Privileged and *Staphylococcus aureus* Impaired Healing: Is there a Connexin Connection?

By

Nicola Davis

Submitted to University College London for the degree of Doctorate of Philosophy

Supervised by Professor David Becker

Cell and Developmental Biology, University College London

September 2014

Declaration

I, Nicola Davis, confirm that the work presented in this thesis is my own. Where information has been derived from other sources, I confirm that this has been indicated in the thesis.

Abstract

Wound healing is a vital process, ensuring re-establishment of homeostasis and protection from pathogens. A few regions exhibit privileged healing, such as buccal mucosa, repairing very rapidly. In contrast, wound healing can be impaired, creating chronic wounds. Connexins (Cx) are a group of proteins that form gap junctions, enabling direct communication between the cytoplasm of connected cells. They play a pivotal role in normal skin wound healing. Cx43 is involved in cell proliferation and migration, but the roles of Cx26 and Cx30 are less well understood.

Connexin expression changes in the privileged healing of buccal mucosa have not previously been determined. Cx26, Cx30 and Cx43 were highly expressed throughout the mucosa epithelium, but became rapidly down-regulated at the wound edge. This is in contrast to skin, where Cx26 and Cx30 are expressed at low levels, but increase at the wound edge, showing that the connexin dynamics differ between the tissues.

Cx26, Cx30 and Cx43 expression also differs in chronic wounds compared to normal skin. They are expressed at abnormally high levels throughout the epidermis, and Cx43 is highly expressed in the dermis. It is thought that bacterial infection is involved in chronic wound development and healing impairment. *Staphylococcus aureus* is found in 90% of chronic wounds, where it forms a biofilm. I found that *in vitro S.aureus* biofilm exotoxins caused senescence in fibroblasts, impaired migration, and reduced Cx43 expression. The bacteria themselves reduced Cx43 expression, which increased their internalisation into fibroblasts. Furthermore, loss of Cx43 expression resulted in increased toxicity of *S.aureus* infection. *In vivo S.aureus* infection impaired healing, and resulted in epidermal hyperplasia and connexin up-regulation, mimicking the aetiology of chronic wounds.

Connexin expression differs in buccal mucosa and *S.aureus* infected wounds compared to normal skin during healing, but their role in the healing status of these tissues is still poorly understood.

Acknowledgements

I would like to thank everyone who has supported me throughout my PhD, and there are many without whom I could not have completed this thesis.

For their intellectual input I would like to thank Professor David Becker, Dr Chris Thrasivoulou, Dr Anthony Phillips, Professor Andy Forge and Dr Dan Jagger. For their help and support in my final year I particularly wish to thank Professor Andy Forge and Dr Dan Jagger. I am also very grateful for the help from all members of the Becker lab, for their thoughts and ideas, encouragement, as well as their technical support. I would also like to thank the confocal unit, particularly Tim Robson and Dr Chris Thrasivolulou for their technical support, and Dr Bambos Charalambous for training me in microbiological techniques. I also wish to thank my supervisor, Professor Becker, for his faith in me and in my abilities, and for his willingness to give me my independence.

Most of all I wish to thank all my colleagues on the 5th and 6th floor, who have made my time at UCL fun and enjoyable. I also want to thank everyone who offered their general help and support following David's departure, and Professor Stephen Davies for allowing us to use his lab and office.

Finally, but most importantly, I wish to thank my husband, Dr John Robert Davis, for his tireless support and complete faith in me. I wish to dedicate this thesis to him.

Table of contents

List of Figures

List of Tables

Abbreviations

A-SMA	α-smooth muscle actin
asODN	Antisense oligodeoxynucleotide
ADP	Adenosine diphosphate
ATP	Adenosine triphosphate
BCM	Biofilm Conditioned Medium
bFGF	Basic fibroblast growth factor
cAMP	Cyclic adenosine monophosphate
CBX	Carbenoxolone
cDNA	Complementary deoxyribonucleic acid
CFU	Colony forming unit
CHX	Cyclohexamide
Cx	Connexin
DBS	Donor bovine serum
DMEM	Dulbecco modified eagle's medium
DNA	Deoxyribonucleic acid
dNTP	Deoxyribonucleotide triphosphate
DTT	Dithiothreitol
ECL	Enhanced chemiluminescence
ECM	Extracellular matrix
EDIN	Epidermal cell differentiation inhibitor
EGF	Epidermal growth factor
EKV	Erythrokeratodermia variablis
EPS	Extracellular polymeric substance
EM	Electron microscopy
EV	Empty vector
FnBP	Fibronectin binding protein
GFP	Green fluorescent protein
GJ	Gap junction
GJIC	Gap junction intercellular communication
GTP	Guanosine triphosphate
H&E	Haematoxylin and Eosin
HKSA	Heat killed Staphylococcus aureus

HRP	Horse radish peroxidase
ICR	Imprinted control region
IGF	Insulin like growth factor
IAP	Integrin associated protein
IFN	Interferon
IL	Interleukin
KID	Keratitis ichthyosis deafness
kDa	Kilo Dalton
KGF	Keratinocyte growth factor
LB	Luria broth
LPS	Lipopolysaccharide
LukS-PV	Panton-Valentine leukocidin
LY	Lucifer yellow
MMP	Matrix metalloproteinase
MOI	Multiplicity of infection
mRNA	Messenger ribonucleic acid
MRSA	Methicillin resistant *Staphylococcus aureus*
MTT	3-(4,5-dimethylthiazol-2-yl)-2,5-diphenyl tetrazolium bromide
NAD(P)H	Reduced nicotinamide adenine dinucleotide phosphate
ODDD	Oculodentodigital dysplasia
PBS	Phosphate buffered saline
PCM	Planktonic conditioned medium
PCR	Polymerase chain reaction
PDGF	Platelet derived growth factor
PFA	Paraformaldehyde
PGN	Peptidoglycan
PI	Propidium iodide
PMN	Polymorphonuclear neutrophil
P/S	Penicillin/streptomycin
qPCR	Quantitative polymerase chain reaction
RIP	RNAIII inhibiting peptide
RIPA buffer	Radioimmunoprecipitation buffer
ROS	Reactive oxygen species
RPM	Revolutions per minute
RWD	Relative wound density

SA	Staphylococcus aureus
SA-β-Gal	Senescent associated β-galactosidase activity
SEM	Scanning electron microscopy
STZ	Streptozotocin
TGF	Transforming growth factor
TIMP	Tissue inhibitor of matrix metalloproteinase
TRAP	Target of RNAIII activating peptide
TNF	Tumour necrosis factor
VEGF	Vascular endothelial growth factor
ZO1	Zonular Occludin 1

Chapter 1. Introduction

1.1. Overview

The capacity to heal is of paramount importance for multicellular organisms. However, there are regions of the body that exhibit rapid, privileged healing. Alternatively, healing can be impaired by bacterial infection, such as in chronic wounds, where pathogenic species like *Staphylococcus aureus* are frequently found. Gap junctions are increasingly acknowledged to play a crucial role in cutaneous wound repair, and the changes in connexin expression during both privileged and *S.aureus* impaired healing are examined in this thesis. The relationship between *S.aureus* infection and connexin expression is explored, as are the implications of this relationship for cellular function and for healing.

1.2. Overview of wound healing

1.2.1. Architecture of the skin and mucosa

Skin is a complex organ that covers the entire surface of the body (Kanitakis 2002; Young et al. 2000). It is continuous with the mucous membranes that line the internal orifices of the body, such as the mouth, creating a continuous protective barrier from the external environment. Skin is comprised of three major layers: the epidermis, the dermis and the hypodermis.

The epidermis is the outermost layer (Kanitakis 2002; Young et al. 2000). It is a stratified epithelium, consisting primarily of keratinocytes but also including a small number of melanocytes, Merkel cells and Langerhans cells. The epidermis also contains several skin appendages, such as pilosebaceous follicles and sweat glands. These terminate in the epidermis, but are predominantly located in the underlying dermis. The epidermis is divided into four layers, the lowest layer being the proliferative stratum basale, or basal layer (figure 1.1.A). The stratum spinosum (prickle cell layer) is next, followed by the stratum granulosum (granular layer), and the most superficial stratum corneum (cornified layer). Cells divide basally, differentiating and changing morphologically as they pass through the layers. They become more flattened, losing their nuclei and many organelles as they become increasingly superficial, until they are anucleate and flattened in the cornified layer, where the most superficial are shed.

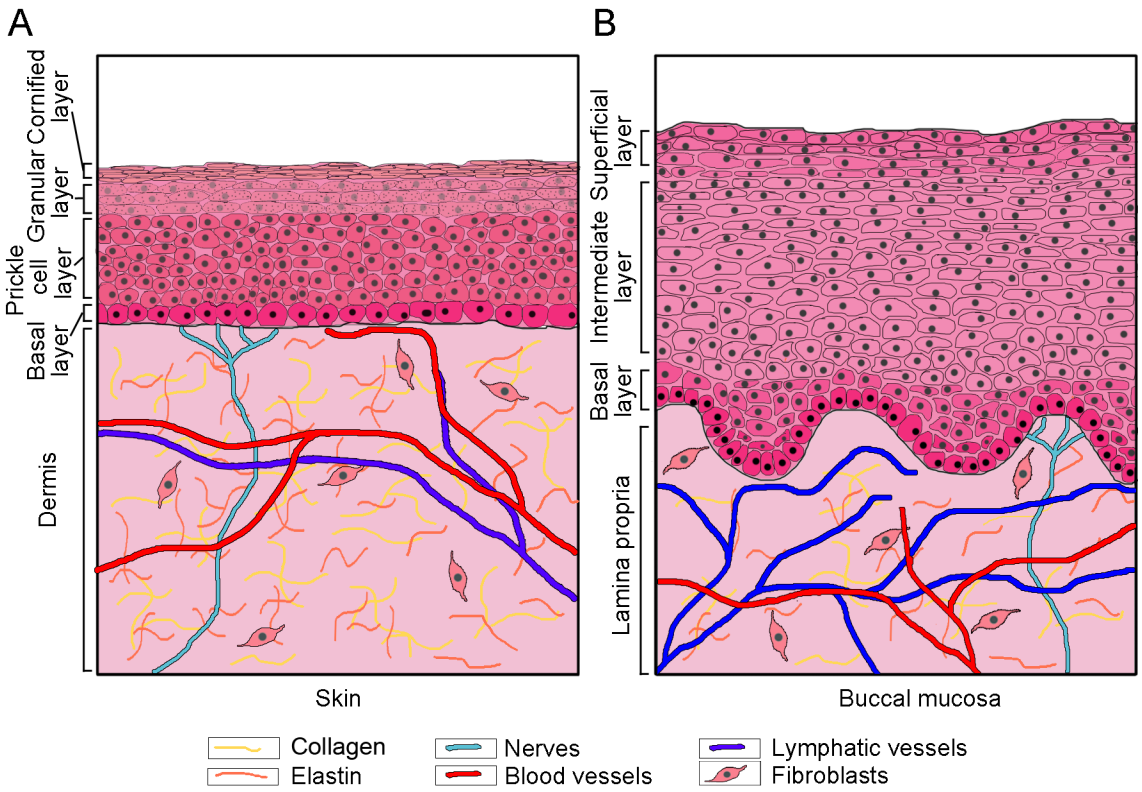

Figure 1.1. Diagrams of the skin and oral mucosa. The epithelial and underlying connective tissue layer of **(A)** skin, and **(B)** oral mucosa are shown. The layers of the epithelium are labelled on the left of each diagram, and demarked by differing colours and morphologies (the information used in the creation of these images was taken from the following references (Diegelmann & Evans 2004; Martin 1997; Shaw & Martin 2009; Abiko & Selimovic 2010; Squier & Brogden 2011; Squier & Kremer 2001; Young et al. 2000)).

Underlying the epidermis, and only separated by a basement membrane, is the dermis (Kanitakis 2002; Young et al. 2000). This is a connective tissue, and is largely comprised of collagen type I bundles, arranged in a loose basket weave structure, and interlaced by elastic fibres. The dermis is richly supplied by nerve fibres and lymphatic vessels, as well as having a dense vascular network. Additionally, epidermal structures such as pilosebaceous follicles and sweat glands are also located in the dermis. The main resident cells within the dermis are fibroblasts. They both synthesise and degrade the connective tissue fibres that are continuously being turned over in the dermis, but the majority are quiescent in healthy undamaged skin. In addition to fibroblasts, the dermis is sparsely populated by mast cells, immune cells that are quickly activated upon wounding.

The hypodermis (Kanitakis 2002; Young et al. 2000) is the deepest layer of the skin. It is often referred to as subcutaneous fat as it comprised almost entirely of adipocytes. It provides protection from mechanical injury, and is involved in insulation and thermoregulation, as well as acting as a nutritional store.

Mucous membranes have the same protective role as skin, as well as other additional functions such as secretion or absorption, depending on the anatomical location (Squier & Kremer 2001; Markiewicz et al. 2007; Squier & Brogden 2011; Young et al. 2000). Oral mucosa is continuous with skin, and can be either keratinised or non-keratinised. Keratinised epithelium closely resembles skin and is found on the gingiva, hard palate and dorsum of the tongue, surfaces that are subject to mechanical force as they come into contact with food during chewing. The majority of the remaining oral mucosa though is non-keratinised. This includes labial mucosa (inside the lips) and buccal mucosa (inside the cheeks). In many ways, oral mucosa largely resembles skin. It is also made up of three layers; a stratified squamous epithelium overlying connective tissue, which is referred to as the lamina propria, with an underlying fatty submucosa.

The epithelium of keratinised mucosa closely mimics the epidermis of skin, containing the same four layers (Squier & Kremer 2001; Markiewicz et al. 2007; Squier & Brogden 2011; Young et al. 2000). The epithelium of non-keratinised

lining mucosa, though, is a little different (figure 1.1.B). It is substantially thicker, and is comprised of only the two lower layers, the basal layer and an intermediate layer similar to the stratum spinosum, plus an uppermost layer referred to as the superficial layer (Squier & Kremer 2001). Cells in the basal layer proliferate, and differentiate as they pass through to the upper layer, but the upper most cells show less morphological differences than the cells in skin. They do become enlarged and flattened and develop cross-linked protein envelopes, but they retain their nuclei and organelles. This makes non-keratinised epithelium more permeable than keratinised epithelia (Squier & Kremer 2001).

The lamina propria is thin, but still closely reflects the dermis (Squier & Kremer 2001; Markiewicz et al. 2007; Squier & Brogden 2011; Young et al. 2000). It is made of loose bundles of collagen type I fibres and is innervated by nerves and vasculature. Non-keratinised mucosa also contains elastin, and the extracellular matrix (ECM) is looser than in skin and keratinised mucosa. The predominant cell type is fibroblasts, but macrophages and mast cells are also present. Like skin there are also appendages in the form of sebaceous follicles, but unlike skin there are no pilosebaceous (hair) follicles. The submucosa also closely resembles the hypodermis, containing mostly adipocytes, but is only present in regions of non-keratinised mucosa (Glim et al. 2013).

1.2.2. Acute wound healing in the skin

1.2.2.1. Introduction to acute wound healing

The ability of skin to heal is of enormous importance in maintaining homeostasis within the body and preventing infection, as skin is the body's main protective barrier from the external environment. Full thickness injuries through the skin result in damage to several different cellular layers. Healing requires a plethora of coordinated signals and events, but is often described as proceeding through four key phases, which overlap: haemostasis, inflammation, proliferation and re-modelling (figure 1.2). This process is discussed in greater depth in the following reviews (Martin 1997; Shaw & Martin 2009), but each phase is reviewed briefly below.

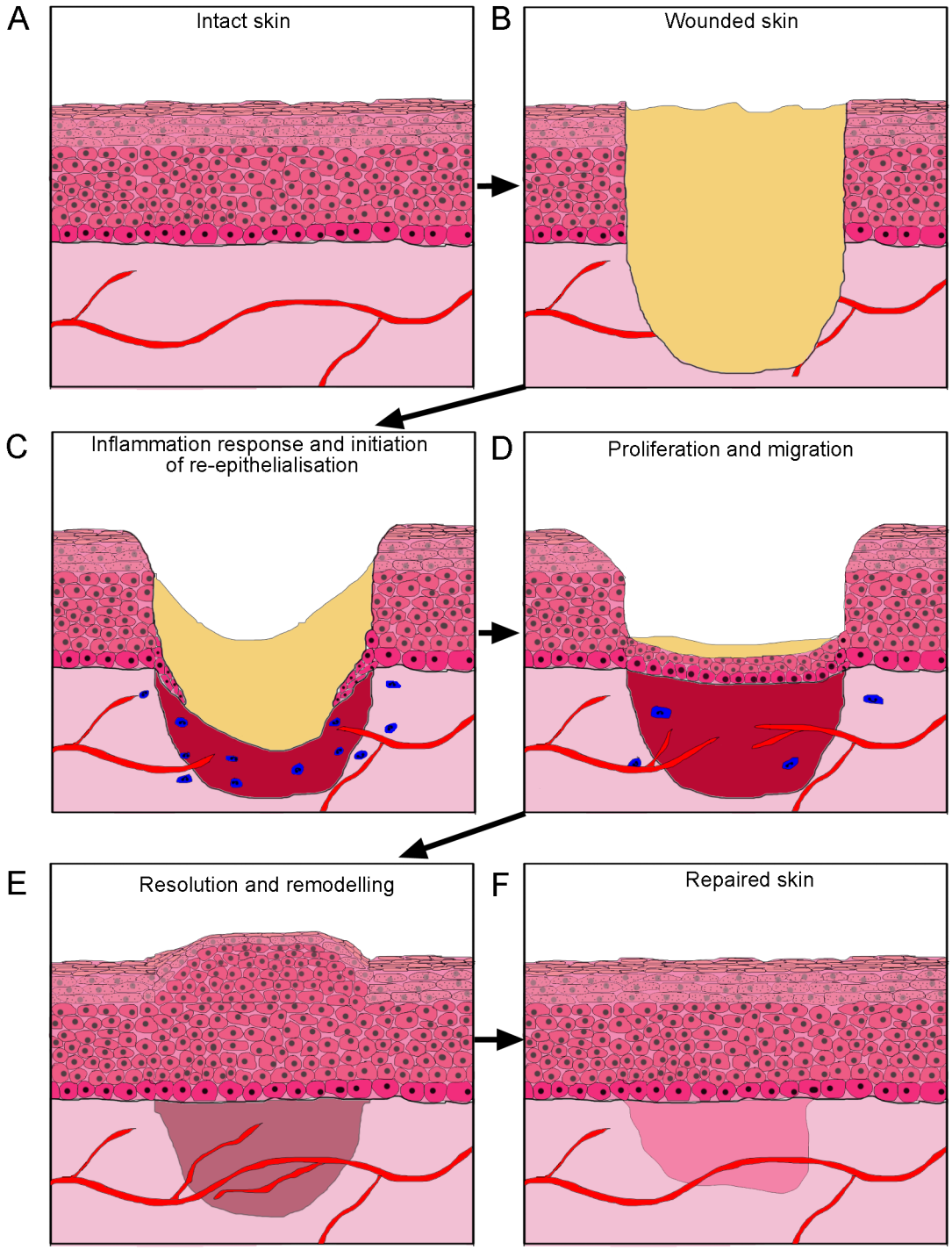

Figure 1.2. Diagrams showing the stages of wound healing in skin. (A) Intact skin prior to injury. **(B)** Wounded skin immediately after injury, showing a clot (yellow) and broken blood vessel (red). **(C)** The initial stages of healing, showing inflammation and the start of re-epithelialisation. Leukocytes (blue) infiltrate the wound, blood vessels begin to grow into the wound bed, and keratinocytes from the epidermis (pink) begin to migrate over the granulation tissue (dark red). **(D)** Re-epithelialisation is complete, restoring barrier function. Keratinocytes continue to proliferate at the wounded site. **(E)** The dermis and epidermis, which is hyper-thickened, begins to remodel. **(F)** Skin is repaired and full barrier function restored (the information used in the creation of these images was taken from the following references (Diegelmann & Evans 2004; Martin 1997; Shaw & Martin 2009; Young et al. 2000)).

1.2.2.2. Haemostasis

During injury to the skin blood vessels are invariably damaged (figure 1.2.B). Platelets in the blood are activated upon contact with the ECM at the wound site. They aggregate and form a clot of insoluble cross-linked fibrin fibres that block blood vessels and prevent further bleeding. Furthermore, platelets release cytokines and growth factors as they degranulate, which are sequestered at the site of injury by the network of fibrin fibres.

1.2.2.3. Inflammation

The inflammatory response is initiated immediately upon wounding by the leakage of circulating leukocytes from damaged blood vessels (figure 1.2.C). Mast cells present in connective tissue around the wound site are also rapidly activated by the innate immune system, releasing granules of pro-inflammatory molecules. These increase vasopermeability, vasodilation, and leukocyte recruitment (Artuc et al. 1999; Diegelmann & Evans 2004). Increased blood vessel leakiness means an increase in exudate production. The exudate dilutes any irritants, and the fibrin clot traps any foreign material. The mast cells also release hyaluronic acid and proteoglycans, which interact with the exudate to form a gel, which further prevents movement of foreign material.

Neutrophils, macrophages and fibroblasts are recruited by pro-inflammatory cytokines released by mast cells, platelets and endothelial cells. They are also recruited by the presence of epitopes recognised as foreign by cells, such as pathogen associated molecular patterns (PAMPs) found on bacteria. Neutrophils are the first to arrive, as they circulate within the bloodstream, and extravasate at the site of injury within minutes. Neutrophils phagocytose contaminants such as bacteria, resulting in the production of bactericidal reactive oxygen species (ROS). Additionally they undergo degranulation, releasing DNA and bactericidal enzymes. Neutrophil infiltration is normally resolved within 1-2 days in uninfected wounds (Martin & Leibovich 2005).

Macrophages are recruited at the same time as neutrophils and by many of the same pro-inflammatory cytokines, though they take longer to respond, typically accumulating in the wound 48-96 hours after wounding. Monocytes, precursors to macrophages, circulate within the blood and are recruited to damaged

tissues. They extravasate into the inflamed tissue and differentiate into macrophages, which phagocytose opsonized bacteria and necrotic tissue. Macrophages also remove remaining neutrophils, but unlike neutrophils, macrophage recruitment will typically continue to increase until 5 days after wounding, even in the absence of infection. Their presence decreases slowly and persists during granulation tissue formation. Macrophages are very sensitive to their environment and can release a range of molecules including cytokines, complement, coagulation factors, ECM proteins, ROS and growth factors. Macrophages also recruit lymphocytes of the adaptive immune system (Diegelmann & Evans 2004; Martin & Leibovich 2005).

1.2.2.4. Proliferation

As the presence of neutrophils declines the proliferative phase begins (figure 1.2.C-E). Macrophages release growth factors, such as platelet derived growth factor (PDGF) and transforming growth factor (TGF) –β, that attract fibroblasts to the wound site, primarily from the surrounding healthy dermis. These proliferate and migrate into the wound bed, depositing ECM, predominantly type III collagen. At the same time as fibroblasts are migrating into the wound bed, angiogenesis of new blood vessels into the wound bed also occurs. The combination of ECM, fibroblasts and new blood vessels is called granulation tissue, and it provides a bed for epithelial cells to migrate over. Wound closure can also be aided by wound contraction. This is mediated by myofibroblasts, differentiated fibroblasts that attach to fibronectin and other ECM components within the granulation tissue and contract, though how this occurs and its importance is still contentious (Martin 1997; Diegelmann & Evans 2004)). Simultaneously, epidermal growth factor (EGF) and TGF-α stimulate proliferation of basal keratinocytes in the epidermis. Keratinocytes at the wound edge, in front of the site of proliferation, become migratory and a tongue of collectively moving cells proceeds over the granulation tissue (figure 1.2.C). This process is termed re-epithelialisation, and continues until migrating keratinocytes at the wound edges come into contact, enabling the closure of the wound (figure 1.2.D). The cells will continue proliferating and differentiating until a fully stratified epithelium is reinstated and the barrier function of the skin is restored (figure 1.2.E) (Shaw & Martin 2009).

1.2.2.5. Tissue remodelling

After re-epithelialisation is complete, tissue remodelling begins (figure 1.2.E). In the dermis, excess blood vessels are retracted and new vasculature is matured to reform a functional network (Martin 1997; Diegelmann & Evans 2004; Shaw & Martin 2009). ECM laid down hastily during granulation tissue formation is also remodelled, and type III collagen is gradually exchanged for type I, the normal collagen found in healthy skin. Moreover, inflammatory cells disperse or apoptose, and myofibroblasts undergo apoptosis.

1.3. Privileged healing in oral mucosa

1.3.1. Introduction to privileged healing

Oral mucosa is described as “proceeding through the same stages of healing as other parts of the body” (Enoch & Stephens 2009). However, clinical observations by periodontists suggest that this anatomical location within the adult body exhibits rapid healing with reduced scar formation (Häkkinen et al. 2000; Ferguson & O’Kane 2004). Evidence for rapid and scarless healing has also been obtained using animal models (Szpaderska et al. 2003; Wong et al. 2009; Mak et al. 2009). Although differing in a number of ways, oral mucosa healing is frequently compared to the rapid and scarless healing seen in foetuses, and so has been called ‘privileged healing’ (Sciubba et al. 1978; Szpaderska et al. 2003). Some of the potential reasons for this privileged healing status are discussed here and are reviewed in more detail by (Glim et al. 2013).

1.3.2. Features and differences in privileged healing

1.3.2.1. Reduced inflammatory response in privileged healing

An important difference between skin and oral mucosa during healing is the inflammatory response. Foetuses heal without scarring; embryonic wounds exhibit little or no inflammatory response, and this is thought to be part of the reason for the fast and scarless healing (Degen & Gourdie 2012). Inflammation in adult skin is clearly vitally important for control of infections as it is exposed to the environment and pathogens. It was thought that inflammation is necessary for adult skin healing, as inflammatory cells provide growth factors and cytokines that are necessary for repair. However, removal of neutrophils and

macrophages in a transgenic mouse found no delay in healing (Martin et al. 2003), and so the role of inflammation in either improving or delaying healing in adults is uncertain. It is acknowledged though that inflammation can be detrimental to wound healing, and inflammation has also been comprehensively linked to fibrosis (Shaw et al. 2010; Grose & Werner 2004). Like embryonic healing, a reduced inflammatory response has been observed in oral mucosa wounds compared to dermal wounds (Chen et al. 2010; Szpaderska et al. 2003; Mak et al. 2009; Schrementi et al. 2008). In tongue mucosa compared to skin it was found that there was significantly less infiltration by neutrophils, macrophages and T cells, with earlier resolution of inflammation (Szpaderska et al. 2003). Fewer macrophages and mast cells were similarly found to infiltrate a pig gingival wound compared to the skin (Mak et al. 2009). The authors suggest that the reduced inflammatory response in oral mucosa wounds may underlie or support rapid healing and reduced scar formation.

In conjunction with a reduced infiltration of leukocytes, a reduction in pro-inflammatory cytokines has also been shown in oral mucosa wounds. Whole transcriptome analysis of oral mucosa and skin during wound healing in mice found considerably more inflammatory response genes were expressed in the skin than mucosa (Chen et al. 2010). Particularly, differences in TGF-β expression have been highlighted (Schrementi et al. 2008; Szpaderska et al. 2003; Mah et al. 2014; Mak et al. 2009; Eslami et al. 2009). TGF-β is a cytokine with both pro- and anti-inflammatory roles (Han et al. 2012). It has three isoforms: TGF-β1, TGF-β2 and TGF-β3, with TGF-β1 being the most abundant. Following wounding, significantly less TGF-β1 was produced in both porcine and murine oral mucosa than skin (Schrementi et al. 2008; Szpaderska et al. 2003). Similarly human gingival fibroblasts produced less TGF-β than skin fibroblasts (Mah et al. 2014). Increased and more persistent TGF-β expression was also found in skin wounds compared to oral wounds in red Duroc pigs, although the β1 and β3 isoforms were not distinguished in this study (Mak et al. 2009). Another study in red Duroc pigs though found increased TGF-β3 expression significantly earlier in mucosa than in skin (Eslami et al. 2009). Interestingly, TGF-β3 expression was lower in unwounded murine oral mucosa compared to skin. Following wounding though, levels increased to be similar to those in skin, while expression in skin did not change. This means the ratio of

TGF-β1 to TGF-β3 was considerably lower in oral mucosa than skin (Schrementi et al. 2008). High levels of TGF-β1 have been closely associated with increased scar formation, and the ratio of TGF-β1 to TGF-β3 is thought to be particularly important; lower ratios are related to reduced scar formation, while higher ratios are related to increased scarring, so the ratio observed here may be contributing to the improved scar outcome (Beanes et al. 2004). Other cytokines have also been shown to differ between skin and oral mucosa (Szpaderska et al. 2003; Liechty et al. 2000; Graves et al. 2001; Chen et al. 2010). Szpaderska et al reported lower expression and a more rapid reduction in the pro-inflammatory cytokines interleukin-6 (IL-6) and cytokine-induced neutrophil-attracting chemokine (KC, a murine homolog of human IL-8) in mouse tongue wounds compared to back skin wounds. Interestingly they didn't find an increase in IL-10, the anti-inflammatory cytokine that suppresses expression of IL-6 and IL-8 (Szpaderska et al. 2003). Using knockout mice, IL-10 has previously been shown to be important for both foetal and hard palate mucosal healing, but not skin healing (Liechty et al. 2000; Graves et al. 2001). Wounds in IL-10 knock out foetal skin and adult mucosa had delayed closure and exhibited excessive inflammation. However, healing of the mucosal wounds was rescued by administration of antibiotics, suggesting that IL-10 is involved in protection from bacteria within oral mucosa (Graves et al. 2001). It was also found that stimulation of murine skin keratinocytes with IL-1β stimulation, a pro-inflammatory cytokine, produced significantly greater amounts of the pro-inflammatory cytokines tumour necrosis factor-α (TNF-α) and IL-6 than stimulation of oral keratinocytes (Chen et al. 2010). This shows that not only is the inflammatory response reduced, but oral mucosa cells also respond differently to pro-inflammatory stimuli compared to their cutaneous counterparts.

It is evident that oral mucosa wounds have a reduced inflammatory response compared to skin. However, oral mucosa is nonetheless exposed to environmental pathogens, and oral epithelia have a rich microbiota, found both extracellularly (Mancl et al. 2013)) and intracellularly (Rudney et al. 2001). Interestingly, it has also been reported that mild inflammation of rat oral mucosa, induced by injection of turpentine, increased proliferation of keratinocytes peripheral to the site of inflammation, both basally and suprabasally (Willoughby et al. 1986). This suggests that while a reduction in the inflammatory response

may be contributing to the privileged healing status of oral mucosa, inflammation may still play an important role in this tissue.

1.3.2.2. Keratinocytes and the epithelium in privileged healing

Keratinocytes are the major cell type found in the epidermis and mucosal epithelium. They play a central role in wound healing, as they must proliferate and migrate in order to close the wound. Wound closure is clinically reported to be faster in oral mucosa wounds that in skin, and re-epithelialisation in particular was found to occur more rapidly in murine mucosa than skin (Schrementi et al. 2008; Szpaderska et al. 2003). Earlier onset of re-epithelialisation was also observed in the healing of parakeratinised rat tongue, commencing at 4 hours in the mucosa compared to 12 hours in the dorsal skin. The mucosal keratinocytes at the migrating edge were also observed to retain their cuboidal morphology, whereas the epidermal keratinocytes became elongated (Sciubba et al. 1978).

Proliferation in intact oral mucosa epithelium is also faster than in skin, with an accordingly higher turnover rate, as shown in mouse buccal mucosa (Susi 1968). Similarly, staining of human soft palate (a non-keratinised mucosa) with Ki67, a proliferation marker, showed more proliferating keratinocytes in the oral mucosa, which were also present suprabasally, compared to only in the basal layer of the epidermis (Glim et al. 2014). The more extensive proliferation of keratinocytes in oral mucosa might in part be due to the presence of saliva (Gröschl et al. 2005). Application of salivary leptin is able to improve wound healing in mice and enhances proliferation of human dermal keratinocytes *in vitro* (Frank et al. 2000). Applying leptin to oral keratinocytes similarly increased proliferation (Gröschl et al. 2005). It also resulted in a significant increase in epidermal growth factor (EGF) and keratinocyte growth factor (KGF) production and secretion. Both EGF and KGF are involved in proliferation of keratinocytes. Furthermore, murine oral keratinocytes were found to produce decreased levels of vascular endothelial growth factor (VEGF) compared to cutaneous keratinocytes (Szpaderska et al. 2005). VEGF stimulates angiogenesis, and it has been suggested that excessive angiogenesis can contribute towards scarring ((Szpaderska et al. 2005; Bloch et al. 2000), reviewed by (Johnson & DiPietro 2013)).

1.3.2.3. Fibroblasts and granulation tissue in privileged healing

Fibroblasts play a vital role in wound healing. They deposit granulation tissue, stimulate re-epithelialisation, remodel granulation tissue after the wound has closed, and differentiated fibroblasts induce wound contraction. Fibrosis and scarring is, however, associated with excessive formation of ECM proteins and increased myofibroblast transformation, factors associated with fibroblasts (Kendall & Feghali-Bostwick 2014). Oral mucosa wounds, in addition to closing more rapidly, heal with minimal scar formation compared to dermal wounds (Mak et al. 2009; Wong et al. 2009; Schrementi et al. 2008; Eslami et al. 2009). Unsurprisingly, differences compared to skin have been observed in the composition of intact lamina propria, the repair of connective tissue, and the activity and gene expression of oral fibroblasts.

The unwounded lamina propria of human palate non-keratinised oral mucosa was reported to differ somewhat from the dermis of skin in its composition (Glim et al. 2014). Several ECM components including fibronectin, chondroitin sulphate and elastin were differentially expressed between the tissues, with the oral mucosa more closely resembling foetal skin. Collagen bundles in the lamina propria of pigs and mice were also found to be smaller and looser than in dermis (Mak et al. 2009; Schrementi et al. 2008). An increased number of blood vessels in the oral mucosa compared to skin has also been reported, in humans, mice and pigs (Glim et al. 2014; Szpaderska et al. 2005; Mak et al. 2009). However, the increase in blood vessels normally observed following injury was not as pronounced in oral mucosa as it was in the skin (Szpaderska et al. 2005; Mak et al. 2009). This is interesting, as a vigorous angiogenic response often precedes fibrosis in *in vivo* models of scarring, and might be related to it (Johnson & DiPietro 2013). Consequently a less robust response could contribute to the minimal fibrosis seen in oral mucosa wounds.

Differences have also been observed in the formation of granulation tissue. In porcine wounds fewer cells were immuno-positive for pro-collagen type I in the lamina propria granulation tissue than in the dermis, and there was reduced fibronectin content (Wong et al. 2009). In culture, human oral fibroblasts also produced less collagen I and III, osteopontin and elastin than dermal fibroblasts

(Mah et al. 2014). Expression of many matrix proteins including collagen type I, fibronectin and osteopontin are associated with and actively contribute to scarring (Mori et al. 2008; Bhattacharyya et al. 2014; McKleroy et al. 2013), and so it is likely that reduced production of these matrix proteins may be contributing to the reduced fibrosis seen in oral mucosa wounds. Additionally, in cutaneous wounds collagen fibrils normally appear immature; they have a reduced diameter compared to those in unwounded dermis, with a more random organisation. However, in porcine and murine oral mucosa wounds the thickness of collagen bundles and their orientation was instead similar to that seen in unwounded mucosa (Mak et al. 2009; Schrementi et al. 2008). Mak et al also observed that at days 28 and 60, in porcine oral mucosa wound beds there were fewer but better aligned fibroblasts compared to skin wounds (Mak et al. 2009); lower cell density is associated with improved maturation of granulation tissue. These results indicate that granulation tissue remodelling is superior in oral mucosa compared to in the dermis. Granulation tissue remodelling is partially achieved through the actions of matrix metalloproteinases (MMPs), which degrade ECM, and unsurprisingly differences too have also been reported in their expression. Oral fibroblasts were found to express significantly elevated levels of active MMP-2, MMP-3 and MMP-10 compared to dermal fibroblasts, but reduced levels of MMP-7 and MMP-11. MMP-3 activity in particular was also shown to be important for the contractile ability of oral fibroblasts, but not skin fibroblasts (Mah et al. 2014; McKeown et al. 2007; Stephens et al. 2001). The exact role of each MMP in wound healing and granulation tissue remodelling is still uncertain, but the balance of different MMPs and their inhibitors, (tissue inhibitors of metalloproteinases-TIMPs) is thought to be important in determining the healing outcome, and may well be contributing to the privileged status of oral mucosa (McCarty et al. 2012).

Increased transformation of fibroblasts into contractile myofibroblasts, alongside increased matrix production, is also associated with fibrosis (Kendall & Feghali-Bostwick 2014). Interestingly, no differences in the number of myofibroblasts (as assessed by α-SMA staining) were found in porcine oral mucosa when small incisional wounds were made, but there was a significant increase in myofibroblasts in both intact and wounded oral mucosa when larger wounds

were made. In these the myofibroblasts also persisted in the region for longer, although the oral mucosa wounds exhibited less contraction than the skin wounds (Mak et al. 2009; Wong et al. 2009). This is in spite of the finding that both human and murine oral fibroblasts were found to have greater contractile ability compared to dermal fibroblasts (P Stephens 1996; Lygoe et al. 2007; Shannon et al. 2006; Lee & Eun 1999; McKeown et al. 2007). Furthermore, increased basal levels of α-SMA expression has been shown in oral fibroblasts (Lygoe et al. 2007), although the opposite has also been shown (Shannon et al. 2006; Mah et al. 2014; McKeown et al. 2007). Additionally, oral fibroblasts were found to be more sensitive to TGF-β, which stimulates their differentiation into contractile myofibroblasts (Lygoe et al. 2007; Lee & Eun 1999), although less TGF-β production has also been reported in oral mucosa (Schrementi et al. 2008; Szpaderska et al. 2003). As such, for the moment the role of myofibroblasts in oral mucosa wounds, and their contribution to the minimal scar formation remains uncertain.

Like keratinocytes, oral fibroblasts also differ in their production of growth factors compared to dermal fibroblasts. Human buccal oral fibroblasts were found to produce more keratinocyte growth factor (KGF) and hepatocyte growth factor (HGF) (Shannon et al. 2006), while gingival produced more VEGF-α (Mah et al. 2014) and insulin like growth factor 2 (IGF-2) (Ebisawa et al. 2011), promoting epithelial and endothelial proliferation. Furthermore, human oral fibroblasts were found to proliferate significantly faster than dermal fibroblasts derived from breast skin (Mah et al. 2014). They were also found to have a longer replicative lifespan than dermal fibroblasts; they had longer telomeres than skin fibroblasts, which enables a greater number of cell divisions, and delayed senescence (Enoch et al. 2009).

1.3.3. Summary of privileged healing

Although oral mucosa shares many similarities with skin, examining its privileged healing status has also revealed many differences. Oral fibroblasts and keratinocytes are phenotypically distinct from their cutaneous counterparts, displaying differences in their contractile and proliferative capabilities, as well as in their growth factor and cytokine production. The inflammatory response is

also markedly dampened compared to skin, and this is all thought to contribute to the improved healing observed in these exceptional tissues.

1.4. *Staphylococcus aureus* impairment of wound healing

1.4.1. Introduction to *S.aureus* impairment of healing

Staphylococcus aureus is able to transiently but harmlessly populate the human skin and mucous membranes, but it is frequently a pathogenic species, and is the most common cause of skin infections. Infection results in an acute inflammatory response (discussed in detail by (Fournier & Philpott 2005)), which *S.aureus* has derived numerous mechanisms to avoid or overcome (discussed in detail by (Kraus & Peschel 2008)). Infection with *S.aureus* can cause serious health problems, including wound infection, osteomyelitis and sepsis; chronic wounds (wounds that remain open for longer than 3 months) are attributed, at least in part, to persistent infections, with *S.aureus* seen as a major player (Davies et al. 2004; Gjødsbøl & Christensen 2006). In chronic wounds *S.aureus* is predominantly found within a biofilm, an antibiotic resistant community of sessile bacteria encased in a self-produced matrix (James et al. 2007). Increasingly, evidence suggests that the formation of biofilms is an important part of the ability of *S.aureus* to prevent healing in chronic wounds (Mustoe et al. 2006). Research has shown that *S.aureus* can produce 300-400 virulence factors, some of which are toxic to cells and others which affect cell function (specific toxins are not discussed here in detail. For more information see the review by (Kraus & Peschel 2008)). The toxins secreted vary between strains, but moreover, they can change depending on whether the bacteria are planktonic or within a biofilm (Resch & Rosenstein 2005; Secor et al. 2011). Thus, the consequences of an infection for the host will differ depending on the location or state (planktonic or biofilm) of the contaminating *S.aureus* (Secor et al. 2011; Kirker & James 2012). Moreover, biofilms are notoriously difficult to destroy, and persistent infection by them is also thought to be responsible for the prolonged inflammation found in chronic wounds, which is highly damaging (Fazli et al. 2011).

As well as the formation of biofilms, *S.aureus* internalisation into host cells is increasingly thought to play a role in the virulence of this pathogen (Kubica et al. 2008; Menzies et al. 2002; Hamza et al. 2013; Edwards et al. 2010). *S.aureus* is a facultative intracellular pathogen, and internalisation into host cells is thought to be an immune evasive mechanism. There is even evidence that it may also aid the dispersal of *S.aureus* throughout a host, and so be involved in bacterial dissemination (Kubica et al. 2008). Intracellular *S.aureus* are now implicated in the recurrence of a growing number of diseases, including cystic fibrosis, bovine chronic mastitis and chronic rhinosinusitis (Jarry & Cheung 2006; Hébert et al. 2000; Clement et al. 2005). Thus there is growing evidence that invasion of host cells may be an important part of *S.aureus* virulence. However, the role of intracellular *S.aureus* in impairing skin wound healing has not been well studied and so is poorly understood.

1.4.2. Biofilm *S.aureus* in impaired wound healing

1.4.2.1. Brief introduction to chronic wounds

S.aureus is commonly found colonising the skin, and can easily contaminate cutaneous wounds. Despite the array of 300-400 virulence factors that *S.aureus* possesses, the immune system of a healthy individual is usually capable of controlling the contamination before it becomes an infection (Fournier & Philpott 2005). However, in individuals with compromised health there is a greater risk of contamination developing into infection, and this is particularly true in individuals with poor healing (Falanga 1993; Mustoe et al. 2006). Thus, unsurprisingly, *S.aureus* is one of the most commonly reported species found in chronic wounds (Davies et al. 2004; Gjødsbøl & Christensen 2006). It is also associated with a non-healing phenotype, as it was found in 60% of non-healing chronic wounds, compared to only 25% of healing wounds (Davies et al. 2004). Consequently, *S.aureus* infection has most commonly been researched in relation to chronic wounds, where bacterial infection is increasingly considered to be a major contributing factor in their chronicity (Mustoe et al. 2006; Bjarnsholt et al. 2008).

Chronic wounds are wounds that fail to heal in a timely fashion (Stadelmann et al. 1998). They fail to proceed through the normal stages of acute wound healing. Instead they become locked in the inflammatory phase, and a

sustained low grade inflammation is one of the hallmarks of chronic wounds; sustained inflammation though impedes the healing process (Menke et al. 2007). Chronic wound keratinocytes are often hyperproliferative, and divide suprabasally, rather than in just the basal levels, forming a hyper-thickened epidermis around the wound. They have been reported to display hyperkeratosis (thickened cornified layer) and parakeratosis (nuclei present in the cornified layer), and to be negative for markers of differentiation and migration (Stojadinovic et al. 2005; Usui et al. 2008; Brem et al. 2007; Stojadinovic et al. 2008). Keratinocytes isolated from chronic wound can also display a reduced ability to respond to growth factors (Stojadinovic et al. 2005; Waikel et al. 2001). Chronic wounds also characteristically exhibit dermal fibrosis, defective granulation tissue formation and poor ECM remodelling (Herrick et al. 1992). Differences observed in fibroblasts from chronic wounds compared to those from acute wounds include an induction of senescence (Ågren & Steenfos 1999; M. V Mendez et al. 1998; A. C. Stanley et al. 1997; Vande Berg et al. 1998), reduced proliferation (Brem et al. 2007), reduced migration (Brem et al. 2007), and changed responses to growth factors (Ågren & Steenfos 1999; Hasan et al. 1997). Research into chronic wounds has shown that ischaemic reperfusion, hypoxia, intrinsic host disease and bacterial infection are all major factors contributing towards impaired healing (Mustoe et al. 2006).

1.4.2.2. Formation and persistence of *S.aureus* biofilms

S.aureus have been studied extensively over the years, predominantly as freely moving planktonic bacteria in single species, nutrient rich, liquid cultures. However, this is not how these bacteria are found naturally. Instead they exist preferentially within biofilms (Figure 1.3), complex adherent matrices of self-synthesised extracellular polymeric substances (EPS), often alongside multiple species (Donlan & Costerton 2002). This is how *S.aureus* are predominantly found within wounds, and it is becoming increasingly apparent that biofilm formation is involved in bacterial impairment of healing (Bjarnsholt et al. 2013).

Biofilm formation is initiated when planktonic bacteria become reversibly adhered to a surface, priming the surface for irreversible attachment (figure 1.3.A). Irreversibly adherent bacteria then proliferate clonally and produce EPS,

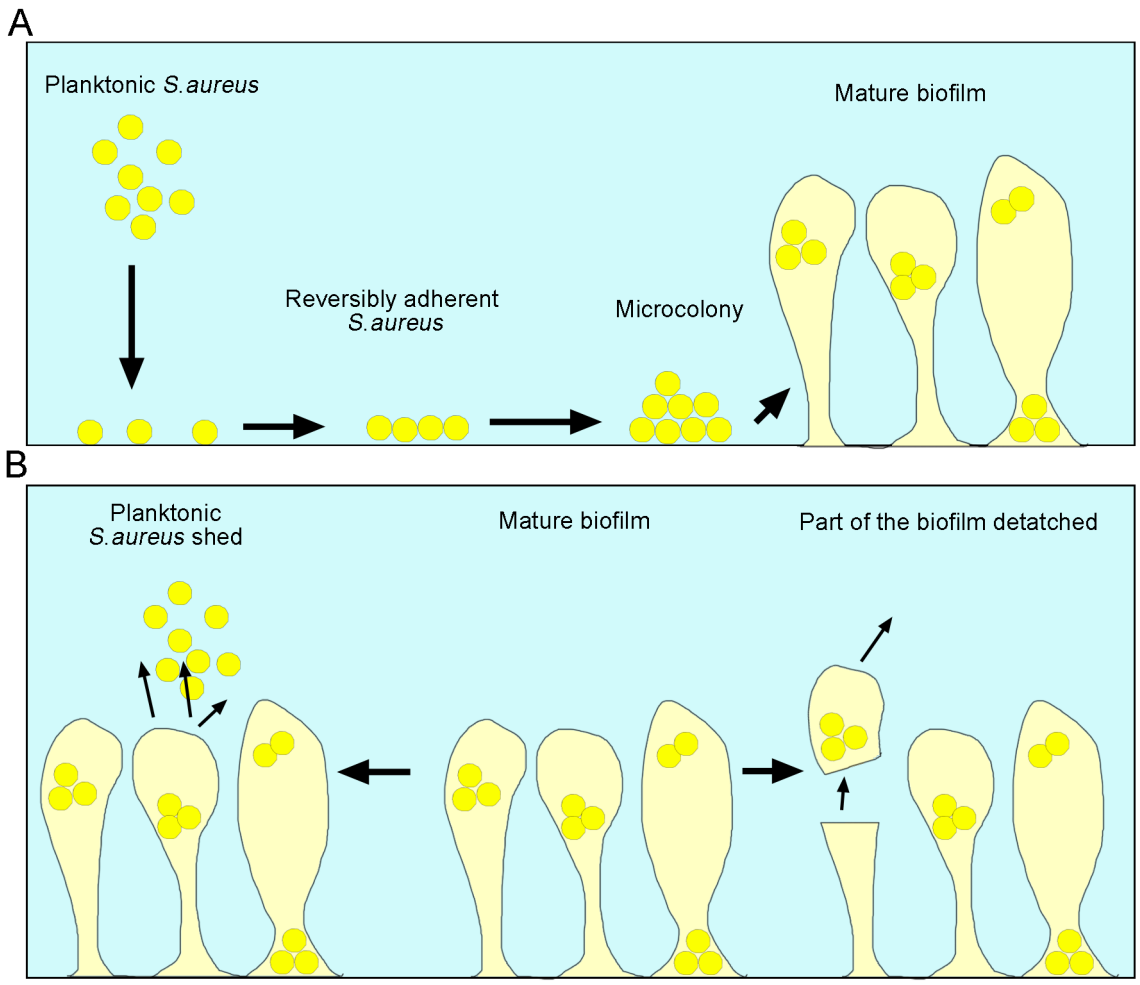

Figure 1.3. Diagrams of biofilm formation and dispersal. (A) The stages of planktonic *Staphylococcus aureus* forming a biofilm are shown from left to right. Planktonic *S.aureus* adhere to a surface, first reversibly, then irreversibly. They form a micro-colony, producing extracellular polymeric substances that encase them. Mature biofilms appear as 'mushrooms' or 'towers'. **(B)** Two methods of *S.aureus* dispersal from a biofilm are shown. On the left, planktonic *S.aureus* are shed from the biofilm. On the right, part of the mature biofilm breaks away (the information used in the creation of these images was taken from the following references (Donlan & Costerton 2002; Costerton et al. 1999; Mancl et al. 2013; Bjarnsholt et al. 2013)).

a process referred to as biofilm maturation. EPS is comprised of polysaccharides, proteins, and extracellular DNA (Donlan & Costerton 2002). It encases the increasingly sessile bacteria, forming “mushrooms” or “towers” (Figure 1.3.A) (Mancl et al. 2013). Bacteria within biofilms are phenotypically distinct from planktonic bacteria, displaying reduced growth rates, altered gene expression, and producing different virulence factors (Donlan & Costerton 2002). A mature biofilm is normally polymicrobial. It will be comprised of heterogeneous populations with species-specific niches, linked by channels (Costerton et al. 1999). These channels enable the passage of nutrients and waste products. They also enable the transportation of signalling molecules used in quorum sensing (a system used to coordinate gene expression of the bacteria based on nutrient availability and population density, amongst other things) and of genetic material. Furthermore, biofilms are not static, but develop temporally as the population density, nutrient availability and combination of species changes.

Biofilms often display a marked resistance to the host immune system and to antibiotic treatment. This resistance is a common feature of biofilms. It is thought to be due to multiple factors, although it is still not fully understood. These factors include, but are not limited to, increased resistance to antibiotics, reduced penetration of antimicrobial agents, and physiological changes in the bacteria due to them being found within the biofilm (Van Acker et al. 2014). These mechanisms appear to be highly conserved, and are often very similar between only distantly related species.

In order to be effective, antimicrobial agents must penetrate the biofilm to reach the bacteria within. Biofilms have been shown to reduce penetrance of antibiotics, although this appears to be very specific to both the bacterial species and strain, and the antibiotic. It was shown that *Pseudomonas aeruginosa* biofilms significantly impeded the movement of the antibiotic ciprofloxacin (Suci et al. 1994), whereas *S.aureus* biofilms did not, but they instead impeded the penetration of oxacillin, cefotaxamine and vancomycin, (Singh et al. 2010). Another study showed though, that the antibiotic vancomycin did penetrate an *S.aureus* biofilm, but took over 1 hour to penetrate to the centre (Jefferson et al. 2005). It was also shown that *S.aureus* at the

centre of a biofilm remained intact when challenged with cefuroxime (an antibiotic that significantly affected the biofilms viability), while the cell walls of peripheral bacteria were destroyed (Amorena & Gracia 1999), demonstrating the reduced penetration of the antibiotic to the centre of the biofilm. Slower penetration of antibiotics means bacteria would be exposed to initially low but gradually increasing doses of antibiotics. It has been suggested that this might provide a window in which the bacteria are able to mount a defence (Jefferson et al. 2005). Furthermore, microenvironments within the biofilms might directly influence the efficacy of antibiotics; there are anaerobic niches in biofilms (de Beer et al. 1994), and aminoglycosidase antibiotics are less effective against many aerobic bacterial species, including *S.aureus*, in anaerobic conditions (Tack & Sabath 1985).

Biofilms have been shown to reduce the penetrance of some antibiotics, but the actual bacteria within the biofilm have also been shown to be more resistant than in planktonic cultures (Van Acker et al. 2014). This is thought to be because of phenotypic changes and differences in gene expression. Biofilm bacteria grow significantly slower than planktonic cultures, with distinct zones observed within biofilms where bacteria proliferate at different rates (Xu et al. 2000). Slower growing bacteria have been found to be less susceptible to antimicrobials (Evans et al. 1990); It was reported that the sensitivity of *E.coli* to the antiseptic centrimide was dependent on the growth rate of the bacteria, with the fastest growing bacteria the most sensitive (Evans et al. 1990). It was also found that faster growing young *S.aureus* biofilms (6 hours) were more sensitive to antibiotics than older biofilms (24 hours) (Amorena & Gracia 1999). This was similarly shown using *P.aeruginosa* biofilms. Treatment of young biofilms (2 days old) with tobramycin or pipercillin eradicated the bacteria, but this could not be achieved when 10 day old biofilms underwent the same treatment (Anwar et al. 1992). In addition to changes in growth rate, it is well established that biofilm gene expression differs from planktonic gene expression (Sauer 2003). Although not widely studied yet, some of the differently expressed genes have been associated with antibiotic resistance. For example *P.aeruginosa* biofilm cells express the *ndvB* gene, which encodes for a cyclic glucan that is thought to sequester antibiotic molecules (Beaudoin et al. 2012). Similarly, expression of the *agr* quorum sensing gene by *S.aureus* in biofilms was found

to influence their susceptibility to the antibiotic rifampin (Yarwood et al. 2004). Additionally, it has recently been shown the frequency of mutations giving rise to antibiotic resistance in *S.aureus* biofilms was increased 60 fold compared to planktonic cultures, as a result of oxidative stress (Ryder et al. 2012). Furthermore, the rate of horizontal transfer of antibiotic resistance genes was higher in *S.aureus* biofilms compared to planktonic cultures (Savage et al. 2013). Increased frequency of both antibiotic resistance mutations and transfer have similarly been shown in *Pseudomonas ssp* (Ehlers & Bouwer 1999; Driffield et al. 2008).

In addition to being antibioticsresistant, biofilms are often described as resistant to host defences. Although there is extensive research into how planktonic bacteria evade host responses, research into the relationship between the immune system and biofilm bacteria is limited, and so is poorly understood. For a long time it was thought that biofilms reduced the penetrance of host immune cells. However, evidence is emerging showing that this is not always the case. It has been demonstrated that leukocytes are attracted to *S.aureus* biofilms and are able to attach to them (Leid & Shirtliff 2002; Günther et al. 2009; Thurlow et al. 2012). One group found that human leukocytes (mostly monocytes and T and B cells) were unable to penetrate a 2 day old *S.aureus* biofilm, but were readily able to penetrate 7 day old biofilms, although they failed to phagocytose the bacteria within (Leid & Shirtliff 2002). Similarly, using a mouse model, it was observed that there was only limited invasion of macrophages into *S.aureus* biofilms, and that successfully invading macrophages had minimal phagocytic activity or were killed (Thurlow et al. 2012). In contrast, human polymorphonuclear neutrophils (PMNs) were found to readily enter *S.aureus* biofilms and phagocytose the bacteria, but they too were found to be less effective against 15 day old biofilms than against 2 or 6 day old biofilms (Günther et al. 2009). Additionally, *S.aureus* biofilms in mice were found to cause a significant reduction in cytokines and chemokines normally increased during infection, including TNF-α and IL-1β (Thurlow et al. 2012).

Within biofilms there are small populations of dormant bacteria that are very tolerant to antibiotics, called ‘persister cells’, which are thought to repopulate the biofilm following antibiotic treatment (Lewis 2010). However, repeated

cycles of antibiotics results in the selection of strains with higher levels of persister cells, a mechanism which has been shown to result in persistent lung infection by *Pseudomonas* in cystic fibrosis (Mulcahy et al. 2010). Thus, persister cells contribute to the persistence of biofilm infections.

Furthermore, mature biofilms can shed planktonic bacteria or entire parts of the biofilm in a process called dispersion (figure 1.3.B) (Donlan & Costerton 2002). This means that when bacteria are present as biofilms within a host, the biofilm infection and release of planktonic bacteria is persistent, and therefore difficult to treat. Bacteria, and biofilms specifically, are increasingly being recognised as an important part of the poor healing seen in chronic wounds (Bjarnsholt 2013).

1.4.2.3. *S.aureus* and biofilms during wound healing

S.aureus form biofilms in physiological conditions (Davis et al. 2008; Han et al. 2011), and an SEM study of human chronic wounds showed that 60% of the chronic wounds tested contained biofilms, compared to only 6% of acute wounds (James & Swogger 2008), suggesting that in chronic wounds *S.aureus* is predominantly found within biofilms. In fact, it is now commonly accepted that bacteria in chronic wounds exist predominantly in the form of biofilms, although mature biofilms also continuously shed planktonic bacteria (Bjarnsholt et al. 2013). Several animal models have been made that attempt to mimic this *in vivo,* enabling investigation of the effects of *S.aureus* infection and the role of biofilm formation within wounds. Using these infected wound models, the presence of mature *S.aureus* biofilms has been confirmed at 24 hours in rabbits and mice, and at 48 hours in pigs (Akiyama et al. 1996; Davis et al. 2008; Gurjala et al. 2011). In mouse, pig and rabbit wound models, it was shown that infection with *S.aureus* delayed wound healing, particularly by reducing re-epithelialisation (Schierle et al. 2009; Gurjala et al. 2011; Akhil K. Seth et al. 2012; A. Seth et al. 2012; Pastar et al. 2013). In a rabbit wound model a predominantly biofilm phenotype was established by topical application of the antibiotic mupirocin, which eliminated planktonic *S.aureus*. This was compared to an ‘active’ infection which hadn’t been treated, where both biofilm and planktonic *S.aureus* were present; both forms of infection delayed re-epithelialisation and reduced the granulation tissue area, indicating that *S.aureus* within a biofilm was important for the delay in healing (Gurjala et al.

2011). Furthermore, in a mouse model it was demonstrated that disruption of biofilms with RNAIII inhibiting peptide (RIP), which disrupt biofilms but has no effect on *S.aureus* viability, restored normal healing (Schierle et al. 2009). Similarly, infection with an *S.aureus* TRAP-null mutant, which has retarded ability to form a biofilm, improved the rate of healing compared to wild type *S.aureus* (Schierle et al. 2009). This demonstrated the importance of biofilm formation for *S.aureus* impairment of healing. Similar results were obtained with *P.aeruginosa* biofilms in diabetic mouse wounds (Zhao et al. 2010), confirming biofilm-induced prevention of healing is not specific to *S.aureus* infections.

In addition to comparing the rate of healing, the effect of *S.aureus* biofilms on the immune response has also been observed. Using the *S.aureus* wound infected rabbit model previously described, Gurjala et al found that the 'active' infection created a greater inflammatory response than the predominantly biofilm wounds; they reported significantly higher levels of TNF-α and IL-1β in the 'active' infection wounds compared to the predominantly biofilm wounds at day 6, despite similar bacterial loads (Gurjala et al. 2011). These inflammatory markers remained elevated between 6 and 12 days in the predominantly biofilm wounds, showing a sustained low-grade infection. In contrast, no differences were observed in the mouse immune response when implanting tissue cages coated with either wild type *S.aureus* or *ica*-null *S.aureus*, which are unable to form biofilms. The immune response was assessed by the production of TNF-α, IL-8, MIP-2, and the presence of leukocytes (Kristian et al. 2004). Cutaneous wound healing involves multiple cell types, including keratinocytes and fibroblasts, as well as leukocytes, and it has been shown in cell culture that secreted biofilm products affect the cytokine production of different cell types in different ways (Secor et al. 2011; Kirker & James 2012; Sadowska et al. 2013; Tankersley et al. 2014). It is therefore possible that the differences in host responses might be a product of the *in vivo* model used.

As well as investigating *S.aureus* infection in animal models, it has also been investigated *in vitro*, again in relation to chronic wounds and biofilm formation. Biofilm and planktonic bacteria have distinctly different gene expression (Sauer 2003). Analysis of *S.aureus* gene expression showed that the biofilm bacteria expressed lower levels of toxins and proteases compared to planktonic

S.aureus (Resch & Rosenstein 2005). Differences were similarly observed in a proteomic analysis of secretions by biofilm and planktonic *S.aureus*, where a different strain was used (Secor et al. 2011). However, a comparison of several soluble products secreted by four different *S.aureus* strains found no differences in the levels of peptidoglycan, lipoteichoic acid, α-haemolysin and staphylokinase between planktonic and biofilm cultures (Sadowska et al. 2013). These conflicting results suggest that differences in secretions by biofilm and planktonic *S.aureus* are not in all products and may also be strain specific, but it is clear that there are differences in the secretions from some strains of *S.aureus* in the two states. While the effects of some individual toxins produced by planktonic *S.aureus* have been explored in some detail (see review by (Bronner et al. 2004) for more detail), there have been few studies that have compared the effect on cells of *all* the products secreted by either planktonic or biofilm *S.aureus.* Those that have, used cell culture media that had been conditioned with the exotoxins produced either by planktonic *S.aureus* (PCM), or biofilm *S.aureus* (BCM) (Kirker et al. 2009; Kirker & James 2012; Secor et al. 2011; Tankersley et al. 2014). Kirker et al showed that exposing human keratinocytes to BCM, but not PCM, created using a clinical isolate of *S.aureus*, caused morphological changes in the keratinocytes, including dendritic extensions and disorganisation of the actin cytoskeleton (Kirker et al. 2009). They also reported that exposure to both PCM and BCM impaired scratch wound closure, but that exposure to BCM significantly reduced viability and increased apoptosis within 3 hours compared to PCM incubated cell (Kirker et al. 2009). In line with these findings, it was shown that BCM caused an up-regulation of genes involved in apoptosis in keratinocytes (Secor et al. 2011). It was also reported that after 4 hours of incubation BCM caused an increase in cytokine production (IL-1β, IL-6, TNF-α, etc.) but by 24 hours this was reduced, resulting in a low grade sustained production of cytokines. In contrast, incubating keratinocytes with PCM resulted in continuously increasing production of cytokines, so at 24 hours all cytokines assessed were produced at significantly higher levels by keratinocytes exposed to PCM than BCM (Secor et al. 2011). Similarly, analysis of the effect of BCM created using a different strain of *S.aureus* (ATCC 6538) on human keratinocytes found an increase in numerous inflammatory genes compared to PCM exposed cells after 2 hours of exposure (Tankersley et al. 2014). The effect of incubating human fibroblasts

with either BCM or PCM, derived from the *S.aureus* clinical isolate, was also compared. However, while the viability, apoptotic rate and scratch wound closure in fibroblasts exposed to BCM or PCM differed from controls, it was found not to differ between BCM and PCM exposed fibroblasts (Kirker & James 2012). Differences were, however, observed in cytokine production, with fibroblasts exposed to BCM producing less pro-inflammatory IL-6 and IL-8 than those exposed to PCM at all time points assessed over 72 hours, but more TNF-α (Kirker & James 2012). Interestingly, no differences were observed in the production of TNF-α over 24 hours by murine leukocytes when stimulated with either PCM or BCM created from four different *S.aureus* strains. BCM from two of the strains, however, stimulated increased production of IL-6, IL-10 compared to PCM (Sadowska et al. 2013). These experiments suggest that the effects of planktonic and biofilm soluble products on host cell function and inflammatory response do differ, but that it is dependent on both the strain of *S.aureus* and the cell type investigated.

Most *in vitro* and *in vivo* experiments investigating the inflammatory response to *S.aureus* biofilms observed differences to those seen in response to planktonic *S.aureus.* Interestingly, the inflammatory response in chronic wounds is also abnormal, compared to acute wounds. In acute wounds neutrophil infiltration is normally resolved within 72 hours; in chronic wounds neutrophils are present throughout, and there is sustained low grade inflammation (Diegelmann 2003). This is reminiscent of the inflammatory response observed in the *in vivo S.aureus* biofilm wound model, which was found to exhibit a sustained low grade inflammatory response (Gurjala et al. 2011). Similarly, there is an unusual cytokine and growth factor profile in chronic wounds. Analysis of a range of cytokines in diabetic foot ulcers found an increase in factors associated with keratinocyte migration and proliferation, as well as monocyte recruitment. In contrast there was a reduction in angiogenesis promoting factors (Galkowska et al. 2006). There is mounting evidence indicating that biofilm bacteria, and *S.aureus* in particular, within the wound are involved in sustaining the inflammation (Fazli et al. 2011). However, sustained inflammation, instead of removing the biofilm, results in damage to the host's own tissues, a feature commonly observed in chronic wounds (Menke et al. 2007). Neutrophils secrete proteases such as MMPs and neutrophil elastase, which degrade tissue;

neutrophil infiltration in chronic wounds is excessive and sustained, and MMPs are also expressed at persistently high levels (Tarnuzzer & Schultz 1996; Diegelmann 2003). Neutrophil activity results in a large production of ROS. Neutrophils recruit more neutrophils, resulting in sustained inflammation and consistently high levels of pro-inflammatory cytokines, such as TNF-α and IL-1β (Tarnuzzer & Schultz 1996). TNF-α can further stimulate the production of MMPs, altering the delicate balance between MMPs and TIMPs. Furthermore it has been shown that *S.aureus* can induce the expression of multiple MMPs in human dermal fibroblasts, as well producing proteases themselves (Kanangat et al. 2006; Vollmer et al. 1996). This imbalance shifts the wound towards a predominantly degrading environment, where ECM deposited by fibroblasts is destroyed at a more rapid rate than it is produced. As keratinocytes in the epidermis migrate over granulation tissue, this can prevent keratinocyte migration, and thus prevent re-epithelialisation and closure of the wound. As well as destroying bacteria, neutrophils and macrophages secrete chemokines and cytokines involved in angiogenesis (e.g. VEGF), and the proliferation of keratinocytes and fibroblasts (e.g. IL-8, IL-1β) (Taichman et al. 1997; Gillitzer & Goebeler 2001). The persistent presence of these leukocytes can therefore alter the balance of cytokines and thus the cellular function of the target cells (Zhao et al. 2013). Furthermore, excessive proteases can degrade important growth factors and cytokines, leading to reduced levels of basic fibroblasts growth factor (bFGF), EGF and PDGF, amongst others (Galkowska 2006), subsequently reducing the mitogenic activity of cells. Thus a delicate balance is needed in wounds to enable healing, and when persistent infection causes sustained inflammation, the wound environment is tipped towards a degrading phenotype.

1.4.3. Intracellular *S.aureus* in infections and wounds

1.4.3.1. *S.aureus* internalisation into host cells

For many years *S.aureus* was considered a purely extracellular pathogen. However, it is now well established that *S.aureus* can invade a variety of non-professional phagocytic cell types and persist for varying lengths of time *in vitro*. These cell types include endothelial cells, fibroblasts, keratinocytes and osteoblasts (Fraunholz & Sinha 2012). Intracellular survival has even been reported in professional phagocytes, such as macrophages and neutrophils

(Kubica et al. 2008; Gresham et al. 2000). Importantly, there is mounting evidence that this too occurs *in vivo*, where invasion by *S.aureus* is thought to be responsible for the persistent recurrent infection in several diseases, including rhinosinusitis, chronic osteomyelitis and chronic mastitis (Garzoni & Kelley 2009). Internalisation and intracellular persistence has been suggested to be a mechanism enabling *S.aureus* to evade the immune response and antibiotics, and thus contributing to persistent and repeated infection.

S.aureus are able to invade cells via an inactive process on their part, mediated by fibronectin and integrin α5β1 (Sinha et al. 1999; Dziewanowska et al. 1999). Integrin α5β1 is found in numerous cell types, including fibroblasts and keratinocytes, and is a component of focal adhesions, which form the attachment between cells and the ECM (Watson et al. 2009; Xu & Clark 1996; Collo & Pepper 1999). It binds to fibronectin, a major component of the wound blood clot. *S.aureus* express fibronectin-binding protein (FnBP) A and FnBP-B on their surface, which too bind to multiple fibronectin molecules. Fibronectin then acts as a bridge between the FnBPs on *S.aureus,* and integrin α5β1 on the host cell. The interaction between FnBPs and fibronectin leads to a sequestering of α5β1, resulting in a signal relay that causes actin rearrangement at focal adhesions, and eventually in endocytosis of the bacterium (Agerer et al. 2005; Schröder & Schröder 2006). Binding of FnBPs is sufficient to induce the uptake of *S.aureus* via zipper-type mechanism (Sinha et al. 2000), and so both heat killed and formalin fixed *S.aureus* are also taken up by host cells (Sinha et al. 1999; Kahl et al. 2000; Krut et al. 2003). An alternative FnBP-independent mechanism has been reported in primary human keratinocytes involving the *S.aureus* Eap protein, although the mechanism by which this occurs remains to be elucidated (Bur et al. 2013; Kintarak et al. 2004).

The fate of intracellular *S.aureus* and its host appears to be dependent on both the cell type and the particular *S.aureus* strain. The bacteria can persist within the cell, or induce cell death through apoptosis or necrosis pathways. Krut et al determined the intracellular fate of 23 different *S.aureus* strains when internalised into fibroblasts and keratinocytes, and found that the majority, 16, were killed within the cell, probably via the phagolysosomal pathway (Krut et al. 2003). Survival of the bacteria within non-professional phagocytes appears to

be dependent on the ability of the bacteria to escape from the phagosome into the cytoplasm or vacuoles (Krut et al. 2003; Klein et al. 2006). Prolonged persistence of *S.aureus*, of 2 weeks or more, has been reported in human epithelial cells, both *in vitro* and *in vivo* (Clement et al. 2005; Garzoni et al. 2007). *In vitro* it was shown that the persistent intracellular *S.aureus* changed their own gene expression, reducing metabolic activity and cell division as well as down-regulating the expression of several toxins (Garzoni et al. 2007); no morphological changes were observed in the host cell though, which remained viable. However, not all strains of *S.aureus* that escape phagolysosomal degradation will persist intracellularly. Most are toxic and will induce either apoptosis or necrosis of the host cell. The toxicity and mechanism of cell death is difficult to predict, but it is largely dependent on the particular *S.aureus* strain (Krut et al. 2003). It has been suggested that this is a result of the secretion of different virulence factors; it is also influenced by the type of host cell infected, as the sensitivity of a cell to a particular toxin can depend on its origin (Fraunholz & Sinha 2012). For example, apoptosis in human endothelial cells was dependent on both invasion and the expression of haemolysis toxins; non-haemolytic strains were unable to induce apoptosis but expression of α-haemolysin partially restored apoptosis induction (Haslinger-Löffler et al. 2005). Similarly, in human keratinocytes a correlation was found between the production of haemolysins and the toxicity of invading *S.aureus* strains, where more haemolytic strain caused cytotoxicity and less haemolytic strains induced apoptosis (Mempel et al. 2002). Evidence is also mounting that induction of apoptosis, but not necrosis, by *S.aureus* is dependent on internalisation of the bacteria (Mempel et al. 2002; Krut et al. 2003; Haslinger-Löffler et al. 2005; Kubica et al. 2008).

1.4.3.2. *S.aureus* internalisation in infection and wounds

It is now well established that *S.aureus* is internalised by a number of cell types *in vitro*, including fibroblasts, keratinocytes and endothelial cells, as well as professional phagocytes such as macrophages and neutrophils (Kubica et al. 2008; Gresham et al. 2000; Sinha et al. 1999; Kintarak et al. 2004). The evidence for a physiological role for intracellular *S.aureus* specifically in cutaneous wounds is very limited, but there is growing evidence of *in vivo*

intracellular *S.aureus* in other infections and diseases, where it is thought to be an important mechanism for *S.aureus* immune evasion and dissemination.

Internalised *S.aureus in vivo* have been identified in several diseases where recurrent infections are common. Intracellular reservoirs of *S.aureus* were identified in the nasal mucosa cells of people experiencing recurrent rhinosinusitis, caused by patient specific strains of *S.aureus* (Clement et al. 2005; Plouin-Gaudon et al. 2006). Similarly viable internalised *S.aureus* were found inside bovine macrophages and alveolar cells in milk produced by cows with chronic bovine mastitis (Hébert et al. 2000). Furthermore intracellular *S.aureus* have been identified in buccal and gingival epithelial cells in people suffering with periodontal disease (Colombo et al. 2013), and the invasion of airway epithelial cells by *S.aureus* has been linked to recurrent infection in cystic fibrosis (Jarry & Cheung 2006).

Experimental infections *in vivo* have also provided evidence purporting an important role for *S.aureus* invasion in the persistence and spread of infection. Chronic osteomyelitis is often hard to treat and recurrent, and *S.aureus* has been identified as the causative pathogen in over 80% of cases. *S.aureus* are able to invade osteoblasts both *in vitro* and *in vivo* (Reilly et al. 2000; Ellington et al. 1999), and it was found that the death of intracellularly infected osteoblasts released viable *S.aureus*, which were then able to infect other osteoblasts, suggesting a mechanism for reinfection (Ellington et al. 2003). Transplant of osteoblasts containing intracellular *S.aureus* into a bone fracture was then sufficient to cause bone infection in rats (Hamza et al. 2013). Additionally, internalised *S.aureus* have been associated with an *in vivo* model of biofilm related implant infection (Murillo et al. 2009). A tissue cage was inserted subcutaneously in a rat and infected with *S.aureus,* which formed a biofilm, mimicking chronic prosthetic infection. Collection of fluid from the tissue cage revealed that the majority of *S.aureus* present were intracellular, presumably within leukocytes (Murillo et al. 2009). Invasion of cells by *S.aureus* is predominantly through the binding of *S.aureus* to fibronectin by FnBPs. Fibronectin interacts with α5β1 integrin on the host cell and facilitates the pathogen's uptake (Sinha et al. 1999). It was found that the addition of recombinant fragments of FnBP prevented invasion of *S.aureus* into cells in

culture, and furthermore, significantly impaired the establishment of *S.aureus* infection in a guinea pig model of intramuscular wound infection (Menzies et al. 2002). The authors speculated that by blocking internalisation of *S.aureus* by host cells the bacteria might have been more easily killed by host defences, thus reducing the infection. Similarly, *S.aureus* mutants lacking the non-identical repeated FnBP binding domains were unable to invade mouse endothelial cells (Edwards et al. 2010). *S.aureus* with either full length FnBP or FnBP lacking the binding domains were injected intravenously into mice. Full length FnBP *S.aureus* caused significantly greater weight loss and mortality (60% versus 20%) in the mice. The authors concluded that invasion of host cells by *S.aureus* was necessary for *S.aureus* virulence and ability to cause sepsis. Of interest, it was also recently found that internalisation of *S.aureus* by human epithelial cells can affect proliferation of the host cell by delaying the G2/M phase transition, a phenomena which the authors suggested was used by *S.aureus* to aid their intracellular proliferation within the host (Alekseeva et al. 2013).

As well as invading non-phagocytic cells, *S.aureus* has been shown to invade and persist within professional phagocytes, such as macrophages, neutrophils and mast cells (Kubica et al. 2008; Gresham et al. 2000; Abel et al. 2011). This was described as “an infection reservoir” that contributed to reinfection and chronicity (Abel et al. 2011). *S.aureus* phagocytosed by monocytes were shown to survive intracellularly within the vacuole for 3-4 days. They then escaped into the cytoplasm and induced cell lysis, but prior to lysis the monocytes appeared healthy (Kubica et al. 2008). Koziel et al further showed that the infected macrophages had increased expression of anti-apoptotic genes (Koziel et al. 2009), and the authors suggested that this might be an additional mechanism by which *S.aureus* persist and spread infection. Similarly, reservoirs of *S.aureus* were found in the macrophages of infected zebra fish, and found to disseminate the pathogen (Prajsnar et al. 2012). Gresham et al found viable *S.aureus* inside vacuoles in polymorphonuclear neutrophils (PMNs) isolated from the site of an infection (Gresham et al. 2000). When transferred to another healthy mouse the infected neutrophils were sufficient to cause infection, as well as induce an influx of endogenous neutrophils. However, using transgenic mice with limited capacity for neutrophil migration (IAP-deficient mice), they found that limiting

neutrophil influx to the site of infection enhanced survival rates. They proposed that *S.aureus* invasion of neutrophils is a virulence mechanism which contributes to the infection (Gresham et al. 2000).

S.aureus is well established as a pathogen in many diseases. The physiological importance of its ability to invade host cells, both professional phagocytes and non-phagocytic cells, is becoming increasingly apparent, and research into this area is enhancing our understanding of the persistence and recurrence of *S.aureus* infections.

1.5. Connexins

1.5.1. Overview of connexins

Connexins are a groups of proteins found in almost all vertebrate tissues. They combine to form channels in the plasma membrane called connexons. These dock to connexons on adjacent cells, forming channels that allow the direct passage of small molecules between the cytoplasms of the connected cells, in a process called gap junction intercellular communication (GJIC). GJIC is vitally important for the coordination of individual cells within a tissue, and so gap junction activity is tightly regulated. However, connexins do not just exert their influence through gap junctions. Undocked hemichannels can also allow molecules to pass through, enabling intracellular to extracellular communication. This is particularly important in the stress response. Moreover, evidence is accumulating showing non-junctional roles for some connexins in several cellular processes, including cell migration, proliferation and apoptosis. These processes are all important during wound repair, and several connexins are expressed in skin. In particular connexin43 (Cx43), connexin26 (Cx26) and connexin30 (Cx30) are expressed, and their expression changes dynamically during healing. There is mounting evidence that they are involved in cutaneous healing and can influence the outcome of wound repair. Throughout this thesis, particular attention is therefore paid to these three connexins.

1.5.2. Connexin structure and function

1.5.2.1. Connexin structure

Connexins are comprised of four α helical transmembrane domains (figure 1.4.A-B). These are linked by two highly conserved extracellular loops, and a variable intracellular loop. They also have a variable C-terminus 'cytoplasmic tail' (Yeager et al. 1998). There are 20 connexins in mice and 21 in humans. Many of these show high sequence homology between murine and human orthologs, including Cx26, Cx30 and Cx43 (Willecke et al. 2002; Sohl & Willecke 2003). Cx26 and Cx30 have relatively short cytoplasmic 'tails', at 18 and 55 amino acids respectively. The tails of the highly homologous Cx26 and Cx30 are not thought to be subject to phosphorylation (Dahl et al. 1996). Cx43 on the other hand has a fairly long C-terminus, comprised of 155 amino acids, which can be phosphorylated at multiple sites (Evans & Martin 2002; Solan & Lampe 2009).

Six connexins combine to form a connexon which amass in the plasma membrane (figure 1.4.C). Connexons can be made of only one type of connexin (homomeric) or several (heteromeric), although not all connexins are compatible (Stauffer 1995; Sosinsky 1995; Jiang & Goodenough 1996; Diez et al. 1999). Each adjacent cell provides a connexon, and these dock to one another, creating a gap junction (figure 1.4.D). Gap junctions allow a direct connection between the cell's cytoplasms, enabling direct communication. Many gap junctions will accumulate together to form a gap junction plaque (figure 1.4.E). Like connexons, gap junctions can be homotypic (formed from hemichannels of the same connexin type), or heterotypic (formed from hemichannels of different connexins) (Werner et al. 1989; Swenson et al. 1989), though this is dependent on the compatibility of the connexins. For example Cx26 and Cx43 can't form functional gap junctions, while Cx26 and Cx30 can (Tomasetto et al. 1993; Elfgang et al. 1995; Yum et al. 2007). Alternatively, connexons can remain undocked, accumulating in non-junctional regions of the plasma membrane. These undocked connexons are referred to as hemichannels. They are receiving increasing attention as it is becoming evident that they are also able to act as transmembrane channels. Instead of enabling intercellular communication, they provide a route for intracellular-extracellular communication (Evans et al. 2006).

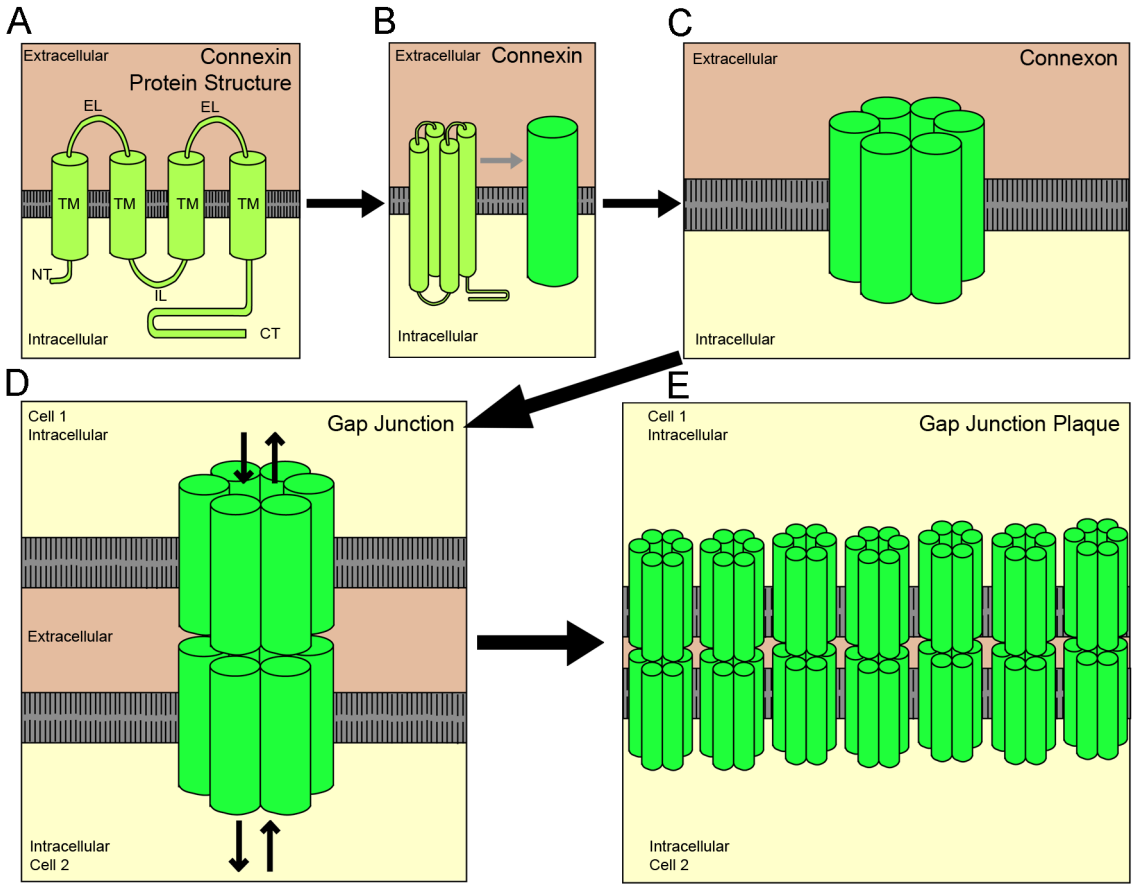

Figure 1.4. Diagrams of connexin and gap junction structure. (A) Diagram of the connexin protein structure, showing each structural region. **(B)** Representation of a single connexin, as the protein regions fold. **(C)** Six connexins combined to show an individual connexon or hemichannel. **(D)** Two connexons, one provided from cell 1 and one from cell 2, docked to form a gap junction channel between the two cells. **(D)** Many gap junctions come together to form a plaque between the two cells. (NT= amino terminal, CT= carboxyl terminal/cytoplasmic loop, TM= transmembrane domain, EL= extracellular loop, IL= intracellular loop) (the information used in the creation of these images was taken from the following references (Evans & Martin 2002; Hervé et al. 2012; Vinken et al. 2006)).

1.5.2.2. Connexin selectivity and permeability

Gap junctions enable the passive diffusion of metabolites smaller than 1.2 KDa across them, including Ca^{2+}, inositol triphosphate (IP_3), adenosine triphosphate (ATP) and cyclic adenosine monophosphate (cAMP) (Romanello & D'Andrea 2001; Kang et al. 2008; Cotrina et al. 2000; Isakson et al. 2001; Sáez et al. 1989; Niessen et al. 2000; Lawrence et al. 1978; Bevans et al. 1998; Kanaporis et al. 2008). Hemichannels are thought to allow the passage of similar molecules to gap junctions, though this remains to be extensively investigated (Trexler et al. 1996; Verselis et al. 2000; Li et al. 2001; Gomes et al. 2005; Kang et al. 2008; Romanello & D'Andrea 2001). They have been shown to mediate intercellular calcium signal propagation by releasing ATP, which activates purinergic receptors on nearby cells (Isakson et al. 2001; Kang et al. 2008). Classically gap junctions were thought to be non-selective, but interestingly, not all gap junctions have the same permeability to metabolites. Selectivity is based on both the size and charge of the molecules, and appears to be largely dependent on which connexins gap junctions are comprised of (Elfgang et al. 1995). However, the permeability of gap junctions can also be modified by a number of factors including transjunctional voltage (the voltage difference between coupled cells), calcium concentrations, pH and post translational modifications like phosphorylation (Turin & Warner 1977; Rose & Loewenstein 1975; Rook et al. 1988; Somogyi et al. 1989; Reynhout et al. 1992). Similarly, hemichannels are influenced by intracellular signals including intracellular pH, redox status and phosphorylation (Retamal et al. 2007; Bao et al. 2007; Liu et al. 2011). Many external stresses, such as mechanical and ischaemic stress, induce hemichannel opening, indicating a role in the stress response (Contreras et al. 2002; Cherian et al. 2005; Thompson et al. 2006; Batra et al. 2012; Gomes et al. 2005). Consequently the specificity of gap junctions and hemichannels is highly selective and their permeability can be rapidly modified. Likewise, their turnover is fast and tightly regulated; *in vivo* hepatic murine connexins have a half-life of 5 hours (Fallon & Goodenough 1981), while *in vitro* the half life of connexins, including Cx26 and Cx43, is reported to be 1-3 hours (Traub et al. 1989; Laird et al. 1991; Darrow et al. 1995). This enables rapid gap junction remodelling to suit physiological requirement.

1.5.2.3. Connexin roles and function

Connexons are found as part of multiprotein complexes located at the membrane, targeting proteins to particular regions in the membrane. A number of different connexins are able to bind cytoskeletal proteins, junctional proteins, scaffold proteins and receptors (see (Hervé et al. 2012) for a comprehensive list), though the precise functional role of many of these interactions has not yet been elucidated. However, it is known that these complexes anchor proteins that can modify connexins, such as protein kinases, enabling swift modification of gap junctions and facilitating a rapid response to physiological requirements (Hervé et al. 2012). Multiprotein complexes also enable connexins to indirectly influence other binding proteins via their interactions, such as cytoskeletal and signalling proteins. Furthermore, changes in Cx43 expression have been shown to result in significant gene transcription alterations in genes with diverse functions, and it has been suggested that Cx43 forms the centre of a protein 'nexus' that enables it to influence the expression of multiple genes (Iacobas et al. 2004). Consequently it is becoming increasingly clear that, in addition to their role in intercellular and intracellular-extracellular communication, connexins are involved in modulating cellular functions through non-junctional means. These functions include cell migration, differentiation, proliferation and apoptosis (Xu et al. 2006; Man et al. 2007; Wright et al. 2009; Mendoza-Naranjo, Cormie, A. Serrano, et al. 2012; Brissette et al. 1994; Churko et al. 2012; Zhang et al. 2001; Zhang et al. 2003; Djalilian et al. 2006; Huang et al. 2001; Klee et al. 2011).

Connexins are involved in determining cell morphology and polarity. They also affect the adhesions between cells, and can regulate the rearrangement of the cytoskeleton. Thus they have a function in cell motility and migration. This is complex though, and the role appears to be cell type specific (Matsuuchi & Naus 2013). For example, knockout of Cx43 expression causes cell migration defects in cardiac neural crest cells, as well as in neurons (Huang et al. 1998; Fushiki et al. 2003). Conversely, increased migration from Cx43 knockdown or attenuation of GJIC has been observed in epithelial cells and fibroblasts (Mori et al. 2006; Simpson et al. 2008; Wright et al. 2009; Mendoza-Naranjo, Cormie, A. Serrano, et al. 2012). Cx26 expression was found to inhibit migration in a gap junction independent manner in a breast tumour cell line (Kalra et al. 2006),

whereas overexpression in keratinocytes increased migration (Man et al. 2007). Cx30 over-expression in keratinocytes also increased migration (Man et al. 2007).

Connexins can propagate proliferative signals between adjacent cells through gap junctions and hemichannels in opposing membranes. They have been shown to interact either directly or indirectly with a number of important proliferation molecules, and can even influence their production or activity. Extensive research in cancer cells has shown connexins are involved in regulating the cell cycle, and addition of connexin genes to gap junction deficient tumour cells can restore normal growth (Vinken, Decrock, Leybaert, et al. 2012). Consequently, many members of the connexin family are considered to have tumour-suppressing roles, including Cx43 and Cx26. However, research in non-tumorigenic cells has shown some contrasting results. For example constitutive knockdown of Cx43 reduced proliferation in fibroblasts (Mendoza-Naranjo, Cormie, A. Serrano, et al. 2012), as did conditional knockout in astrocytes (Liebmann et al. 2013). Inducing expression of Cx26 has been associated with increased proliferation in keratinocytes (Lucke et al. 1999; Djalilian et al. 2006; Man et al. 2007). Cx30 expression in head and neck cancer cells, and in keratinocytes, also increased proliferation (Ozawa et al. 2009; Man et al. 2007), but knockout of Cx30 in mice also increased the number of BrdU positive cells in the hippocampus (Liebmann et al. 2013).

In addition to regulating proliferation through the cell cycle, connexins are involved in controlling apoptosis (Vinken et al. 2006). Just as with proliferation, apoptotic signals (calcium in particular) can be passed between cells through gap junctions and hemichannels, inducing a wave of apoptosis (Kameritsch et al. 2013; Decrock et al. 2009). Conversely, ‘rescue signals’ can also be passed from healthy cells to their afflicted neighbours (Blanc et al. 1998). Moreover, Cx43 is able to control the expression of a number of both pro- and anti-apoptotic genes (Vinken, Decrock, Vanhaecke, et al. 2012). This all suggests that connexins can influence apoptosis but the ultimate outcome depends on the balance of several interconnected factors.

Finally, connexins are thought to be important for the differentiation of cells, particularly in the epidermis of the skin. Several connexins are expressed in the epidermis, confined to particular layers (Di et al. 2001). Mutations in connexins, including Cx26 and Cx43, result in skin diseases associated with poor differentiation of keratinocytes (Lucke et al. 1999; Djalilian et al. 2006; Churko et al. 2012). However, the roles connexins play in epidermal differentiation are still poorly understood.

1.5.3. Connexins in skin

Connexins are expressed in almost all tissues in vertebrates, and are thought to play a vital role in maintaining tissue homeostasis through their role in gap junction intercellular communication. Some are expressed in numerous tissues, such as the near ubiquitous Cx43, but expression of others is confined to particular tissues, suggesting that they may have more specific roles within these tissues. Ten different connexins with overlapping distributions are expressed in the human epidermis, and 8 in the mouse epidermis (see table 1.1) (Di et al. 2001; Risek et al. 1992; Goliger & Paul 1994; Kretz et al. 2003). A number of diseases have been attributed to mutations in connexins, and most of these cause skin abnormalities (Kelsell et al. 2001; Laird 2014). Briefly, a specific mutation in Cx26 causes Vohwinkel syndrome, a disorder characterised by hyperkeratosis (thickening of the stratum corneum) at regions of flexion with diffuse palmoplantar keratoderma (hyperkeratosis specifically on the palms and soles) (Maestrini et al. 1999; Kelsell et al. 2000). Several Cx26 mutations also cause palmoplantar keratoderma, (Richard, White, et al. 1998; Kelsell et al. 2000), as do mutations in Cx31 (Kelsell et al. 2000). Other Cx31 mutations cause erythrokeratodermia variablis (EKV), another skin disease that is characterised by hyperkeratosis amongst other features (Richard, Smith, et al. 1998; Wilgoss et al. 1999; Gottfried et al. 2002). Mutations in Cx30 cause hidrotic ectodermal dysplasia, which similarly exhibits palmoplantar hyperkeratosis (Lamartine et al. 2000). Interestingly, although Cx43 is the most ubiquitously expressed connexin only one diseases has been attributed to mutations in the Cx43 gene (GJB1), Oculodentodigital dysplasia (ODDD) (Paznekas et al. 2003). ODDD is not primarily a skin disease, but some patients do develop palmoplantar hyperkeratosis. These mutations highlight the importance of these connexins for the normal function and structure of skin.

The connexins in the epidermis have specific distributions. The distribution differs somewhat between humans and mice, and the murine distribution has been focused on here. In intact adult skin Cx43 is normally expressed at moderate levels in the lower spinous and basal layers of the epidermis. Cx26 and Cx30 are both expressed at very low levels within the granular layer with a highly overlapping distribution (Goliger & Paul 1994; Coutinho et al. 2003; Risek et al. 1992; Kretz et al. 2003). Cx43 is also expressed throughout the dermis, in hair follicles, fibroblasts, sebaceous glands and endothelial cells (Liu et al. 1997; Risek et al. 1992; Little et al. 1995).

Table 1.1. Connexin expression in skin and the related diseases. The connexins expressed in the epidermis of humans and mice are listed. The human skin diseases related to mutations in each connexin gene are also shown. Information reviewed in (Kelsell et al. 2001) and (Richard 2000).

Human	Mouse	Mutations linked to human skin diseases
Cx26	Cx26	Vohwinkel syndrome Palmoplantar hyperkeratosis
Cx30	Cx30	Hidrotic ectodermal dysplasia
Cx30.3	Cx30.3	Erythrokeratodermia variablis
Cx31	Cx31	Erythrokeratodermia variablis
Cx31.1	Cx31.1	
Cx32		
Cx37	Cx37	
Cx40	Cx40	
Cx43	Cx43	Oculodentodigital dysplasia
Cx45		

1.6. Connexins in wound healing

Upon wounding of skin, connexin expression changes dynamically throughout the healing process (Goliger & Paul 1995). The changes in three connexins, Cx26, Cx30 and Cx43, are focused on here (figure 1.5).

1.6.1. Connexin 43 in wound healing

Experiments using incisional wounds in 10 day old rat tail, and in neonatal mice showed that Cx43 became down-regulated within 6 hours in the epidermal wound edge and for some distance from the wound (Figure 1.5.A), remaining low peripherally until returning to normal expression levels following complete

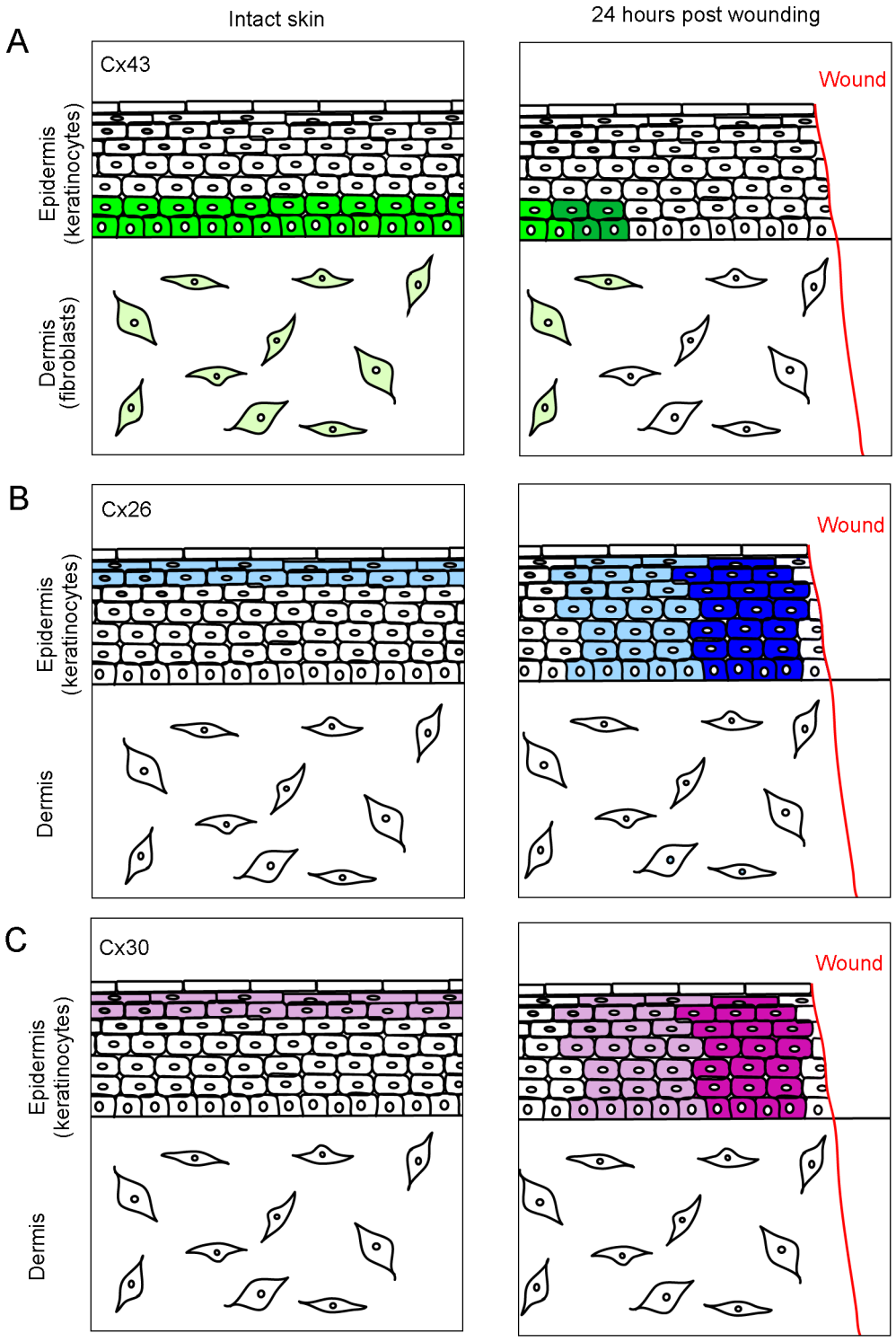

Figure 1.5. Connexin43, Connexin26 and Connexin30 expression in skin and during wound healing. Connexin expression is shown in intact epidermis and dermis (left), and 24 hours after wounding (right). Darker colours indicate higher expression levels (the information used in the creation of these images was taken from the following references (Goliger & Paul 1995; Coutinho et al. 2003; Mendoza-Naranjo, Cormie, A. E. Serrano, et al. 2012; Mendoza-Naranjo, Cormie, A. Serrano, et al. 2012)).

re-epithelialisation (Goliger & Paul 1995; Coutinho et al. 2003). Once re-epithelialisation was complete, though, Cx43 increased in the hyperproliferative epidermis at the wound site (Goliger & Paul 1995; Coutinho et al. 2003). An additional study in 8 week old ICR mice found that, while most of the connexin distribution was the same as in the neonatal rodents, instead of decreasing expression peripherally from the wound edge, in adult mice Cx43 was elevated at 6 hours in hyperproliferative epidermis behind the wound edge (Mori et al. 2006). It is known that connexin expression in the skin changes through development, and that expression and distribution of some connexins differ between neonatal and adult rodents (Goliger & Paul 1994); this is likely the reason for the differences observed. Cx43 is also expressed in the dermis, and was down-regulated both in human and mouse dermis near the wound edge within 4 hours of wounding (Mendoza-Naranjo, Cormie, A. Serrano, et al. 2012). In contrast Cx43 was up-regulated in the endothelial cells of the vasculature around the wound edge in mice within 6 hours of injury, and expression remained elevated during healing (Coutinho et al. 2003).

In vivo observations of connexin dynamics during healing have led to the assertion that Cx43 needs to be down-regulated in the cells at the wound edge in order for their migration to occur (Qiu et al. 2003; Kretz et al. 2003; Mori et al. 2006). This is supported by observations of the levels of connexin expression in a variety of human chronic wounds, which exhibit severely delayed healing. Brandner et al observed that Cx43 down-regulation at the wound edge did not occur in a mixed selection of chronic wound biopsies, and that expression was retained at the epidermal wound edge (Brandner et al. 2004). Another study found Cx43 expression was actually elevated throughout the dermis of venous leg ulcer biopsies compared to patient matched unwounded tissue, and there was a failure to reduce expression at the wound edge in these non-healing wounds (Mendoza-Naranjo, Cormie, A. Serrano, et al. 2012). Examination of Cx43 specifically in diabetic foot ulcers, venous leg ulcers and pressure ulcers found a significant increase in expression up to 4 mm from the wound edge in both the epidermis and dermis ((Mendoza-Naranjo, Cormie, A. E. Serrano, et al. 2012), Sutcliffe et al, data from the Becker group, manuscript submitted). The abnormal expression and dynamics seen in chronic wounds are proposed to contribute to the wound healing delay, and this is corroborated by a number of

experiments where Cx43 expression in wounds has been purposely down-regulated.

Cx43 knockout mice die at birth due to heart defects (Reaume et al. 1995), but inducible knockout of Cx43 in mice was used to assess cutaneous healing in the absence of Cx43 (Kretz et al. 2003). Healing rates were enhanced in the Cx43 knockout mice, with wounds typically closing a day earlier than in littermate controls. Similarly, healing was sped up in mice where Cx43 expression was targeted by application of Cx43 antisense oligodeoxynucleotides (Cx43 asODNs) (Qiu et al. 2003; Coutinho et al. 2005; Mori et al. 2006). Transient knockdown of Cx43 increased the re-epithelialisation rate, alongside increasing the proliferation of keratinocytes in the migrating epithelial tongue (Mori et al. 2006). Cx43 knockdown also resulted in many factors that suggested more rapid granulation tissue formation and maturation: an increase in fibroblasts at the wound edge at day 2; earlier blood vessel formation; increased collagen type I and hydroxyproline; earlier presence and resolution of myofibroblasts, and a reduction in the amount of granulation tissue present at days 7 and 12 after wounding (Qiu et al. 2003; Mori et al. 2006). Furthermore, Cx43 asODN also improved healing in diabetic rats (Wang et al. 2007). Induction of diabetes with streptozotocin (STZ) resulted in a thickened bulb of non-migratory keratinocytes reminiscent of chronic wounds, with an abnormally increased Cx43 expression at the wound edge, and delayed re-epithelialisation compared to controls rats. Preventing the abnormal increase in Cx43 expression, by applying Cx43 antisense, rescued re-epithelialisation, and even enhanced it compared to untreated controls (Wang et al. 2007).

In order to investigate the mechanism of improved healing *in vitro* Cx43 expression was knocked down in NIH3T3 fibroblasts, both transiently with Cx43 asODN and permanently with Cx43 shRNA. A reduction in Cx43 expression increased the rate of migration, as well as polarisation of the Golgi body towards the wound edge. This was lost when wild type Cx43 was overexpressed in the cells. Cx43 knockdown also decreased cell-adhesion and, interestingly, proliferation (Mendoza-Naranjo, Cormie, A. Serrano, et al. 2012; Mori et al. 2006). This indicated a positive correlation between Cx43 expression and cell proliferation in skin. This correlation was similarly observed in

keratinocytes during wound healing in mice, where Cx43 expressing cells were found to be also Ki67 positive (Coutinho et al. 2003).

Similar results to those found using Cx43 asODN *in vivo* were described when murine and porcine wounds were treated with ACT1 (Ghatnekar et al. 2009). ACT1 consists of the terminal 9 peptides of the Cx43 cytoplasmic tail, which are linked to the internalisation protein, antennapedia. In cell culture, ACT1 was found to interact with Cx43 binding partners (particularly Zonular Occludin 1 (ZO1)), thus competing with the endogenous cytoplasmic Cx43. Its use in cells resulted in larger Cx43 gap junction plaques; the enlarged plaques were a result of an increased accumulation of gap junctions from non-junctional pools of Cx43, not of changes in the protein expression or turnover (Hunter et al. 2005). When ACT1 was applied directly to the wounds of mice and pigs, the authors too reported improved wound closure rates, reduced inflammation, less granulation tissue, and faster maturation of the healed skin. However, as overall Cx43 expression was not altered by ACT1 the authors suggest that the beneficial effects of ACT1 is likely through a separate mode of action to Cx43 asODN.

In addition to the ACT1 peptide, healing rates have also been investigated after treatment with mimetic Cx43 peptides, particularly Gap27 (Kandyba et al. 2008; Wright et al. 2009; Pollok et al. 2011). This peptide binds to one of the highly conserved extracellular loops of connexins. Instead of preventing binding to cytoplasmic proteins, it prevents two connexons docking, ostensibly inhibiting gap junction formation and therefore communication, without altering Cx43 expression or inhibiting protein interactions. There is also growing evidence that Gap27 can inhibit hemichannel function. Experiments have shown that Gap27 increases cell migration rates in mouse epidermal keratinocytes (Kandyba et al. 2008), human keratinocytes and dermal fibroblasts (Wright et al. 2009). They also increased migration in human organotypic skin models and an *ex vivo* porcine skin model (Pollok et al. 2011). Interestingly, Gap27 also increased proliferation of both adult human primary keratinocytes and fibroblasts at the leading edge of scratch wounds, and increased the number of ki67 positive keratinocytes in the migrating epithelial tongue in the *ex vivo* porcine wound model (Pollok et al. 2011). This is in opposition to findings where Cx43

expression was reduced in fibroblasts; loss of expression resulted in reduced proliferation (Mendoza-Naranjo, Cormie, A. Serrano, et al. 2012). The authors suggest that the differences observed may reflect a non-junctional role for Cx43 protein in proliferation.

In contrast with other data described above, an increase in Cx43 expression was reported to enhance granulation tissue formation in rat skin (Moyer et al. 2002), as assessed by an increase in blood vessel formation and decrease in cellular density. However, Cx43 expression was increased by application of lithium chloride (LiCl). LiCl is non-specific; it enhances Cx43 expression through activation of canonical Wnt signalling. Wnt signalling also activates the expression of numerous other genes through β-catenin, which has also been shown to mediate wound healing (Cheon et al. 2006), making the specific role of Cx43 in this experiment difficult to determine.

More recent studies have also investigated the functional consequences of two Cx43 mutations related to Oculodentodigital dysplasia (ODDD), a human disease discovered in 2003 to be caused by Cx43 mutations, and which can cause skin abnormalities (Churko et al. 2012; Churko et al. 2011; Paznekas et al. 2003). Primary fibroblasts from one ODDD patient with a missense D3N mutation were able to form gap junction plaques, while fibroblasts from another patient carrying a V216L mutation were not. However, gap junction intercellular communication was reduced by both mutations. The fibroblasts from both patients migrated and proliferated slower than fibroblasts derived from closely related but healthy donors, showing the importance of normal Cx43 expression (Churko et al. 2011). Additionally, a mouse with a Cx43 missense mutation in the first extracellular loop (G60S) also showed delayed healing of cutaneous injury, apparently due to reduced contraction of the wounds (Churko et al. 2011). Investigations into this revealed an inability for the patient derived fibroblasts to differentiate into myofibroblasts in response to stimulation with TGF-β1 (Churko et al. 2011). The authors also report abnormal Cx43 dynamics in the healing epidermis of the G60S mutant mice; they report higher expression at the wound edge in G60S mice compared to controls at 24 hours, a characteristic also seen in STZ diabetic rats (Wang et al. 2007). Interestingly, primary keratinocytes derived from these mice were found to proliferate faster but migrated and

differentiated normally (Churko et al. 2012). Unfortunately, the authors did not comment on whether a thickened bulb of keratinocytes also developed at the wound edge in the mice, as is seen in diabetic mice and in human chronic wounds where Cx43 is also elevated at the wound edge (Wang et al. 2007; Herrick et al. 1992; Brandner et al. 2004; Mendoza-Naranjo, Cormie, A. E. Serrano, et al. 2012).

These experiments demonstrate the important role Cx43 plays in the wound healing process, in both the dermis and epidermis. Nevertheless the role Cx43 plays in wound healing is complex, and is still poorly understood. Moreover, Cx43 is not the only connexin expressed in the skin, or to dynamically change expression during the healing process. Two other connexins, Cx26 and Cx30, are also thought to be involved in wound healing.

1.6.2. Connexin 26 and Connexin 30 in wound healing

Like Cx43, in both rat tail and mouse back epidermis Cx26 and Cx30 were down-regulated at the wound edge within 6 hours of wounding. However, they both became highly up-regulated directly behind the wound edge through several epidermal layers and for up to 500 μm from the wound (figure 1.5.B-C). Following wound closure expression levels remained high in the hyperproliferative epidermis during differentiation, but returned to normal following completion of full barrier restoration (Coutinho et al. 2003; Goliger & Paul 1995).

Both Cx26 and Cx30 have been implicated in the pathology of chronic wounds, which are characterised by hyperproliferative epidermis peripheral to the wound and by a bulb of non-migratory keratinocytes at the wound edge (Herrick et al. 1992). Brander et al reported that Cx26 and Cx30 were both expressed at the wound edge of a mixed selection of chronic wounds, and for some distance peripherally, whereas in healing wounds both were down-regulated at the wound edge (Brandner et al. 2004). Additionally Cx26 and Cx30 were found to be significantly up-regulated at the wound edge and up to 4 mm peripherally in both diabetic foot ulcers and venous leg ulcers, and to a lesser extent in pressure ulcers (Sutcliffe et al, manuscript submitted). These finding suggest that high expression at the wound edge may be detrimental to healing. This is

supported by experiments where Cx26 was overexpressed ectopically in the epidermis of transgenic mice and impaired healing (Djalilian et al. 2006). Homozygous mutations were lethal due to impaired skin barrier function, but a heterozygous mutation resulted in a hyper-thickened epidermis, though differentiation of the epidermis was normal. However, these mice exhibited very poor wound healing compared to wild type littermates, and interestingly this was alongside an increased inflammatory response. Cx26 expression also remained elevated at the wound edge in the transgenic mice following injury, and maintained keratinocytes in a hyperproliferative state even after re-epithelialisation was complete. The re-epithelialising epidermis also displayed hyperkeratosis, parakeratosis, hypogranulosis and acanthosis, and the authors proposed that Cx26 down-regulation is necessary for the return of full skin barrier function (Djalilian et al. 2006). Alternatively, Cx30 deletion in mice was not observed to cause any abnormalities in skin, and wounding experiments conducted on the tail revealed no improvement or delay in healing compared to wild type litter mates (Teubner et al. 2003; Kretz et al. 2003). The effect of overexpressing wild type Cx30 on skin formation and wound healing remains to be determined.

Cx26 and Cx30 are normally expressed at very low levels, but are highly expressed in regions of hyperproliferative epidermis during healing in rodents (Goliger & Paul 1995; Coutinho et al. 2003). Interestingly, high levels of Cx26 and Cx30 are also found in hyperproliferative epidermis such as viral warts, psoriasis and porokeratosis (Hivnor et al. 2004; Lemaître et al. 2006; Lucke et al. 1999; Labarthe et al. 1998). Thus, both Cx26 and Cx30 have been suggested to be markers of hyper-thickened epidermis. Furthermore, many of the hyperproliferative skin diseases where Cx26 and Cx30 expression are increased are also associated with abnormalities in differentiation, prompting authors to suggest they may be involved in abnormal differentiation, or at least reliable markers (Labarthe et al. 1998; Lucke et al. 1999). Like other differentiation markers connexins are expressed in specific layers of epidermis, and induction of differentiation of keratinocytes *in vitro* with calcium resulted in changes in the connexins expressed (Brissette et al. 1994). Additionally, treatment of human epidermis with retinoic acid, known to significantly modify keratinocyte differentiation, also modified connexin expression, particularly

increasing expression of Cx26 (Masgrau-Peya et al. 1997). Cx26 and Cx30 mutations have also been linked to hyperproliferative and poorly differentiated epidermis through connexin related diseases, where patients frequently present with hyperkeratosis and parakeratosis (Richard, White, et al. 1998; Lamartine et al. 2000; Kelsell et al. 2000). Expression of one Cx26 human mutation (R143W) that appears to prevents Cx26 trafficking, in keratinocytes *in vitro* resulted in hyper-thickened organotypic cultures in comparison to wild type Cx26. Surprisingly though, this was not in conjunction with abnormal differentiation (Man et al. 2007). Expression of another, encoding a stop mutation (35delG) that effectively knocks out Cx26, instead reduced the thickness of keratinocyte organotypic cultures. However, a Cx30 mutation that causes hidrotic ectodermal dysplasia, G11R, caused no apparent differences (Wiszniewski et al. 2001). Alternatively, expression of a different hidrotic ectodermal dysplasia Cx30 mutation (A88V) driven by the endogenous promoter caused mild hyperkeratosis in transgenic mice (Bosen et al. 2014), though its effect on differentiation and wound healing remains to be tested. A further loss of function Cx26 dominant mutation was expressed in a rat epidermal keratinocyte line, alongside overexpression of wild type Cx26 (Thomas et al. 2007). Surprisingly, neither caused a difference in epidermal thickness or differentiation of the keratinocytes. Moreover, neither altered proliferation or migration of the cells. Oppositely, over-expression of wild type Cx26 in a human keratinocyte cell line (nTERT) resulted in significantly increased proliferation in organotypic cultures (Man et al. 2007). It also increased migration rates compared to vector only controls. Similarly, overexpression of Cx30 in nTERT keratinocytes caused a significant increase in proliferation and migration. Enhanced cell proliferation was also observed in head and neck squamous cancer cells where full length and partial length Cx30 was over-expressed (Ozawa et al. 2009). Nevertheless, *in vivo* observations do not support a direct association between proliferation and either connexin. While Goliger et al observed Cx26 in hyperproliferative epidermis during healing, they noted that it was present predominantly in the differentiated layers rather than in the proliferative layers (Goliger & Paul 1995). Double labelling for Cx26 and Ki67, a marker for proliferation, in human hyperproliferative psoriatic lesional epidermis similarly showed most Cx26 expressing cells did not express Ki67 (Lucke et al. 1999). Additionally a negative correlation between the connexins Cx26 and Cx30, and Ki67 was

reported during wound healing in the mouse epidermis (Coutinho et al. 2003). These conflicting results means that while it is clear Cx26 and Cx30 are involved in the wound healing process, the roles they play in proliferation, differentiation and migration are elusive, and their ultimate importance is still highly contentious.

1.6.3. Connexins in inflammation during wound healing

Upon wounding, an inflammatory cascade is initiated that results in the release of a plethora of pro-inflammatory cytokines and the recruitment of leukocytes. Bacteria or other contaminants, which are recognised by the innate immune system, also induce an inflammatory response. Cytokines and inflammatory stimuli are able to modulate connexin expression and gap junction communication in both local cells and recruited immune cells. Both TNF-α and IL-1α decreased GJIC in endothelial cells, with TNF-α also decreasing the expression of Cx40 and Cx37 (Hu & Xie 1994; van Rijen et al. 1998). Alternatively, *Staphylococcus epidermidis* peptidoglycan, a cell wall component, induced Cx43 expression in endothelial cells, alongside increasing GJIC (Robertson et al. 2010). Similarly *Staphylococcus aureus* peptidoglycan induced Cx43 expression and GJIC in microglia (Garg et al. 2005). Bacterial lipopolysaccharide (LPS), another cell wall component recognised by the innate immune system, also increased Cx43 expression, but in kidney cells (Fernandez-Cobo et al. 1998). Cx43 is not expressed by circulating neutrophils or macrophages, but expression and GJIC was induced when activated by a number of growth factors and pro-inflammatory cytokines, such as TNF-α and IFN-γ (Eugenin et al. 2003; Jara et al. 1995; Hu & Xie 1994; Zahler et al. 2002). Activated leukocytes also form functional gap junctions with endothelial cells (Zahler & Hoffmann 2003; Eugenin et al. 2003; Oviedo-Orta et al. 2002).

In reverse, manipulation of connexin expression during wounding has been shown to alter inflammation (Qiu et al. 2003; Coutinho et al. 2003; Mori et al. 2006; Ghatnekar et al. 2009; Djalilian et al. 2006). Reduced neutrophil recruitment was observed in pig wounds when they were treated with Cx43 ACT1 peptide (Ghatnekar et al. 2009). Similarly, transient knockdown of Cx43 expression in mice with antisense immediately following wounding was found to result in reduced neutrophil and macrophage recruitment (Qiu et al. 2003;

Coutinho et al. 2005; Mori et al. 2006). It also modulated the expression of TGF-β1 (Mori et al. 2006), a cytokine involved in the recruitment of leukocytes and fibroblasts (Beanes et al. 2004). Loss of Cx43 was also found to increase neutrophil transendothelial migration, whereas blocking gap junction function prevented monocyte transendothelial migration (Zahler & Hoffmann 2003; Eugenin et al. 2003), suggesting an important role for Cx43 GJIC in controlling leukocytes extravasation, which may in part explain the reduced leukocyte recruitment in Cx43 antisense and ACT1 peptide treated wounds.

However, Cx43 is not the only connexin involved in inflammation. When transgenic mice that ectopically overexpressed Cx26 in the epidermis were wounded there was a heightened inflammatory response, with excessive infiltration of neutrophils and lymphocytes (Djalilian et al. 2006). Interestingly, KID syndrome is caused by mutations in Cx26, and is often associated with inflammation. Challenging HeLa cells transfected with Cx26 KID mutations with inflammatory stimuli resulted in an increase in hemichannel opening (Donnelly et al. 2012), a phenomena which is often also associated with inflammation (Eugenin 2014).

1.7. Connexins in oral mucosa and privileged healing

Connexin expression has been shown to be dynamically regulated in cutaneous wound healing, and manipulation of connexin expression and GJIC has shown that this is an important part of the healing mechanism (Churko & Laird 2013). Oral mucosa exhibit privileged healing status, healing more rapidly and with reduced scar formation (Enoch & Stephens 2009). However, little is known about connexin expression and dynamics during wound healing in oral mucosa. The little that is known is discussed here.

Cx43 is the most studied connexin in oral mucosa. It was found to be expressed weakly in the basal layers of parakeratinised rat tongue, expressed more strongly in the stratum spinosum and granulosum, but absent from the stratum corneum (Xia et al. 2009). A similar distribution was also observed in keratinised rat gingiva, but in the rat gingiva expression of Cx43 was absent from stratum granulosum (Muramatsu et al. 2008). However, in human gingiva

Cx43 was found only in the stratum spinosum (Hatakeyama et al. 2006). Mouse gingival keratinocytes were found to express Cx26, Cx30.3, Cx31, Cx32 mRNA in addition to Cx43 mRNA (Hatakeyama et al. 2011). In non-keratinised mouse labial mucosa Cx43 was simply described as being expressed suprabasally (Riau et al. 2008). However, in human non-keratinised buccal mucosa it was expressed weakly in the stratum basale and strongly in the intermediate layer, but not in the most superficial layer. A similar distribution was also described for Cx26 in human buccal mucosa and tongue (Lucke et al. 1999; Ozawa et al. 2007). However, in parakeratinised rat gingiva Cx26 was found to be expressed only in the stratum granulosum and upper part of the stratum spinosum (Muramatsu et al. 2008). In human tongue, Cx30 was reported to be expressed only in the stratum spinosum (Ozawa et al. 2007). There are considerable differences between these finding, suggesting that the distribution of Cx26, Cx30 and Cx43 is both species and location dependent in the oral mucosa.

Only one study has investigated connexin expression and dynamics within oral mucosa during wound healing. They observed hamster tongue, a parakeratinised epithelium, following an excisional wound (Saitoh et al. 1997). Immunofluorescence revealed Cx43 expression in the stratum basale and lower stratum spinosum of intact tongue, and Cx26 expression in the upper stratum spinosum and throughout the stratum granulosum. Upon wounding, expression of both connexins decreased within 6 hours at the wound edge, and remained low at 24 hours. However, where the connexins were expressed in the epithelium near the wound edge, they were expressed throughout the stratum basale to the stratum granulosum, with considerable overlap. Additionally, despite a reduction in immunofluorescence at the wound edge, *in situ* hybridisation showed that connexin mRNA levels remained constant at the wound edges, suggesting post-transcriptional regulation. Expression remained high for several days, but began to return to normal after epithelialisation was complete. Cx43 dynamics in the hamster tongue epithelium mimicked those normally seen in rat and mouse skin. Interestingly though, Cx26 dynamics differed from those typically seen in skin, where Cx26 becomes up-regulated behind the wound edge following injury (Coutinho et al. 2003; Goliger & Paul 1995).

1.8. Connexins and *S.aureus*

Infection with bacteria results in an inflammatory response, both from cells in the vicinity, and from leukocytes that are subsequently recruited. A number of pro-inflammatory cytokines are able to influence connexin expression and function in these cells, and it's becoming clear that connexins play an important role in inflammation (see review by (Eugenin 2014)). However, evidence is also starting to emerge showing that a variety of bacterial species can influence hemichannel activity, gap junction intercellular communication and the expression of connexins. There are also reports that several pathogens use their influence on connexins to alter inflammation, their virulence and even their invasion into cells (see review by (Ceelen et al. 2011)). The influence of the pathogen *S.aureus* on connexins will primarily be focused on here, although research into the relationship between *S.aureus* and connexins is still in its infancy.

Peptidoglycan (PGN) is a component of all bacterial cell walls, though it is much more abundant in Gram positive than Gram negative species (Fournier & Philpott 2005). Due to the propensity for *Staphylococcal* infections in skin, the effect of PGN on endothelial cells and keratinocytes was investigated (Donnelly et al. 2012; Robertson et al. 2010). PGN (10 μg ml^{-1}) derived from *S.aureus* was found to increase the expression of Cx43 mRNA after 6 hours in human endothelial cells (HECs) (Donnelly et al. 2012). Similarly, at 6 hours PGN derived from the highly related *Staphylococcus* species *S.epidermidis*, also increased Cx43 mRNA and protein expression in HECs, alongside an increase in Cx43 phosphorylation (Robertson et al. 2010). Increased Cx43 expression following challenge with *S.epidermidis* PGN was concomitant with an increase in gap junction intercellular communication (GJIC), as assessed by microinjection of Lucifer yellow. However, *S.aureus* PGN was unable to stimulate Cx43 mRNA expression in the human keratinocyte HaCaT cell line, but instead increased Cx26 mRNA expression (Donnelly et al. 2012). In addition to affecting connexin expression levels, PGN was also found to alter hemichannel activity. When HaCaT cells overexpressing Cx26 were incubated with *S.aureus* derived PGN for 15 minutes they opened their hemichannels, as determined by a 2 fold increase in ATP release, which could be blocked by the gap junction blocker carbenoxolone (CBX) (Donnelly et al. 2012). PGN derived

from *S.epidermidis*, though, could not elicit this response in the keratinocyte HaCaT cells, but it was found to cause hemichannel opening in HeLa cells (HeLa cells are connexin deficient) transfected with Cx26, as assessed by the same parameters (Donnelly et al. 2012). Furthermore, *S.epidermidis* PGN also caused activation of hemichannels in HeLa cells transfected with Cx43 (Robertson et al. 2010). Interestingly, when the HaCaT cells were transfected with a mutant Cx26, *S.aureus* PGN increased ATP release 3-4 fold, a significant increase in the hemichannel activity seen when overexpressing wild type Cx26 (Donnelly et al. 2012). The Cx26 mutant was from a Keratitis ichthyosis deafness (KID) syndrome mutation, a skin disease where patients are prone to inflammation and infection, particularly with Gram-positive bacteria. The same response wasn't seen in Cx26 mutants derived from other Cx26 related diseases which are not related to increased skin infection (Vohwinkel syndrome and other palmoplantar keratoderma mutants), suggesting that Cx26 hemichannel activity might be involved in the excessive inflammatory response seen in KID patients. A role for Cx43 hemichannels in inflammation has also been reported. PGN is recognised by host cells and elicits the release of several pro-inflammatory cytokines. Challenging HaCaT and HEC cells with *S.aureus* PGN for 24 hours resulted in the concentration dependent production of IL-6 (Donnelly et al. 2012). PGN from *S.epidermidis* also caused HECs, but not HaCaT cells to release IL-6 (Donnelly et al. 2012; Robertson et al. 2010). Interestingly, blocking hemichannel activity with CBX in HEC cells prevented the increase in IL-6 release caused by *S.epidermidis* PGN, suggesting Cx43 hemichannels might be involved in the initial inflammatory response (Robertson et al. 2010). At this point it is not known whether the same response will be elicited when challenged with *S.aureus* PGN. Although *S.aureus* and *S.epidermidis* are highly related, it is clear that PGN derived from these two *Staphylococci* differ in their effects on cells. Moreover, the effect of *S.aureus* PGN on connexins is not universal, but dependent on the cell type.

The effect of *S.aureus* PGN has also been investigated in neuronal cells, as *S.aureus* infection is commonly involved in brain abscesses (Garg et al. 2005; Esen et al. 2007; Karpuk et al. 2011). Looking at mouse primary astrocytes, and again using a concentration of 10 μg ml^{-1}, it was found that incubation with *S.aureus* derived PGN for 6 or 24 hours significantly attenuated Cx43 mRNA

and protein expression (Esen et al. 2007). Incubation with 10^7 colony forming units (CFU) of intact but heat killed *S.aureus* (HKSA) similarly reduced Cx43 expression. The group also investigated the effect of PGN and HKSA on Cx30 and Cx26 expression. Cx30 expression was attenuated similarly to Cx43, but in contrast, Cx26 mRNA and protein expression was induced by the stimulation. By blocking protein production with cyclohexamide (CHX) they investigated whether the reduction in Cx43 and Cx30 expression was a direct result of interaction with the HKSA or PGN, or whether it was in response to inflammatory cytokines produced by the stimulated cells. CHX inhibits protein synthesis so prevents astrocytes from producing pro-inflammatory cytokines after stimulation with HKSA or PGN. Incubation with CHX did not prevent the reduction in Cx30 and Cx43 expression caused by stimulation with PGN or HKSA, suggesting that interaction with the bacteria, and not stimulation of pro-inflammatory cytokines, was responsible for the change in connexin expression (Esen et al. 2007). The consequence of *S.aureus* infection on astrocytes was also investigated *in vivo* (Karpuk et al. 2011). Mice with GFP astrocytes were given an intracerebral inoculation of live *S.aureus*, and their brain slices examined after 3 or 7 days. In contrast, it was found that immunofluorescence of Cx43 and Cx30 at 3 and 7 days respectively increased in cells for a large region around the *S.aureus* brain abscess. The authors did not directly address the discrepancies between the *in vitro* and *in vivo* findings, but did state that the *in vivo* brain slices were comprised of multiple cell types, including neurons and microglia (Karpuk et al. 2011). Microglia are mononuclear phagocytes of the central nervous system, and observations of primary mouse microglia in culture showed that incubation with 10 μg ml^{-1} of *S.aureus* derived PGN increased Cx43 mRNA and protein expression (Garg et al. 2005), which may have contributed to the increase in Cx43 seen in the brain slices. Microglia in cell culture do not form functional gap junctions, but after 48 hours incubation with PGN there was a small but significant increase in microglia GJIC. In contrast, cultured astrocytes are usually gap junction coupled, and Lucifer yellow dye injection showed that HKSA and PGN significantly reduced GJIC (Esen et al. 2007). Similarly, whole patch clamp recording of astrocytes surrounding the *S.aureus* brain abscesses revealed that astrocyte GJIC was impaired in the region immediately around the abscess, with communication increasing in relation to the distance from the abscess (Karpuk et al. 2011). In contrast,

analysis of ethidium bromide uptake (which could be prevented with gap junction blockers) indicated at day 3 that hemichannel activity was higher nearer the abscess.

In addition to *S.aureus,* connexin expression changes have been reported in response to a number of different bacteria. For example, both *P.aeruginosa* and *Escherichia coli* derived lipopolysaccharide (LPS) have been reported to cause both up and down-regulation of a range of connexins in different cell types (Sarieddine et al. 2009; Yeh et al. 2005; Fiorini et al. 2006; De Maio et al. 2000; Oviedo‐orta et al. 2000; Simon et al. 2004; Liao et al. 2010). An in depth discussion of these are beyond the scope of this thesis, but for more details see (Ceelen et al. 2011). However, the investigations into how these bacteria induced connexin expression changes have revealed that connexin expression changes are brought about by a variety of different mechanisms. Cx43 protein expression was found to be reduced in microglia by Gram negative bacterial lipopolysaccharide (LPS), but without a reduction in Cx43 mRNA levels, suggesting increased protein degradation (Hinkerohe et al. 2010). Alternatively, *S.aureus* PGN decreased Cx43 expression in astrocytes at both the mRNA and protein level (Esen et al. 2007). Decreased Cx32 mRNA in hepatocytes exposed to LPS was found to be through a shortening of the polyA tail, leading to degradation of the mRNA (Gingalewski et al. 1996; De Maio et al. 2000), and increased Cx43 mRNA expression after LPS incubation in hepatocytes was found to be through direct increase in Cx43 promoter activity (Fernandez-Cobo et al. 1998). This illustrates the range of mechanisms adopted when connexin expression is influenced by exposure to different bacterial components.

Like connexin expression, GJIC has been reported to be both increased or decreased in response to bacteria or their components (Uchida et al. 2005; Esen et al. 2007; Eugenín et al. 2007). In some cases this is associated with concomitant changes in connexin expression (Robertson et al. 2010), but this is not always the case; C3 toxin from the Gram positive *Clostridium botulinum* reduced GJIC in primary rat cardiomyocytes but without altering Cx43 expression or phosphorylation, but instead by increasing the interaction between Cx43 and ZO-1 (Derangeon et al. 2008).

Hemichannel opening has also been reported in response to several pathogenic bacteria, including *Shigella flexneri*, *Yersinia enterocolitica*, *Citrobacter rodentium* and *S.aureus* (Tran Van Nhieu et al. 2003; L. A. Velasquez Almonacid et al. 2009; Guttman et al. 2010; Karpuk et al. 2011). This response appears to be involved in the ability of several bacterial species to invade the cells. In Cx43 transfected HeLa cells, Cx43 hemichannel opening was induced by Cx43 phosphorylation, and increased *Y.enterocolitica* uptake (L. A. Velasquez Almonacid et al. 2009). Similarly, *S.flexneri* infection in Cx26 stably transfected HeLa cells caused ATP release via hemichannel opening, which further increased bacterial invasion (Tran Van Nhieu et al. 2003), but expression of Cx30 and Cx31 expression did not (Man et al. 2007). Cx43 expression has also recently emerged as an important determinant of cell death or mortality (Radin et al. 2014; Anand et al. 2008). When epithelial cells were challenged by the *Helicobacter pylori* VacA toxin, a reduction in Cx43 expression was protective; expression of Cx43 in HeLa cells resulted in VacA induced death (Radin et al. 2014). The authors did not determine if Cx43 hemichannel opening was involved, but they speculated that hemichannel activity could potentially be involved in Cx43 expression susceptibility. In contrast, Anand et al found reduced Cx43 expression in Cx43 heterozygous transgenic mice increased the mortality rate following *E.coli* infection (Anand et al. 2008). Interestingly, they also observed this when Cx43 expression was normal but gap junction activity was blocked with oleamide.

The complexity of how bacteria, and *S.aureus* specifically, influence connexin expression, GJIC and hemichannel activity is beginning to emerge. The relationship is dependent on the bacterial species, and the cell type, as well as being tied into the inflammatory response. In order to understand it, comprehension of the consequences for both the host's cells and the bacteria, is needed.

Chapter 2. Materials and Methods

General materials and methods are listed in this chapter. See the beginning of each results chapter for materials and methods specific to that chapter.

2.1. Common Reagents and buffers

Table 2.1. List of common buffers and their composition.

Reagent/ Buffer	Composition
Western blot T/G/S running buffer	(Brought from Bio-Rad) 25 mM Tris, 190 mM glycine, 0.1% sodium dodecyl sulphate (SDS)
Western blot transfer buffer	25 mM Tris, 190 mM glycine, 20% methanol
Western blot blocking buffer	4 % skimmed milk in phosphate buffer saline (PBS, Oxoid) with 0.1 % tween 20
Ponceau S staining buffer	0.1% Ponceau crystals, 5 % acetic acid
Radioimmunoprecipitation (RIPA) buffer	1% Triton X-100, 0.5% sodium deoxycholate, 0.1% SDS, 50 mM Tris-hydrochloric acid, 150 mM sodium chloride
Senescence associated β galactosidase staining solution (SA-β-gal)	40 mM citric acid/ sodium phosphate buffer, 5 mM potassium ferrocyanide, 5 mM potassium ferricyanide, 150 mM sodium chloride, 2 mM magnesium chloride, 1 mg ml^{-1} (5-bromo-4-chloro-3-indolyl-β-D-galactopyranosidase (X-gal, Sigma)) in distilled water. Solution must be pH 6.0 and freshly prepared just prior to use.
Immunofluorescence blocking buffer	0.05% Triton X-100, 0.1 M L-lysine monohydrochloride, made in phosphate buffer saline (PBS, Oxoid)

2.2. Bacterial components

2.2.1. Bacterial strain and growth

Staphylococcus aureus subspecies. *aureus* ATCC® 29213™ (hereafter referred to as *S.aureus*), a strain originally isolated from a wound, was grown in Luria broth (LB) media at 37 °C and 250 RPM over night. Over night suspensions were washed in DMEM (Sigma-Aldrich) supplemented with 10% DBS (Gibco) and re-suspended in the same medium. A CamSpec M330 spectrophotometer

(Spectronic CamSpec) was used to take OD600 absorption readings and cells were diluted to the appropriate concentration. For all experiments, solutions of bacteria were serially diluted, plated on LB agar and incubated at 37 °C overnight. Colonies were counted the following day to confirm bacterial concentration.

2.2.2. Heat Killed *Staphylococcus aureus* (HKSA)

After dilution to the required concentrations, bacterial solutions to be heat killed were placed at 70 °C for one hour, then cooled to room temperature. An aliquot was plated on LB agar and incubated at 37 °C overnight to ensure death.

2.2.3. Biofilm Conditioned Medium (BCM)

This protocol is adapted from the method used in (Kirker et al. 2009). Millicell cell culture inserts with 0.4 µm pores (Millipore) were placed into six well plates with 2.1 ml of DMEM supplemented with 10% DBS in each well. A sterile mixed cellulose ester hydrophilic membrane filter disc with 0.22 µm pore size (Millipore) was placed in each well. An initial overnight culture of *S. aureus* was washed in DMEM with 10% DBS and then resuspended and diluted in in the same media to an optical density of 0.05 at 600 nm. Seven 10 µl drops of the diluted overnight culture were placed onto the filter disc in each culture insert and biofilms were allowed to develop and mature for 72 hours. Every 24 hours for four days thereafter, the growth medium was collected, filter sterilized, pH adjusted to 7.2, and replaced with fresh media. The collected medium is referred to as biofilm conditioned media (BCM), and was pooled to provide sufficient quantities of media to perform all experiments, and to eliminate daily variations that might occur in the biofilm cultures.

2.3. General *In Vitro* experimental methods

2.3.1. Cell culture

NIH 3T3s (mouse embryonic fibroblasts cell line) were grown in Dulbecco's Modified Eagle Medium (DMEM, Sigma-Aldrich) supplemented with 10% donor bovine serum (DBS, Gibco) and 2% penicillin/streptomycin (P/S, Gibco) in 5% CO_2 at 37 °C. Cells were washed prior to all experiments to remove traces of

antibiotics. All experimental media contained no antibiotics. Cells will be referred to as 3T3s hereafter.

2.3.2. Transfection of fibroblasts

A stable 3T3 cell line with Cx43 expression knocked down, and an empty vector control, was previously created by Dr Peter Cormie, a post doc previously of University College London, and kindly made available for my use (Mendoza-Naranjo, Cormie, A. Serrano, et al. 2012). The knocked down cell line was made by transfecting 3T3 cells with a pSuper.retro.puro vector (OligoEngine) containing the Cx43 specific shRNA sequence (GGTGTGGCTGTCAGTGCTC), kindly donated by W.H. Moolenar. An empty vector control (hereafter referred to as EV) was also created using a retroviral pSuppressor vector (Imgenex Corporation). GP2-293 (Clontech) packaging cells were seeded at 20% confluence in DMEM with 10% foetal calf serum (Gibco) and transfected with 15 µg of retroviral plasmid by calcium phosphate precipitation to produce retroviral supernatants. The culture media was collected after 2 days and filtered, and used to infect 3T3 fibroblasts. 3T3 fibroblasts containing the Cx43 shRNA retrovirus were selected and maintained by incubation with 2 µg ml^{-1} of puromycin (Invitrogen). Cells containing the Psuppressor empty vector were selected and maintained by incubation with 500 µg ml^{-1} of gentamicin (Sigma-Aldrich).

2.3.3. Live imaging of proliferation and propidium iodide uptake

Cells were grown in flat bottom 96 well plates. Prior to imaging, cells were incubated with media containing 0.5 µg ml^{-1} Hoechst for 30 minutes. This concentration was selected following a pilot study and was not toxic to the cells. The media containing Hoechst was removed, the cells washed with PBS, and media (DMEM supplemented with 10% DBS) or BCM was added which contained 1 µg ml^{-1} of propidium iodide. *S.aureus* or HKSA was added as appropriate. Cells were then live imaged every hour for 24 hours on an ImageXpress® Micro XL system (Molecular Devices). MetaXpress 5.0 software (Molecular Devices) cell count analysis was used to determine the total number of cells in each image (Hoechst positive) and the number of dead cells (cells that had taken up propidium iodide from the media).

2.3.4. Western blotting

Protein extraction

Cells were grown in 6 well plates to 90-100% confluence before commencing experiments. They were incubated in experimental conditions for the time indicated in the figures. Following the incubation period, cells were placed on ice and washed with cold PBS. Samples were harvested using cold RIPA buffer (see table 2.1) supplemented with phosphatase inhibitors and protease inhibitors (Roche), and using a cold cell scraper (Greiner bio-one). Samples were sonicated for 30 seconds in a USC100T Ultrasonic cleaner (VWR), then kept on ice for 30 minutes, before centrifuging for 30 minutes at 15000 x g at 4 °C. Protein concentrations were quantified using a Pierce BCA protein assay kit (ThermoScientific), following the manufacturer's protocol and determining absorbance with an ELx800 Absorbance Microplate Reader (BioTek) using Gen5 plate reading software (BioTek).

Western blots

Equal amount of protein were re-suspended in 4x Laemmli buffer (Bio-Rad), supplemented with β-mercaptoethanol as per the manufacturer's instructions. Samples were then boiled at 95 °C for 5 minutes. Samples were separated on 10% Mini-Protean® TGX™ gels (Bio-Rad), alongside a Precision Plus Protein™ Dual Colour Standard (Bio-Rad) in a mini protean Tetra cell tank (Bio-Rad) in T/G/S running buffer (Bio-Rad) at 100 volts for up to 2 hours. Samples were then transferred to a Hybond™ C nitrocellulose membrane (Amersham Biosciences) for 1 hour at 100 volts in western blot transfer buffer (see table 2.1. for recipe). Membranes were blocked in western blot blocking buffer (see table 2.1) for 30 minutes. Blots were incubated with primary antibodies (see table 2.2) made in western blot blocking buffer (see table 2.1) for the time indicated. They were then washed 3 times in PBS containing 0.1% Tween 20, before incubating with the relevant secondary antibody (also made in western blot blocking buffer) for the time indicated. Secondary antibodies were horse-radish peroxidase (HRP) conjugated and protein levels were visualised using an enhanced chemiluminescence (ECL) system (ThermoScientific) on a ChemiDoc™ MP Imaging System (Bio-Rad). Densitometry was used to quantify protein bands using Quantity One® Version 4.6.3 software (Bio-Rad). α-tubulin or GAPDH

expression were used as loading controls, and the ratio of Cx43 to α-tubulin or GAPDH was determined.

Table 2.2. Table of primary and secondary antibodies used to do western blots. Concentrations and incubation periods are shown.

Antibody antigen	Species raised in	Company and code	Concentration	Incubation time
Anti-Cx43	Rabbit	Sigma-Aldrich (C6219)	1:4000	1 hour at room temperature
Anti-α-tubulin	Rat	Abd (MCA77G)	1:2500	1 hour at room temperature
Anti-GAPDH	Rabbit	Sigma-Aldrich (G9545)	1:1000	1 hour at room temperature
Anti-rabbit HRP	Goat	Sigma-Aldrich (A6154)	1:1000	1 hour at room temperature
Anti-rat HRP	Goat	CalbioChem (401416)	1:2000	1 hour at room temperature

2.3.5. Immunofluorescence and auto-fluorescence

Immunofluorescent staining

Cells were grown on Millicell EZ slides (Millipore) to 90-100% confluence before commencing experiments. They were incubated in experimental conditions for the time indicated in the figures. Following the incubation period, cells were washed with PBS then fixed with 4% paraformaldehyde (PFA) for 5 minutes. They were washed twice more with PBS, then blocked in immunofluorescence blocking buffer for 30 minutes (see table 2.1). Samples were incubated with rabbit anti-Cx43 antibody (Sigma-Aldrich, C6219, 1:2000) at room temperature for 1 hour. Samples were washed with immunofluorescence blocking buffer, then incubated with goat anti-rabbit Alexa Fluor® 488 (Invitrogen, A11008, 1:400) for 1 hour at room temperature. Cells incubated with BCM for 7 days had high levels of auto-fluorescence when excited with a 488 laser, so were instead incubated with goat anti-rabbit Alexa Fluor® 633 (Invitrogen, A21070, 1:400). Samples were counterstained with Hoechst (Sigma-Aldrich, H33342, H33258, 1:50,000), washed in PBS and mounted in Citifluor® (Glycerol/PBS solution, Citifluor Ltd).

Confocal Imaging

Immunofluorescence was imaged on a Leica SPE upright or inverted confocal microscope. Optimal gain and offset were set in advance and kept constant during image acquisition. A 488 nm laser was used to excite Alexa 488, a 633 nm laser was used to excite Alexa 488 and a 405 nm laser to excite the Hoechst stain. Where cells were incubated with BCM for 7 days a 488 nm laser was instead used to determine the extent of auto-fluorescence.

The regions imaged were selected at random by only observing the Hoechst channel, and single optical sections were obtained. A minimum of three regions was imaged of each biological replicate. A negative control, using no primary antibody but following all other conditions, was done for each experiment and used to threshold images during quantification.

Quantification of immunofluorescence and auto-fluorescence

Images were imported into Image J (National Institute of Health) for quantification. 8 bit images were identically thresholded, to create a binary image. The total area of connexin expression or auto-fluorescence was measured and was normalised to the number of nuclei in each image. The results from experimental replicates were averaged.

2.4. General *In vivo* experimental methods

2.4.1. Animals

Individually housed 6 week old male imprinting control region (ICR) mice were obtained from Harlan, and kept in accordance with UK Home Office regulations. All animal experiments had UK Home Office approval.

2.4.2. Surgery

Mice were anaesthetised with 4% isofluorane in oxygen at 2 L m^{-1} and nitric oxide at 1 L m^{-1}. 0.1 mg kg^{-1} of buprenorphine (Vetergesic, Recknitt Benckiser Healthcare) was injected subcutaneously in the scruff of the neck. Mice were placed on a heated mat and received either cheek or back wounds, as indicated in figure 2.1. After surgery they were observed to ensure full recovery and returned to their home cages and observed daily.

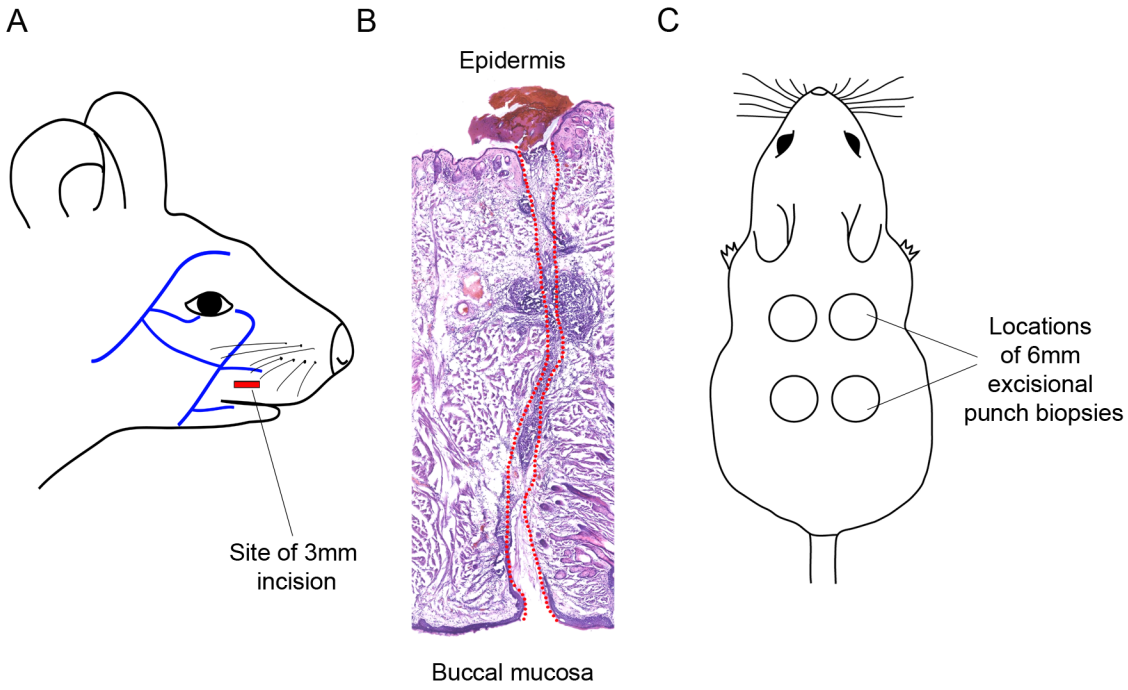

Figure 2.1. *In vivo* wound sites. (A) Schematic of a mouse head with the major blood vessels indicated in blue. The site of incision for cheek wounds is indicated in red. **(B)** H&E of a cheek wound showing the wound passing through the full thickness of the tissue, from external epidermis through to internal mucosa. **(C)** Schematic of a mouse viewed from above, showing the regions of back punch biopsies.

2.4.3. Tissue harvesting and processing

Mice were euthanised by a rising concentration of CO_2, and death confirmed by cervical dislocation using a tool. Tissue was excised and fixed in 4% PFA in PBS overnight at room temperature. The tissue was then washed three times with PBS, then transferred to 20% sucrose in PBS with 0.1% sodium azide at 4 °C overnight. Tissue was frozen into O.C.T (Tissue-Tek, Sakura) and stored at -80 °C until further processing. Cross sections of wounds were cut on a cryostat (Leica) at 10 or 12 µm thickness. Slides with sectioned tissue were stored at -20 °C.

2.4.4. Haematoxylin and & Eosin (H&E) staining

H&E staining

Fixed tissue sections were brought to room temperature, and washed in tap water for 10 minutes to dissolve all O.C.T. Slides were then placed in Harris's Haematoxylin stain (Sigma-Aldrich HH532) for 30 seconds, then washed in running tap water for 5 minutes to remove excess stain. They were briefly dipped in acid alcohol (70% ethanol, 1% hydrochloric acid) then washed again in running tap water for a further 5 minutes. The slides were then counterstained by placing in 1% eosin Y solution (Sigma-Aldrich HT110232,) for 1 minute. Slides were dipped in water to remove excess stain before dehydrating by transferal through increasing concentrations of ethanol as shown in table 2.3. Sections were then mounted on coverslips using DPX (VWR).

Table 2.3. H&E dehydration steps

Solution	Time (minutes)
70% ethanol	1
100% ethanol	2
100% ethanol	2
100% xylene	3
100% xylene	3

Quantification of H&E images

H&E stained sections were imaged on a Leica DMLB microscope (Leica) or on an AxioScan Z1 slide scanner (Zeiss) using x10 or x20 objectives. Images were opened in NIH Image J (http://rsbweb.nih.gov/ij/) or Zen 2012 software (Zeiss) respectively.

Measuring re-epithelialisation

Re-epithelialisation was measured from the wound edge (where the incision was made and normal dermis or sub-mucosa was present) to the tip of the new growth. Re-epithelialisation was measured at both wound edges in a minimum of 2 sections, taken from different regions of the wound. The measurements were averaged.

2.4.5. Immunofluorescence

Immunofluorescence staining

Sections were brought to room temperature and washed in PBS for 10 minutes to remove O.C.T. They were then permeabilised in cold acetone for 5 minutes. Samples were blocked in immunofluorescence blocking solution (see table 2.1) for 30 minutes. Sections were incubated with one of the antibodies listed in table 2.4. for 1 hour at room temperature.

Table 2.4. Primary antibodies used to immuno-stain mouse tissue.

Antigen raised against	Species raised in	Company and code	Concentration	Monoclonal / Polyclonal
Cx26	Rabbit	Millipore (AB8143)	1:100	Polyclonal
Cx30	Rabbit	Invitrogen (71-2200)	1:200	Polyclonal
Cx43	Rabbit	Sigma-Aldrich (C6219)	1:2000	Polyclonal

Sections were washed with immunofluorescence blocking solution, then incubated with goat anti rabbit Alexa Fluor® 488 (Invitrogen, A11008, 1:400). Sections were counterstained with Hoechst (Sigma-Aldrich, H33342, H33258,

1:50,000), washed in PBS and mounted in Citifluor® (Glycerol/PBS solution, Citifluor Ltd).

Confocal imaging and quantification

Immunofluorescence was imaged on a Leica SPE inverted or upright confocal microscope. Optimal gain and offset were set in advance and kept constant during image acquisition. A 488 nm laser was used to excite Alexa 488, and a 405 nm laser to excite the Hoechst stain, and single optical sections obtained. To quantify connexin expression changes in *in vivo* samples single optical section images were taken of a distal region (up to 1 mm from the wound), the wound edges (the region where the wound was made, and the original dermis or lamina propria is still present), and the tip of new growth. Images were taken at x40 magnification (1024x1024 pixels). Images were imported into Image J for quantification. 8 bit images were identically thresholded, to create a binary image, and the region to be measured was demarked. The total area of connexin expression was measured in pixels, normalized to the area of the region of interest, and presented as pixels / μm^2 (Wang et al. 2007). Where indicated, wound edge connexin expression was then normalized to expression distal to the wound, and presented as the percentage connexin was down-regulated at the wound edge.

2.5. Statistical analysis

All N numbers indicate independent experiments conducted separately. Additionally, data from each *in vitro* experiment is an average from several replicates. All error bars on graphs indicate the standard error of the mean (SEM).

Assumptions of statistical tests were checked before commencing each statistical analysis. All parametric tests used assume Gaussian normal distribution, and this was tested using a Shapiro-Wilk test. Data not conforming to a Gaussian normal distribution was transformed by taking the common logarithm or the square root. If this did not result in a normal distribution then the appropriate non-parametric test was used instead. Statistical differences

were inferred if $p<0.05$. All statistical analysis was performed in SPSS® version 21 statistical analysis software (IBM) unless otherwise stated.

2.5.1.1. Student's t-tests

Unpaired Student's t-tests were used to determine statistical differences between two groups, using Welch's correction for data with unequal variances. Mann Whitney U tests were used on data not showing a normal distribution after transformation.

2.5.1.2. One-way ANOVAs

One-way ANOVAs were used when there were more than two groups. Homogeneity of variances was tested using Levene's test. Post hoc tests were performed using Bonferroni or Tukey's adjustments as appropriate when multiple comparisons were made. A Games-Howell post hoc was used if the variances differed significantly.

2.5.1.3. Mixed design ANOVAs

A mixed design ANOVA was used when there were two or more data sets that were subject to repeated measures, in this case time. Sphericity of the covariance matrix was tested using Mauchly's sphericity test, and if sphericity was violated a Greehouse-Geisser correction was used. Homogeneity of variance was tested with Levene's test. A Tukey's post hoc was used to compare individual groups, or Games-Howell if variances between the groups differed significantly.

Chapter 3. Connexin Dynamics in the Privileged Wound Healing of the Buccal Mucosa

This chapter is published. Minor re-formatting of text and figures has been done to fit with the thesis style and figure 3.6 is a new addition. The remainder has not been altered from the published version (Davis et al. 2013).

3.1. Introduction

The ability of skin to heal is of enormous importance in maintaining homeostasis within the body, and in preventing infection. Healing proceeds through four overlapping phases: haemostasis, inflammation, granulation tissue formation and tissue remodelling. Re-epithelialisation involves the proliferation of epidermal keratinocytes, and their migration over granulation tissue in the wound bed in order to re-establish skin integrity (Martin 1997). A plethora of signals from different cells and tissues must be coordinated to ensure correct healing in the skin, and there is a growing body of evidence demonstrating a critical role for gap junctions during the repair process (Goliger & Paul 1995; Qiu et al. 2003; Kretz et al. 2003; Coutinho et al. 2003; Lampe et al. 1998). Gap junctions are intercellular pores comprised of two hemichannels, known as connexons, which in turn consist of 6 connexin (Cx) protein subunits (Makowski et al. 1977). Each adjacent cell provides a hemichannel, which dock to one another and allow a direct connection between the cells' cytoplasm. Gap junctions enable the passive diffusion of small molecules through them but discriminate against molecules larger than 1 kDa (Veenstra et al. 1995; Elfgang et al. 1995).

Ten different connexins have been reported to be expressed in the epidermis including Cx26 and Cx30, though the most highly expressed is Cx43 (Risek et al. 1992; Goliger & Paul 1994; Di et al. 2001; Coutinho et al. 2003). In intact skin Cx43 is normally expressed at moderate levels in the lower spinous and basal layers of the epidermis, whereas Cx26 and Cx30 are both expressed at low levels within the granular layer (Goliger & Paul 1994; Coutinho et al. 2003). Upon wounding of skin, connexin expression changes dynamically throughout the healing process (Goliger & Paul 1995; Coutinho et al. 2003). Cx43 expression becomes down-regulated in the epidermal wound edge keratinocytes as they become migratory over 24-48 hours, returning to normal following complete re-epithelialisation. Conversely Cx26 and Cx30 are up-regulated in the migratory keratinocytes, with levels returning to normal upon wound closure (Goliger & Paul 1995; Coutinho et al. 2003).

Healing rates were observed to be enhanced in Cx43 knockout mice and in mice where Cx43 expression was targeted by application of Cx43 antisense

oligodeoxynucleotides (Cx43asODNs) (Mori et al. 2006; Qiu et al. 2003; Kretz et al. 2003). The requirement for Cx43 reduction at the wound edge, in order for migration to take place normally, is supported by observations that Cx43 was abnormally up-regulated in the wound edge keratinocytes and fibroblasts of diabetic rats and that preventing this with application of Cx43asODNs rescues the rate of healing (Wang et al. 2007; Mendoza-Naranjo, Cormie, A. Serrano, et al. 2012). Fibroblast migration in *in vitro* scratch wound studies also demonstrated a requirement for Cx43 to be down-regulated in order for cells to extend long lamellipodia and migrate rapidly (Mendoza-Naranjo, Cormie, A. Serrano, et al. 2012).

Some regions of the body exhibit privileged healing, whereby they heal more rapidly than other regions and without scarring. One such region is the oral mucosa (Sciubba et al. 1978; Szpaderska et al. 2003), which is comprised of parakeratinised regions such as the tongue and gingiva, and non-keratinized regions such as labial and buccal mucosa (Squier & Brogden 2011). Oral mucosa is described as “proceeding through the same stages of healing as other parts of the body” (Enoch & Stephens 2009). However, some differences such as earlier onset and the shape of the migratory cells have been described in the re-epithelialisation process in parakeratinised rat tongue (Sciubba et al. 1978) and studies investigating privileged healing in the oral mucosa have identified features including a reduced inflammatory response (Szpaderska et al. 2003) and increased fibroblast migration rate (P Stephens 1996).

Despite the importance of connexin expression and dynamics in skin healing, little research has been performed on connexin expression in oral mucosa during the healing process. The aim of this work was to observe healing in buccal mucosa, and to ascertain if connexin expression and dynamics may contribute towards the privileged healing status of this epithelium.

3.2. Materials and methods

3.2.1. Animals

Individually housed 6 week old male ICR mice were kept in accordance with UK Home Office regulations. Mice were anaesthetized with 4% isofluorane in oxygen at 2 L m^{-1} and nitric oxide at 1 L m^{-1}, and then 0.1 mg kg^{-1} of buprenorphine was injected subcutaneously in the scruff of the neck. Mice were then injected intraperitoneally with 75 mg kg^{-1} ketamine, and 1 mg kg^{-1} medetomidine. A full thickness incision through the skin and buccal mucosa of 3 mm width was made in each cheek with a scalpel above the lip as indicated (Figure 2.1. A, B), avoiding the major blood vessels in the region. Mice were subsequently revived by administration of 1 mg kg^{-1} of subcutaneously injected antipamezole. They were observed to ensure full recovery and returned to their home cages. Soft wet food was made available to these mice. All animal experiments had UK Home Office approval.

3.2.2. Tissue harvesting and processing

Mice were anaesthetised then euthanized by cervical dislocation using a tool to prevent trauma to the facial tissue. Nine mice were harvested at each time point: 6 hours, 24 hours and 48 hours. Wounds were excised and fixed in 4% PFA overnight, washed, then transferred to 20% sucrose in PBS with 0.1% sodium azide at 4 °C overnight. Tissue was frozen into O.C.T and stored at -80 °C until further processing. Cross sections of wounds were cut on a cryostat at 10 μm thickness, or at 5 μm for H&E staining.

3.2.3. Measuring re-epithelialisation

Sections were H&E stained and imaged on a Leica DMLB microscope or a slide scanner (Laser 2000). The extent of re-epithelialisation was measured from the wound edge (where the incision was made and normal dermis/submucosa was present) to the tip of new growth using an eyepiece graticule and a stage micrometre. Results from a minimum of 2 sections per sample, from different regions of the wound, were averaged.

3.2.4. Immunofluorescence imaging and quantification

Sections were permeabilised in cold acetone for 5 minutes, and blocked in PBS lysine (0.1 M) for 30 minutes. Sections were incubated with rabbit anti-Cx43 antibody (Sigma-Aldrich, C6219), rabbit anti-Cx26 (Millipore, AB8143) or rabbit anti-Cx30 (Invitrogen, 712200) at room temperature for 1 hour. Sections were washed with PBS lysine (0.1 M) then incubated with goat anti rabbit Alexa Fluor® 488 (Invitrogen, A11008). Sections were counterstained with Hoechst (Sigma-Aldrich, H33342, H33258), washed in PBS and mounted in Citifluor® (Glycerol/PBS solution). Immunofluorescence was imaged on a Leica SPE inverted confocal microscope. A 488 nm laser was used to excite Alexa 488, and a 405 nm laser to excite the Hoechst stain, and single optical sections obtained. To quantify connexin expression changes following wounding single optical section images of a distal region (up to 1 mm from the wound) and the wound edges were taken at x40 magnification (1024 pixels X 1024 pixels). Microscope settings were kept constant when comparing connexin expression levels between the cheek epidermis and the buccal mucosa, using the buccal mucosa region to select settings. Images were imported into image J (NIH) for quantification. 8 bit images were identically thresholded, to create a binary image, and the region of the epithelium to be measured was demarked. The total area of connexin expression was measured and normalized to the total demarked area (Wang et al. 2007). Wound edge connexin expression was then normalized to expression distal to the wound, and presented as the percentage connexin was down-regulated at the wound edge.

3.2.5. Statistics

Unpaired Student's t-tests were used to determine statistical differences between the epidermis and buccal mucosa for data having normal Gaussian distribution, using Welch's correction for data with unequal variances. Data not showing normal distribution was transformed by taking the natural log and, if now normal, t-tests were used. Mann Whitney U tests were used on data not showing a normal distribution after transformation. All analysis was performed in prism V5, statistical analysis software.

3.3. Results

3.3.1. The re-epithelialisation process in buccal mucosa differs from the process in skin

In skin, re-epithelialisation is characterized by a thin tongue of flattened, elongated keratinocytes (figure 3.1.A) that crawl down the edge of the wounded dermis (figure 3.1.Ai) and over the granulation tissue which forms in the wound bed (figure 3.1.Aii). This process continues until the migrating cells from each wound edge meet and form a continuous intact epithelium (figure 3.1.Aiii) (Martin 1997). Despite the fact oral mucosa is considerably thicker than the skin epidermis, and comprised of many more layer of cells, re-epithelialisation in this epithelium has been described as proceeding through the same stages as skin (Enoch & Stephens 2009). However, here it is shown that there are distinct differences in the way the buccal mucosa heals.

It was found that the wound edge epithelial cells of the buccal mucosa migrated in a thick lip or 'wedge' (figure 3.1.Bi), rather than a thin tongue of cells as in the epidermis. In the epidermis in the first 24 hours the leading migratory cells became flattened and elongated; however, in the buccal mucosa the leading cells largely retained their thickness and shape, only becoming slightly thinner (figure 3.2.A-D). The cells migrated rapidly down the wound tract in a 'wedge' (figure 3.1.Bii) until they met and joined up, forming a 'V' in the tissue (figure 3.1.Biii). There appeared to be little or no granulation tissue in the wound bed, with cells migrating instead over the underlying sub-mucosa. The 'V' then rapidly filled with cells until they occupied the entire space between the two sides of the wound leaving a solid 'delta' shape of epithelial cells projecting into the underlying connective tissue (figure 3.1.Biv). The tissue then underwent remodelling and the 'delta' of epithelial cells retracted (figure 3.1.Bv) until there was very little evidence of the wound's location (figure 3.1.Bvi).

Interestingly, a deviation from the accepted model of oral mucosa was also found, as the presence of large hairs was noted within unwounded buccal mucosa in these mice. Hair is not normally found in non-keratinized buccal mucosa, but is usually restricted to keratinized epithelia. While hairs were infrequent very large hair follicles were consistently identified (figure 3.2.E).

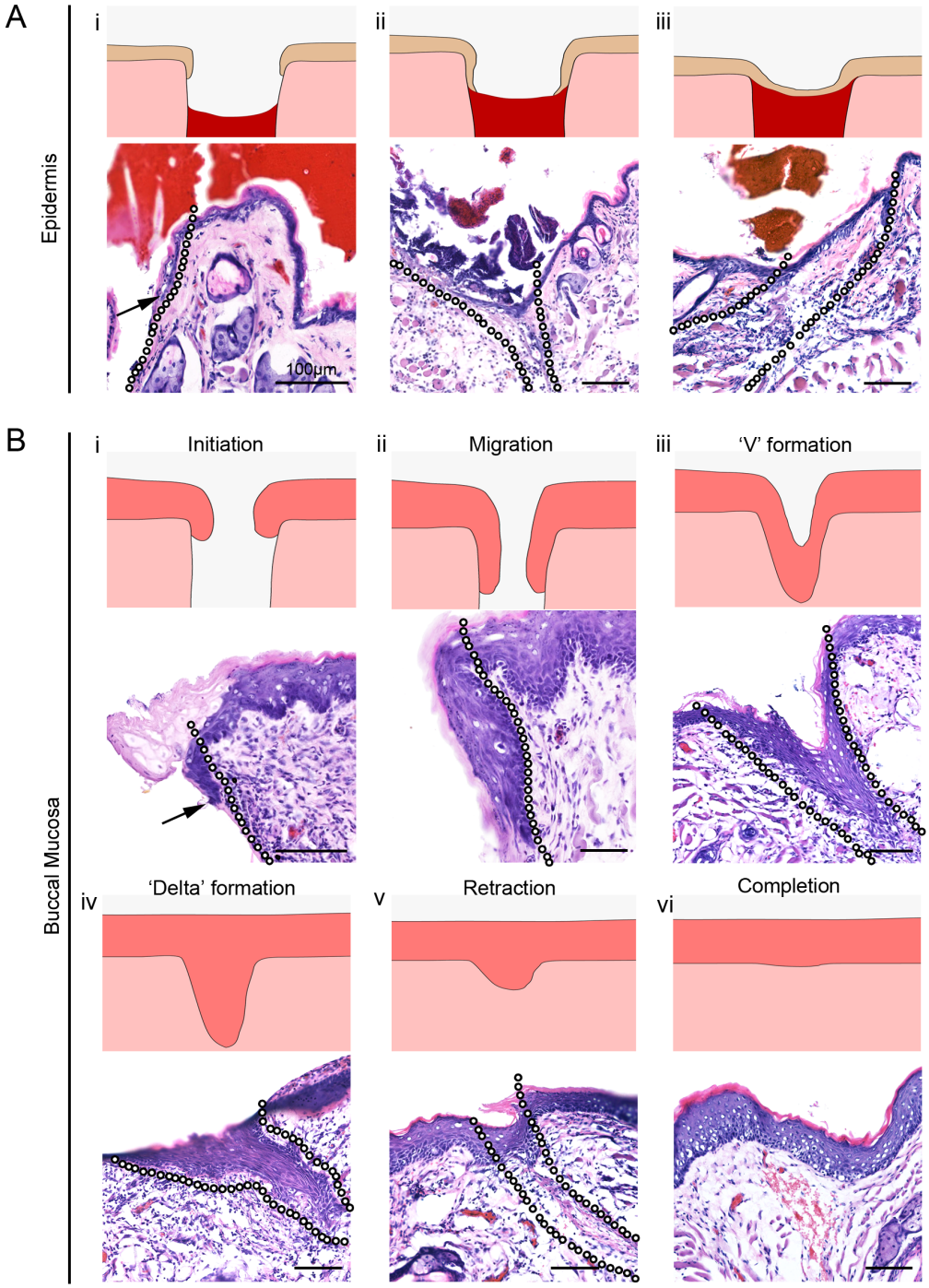

Figure 3.1. The stages of re-epithelialisation in the skin epidermis and the buccal mucosa. In the skin **(A)** the keratinocytes form a thin tongue of cells at the wound edge (i), which migrate over granulation tissue (ii) until the two tongues meet and form a continuous epithelium (iii). In the buccal mucosa **(B**) the epithelial cells form a thicker wedge during the 'initiation' of re-epithelialisation (i), which 'migrate' into the wound (ii) until the two sides meet and form a 'V' (iii). The 'V' becomes filled to form a 'delta' (iv), which is then 'retracted' (v) during remodelling, until the process is 'complete' (vi). The black and white dotted lines indicate the wounded region, where apparent. The black arrows indicate the thin epidermal re-epithelialisation **(A)** and the thicker buccal mucosa re-epithelialisation **(B)** All scale bars indicate 100 µm (Bi-ii= 6 hours; Ai-ii= 24 hours; Biii-vi and Aiii=48 hours).

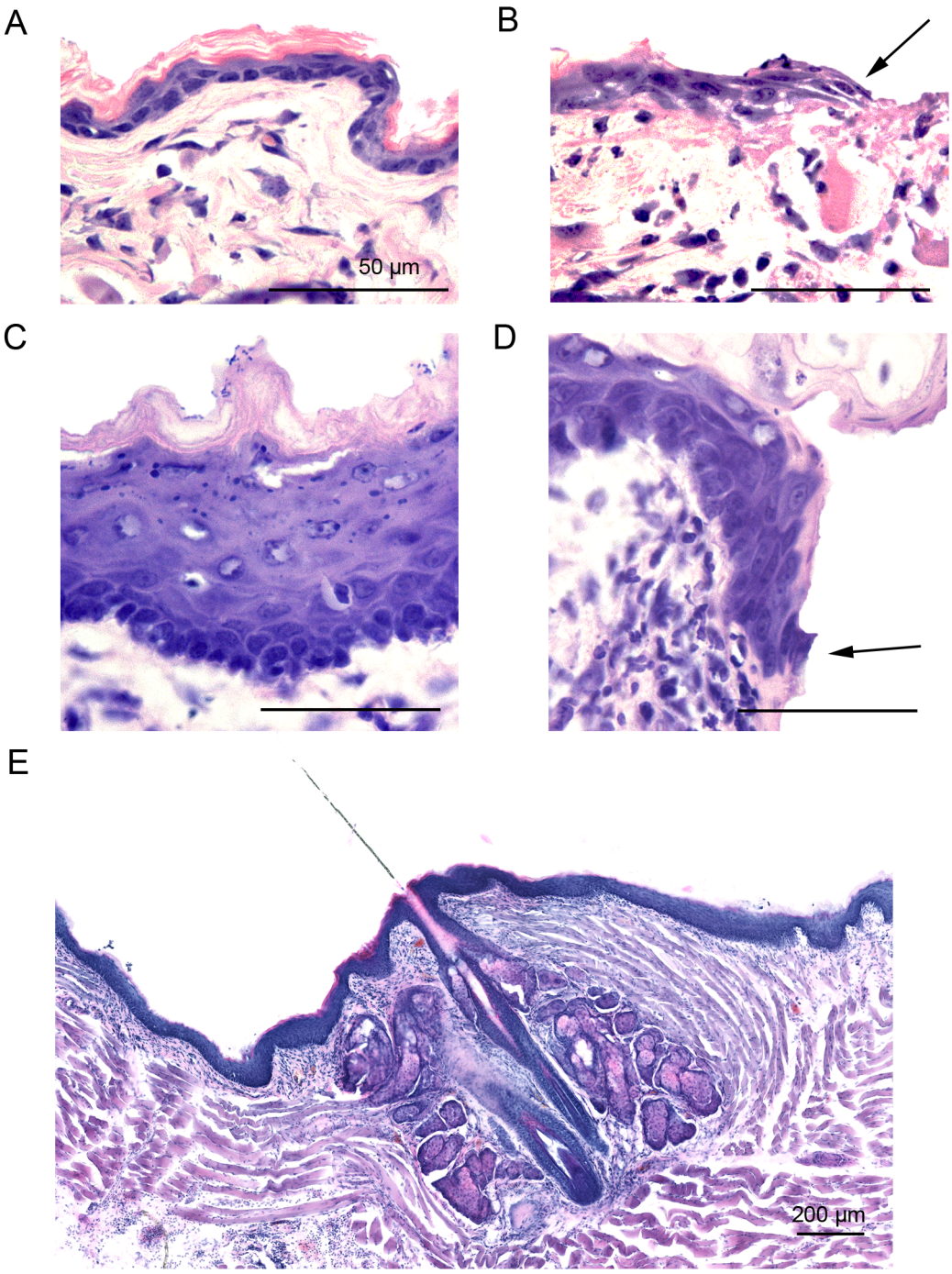

Figure 3.2. Cell shape at the migrating edge differs in skin and buccal mucosa. (A) Distal keratinocytes in the skin epidermis are rounded, but at the wound edge (24 hours post wounding) **(B)** they become thin and elongated. **(C)** Distal cells in the buccal mucosa are also rounded, but at the wound edge (6 hours post wounding) **(D)** they retain their shape fairly well. Arrows indicate the tip of the wound edge. Scale bars indicate 50 µm. **(E)** An example of a hair follicle in buccal mucosa. Scale bar indicates 200 µm.

3.3.2. Re-epithelialisation is more rapid in buccal mucosa than in skin

Full thickness wounds through the cheek skin and the buccal mucosa were made. Tissue was harvested at 6 hours, 24 hours or 48 hours. Histological evaluation of wounds at 6 hours, 24 hours and 48 hours post-wounding were used to determine the extent of re-epithelialisation in the epidermis and buccal mucosa (figure 3.3). Contraction is reported to be greater in the oral mucosa than skin (P Stephens 1996; Shannon et al. 2006; McKeown et al. 2007), so re-epithelialisation was measured rather than wound area to prevent contraction from confounding the results, as this study focuses on epithelial rather than connective cells. After 6 hours no re-epithelialisation could be seen in the epidermis of skin wounds. At 24 hours there was a tongue of migrating keratinocytes with an average re-epithelialisation of 53 μm (±10.16). In the buccal mucosa there was significantly more growth than in the epidermis both at 6 hours and 24 hours ($p<0.05$). At 6 hours the average re-epithelialisation in buccal mucosa was 55 μm (±12.32), and at 24 hours it was 82 μm (±10.59). Due to the manner in which buccal mucosa heals, the exact location of re-epithelialisation initiation wasn't always distinct. To ensure a fair comparison between the tissues, measurements of re-epithelialisation in the buccal mucosa were conservative, and actual re-epithelialisation in this tissue may be greater. By 48 hours 87.5% of buccal mucosa wounds had completed re-epithelialisation, compared to only 55.6% of the epidermal wounds (figure 3.3.Ci). Of the buccal mucosa wounds that had completed re-epithelialisation 66.7% of these had not only joined up but had entirely completed the remodelling process of retracting the delta of wound epithelium, and the wounds were no longer apparent (figure 3.3.Cii).

3.3.3. Cx26, Cx30 and Cx43 expression is significantly higher in buccal mucosa than in skin

Cx26 was expressed at very low levels suprabasally in intact facial epidermis. However, it was much more strongly expressed in the buccal mucosa throughout the intermediate and lower superficial layers but not basal layers (figure 3.4.A-B).

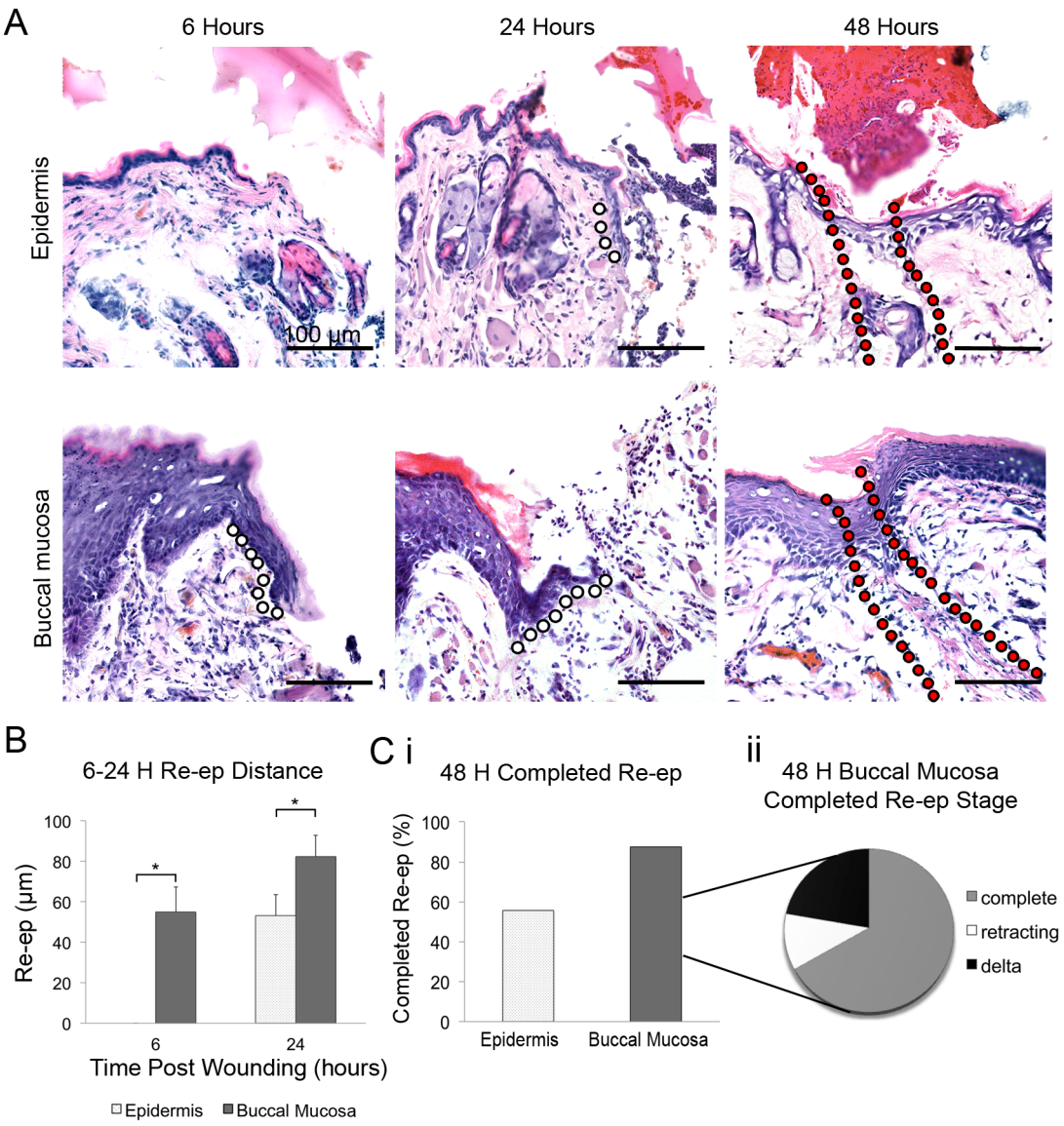

Figure 3.3. Re-epithelialisation of skin and buccal mucosa. (A) Images show examples of re-epithelialisation in skin epidermis (top row) and buccal mucosa (bottom row) at 6, 24 and 48 hours. Black and white dotted lines indicate re-epithelialisation. Red and black dotted lines in the 48 H images indicate the original site of the wound. **(B)** Graph showing the re-epithelialisation distance in skin epidermis and buccal mucosa at 6 and 24 hours. Mean ± SEM are shown (n=7 in the skin and n=6 in the buccal mucosa at 6 hours, and n=8 at 24 hours in both tissues (* $p<0.05$)). **(Ci)** Graph showing the percentage of samples with completed re-epithelialisation at 48 hours. **(Cii)** Pie chart showing, of the buccal mucosa samples that had completed re-epithelialisation, the percentage at each stage of healing as described in figure 3.1.

Cx30 was not easily detectable in the intact facial epidermis, but for the first time it is shown that Cx30 is strongly expressed in the intermediate and lower superficial layers of the buccal mucosa of mice (figure 3.4.A, C). Interestingly neither Cx26 nor Cx30 were strongly expressed in the proliferative basal cells of the buccal mucosa.

Cx43 is the most ubiquitous connexin in skin, and in intact epidermis Cx43 was found in the basal and spinous layers as previously reported (Goliger & Paul 1994). In the buccal mucosa, however, Cx43 was found in all layers except the superficial layer, but had lower expression in the basal than other layers (figure 3.4.A, D).

Cx26, Cx30 and Cx43 were all expressed at significantly higher levels in the buccal mucosa than in cheek skin ($p<0.002$) (figure 3.4.B-D). There was 326-fold more Cx26, 490-fold more Cx30 and 24-fold more Cx43 in the buccal mucosa than in the cheek epidermis.

3.3.4. Cx26, Cx30 and Cx43 are down-regulated rapidly at the buccal mucosa wound edge

Connexin expression changes in the back skin epidermis have previously been reported with Cx26 and Cx30 increasing in wound edge keratinocytes and Cx43 down-regulating concomitantly (Coutinho et al. 2003; Goliger & Paul 1995). Similar results were found in the cheek epidermis. Cx26 expression increased in the epidermis behind the wound edge within 6 hours, and significantly increased between 6 and 24 hours (* $p<0.05$) (figure 3.5.A). Similarly, Cx30 expression increased behind the wound edge but within 24 hours (figure 3.5.C). In contrast, Cx43 became down-regulated at the wound edge within 6 hours by 57% (±13.94%), and expression remained very low at 24 hours (figure 3.5.E).

However, the buccal mucosa wound edge was noticeably different in its connexin response to injury, with a rapid global down-regulation of Cx26, Cx30 and Cx43 at the wound edge within 6 hours of injury (figure 3.5.B, D, F).

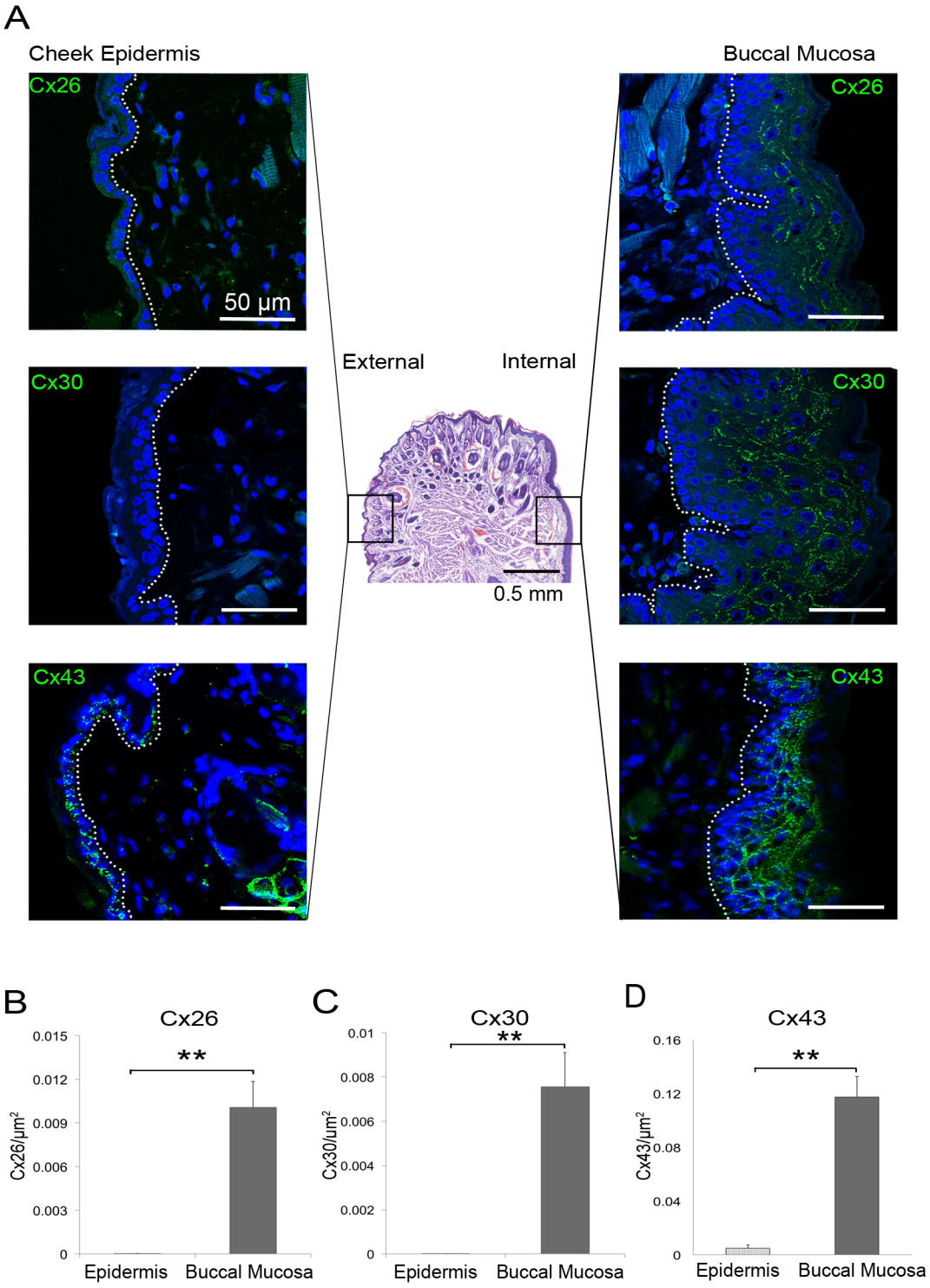

Figure 3.4 Connexin expression in the cheek epidermis and in buccal mucosa. (A) An H&E image is shown of the epidermis transitioning into oral mucosa. Images of Cx26, Cx30 and Cx43 in the cheek epidermis (left) and buccal mucosa (right) are shown. Connexin staining is in green as indicated, and Hoechst is in blue. The epidermal and buccal mucosa images were taken using the same settings (note: the Cx43 expression levels in the epidermal image have been increased in this image only, to enable the Cx43 expression to be seen). The dotted white lines indicate the dermal-epidermal junction, and the mucosal-sub-mucosal junction. **(B)** Graph showing C26, **(C)** Cx30 and **(D)** Cx43 expression per μm^2 in cheek epidermis and buccal mucosa. Mean ± SEM are shown (B and C, n=7; D, n=6 (** $p<0.002$)).

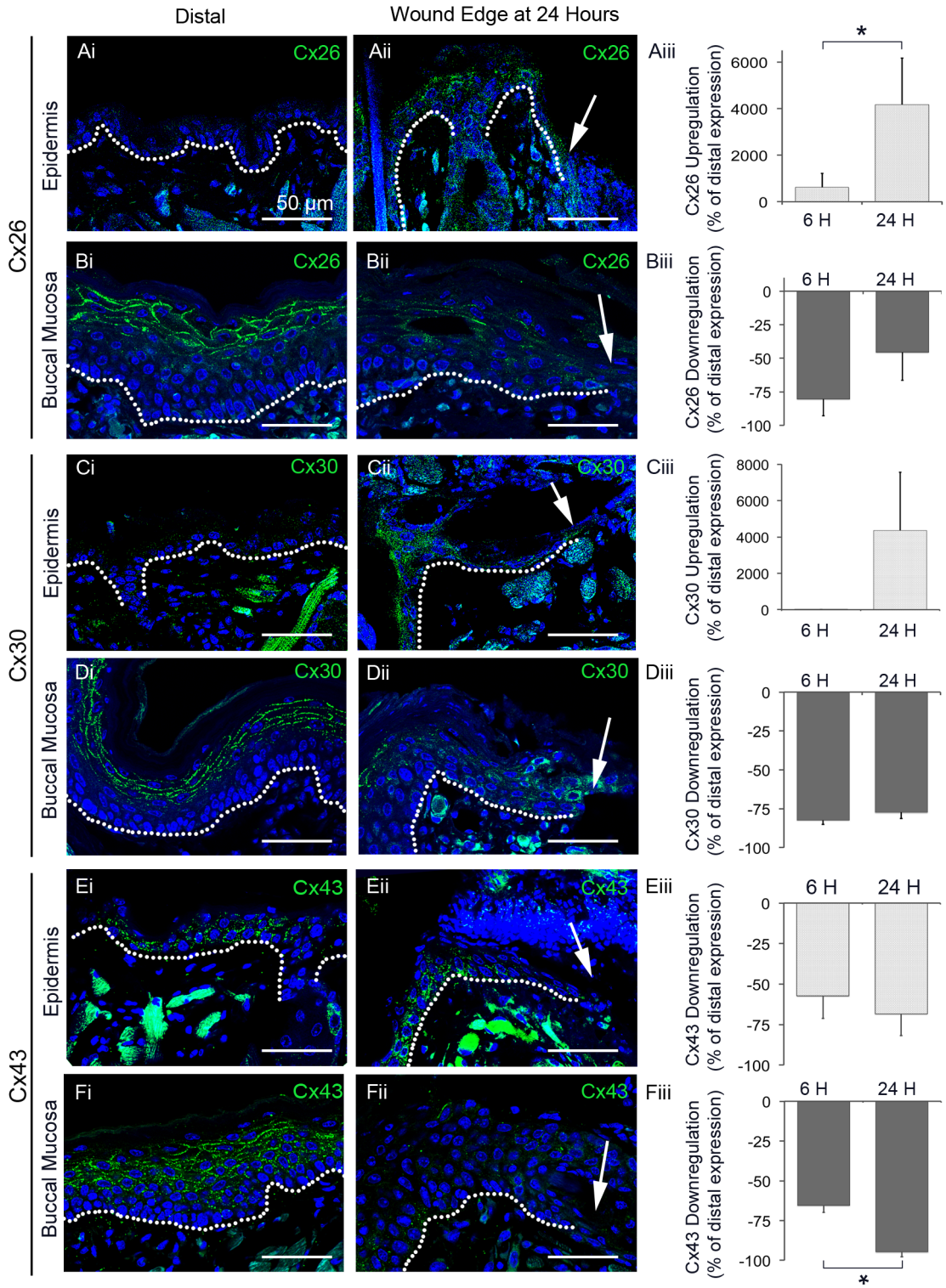

Figure 3.5. Connexin expression in a distal region and at the wound edge in skin and buccal mucosa at 24 hours following wounding for Cx26 **(A-B),** Cx30 **(C-D)** and Cx43 **(E-F)** are presented. Hoechst (nuclei) are in blue, and connexins are green as indicated. Dotted white lines represent the epidermal-dermal, or mucosal-sub-mucosal junction, and the white arrows indicate the tip of the wound edge. Graphs show the connexin down-regulation or up-regulation at the wound edge from the distal region at 6 hours and 24 hours. Mean ± SEM are given (Aiii n=5 at 6 H and n=6 at 24 H; Biii n=4; Ciii n=4 at 6 H and n=5 at 24 H; Diii n=4 at 6 H and n=5 at 24 H; Eiii n=4 at 6 H and n=7 at 24 H; Fiii n=6 at 6 H and n=7 at 24 H; (*p<0.05)).

Cx26 and Cx30 were both rapidly down-regulated by 84% (±9.11%) and 80% (±5.01%) respectively at 6 hours (figure 3.5.B,F). Cx26 expression at the wound edge returned a little at 24 hours, to only 39% (±15.91%) down-regulation, but Cx30 expression remained very low at 70% (±7.01%) down-regulation. By 48 hours, expression of both connexins was starting to return to normal levels. Expression, though, was highly variable, as at this time the majority of buccal mucosa wounds had completed re-epithelialisation and were at various stages in the remodelling process.

At 6 hours after wounding Cx43 expression was 65% (±5.17%) lower at the wound edge than in distal regions (figure 3.5.F). At 24 hours very little Cx43 expression was present, with 95% (±1.69%) of the Cx43 expression down-regulated at the wound edge. At 48 hours, as with Cx26 and Cx30, Cx43 expression levels were starting to return to normal levels. Cx43 dynamics followed a slightly different pattern to Cx26 and Cx30, taking longer to reach its maximal down-regulation.

3.4. Discussion

Buccal mucosa is described as exhibiting “privileged healing” within adults. However, despite the importance of connexin expression and dynamics in the normal skin healing process, no research has been conducted into the connexin dynamics in buccal mucosa. Here, a rapid re-epithelialisation rate was observed, and differences noted in the re-epithelialisation process and connexin expression dynamics when compared to skin.

Re-epithelialisation in oral mucosa is often described as proceeding through the same stages as skin (Enoch & Stephens 2009), although with a dramatically increased proliferation rate (Thomson et al. 1999). However, it was noted in an EM study of healing in rat tongue, a parakeratinised oral mucosa, that re-epithelialisation onset was earlier than in skin epidermis. It was also reported that migratory mucosal cells retained their shape in comparison to skin keratinocytes, which become elongated (Sciubba et al. 1978). In this study, early onset and shape retention of migratory cells in buccal mucosa wounds was similarly observed. Differences in the buccal mucosal re-epithelialisation process are also described, namely the leading cells at the wound edge migrate in a wedge rather than a thin tongue. Whilst other studies have observed re-epithelialisation in various oral mucosae, this phenomenon has not previously been reported. This may be due to several possible reasons. Few studies have examined the histology earlier than 24 hours after wounding, and many report complete re-epithelialisation (Szpaderska et al. 2003; Schrementi et al. 2008; Mak et al. 2009). Furthermore, this mechanism could be limited to incisional wounds that heal by primary intention, and may differ from wounds closing by secondary intention. Alternatively the wound location may influence the mechanism, as buccal mucosa is reported to proliferate more rapidly that keratinised oral mucosa like gingiva or dorsal tongue (see (Squier & Kremer 2001) for more information). The species may also be important, as the thickness and turnover of the oral mucosa differs between species (see (Squier & Kremer 2001)).

Previous research has shown that oral mucosa fibroblasts differ from skin dermal fibroblasts in several ways, one of which is a significantly increased

contractile ability (P Stephens 1996; Shannon et al. 2006). This rapid contraction of the sub-mucosa wound bed may create a different migratory path for buccal mucosa epithelial cells, whereby they migrate into the wound bed rather than over granulation tissue, resulting in the ‘V’ and ‘delta’ described in the results, and a different process to that observed in skin epidermal wound healing.

In addition to differences in the healing mechanism, it was shown that the intact buccal mucosa has a significantly higher level of connexin expression compared to skin (figure 3.6). While Cx26 and Cx43 have previously been reported in various unwounded oral mucosae (Hara et al. 1999; Hatakeyama et al. 2006; Muramatsu et al. 2008; Saitoh et al. 1997), to the best of our knowledge Cx30 expression in normal buccal mucosa is described here for the first time. In addition it was shown that the connexin dynamics in buccal mucosa wound healing differ considerably from those seen in the skin with all three connexins rapidly down regulating at the wound edge within 6 hours of injury (figure 3.6).

It is widely accepted that Cx43 must be down-regulated in order for cells to migrate during wound healing (Qiu et al. 2003; Kretz et al. 2003; Mori et al. 2006; Mendoza-Naranjo, Cormie, A. Serrano, et al. 2012; Wang et al. 2007). Thus, such high levels of Cx43 expression in buccal mucosa compared to skin might be expected to result in slower healing. Nevertheless, these results have shown that buccal mucosa re-epithelialisation is significantly faster, commencing sooner and reaching completion more rapidly. In this regard, the results have also shown here that rapid healing correlates with very rapid down-regulation of Cx43 within 6 hours, with 95% of Cx43 removed within 24 hour. The change in connexin dynamics reported here is consistent with the necessity of Cx43 down-regulation for cell migration. It is possible that this prompt response may enable the rapid onset of buccal mucosa re-epithelialisation, and thus contribute to the privileged healing status of this tissue, though further work is required to confirm this.

The high levels of Cx26 and Cx30 in unwounded buccal mucosa are also interesting. Both Cx26 and Cx30 have been suggested as markers for

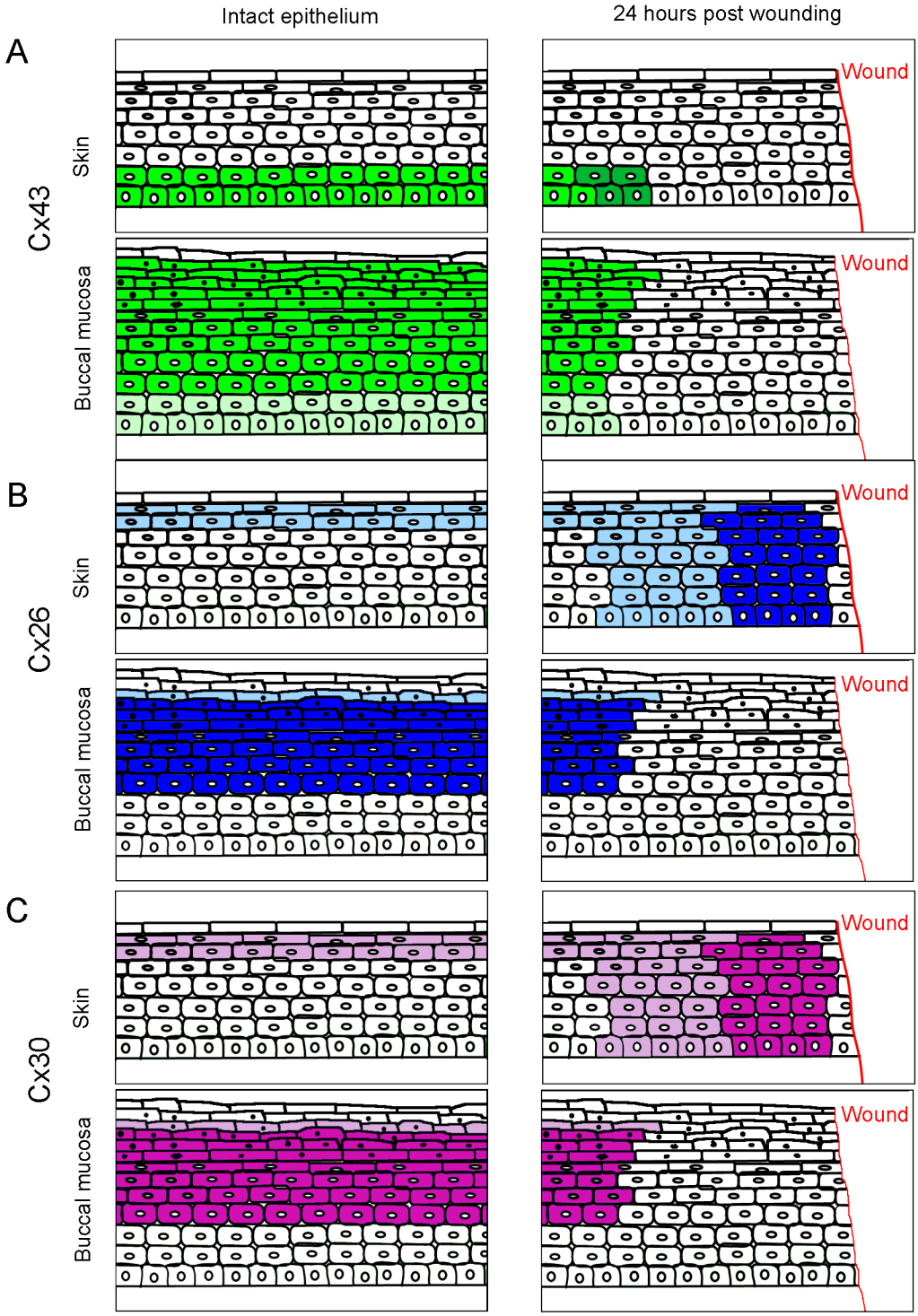

Figure 3.6 Diagram of the connexin expression in the cheek epidermis and in buccal mucosa in intact tissue and at 24 hours after wounding. The expression patterns of Cx43 **(A)**, Cx26 **(B)** and Cx30 **(C)** are shown. The darkness of the colours indicate the extent of expression, with darker colours representing high expression levels, and lighter colours indicating lower expression levels.

hyperproliferative epidermis; high levels of Cx26 are found in hyperproliferative epidermis such as viral warts, psoriasis and porokeratosis (Hivnor et al. 2004; Lucke et al. 1999); and high levels of Cx30 are present in the epidermis in psoriatic and porokeratotic skin (Lemaître et al. 2006). Whilst buccal mucosa isn't hyperproliferative, it is a very thick epithelium with a rapid rate of proliferation, thus sharing some similarities with hyperproliferative epidermis.

Cx26 expression has been implicated in keratinocyte proliferation and differentiation (Brissette et al. 1994; Goliger & Paul 1995), though the precise role Cx26 plays in either process is still contentious. Double labelling for Cx26 and Ki67, a marker for proliferation, in hyperproliferative psoriatic lesional epidermis showed most Cx26 expressing cells did not express Ki67 (Lucke et al. 1999). However, in *in vitro* experiments where Cx26 was over-expressed significantly in keratinocytes, cells exhibited both significantly increased proliferation and migration rates compared to vector-only controls (Man et al. 2007). Furthermore, ectopic over-expression of Cx26 in the epidermis of transgenic mice also increased proliferation of keratinocytes, and resulted in a hyper-thickened epidermis. However, these mice exhibited impaired wound healing compared to wild type litter mates, with only 42% completing re-epithelialisation by day 21 compared to full wound closure in all wild type mice by day 14 (Djalilian et al. 2006). Upon wounding in skin Cx26 becomes elevated in the epidermis at the leading edge (Coutinho et al. 2003), but interestingly, in the faster healing buccal mucosa, it was found to be rapidly down-regulated. Cx26 down-regulation at the wound edge following injury has likewise been shown in hamster tongue, a slower healing parakeratinised oral mucosa that also highly expresses Cx26 (Saitoh et al. 1997).

The presence of high levels of Cx30 in buccal mucosa, and its subsequent rapid down-regulation at the wound edge are shown here for the first time. The rapid reduction in Cx30 expression in the epidermis upon wounding is similar to that of Cx26 (Coutinho et al. 2003), and similarly its role in the process remains elusive. As with Cx26, overexpression of Cx30 in keratinocytes reportedly caused a significant increase in migration and proliferation compared to vector only controls (Man et al. 2007). Enhanced cell proliferation was also observed in Cx30 over-expressing cancer cells (Ozawa et al. 2007), but conversely,

double labelling of Cx30 and Ki67 in *in vivo* wound healing suggest an inverse relationship between Cx30 and proliferation (Coutinho et al. 2003).

Thus, the dynamics of Cx26 and Cx30 in oral wound healing are different from those seen in skin as instead of increasing in expression they rapidly decrease, and this feature may reflect the faster healing process. Both Cx26 and Cx30 are able to bind to other junctional and cytoskeletal proteins such as Zonular Occludens-1, Occludin, Actin and Tubulin (Penes et al. 2005; Nusrat et al. 2000; Qu et al. 2009). Whilst expression of Cx26 and Cx30 may be involved in proliferation, elevated Cx26 and Cx30 expression in the wound edge cells of skin lesions, and the subsequent binding to other junctional and cytoskeletal elements, may slow their migration in skin wounds. It remains to be determined whether re-epithelialisation of skin lesions is improved in the absence of either Cx26 and or Cx30. It is possible the gap junction communication requirements for the healing of these two different epithelia are different and that communication is required in the leading edge cells of the skin but not in the buccal mucosa.

Chapter 4. *Staphylococcus aureus* Biofilm Exotoxins Induce Senescence in Fibroblasts and Impair Their Migration by a Cx43 independent mechanisms

4.1. Introduction

Cutaneous wound healing is a complex process, involving the coordination of a plethora of cell types and signals (Shaw & Martin 2009). Fibroblasts play an important role during healing; they must proliferate and migrate into the wound bed, laying down extracellular matrix to form granulation tissue, over which keratinocytes in the epidermis will migrate in order to restore barrier function.

Wound healing does not always proceed as it should though, which is the case for chronic wounds, which are open for 3 months or more (Menke et al. 2007). These wounds typically have dermal fibrosis, defective granulation tissue formation and poor ECM remodelling (Herrick et al. 1992; Menke et al. 2007). Several abnormal features have been reported in fibroblasts isolated from chronic wounds, including reduced proliferation and migration (M. V Mendez et al. 1998; Brem et al. 2007; Ågren & Steenfos 1999). High levels of senescence have also been reported in chronic wound fibroblasts, with increased rates of senescence observed in one study in regions of higher bacterial load (Ågren & Steenfos 1999; M. V. Mendez et al. 1998; a C. Stanley et al. 1997; Vande Berg et al. 1998).

A common feature of chronic wounds is a sustained but low-level of inflammation, which is associated in part with bacterial contamination. Bacterial infection is in fact thought to be one of the underlying causes of impaired healing in chronic wounds, primarily by causing the sustained inflammation which in turn causes tissue damage (Mustoe et al. 2006; Bjarnsholt et al. 2008). Bacteria in these wounds are typically found within a biofilm, a community of sessile bacteria encased in a self-produced matrix (James et al. 2007). *Staphylococcus aureus* is a pathogenic species, and is one of the species most commonly isolated from chronic wounds, where it was detected in 89-95% of venous leg ulcers (Davies et al. 2004; Gjødsbøl & Christensen 2006). *S.aureus* secrete a range of exotoxins, and proteomic and gene expression analysis has showed that the products they secrete when in biofilms differ from those secreted by freely moving planktonic bacteria (Resch & Rosenstein 2005; Secor et al. 2011). *S.aureus* biofilm secreted products can be collected in cell culture growth medium, and is referred to as biofilm conditioned medium (BCM). BCM

from a methicillin resistant clinical isolate of *S.aureus* was found to reduce the viability and migratory ability of both keratinocytes and fibroblasts (Kirker et al. 2009; Kirker & James 2012).

Connexin43 (Cx43) is expressed by numerous cell types in the skin, including keratinocytes, fibroblasts and endothelial cells, and is important during wound healing (Di et al. 2001; Richard 2000). Its expression affects multiple cellular processes, including apoptosis, proliferation and migration, and low levels of expression have also been suggested as a marker of senescence (Dbouk et al. 2009; Statuto et al. 2002; Stein et al. 2008; Zhao et al. 2004). Cx43 expression changes dynamically during wound healing, initially becoming down regulated at the wound edge in both keratinocytes and fibroblasts (Goliger & Paul 1995; Coutinho et al. 2003; Mendoza-Naranjo, Cormie, A. Serrano, et al. 2012). Genetic knockout of Cx43 in skin, or a rapid reduction in expression through the use of Cx43 antisense, increased the rate of healing by increasing the rate of re-epithelialisation, granulation tissue production and maturation (Qiu et al. 2003; Mori et al. 2006; Kretz et al. 2003).

In chronic wounds Cx43 expression is abnormal, remaining high (Brandner et al. 2004), or even becoming elevated, at the epidermal and dermal wound edge (Mendoza-Naranjo, Cormie, A. E. Serrano, et al. 2012; Mendoza-Naranjo, Cormie, A. Serrano, et al. 2012). The cause of abnormal Cx43 expression in chronic wounds is as yet unknown. However, these wounds are contaminated with bacteria, commonly *S.aureus*. *S.aureus*, or molecules derived from this bacterium, can alter Cx43 expression in multiple cell types including fibroblasts, keratinocytes and endothelial cells (Garg et al. 2005; Esen et al. 2007; Robertson et al. 2010; Donnelly et al. 2012). It is not known whether *S.aureus* biofilm exotoxins also affect Cx43 expression. The hypothesis tested in this chapter is that one mechanism by which *S.aureus* exotoxins impair healing is by contributing to the abnormal Cx43 expression seen in dermal chronic wounds.

4.2. Materials and methods

See Chapter 2 for general materials and methods. Materials and methods used only in this chapter are described here.

4.2.1. Biofilm Conditioned Medium (BCM)

DMEM supplemented with 10% DBS was added to wells in a 6 well plate. Each well held a 0.4 µm pore cell culture insert containing a sterile mixed cellulose ester hydrophilic membrane filter disc with 0.22 µm pore size. An overnight culture of *Staphylococcus aureus* subspecies. *aureus* ATCC® 29213™ (hereafter referred to as *S.aureus*) was washed and diluted to an OD600 of 0.05. Seven 10 µl drops were placed on each filter disc and biofilms were allowed to develop and mature for 72 hours. The media was harvested every 24 hours for four days thereafter and filter sterilized. The collected medium is referred to as BCM.

4.2.2. MTT assay

Cells were grown in flat bottom 96 well plates with good optical quality (Falcon), and incubated with HKSA or BCM at varying concentrations for 24 or 48 hours in 100 µl. At the end point of the experiment 10 µl of 3-(4,5-dimethylthiazol-2-yl)-2,5-diphenyl tetrazolium bromide (MTT, Millipore) was added per well. Cells were incubated at 37 °C for 2 hours. The media was carefully removed, and the MTT formazan dissolved in 100 µl of isopropanol with 0.04 N HCl. The absorbance at 570 nm was measured on an ELx800 Absorbance Microplate Reader (BioTek) using Gen5 plate reading software (BioTek). The absorbance at 630 nm was also measured as a reference wavelength, and deducted from the 570 nm reading. Results were quantified as a percentage of the control's absorbance.

4.2.3. Cell counts

Cells were grown in 6 wells plates in BCM or DMEM supplemented with 10% DBS. At the indicated time points cells were washed, trypsinised, and re-suspended in media. The number of cells in an aliquot were counted using a Scepter™ hand held automated cell counter (Millipore) using 60 µm sensors (Millipore) and gating identically.

4.2.4. Senescence associated β-galactosidase activity stain

Cells were grown for 7 days with BCM, changing the media every 2-3 days. On day 6 the BCM cultured cells and control cells were plated in 24 well cell culture plates for imaging. On day 7 the media was removed and cells washed with PBS before fixing in 4% PFA in PBS for 5 minutes at room temperature. They were washed again and the senescence associated β-galactosidase (SA-βGal) staining solution added to each well (see table 2.1. for the recipe). Cells were incubated with the staining solution in the dark at 37 °C for 24 hours then washed twice in PBS. Cells were imaged on a Ix81-ZDC microscope (Olympus) equipped with an DP72 digital colour camera (Olympus), using Xcellence rt imaging system software (Olympus). 15 regions were imaged per well. The percentage of cells in each image with senescence associated β-galactosidase activity (as determined by the blue colour) was determined. Images were blinded to attenuate potential observer bias.

4.2.5. Measuring nuclear size

Images of cells used to assess (SA-βGal) were imported into Image J. The free hand tool was used to draw around the nuclei and the area was measured in pixels, and then converted to μm^2.

4.2.6. Scratch wound experiments

Cells were plated in 96 well ImageLock tissue culture plate (Essen BioScience) 48 hours before the experiment and grown to confluence. All scratch wound experiments were conducted both with and without the growth inhibitor, mitomycin C. On the day of the experiment, the media was removed from wells that were to be treated with growth inhibitor. This was replaced with DMEM supplemented with 10 μg ml^{-1} mitomycin C from *Streptomyces caespitosus* (Sigma) and incubated for 2 hours. This concentration was chosen after a pilot, and was tested for growth inhibitory effects and cytotoxicity by live imaging of proliferation and propidium iodide uptake (see protocol 2.4.3.). After 2 hours the media was removed from all wells, and cells were washed with PBS. A scratch wound was made using a WoundMaker™ (Essen BioScience), and the cells washed again. BCM, or DMEM supplemented with 10% DBS (controls), was

added and each well imaged every 2 hours for 48 hours on an IncuCyte™ FLR (Essen BioScience). The relative wound density (RWD) was calculated using the IncuCyte 2010A software (Essen BioScience). This is a percentage measure of the density of the wound region relative to the density of the cell region. The distances migrated were calculated by importing 0, 4 and 12 hour images into Image J software (NIH) and manually drawing the leading edge. A plugin, written by Daniel Cintar in UCL Data Analysis, was used to determine the distance migrated from the average central point of the leading edge at 0 hours to the average central point of the leading edge at 4 and 12 hours.

4.3. Results

4.3.1. Incubation with BCM reduces the rate of proliferation

It was determined whether BCM, created using the toxic ATCC® 29213™ *S.aureus* strain, affected the viability of 3T3 fibroblasts. Fibroblasts were incubated with increasing concentrations of BCM for 24 or 48 hours, and then their viability, compared to controls, was assessed using MTT assays (figure 4.1. A and B). The MTT assay is a colorimetric technique often used to assess viability of cells, as only live cells with active NAD(P)H-dependent oxidoreductase enzymes are capable of reducing yellow MTT to insoluble blue formazan crystals; the extent of blue coloration is measured by absorbance at 570 nm and reflects the number of viable cells (Meerloo et al. 2011). A trend was apparent, particularly at the 48 hour time point, whereby increasing concentrations of BCM were associated with decreasing absorbance. At both the 24 and 48 hours incubation with 75% and 100% BCM caused a significant reduction in the absorbance reading, with the effect greatest after 48 hours.

Although MTT assays are normally used as an indicator of the viability of a population of cells, changes in metabolic activity can also influence the results; a reduction in both metabolic activity and the number of viable cells will reduce the production of formazan from MTT (Sumantran 2011). Therefore to support the results of the MTT assays, cell counts were also taken of controls and of fibroblasts incubated with 100% BCM, at 0, 24 and 48 hours (figure 4.1.C). Incubation with 100% BCM resulted in significantly fewer cells than in controls at both 24 and 48 hours. Moreover, the population of control fibroblasts more than doubled between 0 and 24 hours (2.7±0.4 fold), and doubled again between 24 and 48 hours (1.9±0.1 fold), whereas fibroblasts incubated with 100% BCM proliferated slower, growing 1.7±0.3 fold between 0 and 24 hours, but barely proliferating between 24 and 48 hours (1.08±0.004 fold increase in cell count).

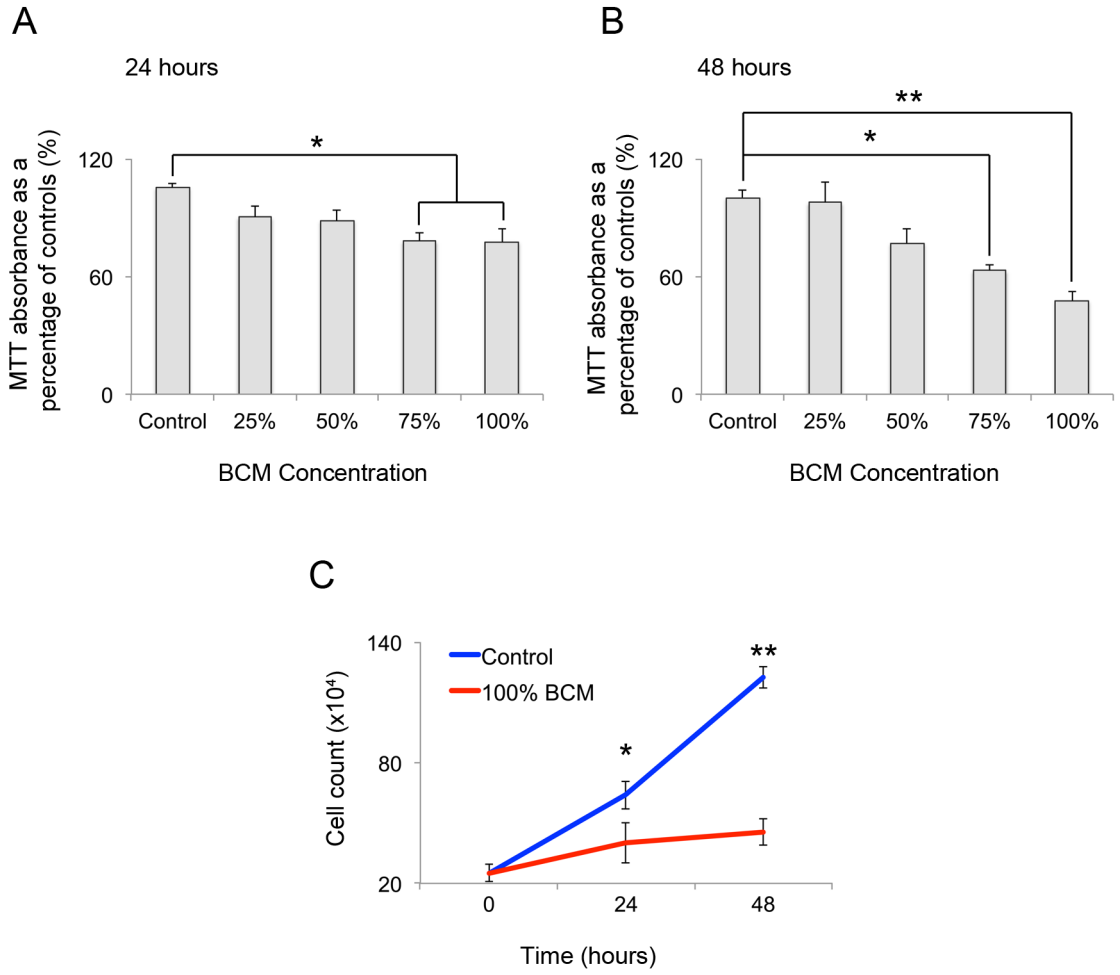

Figure 4.1. Incubation with biofilm conditioned medium (BCM) reduces cell number. (A, B) Graphs illustrating MTT absorbance at 24 **(A)** and 48 **(B**) hours when 3T3 fibroblasts were incubated with increasing concentrations of BCM. A one-way ANOVA showed significant differences between the groups at 24 hours ($p<0.05$) and 48 hours ($p<0.001$). A Tukey's post hoc revealed that incubation with 75% and 100% BCM caused significant differences from controls at both time points. N=4. **(C)** Graph showing the number of cells counted in controls, or after incubation with 100% BCM, over 48 hours. Independent Student's t-tests showed that there were significantly less cells in the 100% BCM group compared to controls at both 24 and 48 hours. N=3. All error bars are SEM. *$p<0.05$, **$p<0.01$.

Cell death is usually accompanied by a change in cell volume: apoptosis causes cell shrinking, while necrosis results in swelling (Orrenius & Sten 2001). The cell counts used to assess cell viability when incubated with 100% BCM were made using a Scepter™ handheld automated cell counter, which creates histograms of the cell's volumes and diameters. However, no statistically significant differences were observed in the volume or diameter of fibroblasts incubated with 100% BCM (figure 4.2.A-B), suggesting that the cells exposed to BCM were not dying. As neither of the techniques previously used to access viability (MTT assays or cell counts) allow a distinction to be made between cytostatic and cytotoxic effects it was possible that the fibroblasts were not dying, but instead failing to proliferate. To investigate this, the nuclei of cells incubated with 100% BCM for 24 hours were visualised by staining with Hoechst, and then observed for signs of apoptosis or necrosis. Apoptosis normally causes nuclear fragmentation and chromatin condensation, and necrotic cells exhibit nuclear swelling (Orrenius & Sten 2001). However, the nuclei of cells incubated with 100% BCM for 24 hours appeared healthy, exhibiting no morphological signs of either necrosis or apoptosis (figure 4.2.C). This agrees with the data showing cell volume and diameter are not altered by incubation with 100% BCM, and indicates that the reductions seen in cell counts and in absorbance in the MTT assays were not the result of reduced viability, but of reduced overall cell number. To determine if this was the case fibroblasts were incubated with 100% BCM or control media and imaged hourly over 24 hours (figure 4.2.D-E). The cell's nuclei were labelled with Hoechst, which enabled the rate of cell proliferation to be assessed by comparing the total number of cells at each time point. Throughout the experiment the medium also contained propidium iodide (PI). This dye is excluded by viable cells but readily enters cells that have lost membrane integrity, and so it is often used to assess cell viability (Johnson et al. 2013). By imaging both Hoechst (total number of cells per image) and PI labelled cells (non-viable cells), the changing percentage of non-viable cells in the population could be determined. By observing the fold change in cell number (figure 4.2.D), it was evident that incubation with 100% BCM significantly reduced the proliferation of 3T3 fibroblasts. The growth rate in the BCM group began diverging from controls at around 8 hours; the fold change of the controls remained exponential, whereas the fold change of BCM incubated cells began to plateau. At 11 hours

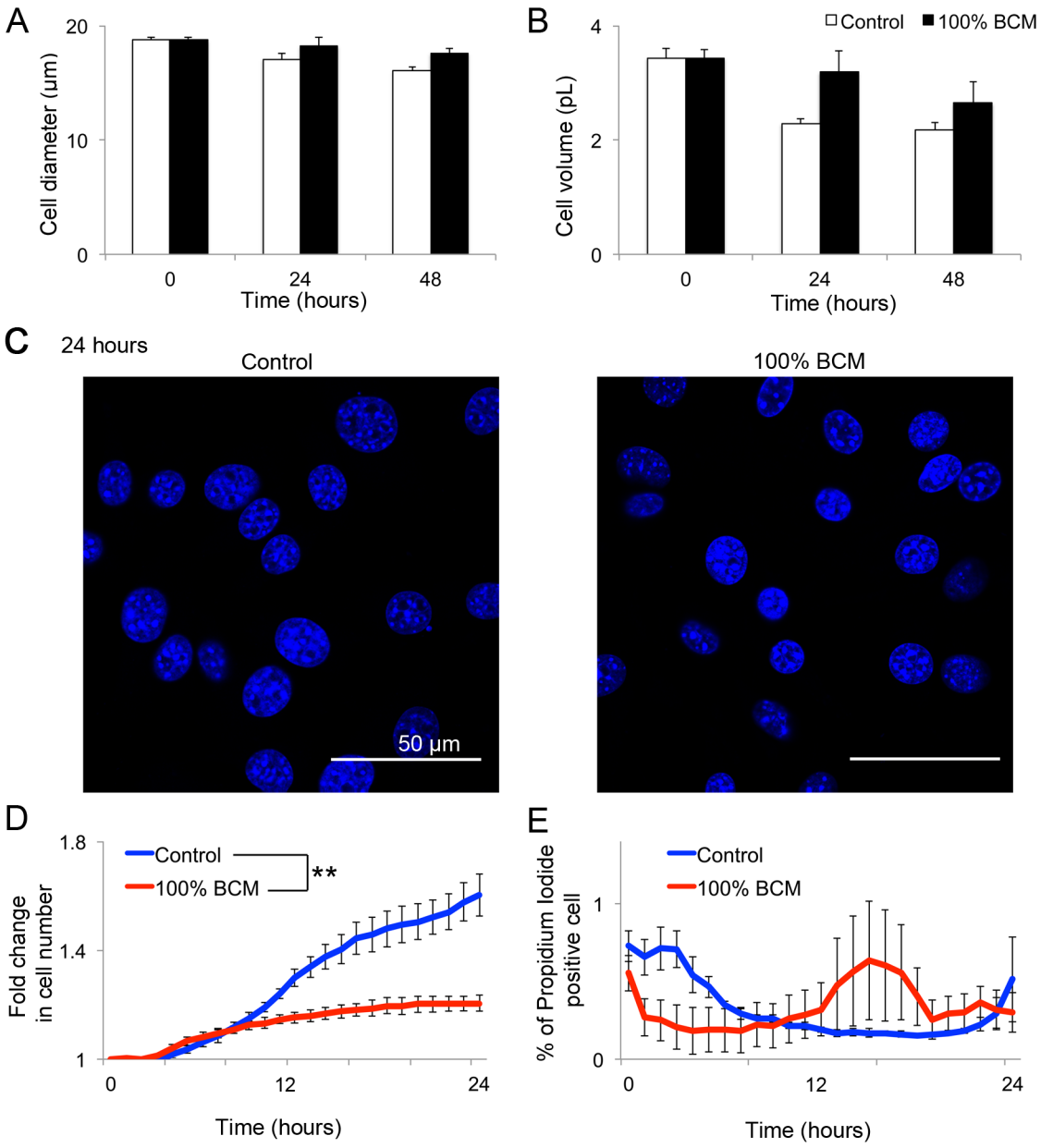

Figure 4.2. Incubation with 100% biofilm conditioned medium (BCM) prevents cell proliferation but doesn't reduce cell viability. (A-B) Graphs demonstrating the **(A)** diameter and **(B)** volume control and 100% BCM incubate cells at 0, 24 and 48 hours. **(C)** Confocal images of nuclei from 3T3 fibroblasts controls (left) and fibroblasts incubated with 100% BCM for 24 hours (right). The images are representative of 3 experiments. Scale bars indicate 50 µm. **(D)** Graph presenting the fold change in cell number over 24 hours as determined by live imaging of Hoechst labelled cells. There were significant differences in proliferation between control and 100% BCM at every time point after 11 hours ($p<0.05$ or <0.01). **(E)** The number of propidium iodide positive cells, as a percentage of the whole population over 24 hours is shown for control 3T3 fibroblasts, and fibroblasts incubated with 100% BCM. Mixed design ANOVAs or independent Student's t tests were used to test statistical differences as appropriate. A-B, N=3; D-E, N=4. All error bars are SEM. *$p<0.05$, **$p<0.01$.

significant differences between control and BCM incubated groups emerged, and the groups differed significantly at every time point thereafter. By 12 hours the fold change in cell number no longer increased in the BCM incubated group, suggesting that the cells had stopped proliferating, and had entered cell cycle arrest. The viability of the population was also assessed, by determining the percentage of the total population that were positive for PI (figure 4.2.E). This was low in both controls and cells incubated with 100% BCM. Less than 1% of cells were PI positive, and there were no differences between the groups

4.3.2. Incubation with 100% BCM for 7 days induces a senescent phenotype

Previous analysis revealed that incubation with 100% BCM attenuates proliferation of fibroblasts without affecting viability (figure 4.2.). Cessation of cell proliferation is the most prominent marker of senescence (Kuilman et al. 2010). Consequently, it was investigated whether cells incubated with BCM also were positive for other markers of senescence.

Cells were incubated with control medium or 100% BCM for 7 days. Senescent cells often exhibit morphological changes, such as enlargement of the cell and nuclei (Kuilman et al. 2010), and observations of the 100% BCM incubated fibroblasts suggested that they were enlarged with increased nuclear size. An example of a cell with these morphological features is indicated by the arrow in figure 4.3.C. Quantification confirmed that incubation with 100% BCM resulted in an increased nuclear size compared to controls (Figure 4.3.A), suggesting that incubation with 100% BCM may be inducing senescence.

Senescence associated β-galactosidase (SA-β-gal) activity is probably the most commonly used biomarker to determine senescence in cell culture. This is a cytochemical technique, which uses the substrate X-gal to detect lysosomal β-galactosidase activity at the suboptimal pH of 6.0 (Dimri et al. 1995; van der Loo et al. 1998). At this pH only senescent cells produce the blue stain, a result of increased levels of the lysosomal β-galactosidase enzyme (Kurz et al. 2000). To assess if BCM was inducing this marker of senescence, 3T3 fibroblasts were incubated with 100% BCM or control medium for 7 days, then examined for SA-

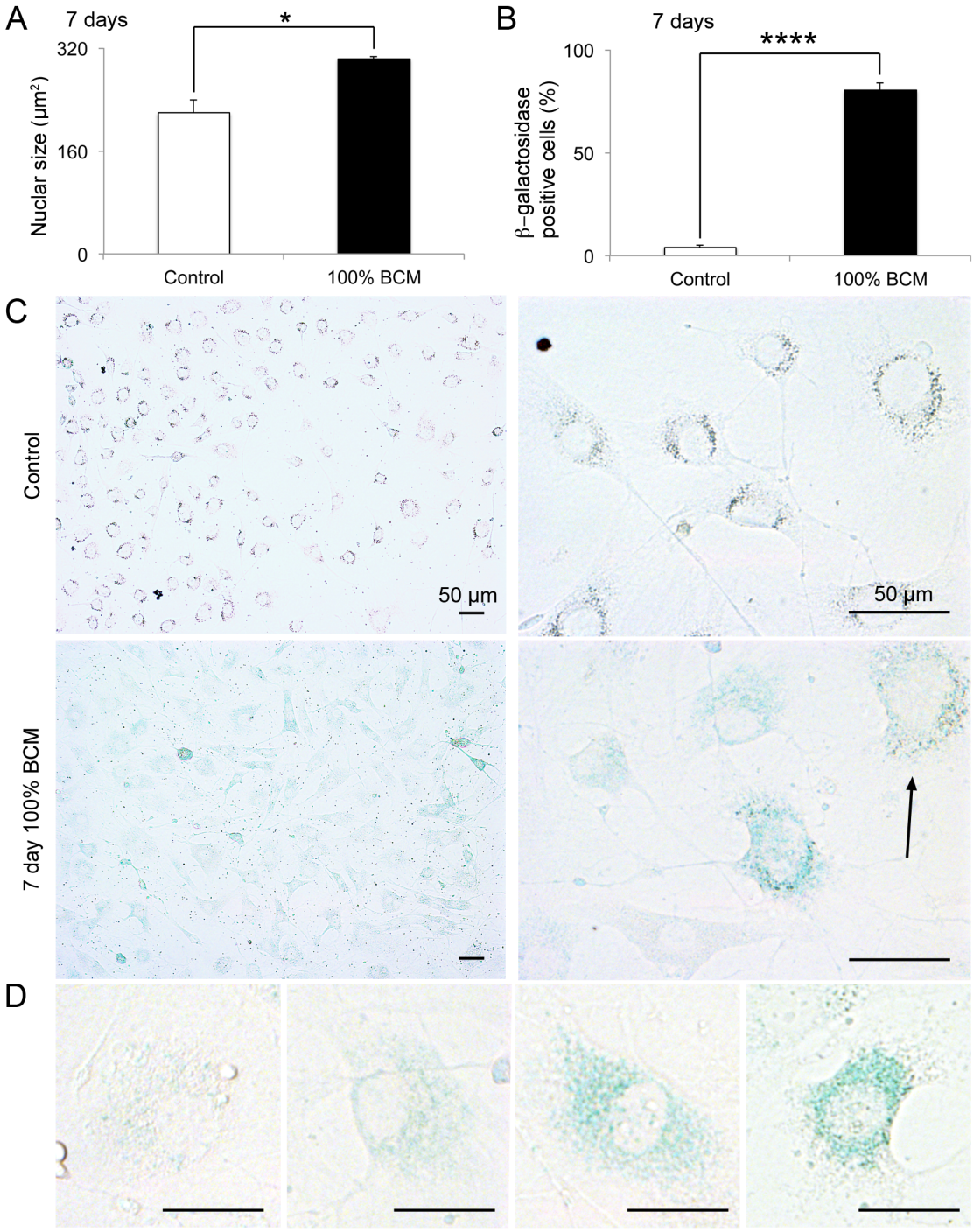

Figure 4.3. β-galactosidase activity in fibroblasts. (A) Graph illustrating the average nuclear area in μm^2. **(B)** Graph showing the percentage of imaged cells that were positive for β-galactosidase activity, as indicated by blue staining. **(C)** Images are shown of the β-galactosidase activity at pH 6.0, of controls (top panel), and of fibroblasts incubated with 100% BCM for 7 days (bottom panel), at both low and high magnification. The arrow indicates an example of an enlarged cell with a enlarged nuclei. **(D)** Example images are shown of cells incubated with 100% BCM, showing varying intensities of β-galactosidase activity, increasing from left to right. Independent Student's t tests were used to test statistical differences. N=3. All scale bars indicate 50 µm. All error bars are SEM. *p<0.05, ****p<0.0001.

β-gal activity (figure 4.3.B-D). Few controls cells exhibited any SA-β-gal staining (4.1% ± 0.9%). Conversely, 100% BCM incubated cells had elevated levels of SA-β-gal activity, with over 80.0% (± 3.7%) of the cells positive for SA-β-gal stain (figure 4.3.B-C). The extent and intensity of blue staining did vary between individual cells as is illustrated in figure 4.3.D. Some cells exhibited only small amounts of granular blue stain, such as in the example on the left of the panel, while others had intense blue stains, as in the example on the right of the panel. This variation suggests that there may be variability in the sensitivity of the population to incubation with BCM.

Another common feature of senescence is an increase in auto-fluorescence (Zglinicki et al. 1995). This is largely due to the lysosomal accumulation of lipofuscin, an auto-fluorescent pigment thought to be comprised of oxidatively damaged protein and lipids (Zglinicki et al. 1995). Fibroblasts were again incubated with 100% BCM or control medium for 7 days, and then examined for auto-fluorescence (figure 4.4). This was assessed on a confocal microscope, using a 488 nm laser. Control cells exhibited only faint auto-fluorescence. Conversely, many of the cells incubated with 100% BCM displayed intense granular cytoplasmic auto-fluorescence. Auto-fluorescence was not limited to excitation with a 488 nm laser, but also occurred to some extent when using a 405 nm laser. Regions that auto-fluoresced with both lasers appear pale blue in the combined 405 and 488 nm images. As with the SA-β-gal staining, the intensity of auto-fluorescence varied from between cells. Quantification of the auto-fluorescence per cell (figure 4.4.C) though, confirmed that the 100% BCM incubated cells exhibited significantly higher levels of auto-fluorescence than control cells. This analytical method normalises to the number of cells per image, so to validate this method it was confirmed that the number of cells per image didn't differ significantly between the groups ($p=0.92$; figure 4.4.D).

The combination of morphological signs of senescence and a reduction in proliferation, as well as increased SA-β-gal activity and auto-fluorescence provides credible evidence that incubation with 100% BCM for 7 days induces senescence in 3T3 fibroblasts.

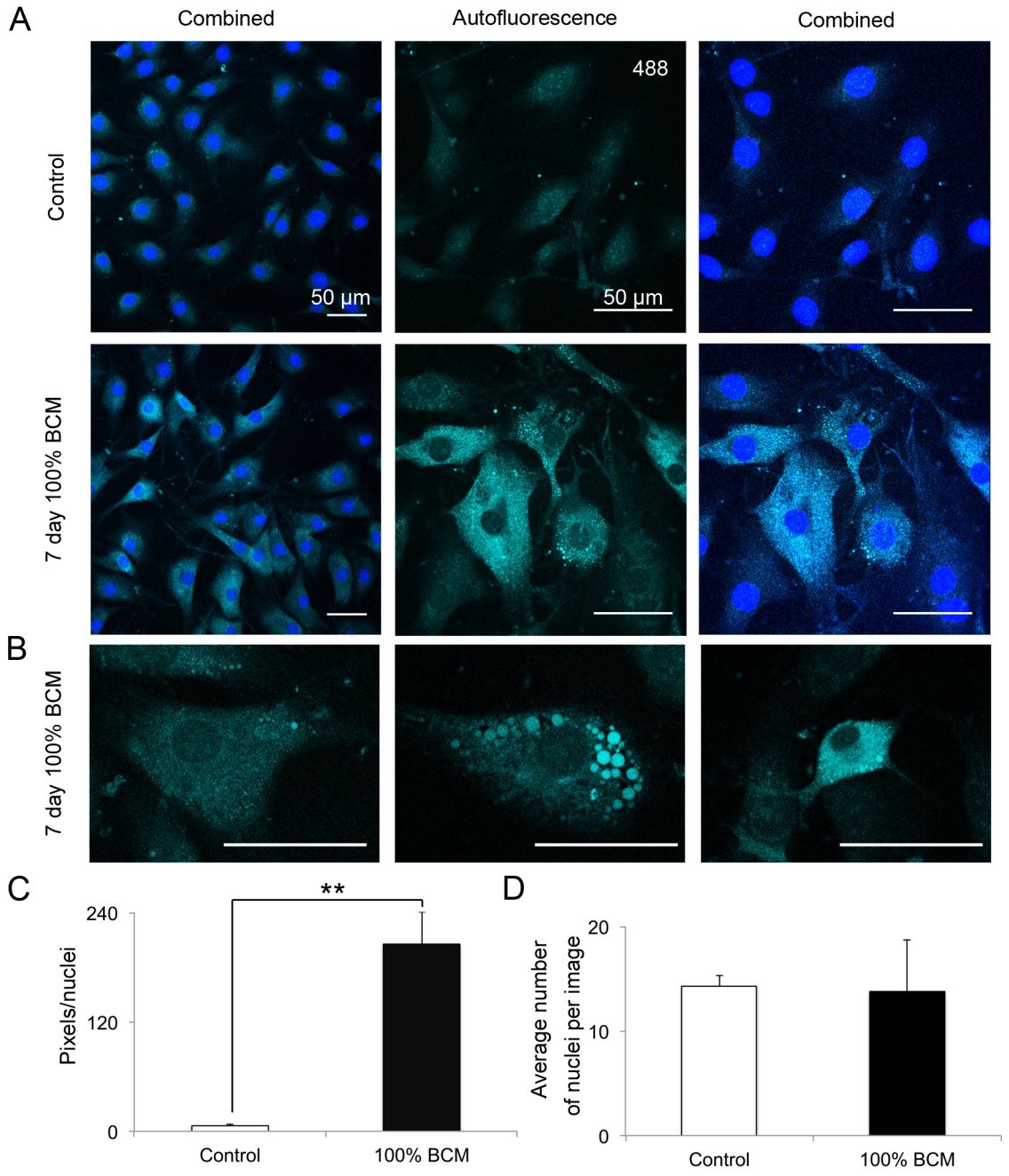

Figure 4.4. Incubation with 100% biofilm conditioned medium (BCM) induces senescent associated auto-fluorescence. (A) Images are shown of the auto-fluorescence emitted when controls (top panel) or fibroblasts incubated with 100% BCM for 7 days (bottom panel) were activated with a 488 nm laser. Low magnification images of auto-fluorescence are shown on the left, with nuclei counterstained with Hoechst (blue). High magnification images are shown of the auto-fluorescence only (middle), and of auto-fluorescence with nuclei counterstained (right). **(B)** Example images are shown of cells incubated with 100% BCM, showing varying intensities of autofluorescence, increasing from left to right. **(C)** Graph showing pixels per nuclei calculated from images of 488 nm auto-fluorescence. **(D)** Graph showing the average number of nuclei in the auto-fluorescent images. Independent Student's t tests were used to test for statistical differences between the groups. There was no difference in the average number of nuclei in each group. N=3. All scale bars indicate 50 µm. All error bars are SEM. **p<0.01.

4.3.3. Incubation with 100% BCM retards cell migration in scratch wound closure

It was determined whether BCM derived from the ATCC® 29213™ *S.aureus* strain impaired scratch wound closure. Confluent fibroblasts were scratched, and 100% BCM added to them immediately afterwards. The wounds were imaged every 2 hours for 48 hours. The impact on overall scratch wound closure was evaluated first (figure 4.5). Over 48 hours control wounds closed completely, leaving no visible sign of the original scratch (figure 4.5.A. top panel). Oppositely, incubation with BCM prevented the full closure of the scratch wounds in this time frame, as can be seen from the representative images taken at 24 and 48 hours after scratching (figure 4.5.A, bottom panel). Towards 48 hours, some BCM incubated cells did succeed in migrating across the whole distance of the scratch, coming into contact with cells from the other leading edge. However the cells did not migrate loosely together as is normal for fibroblasts, but rather individually. Quantification of the relative wound density (RWD, a percentage measure of the density of the wound region relative to the density of the cell region, calculated by the IncuCyte™ software) similarly showed that the scratches failed to close (figure 4.5.B). RWD increased only gradually in the BCM cells and plateaued at 55-60%, unlike the controls, which approached 90% within 30 hours. Significant differences between controls and the BCM incubated groups emerged after 20 hours, although the RWD of the BCM incubated cells appeared to begin diverging from controls after approximately 12 hours.

RWD analysis is a useful measure of wound closure, as it takes into account both the width of the wound and the density of cells within that wound. It thus provides information on the scratch closure that accounts for a combination of both proliferation and cell migration, the two major components of wound closure in cell culture. However, previous analysis of data has shown that incubation with 100% BCM prevents proliferation (figure 4.2). It is not known though, whether failure to close the scratch wounds was due entirely to the effect of BCM incubation on proliferation, or whether BCM also has an effect on cell migration. To determine whether incubation with BCM impairs migration

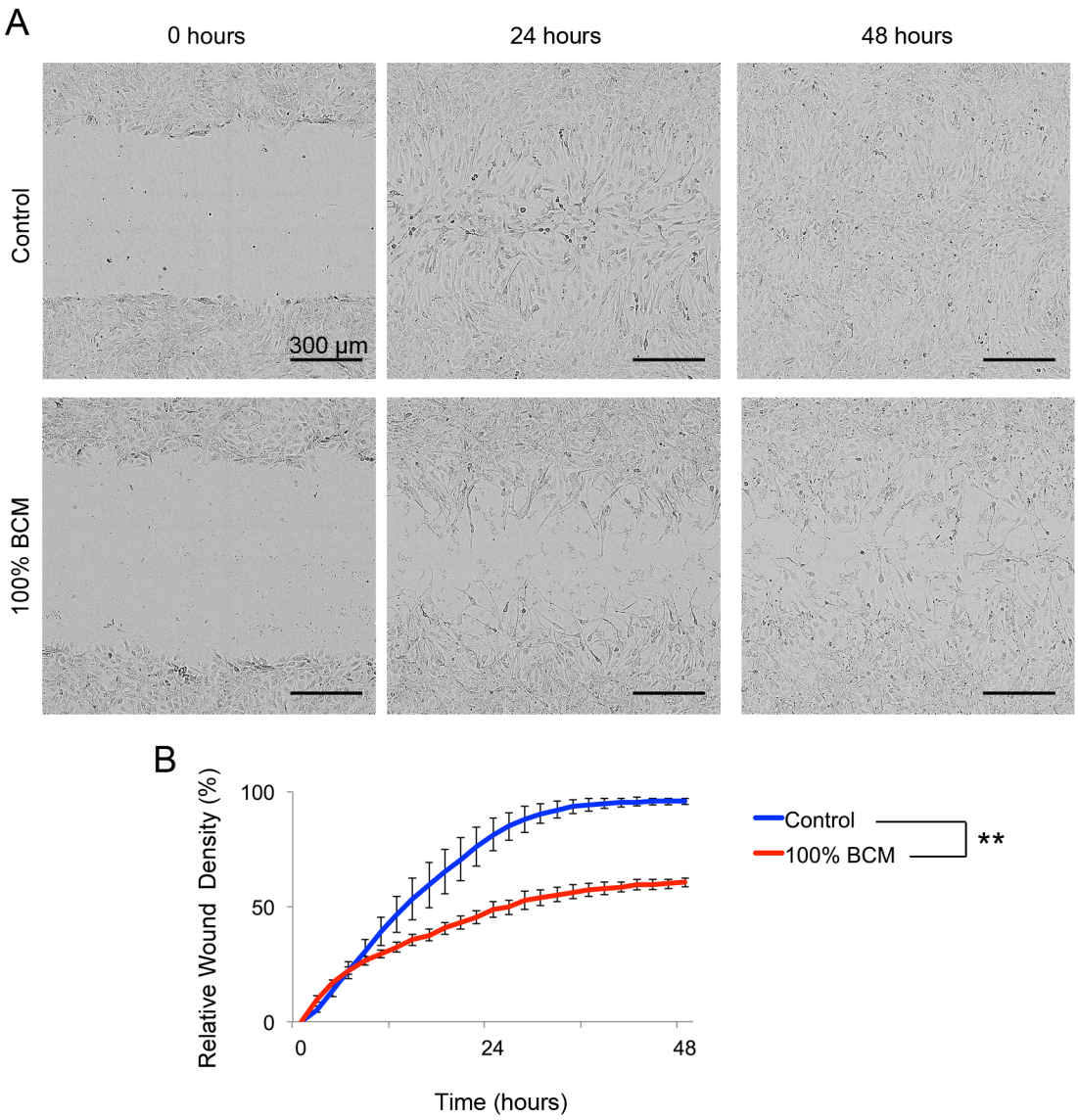

Figure 4.5. Incubation with 100% biofilm conditioned medium (BCM) prevents scratch wound closure of fibroblasts. (A) Images are shown of controls (top panel) and fibroblasts incubated with 100% BCM (bottom panel) at 0, 24 and 48 hours following scratching. Scale bars indicate 300 µm. **(B)** Graph showing the relative wound density, as calculated by Essen Bioscience IncuCyte™ 2010A software. A mixed design ANOVA was performed comparing the relative wound density of controls with 100% BCM incubated cells. The ANOVA showed that there was a significant difference between the groups. Independent Student's t tests showed significant differences at all time points after 20 hours. N=3. All error bars are SEM. **p<0.01.

manual measurements of the average distance migrated by the leading edge of cells was performed (figure 4.6).

Measurements were made at 4 and 12 hours. An early time point of 4 hours was selected, as this would indicate if initiation of migration was prevented. A later time point of 12 hours was also chosen, as this would reveal more subtle differences where migration was reduced, rather than prevented. Time points later than 12 hours could not be measured. This is because the top and bottom leading edge of many control wounds had come into contact, making it impossible to determine which leading edge each cell originated from.

Manual analysis of cell migration at 4 hours showed that there was no difference in the distance the leading edge had moved in controls and 100% BCM incubated cells at this time point (figure 4.6.B). At 12 hours, though, the leading edge of the controls had migrated significantly further than in the 100% BCM incubated group (figure 4.6.C), suggesting that by 12 hours incubation with 100% BCM had retarded migration. As previous analysis had revealed that at 12 hours incubation with BCM there was a significant reduction in proliferation compared to controls (figure 4.2.B), these experiments were also conducted with a proliferation blocker, mitomycin C. Mitomycin C is a powerful DNA crosslinker, which prevents cell proliferation (Tomasz 1995). This attribute means it is commonly used in scratch wound experiments to ensure only migration, and not proliferation, is being observed ((Liu et al. 2009). A concentration of 10 μg ml^{-1} was selected as it stopped proliferation, but was below cytotoxic levels (figure 4.7.A-B). As a control, it was also confirmed that treating control cells with mitomycin C had no significant impact on the distance they migrated compared to cells that had not been incubated with mitomycin C, at both 4 and 12 hours (figure 4.7.C-D). The same comparison was made for fibroblasts incubated with 100% BCM for 4 or 12 hours (figure 4.7.C-D); however, treatment with mitomycin C significantly increased the migration of 100% BCM incubated cells at 12 hours (figure 4.7.D). A comparison was then made of the distances migrated by scratched cells treated with mitomycin C then incubated with either control medium or 100% BCM (figure 4.7.C-D).

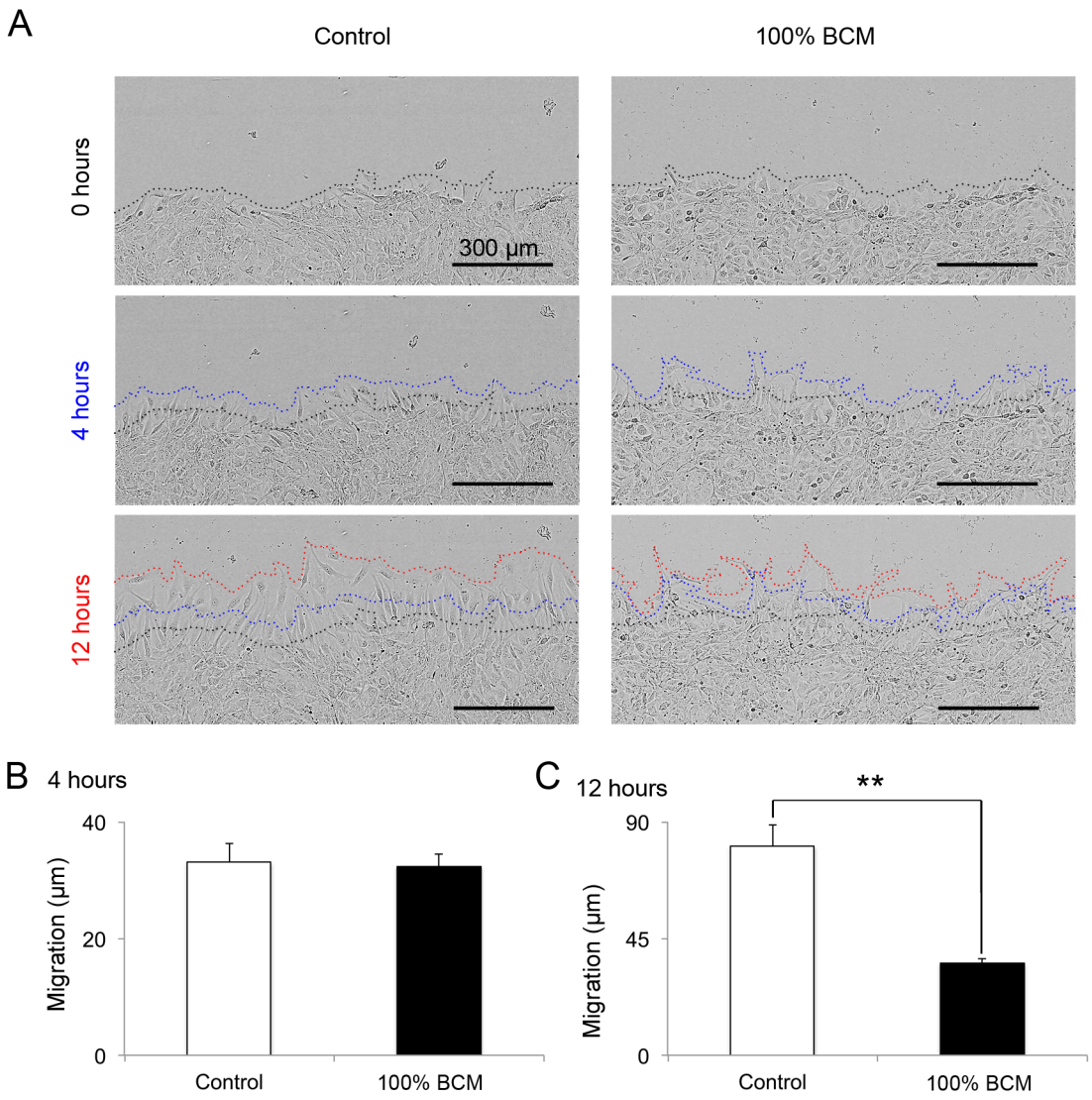

Figure 4.6. Incubation with 100% biofilm conditioned medium (BCM) impairs the migration of 3T3 fibroblasts. (A) Images are shown of controls (left panel) and fibroblasts incubated with 100% BCM (right panel) at 0 (black dotted line), 4 (blue dotted line) and 12 (red dotted line) hours following scratching. Scale bars indicate 300 µm. **(B)** Graph showing the distance migrated by cells by 4 hours. **(C)** Graph showing the distance migrated by cells by 12 hours. Independent Student's t tests showed no significant differences in the distance migrated by the groups at 4 hours, but significant differences at 12 hours. N=3 control, N=4 BCM treated. All error bars are SEM. **p<0.01.

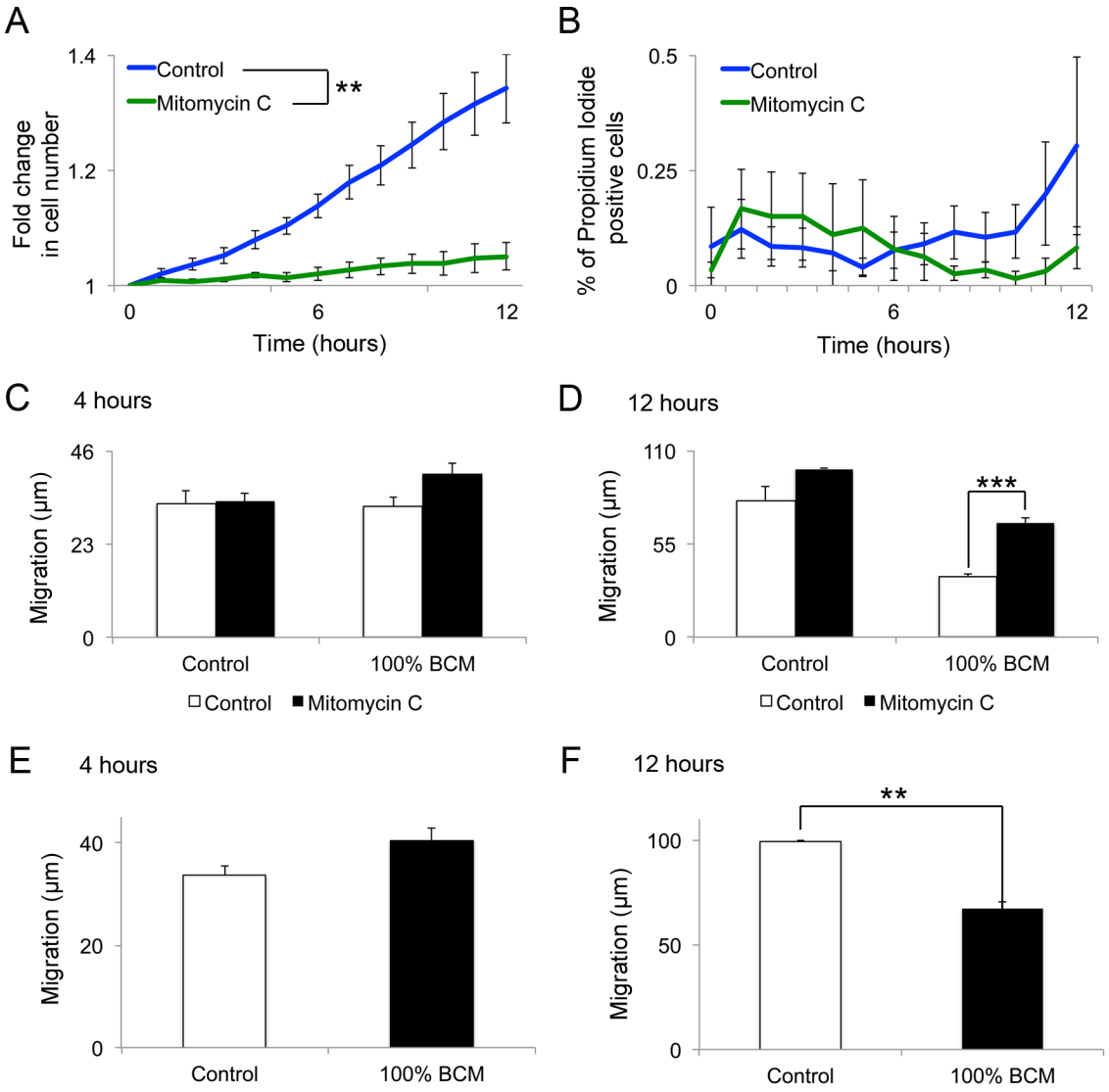

Figure 4.7. Incubation with 100% biofilm conditioned medium (BCM) impairs the migration of 3T3 fibroblasts when proliferation is also blocked. (A) The fold change in cell number, as determined by live imaging cells stained with Hoechst, is shown over 12 hours for controls and fibroblasts incubated with 10 µg ml-1 mitomycin C for 2 hours prior to imaging. A mixed design ANOVA showed there was significantly less proliferation in the 100% BCM group compared to the controls. **(B)** Graph showing the number of propidium iodide positive cells, as a percentage of the whole population over 12 hours. A mixed design ANOVA showed there were no significant differences between the groups. **(C-D)** Graphs showing the distances migrated by control or 100% incubated fibroblasts with and without mitomycin C at **(C)** 4 or **(D)** 12 hours. **(E-F)** Graphs showing the distance migrated by cells at **(E)** 4 or **(F)** 12 hours. Independent Student's t tests were used to determine statistical differences in the distances migrated. N=3. All error bars are SEM. **p<0.01.

Blocking proliferation did not alter the effect incubation with 100% BCM had on the distance migrated by the leading edge of cells; at 4 hours there was no difference in the distance migrated by controls and BCM incubated cells (figure 4.7.C), but at 12 hours the controls had migrated significantly further than the BCM incubated cells (figure 4.7.D), just as seen with the cells not treated with mitomycin C (figure 4.6). This shows that regardless of the impact BCM had on proliferation, incubation with 100% BCM also retarded migration of the leading edge of cells. However, the effect was not immediate as there were no differences in the distance migrated at 4 hours.

As well as differences in the distance migrated, the migrating BCM incubated cells exhibited altered morphology compared to controls (figure 4.8). The controls at the leading edge migrated loosely together, creating a relatively neat and uniform leading edge, where the cells primarily appeared cigar shaped. In contrast, the BCM incubated cells migrated more individually and appear less polarised towards the wound edge. The cells became very thin, their nuclei also appeared more prominent, and their lamellipodia became elongated and thin. Cells extended lamellipodia into the scratched region, but few of the cell bodies appeared to migrate forward compared to the controls, and it appears as though they may not be effectively retracting their tails. Interestingly, this phenotype was only observed when the 100% BCM incubated cells were scratch wounded, and not when they were static.

4.3.4. Prolonged incubation with 100% BCM reduces Cx43 protein expression

It was investigated whether *S.aureus* BCM altered Cx43 expression in 3T3 fibroblasts. An early time point (9.5 hours) was included to examine relatively rapid changes in Cx43 expression, and a 7 day time point to observe the effect of prolonged exposure to 100% BCM. 9.5 hours was selected as at this time point proliferation rates did not differ significantly from controls (section 4.3.1. and figure 4.2.B), which is important as cell density influences Cx43 expression. For the 7 day time point controls, an appropriate number of cells were plated 24 hours prior to the time point, in order to have a control cell density comparable to the BCM incubated cells.

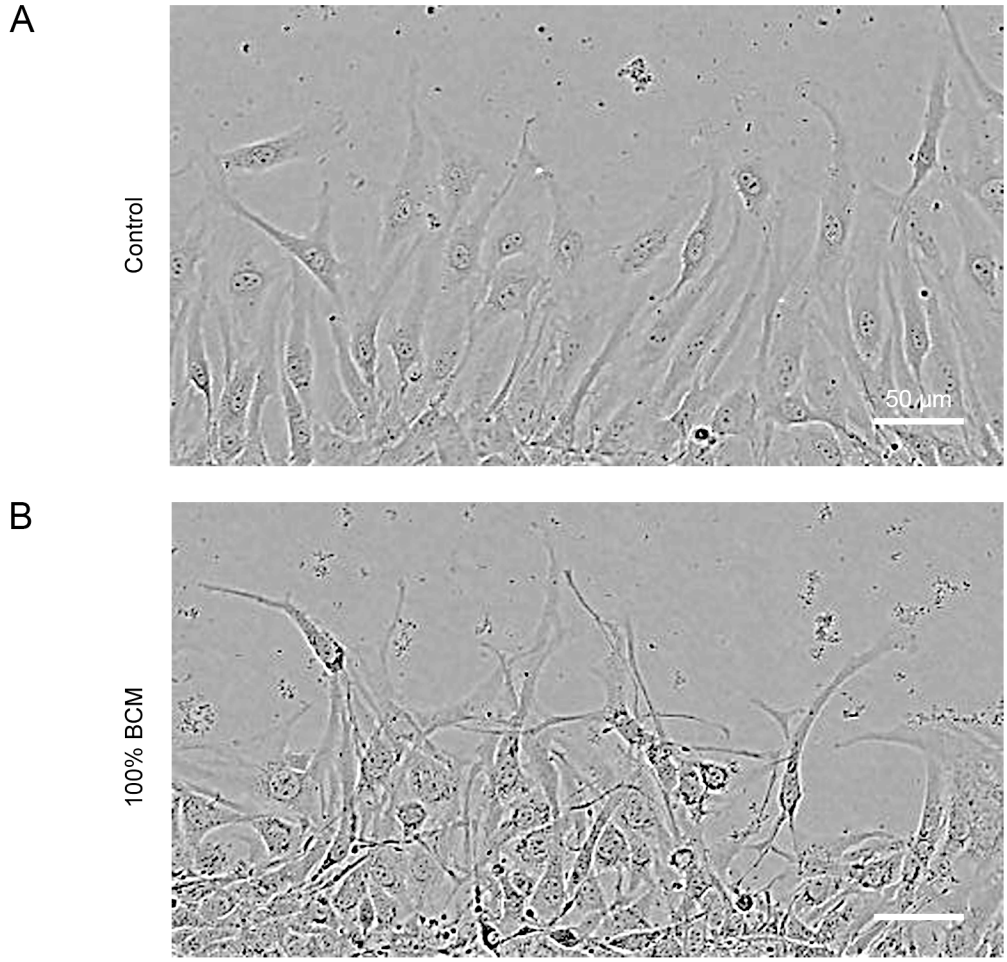

Figure 4.8. Incubation with 100% biofilm conditioned medium (BCM) alters the morphology of migrating cells. Representative images of the leading edge of migrating control cells **(A)** and cells incubated with 100% BCM **(B)** at 12 hours after scratching. Scale bars indicate 50 µm.

After 9.5 hours of incubation with 100% BCM, western blots showed that there was no change in total Cx43 expression compared to controls (figure 4.9.B). A comparison of the α-tubulin expression in each group validated this protein as a loading control, as its expression doesn't differ significantly between controls and BCM incubated cells (p=0.63) (figure 4.9.C). Cx43 separates into three bands when it is visualised by western blot. The fastest migrating band is referred to here as Cx43, and the two slower migrating bands are commonly referred to as Cx43 P1 and Cx43 P2. Cx43 can be phosphorylated at multiple sites, and the proteins at each western blot band are thought to be phosphorylated differently, resulting in different conformations related to the functional location of the protein within the cell (Solan & Lampe 2009). Densiometric analysis of the western blot confirmed that there were no detectable changes in the amount of each protein band (figure 4.9.D). From this it was concluded that incubation with 100% BCM for 9.5 hours does not influence Cx43 expression or phosphorylation in 3T3 fibroblasts. In contrast, incubation with 100% BCM for both 1 and 7 days resulted in a significant reduction in total Cx43 expression (figure 4.10.A-B). A comparison of the levels of each protein band showed that this was due to a significant reduction in expression of the Cx43 and Cx43-P1 protein bands (figure 4.10.E). A comparison of the α-tubulin expression in each group showed that it too was reduced by incubation with 100% BCM (figure 4.10.C). Instead, values were normalised to GAPDH expression. GAPDH was validated as a loading control, as its expression didn't differ significantly between controls and BCM incubated cells (figure 4.10.D).

4.3.5. Incubation with 100% BCM does not alter Cx43 location within cells

Western blots demonstrated that Cx43 protein expression is reduced when incubated with 100% BCM for 7 days, but not for 9.5 hours. However, western blot analysis does not allow visualisation of the location of connexins within the cells. Connexin distribution can be altered by several factors, including infection (Campos de Carvalho et al. 1998; Martínez & Sáez 2000), and so Cx43 protein expression was also visualised using immunofluorescence.

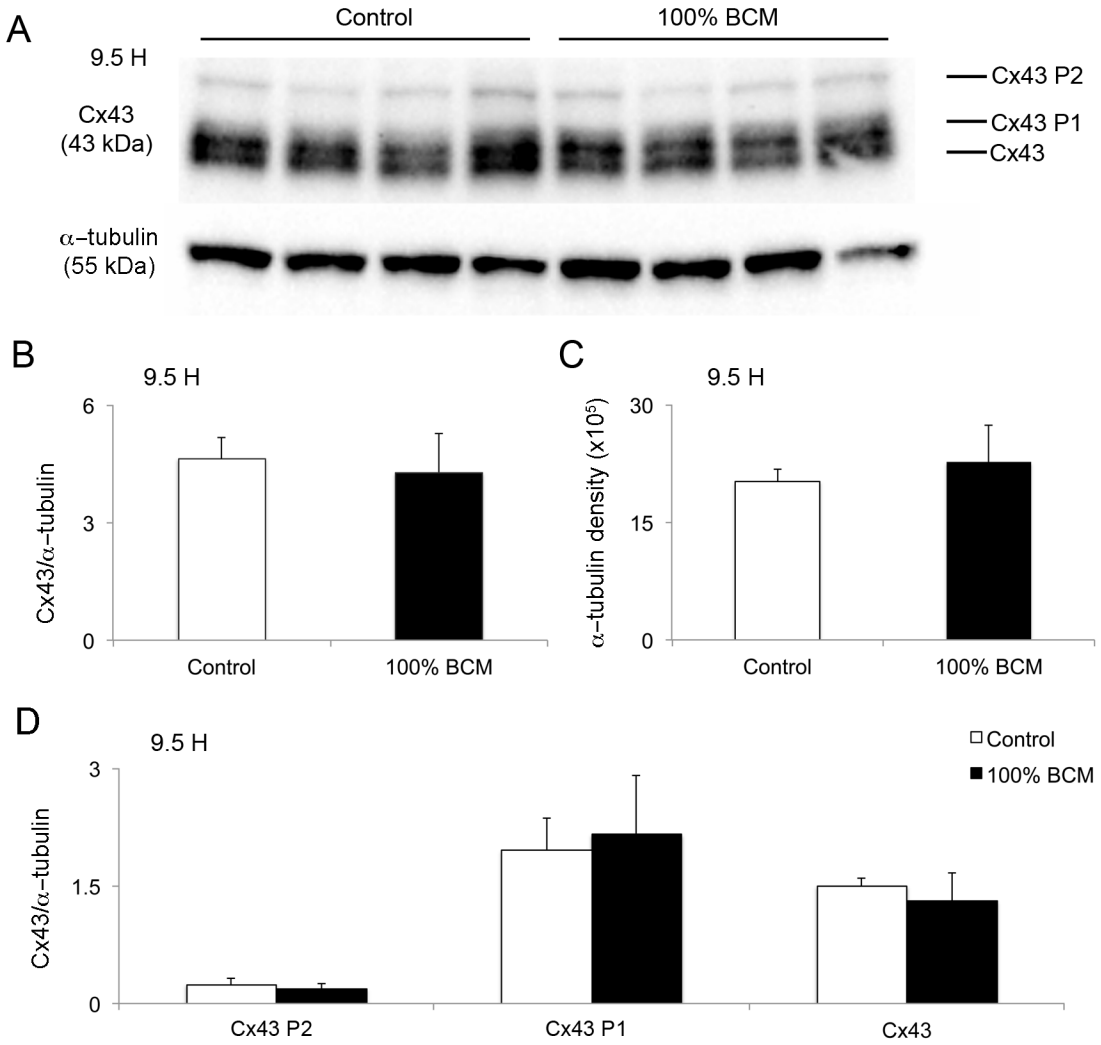

Figure 4.9. Incubation with 100% biofilm conditioned medium (BCM) for 9.5 hours has no effect on Cx43 protein levels. (A) A western blot showing Cx43 protein expression in controls and in fibroblasts incubated with 100% BCM for 9.5 hours. α-tubulin expression was used as a loading control. **(B)** Graph quantifying the total Cx43 expression relative to α-tubulin expression. **(C)** Graph quantifying the α-tubulin expression for control samples, and samples incubated with 100% BCM for 9.5 hours. **(D)** Graph quantifying the different bands of Cx43 seen on the western blot, which indicate the different phosphorylation statuses of Cx43. Expression is relative to total α-tubulin expression. Independent Student's t tests were used to test for statistical differences. These showed no significant differences between controls and BCM incubated. N=4. All error bars are SEM.

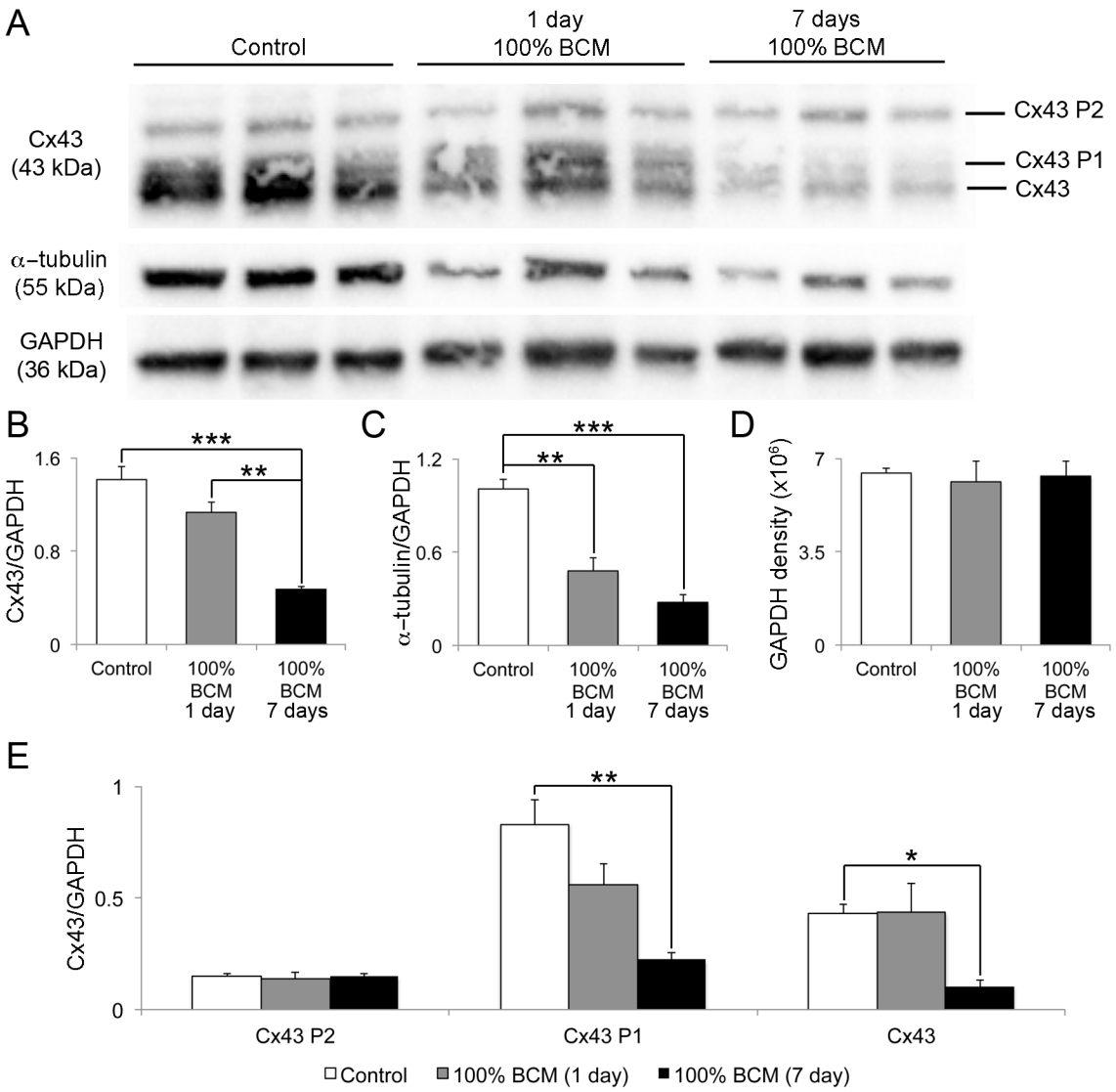

Figure 4.10. Prolonged incubation with 100% biofilm conditioned medium (BCM) reduces Cx43 and α-tubulin protein expression. (A) A western blot showing Cx43 and α-tubulin protein expression from a fibroblast control sample, a sample incubated in 100% BCM for 1 day, and a sample incubated in 100% BCM for 7 days. As a loading control, the GAPDH expression from the samples is also shown. **(B)** Graph quantifying the total Cx43 expression relative to GAPDH. **(C)** Graph quantifying the α-tubulin expression relative to GAPDH. **(D)** Graph quantifying the GAPDH expression. **(E)** Graph quantifying the different bands of Cx43 seen on the western blot, which indicate the different phosphorylation statuses of Cx43. Expression is relative to total GAPDH expression. Independent Student's t tests were used to test for statistical differences. N=3. All error bars are SEM. *p<0.05, **p<0.01, ***p<0.001.

Confocal images were taken of Cx43 immunofluorescence after 9.5 hours or 7 days incubation with 100% BCM (figures 4.11 and 4.12 respectively). Quantification of confocal images of Cx43 immunofluorescence at 9.5 hours (figure 4.11) confirmed the results seen by western blot (figure 4.9), as no differences in Cx43 expression levels were found. As this analytical method normalises to the number of cells per image, it was confirmed that the number of cells per image didn't differ significantly between the groups ($p=0.26$) (figure 4.11.C). Furthermore, no differences in the cellular location of Cx43 immunofluorescence were apparent following incubation with BCM for 9.5 hours. Quantification of confocal images following incubation with 100% BCM for 7 days (figure 4.12.A) also confirmed the results from western blots (figure 4.10), as a significant reduction in Cx43 expression was found (figure 4.12.B). The number of cells per image didn't differ significantly between the groups, validating the use of nuclei number as a normalisation method ($p=1.0$) (figure 4.12.D). Interestingly, as well as a reduction in Cx43 expression, the immunofluorescent images showed a significant reduction in the average Cx43 plaque size (figure 4.12.C). There was also a change in distribution of Cx43. In control cells Cx43 expression was high in foci around the nuclei and at intercellular junctions, with some diffuse cytoplasmic expression. In fibroblasts incubated with 100% BCM for 7 days, Cx43 was instead located diffusely throughout the cytoplasm (figure 4.12.A).

4.3.6. Incubation with 100% BCM reduces proliferation independently of Cx43 expression

It was investigated whether the effect of BCM incubation on proliferation would differ in fibroblasts where Cx43 has been knocked down. An 85% (±5%) reduction in Cx43 expression by 3T3 fibroblasts using shRNA was first confirmed by western blot (figure 4.13). 3T3 empty vector controls (EVs: it was confirmed that there were no statistical differences between EVs and non-transfected 3T3s in any of the assays performed in this chapter, data not shown) and fibroblasts with Cx43 constitutively knocked down (Cx43 shRNAs) were incubated with control medium or 100% BCM and imaged hourly for 24 hours.

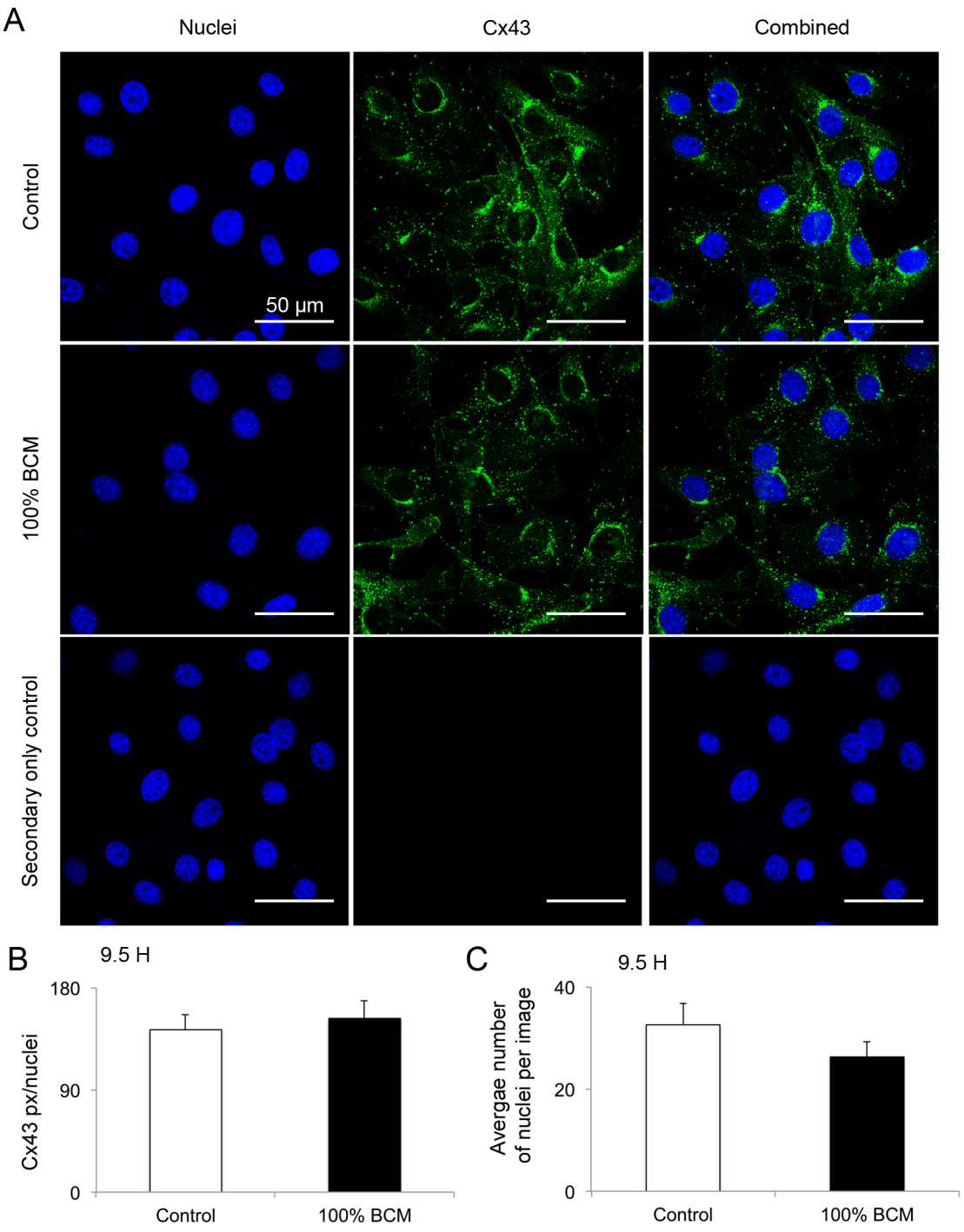

Figure 4.11. Cx43 localisation and expression within the cell is unaffected by incubation with 100% biofilm conditioned medium (BCM) at 9.5 hours. (A) Examples of immunofluorescent confocal images showing nuclei (blue) and Cx43 (green) in controls (top row) and in fibroblasts incubated with 100% BCM for 9.5 hours (middle row). A negative control using secondary antibody only is shown in the bottom panel. Scale bars indicate 50 µm. **(B)** Graph illustrating the Cx43 protein expression levels as quantified from confocal images, shown as Cx43 pixels per nuclei. **(C)** Graph showing the average number of nuclei in the Cx43 immunofluorescent images used to quantify Cx43 expression. Independent Student's t tests were used to test statistical differences. These showed no significant differences. N=4. All error bars are SEM.

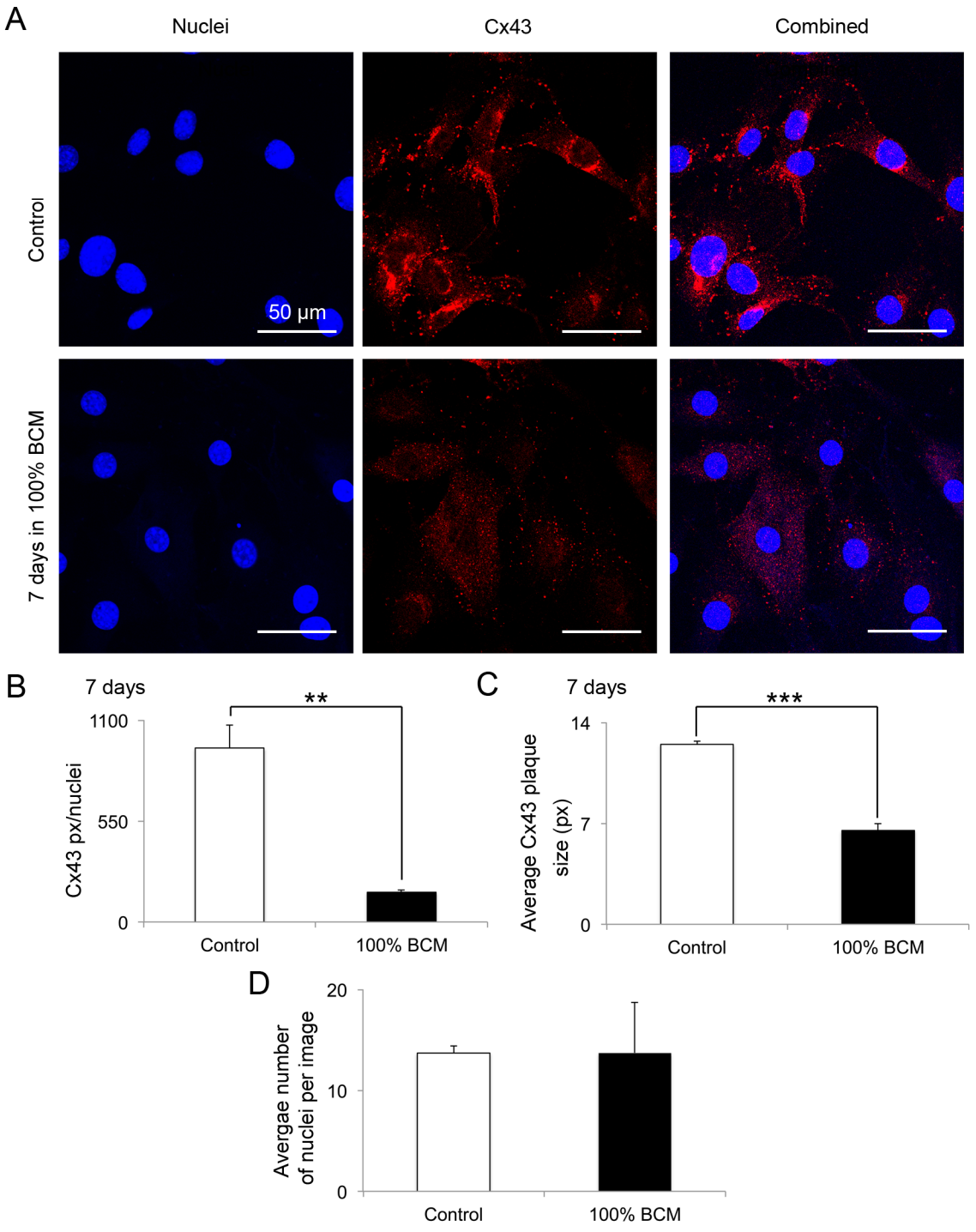

Figure 4.12. Cx43 expression is reduced by prolonged incubation with 100% biofilm conditioned medium (BCM). (A) Examples of immunofluorescent images of nuclei (blue) and Cx43 (red) in controls (top row) and in fibroblasts incubated with 100% BCM for 7 days (bottom row). Scale bars indicate 50 µm. **(B)** Graph showing Cx43 expression as pixels per nuclei. **(C)** Graph showing the average size of Cx43 plaques in pixels. **(D)** Graph showing the average number of nuclei in the Cx43 immunofluorescent images used to quantify Cx43 expression. Independent Student's t tests were used to test statistical differences between control and BCM incubated groups. N=3. All error bars are SEM. **p<0.01, ***p<0.001.

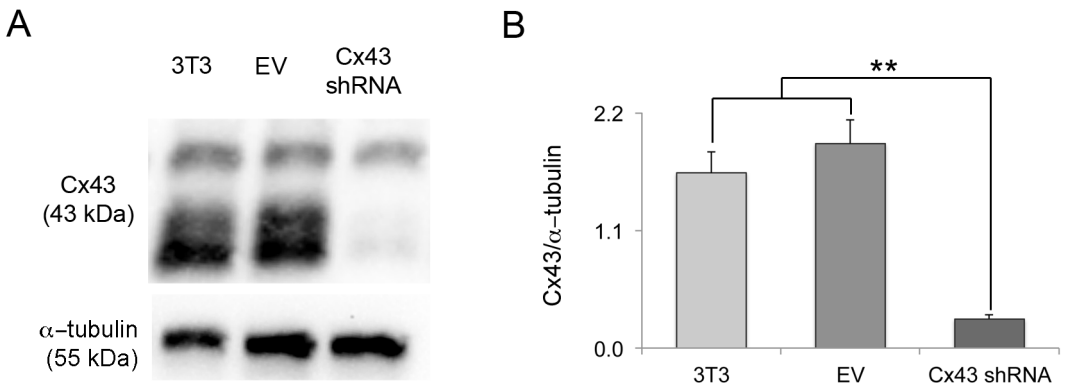

Figure 4.13. Cx43 is knocked down in Cx43 shRNA 3T3 cells. (A) Western blot showing Cx43 and α-tubulin expression in normal 3T3, EV, and Cx43 shRNA cells. **(B)** Graph showing Cx43 expression relative to α-tubulin expression. A One-way ANOVA and Tukey's post hoc showed a significant reduction in Cx43 expression in Cx43 shRNA cells compared to 3T3 and EV controls. N=3. All error bars are SEM. **p<0.01.

The nuclei were labelled with Hoechst and PI was included in the media, enabling determination of both proliferation and viability (figure 4.14). The fold change in cell number was compared (using a mixed design ANOVA) between all four groups: EV controls, EV incubated with 100% BCM, Cx43 shRNA controls and Cx43 shRNA incubated with 100% BCM (figure 4.14). Cx43 knockdown was previously shown to reduce the rate of fibroblast proliferation over 90 hours (Mendoza-Naranjo, Cormie, A. Serrano, et al. 2012). In line with previous evidence, control Cx43 shRNA cells appeared to proliferate slower than EV controls, but there was no statistically significant difference over this time period (24 hours). Incubation with 100% BCM significantly reduced proliferation in EVs and Cx43 shRNAs. However there were no significant differences in the fold changes between BCM incubated EV or Cx43 shRNA cells (figure 4.14.A). Knockdown of Cx43 expression did not alter the cell's proliferative response to incubation with 100% BCM. The percentage of PI positive cells was also compared for all four groups (figure 4.14.B). This was low in both controls and cells incubated with 100% BCM, with less than 1.5% of cells PI positive. Statistical analysis showed that there were no significant differences in the PI uptake of control EVs and Cx43 shRNA cells compared to the 100% BCM incubated counterparts.

4.3.7. The effect of incubation with 100% BCM on migration is independent of Cx43 expression

It was investigated whether the effect of incubation with 100% BCM on migration would differ in Cx43 shRNA cells. Scratch wound experiments were performed on EV and Cx43 shRNA fibroblasts, and the distance migrated by the leading edge was measured. All experiments were performed both with and without the proliferation blocker mitomycin C. As a control, it was first investigated whether treating cells with mitomycin C had an impact on the distance migrated by the cells (figure 4.15), by statistically comparing the distance migrated by the treated and untreated cells in each experimental condition. Blocking proliferation with mitomycin C had no significant impact on the distance migrated by control or 100% BCM incubated EV or Cx43 shRNA fibroblasts at 4 hours (figure 4.15.A and C).

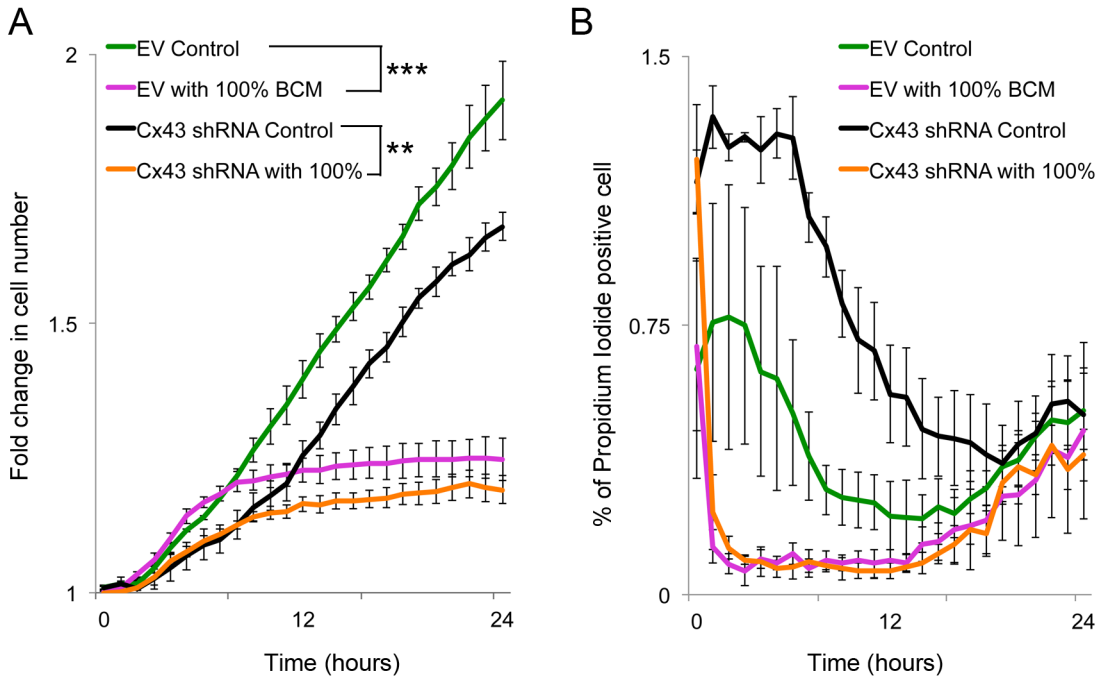

Figure 4.14. Incubation with biofilm conditioned medium (BCM) reduces proliferation in a Cx43 independent manner. (A) The fold change in cell number over 24 hours is shown for EV and Cx43 shRNA fibroblast controls and cells incubated with 100% BCM. A mixed design ANOVA comparing the fold change for all groups revealed significant differences ($p<0.001$). A Tukey's post hoc revealed that treating cells with 100% BCM significantly reduced fold change in cell number in both EV and Cx43 shRNA cells. **(B)** The number of propidium iodide positive cells, as a percentage of the whole population over 24 hours is shown for EVs and Cx43 shRNA fibroblast controls and cells incubated with 100% BCM. A mixed design ANOVA was performed comparing all groups which showed that there were significant differences. However Levene's Test of Equality of Error Variances showed there were considerable differences in variances, and a Games Howell post hoc was conducted which revealed that treating cells with 100% BCM had no significant effects on the percentage of propidium iodide positive cells. N=3. All error bars are SEM. **$p<0.01$, ***$p<0.001$.

Interestingly though, at 12 hours there was a significant increase in the distance migrated by mitomycin C perturbed control EV and Cx43 shRNA cells compared to untreated controls (figure 4.15.B). The reason for this is unclear but suggests incubation with mitomycin C may have unexpected off target effects on migration in these cells. However an increase in migration when treated with mitomycin C was also apparent in the 100% BCM incubated EV and Cx43 shRNA cells, as these also migrated significantly further than their untreated counterparts (figure 4.15.D). This means that although mitomycin C may be increasing the rate of migration, it is occurring independently of the BCM perturbation of migration. As migration of both control and BCM incubated cells is similarly increased, the migration of cells treated with mitomycin C can still be compared.

Manual analysis was performed of the distance migrated by EV and Cx43 shRNA fibroblasts at 4 and 12 hours, with and without mitomycin-C (figure 4.16). In agreement with previous findings (Mendoza-Naranjo, Cormie, A. Serrano, et al. 2012) at 4 hours the Cx43 shRNA controls migrated significantly further than the EV controls, both with and without mitomycin C. Cx43 shRNA cells also migrated significantly further at 12 hours without pre-treatment with mitomycin C. This demonstrates that Cx43 knockdown with shRNA increases the rate of migration (figure 4.16.A and C). In contrast, at 4 hours incubation with 100% BCM (without mitomycin-C) had no significant effect on the distance migrated by the cells compared to controls in either the EV or Cx43 shRNA fibroblasts (figure 4.16.A). However, at 12 hours, incubation with 100% BCM (without mitomycin-C) had significantly reduced the distance migrated compared to controls in cells both with and without Cx43 expression (figure 4.16.B). Moreover, there were no differences in the distances migrated by BCM incubated EV or Cx43 shRNA BCM cells. The same results were obtained at both time points when the experiments were repeated with the proliferation blocker mitomycin C (figure 4.16.C and D). As the inhibitory effect incubation with 100% BCM has on migration occurs both in EV and Cx43 shRNA cells, the effect incubation with 100% BCM has on migration is independent of Cx43 expression.

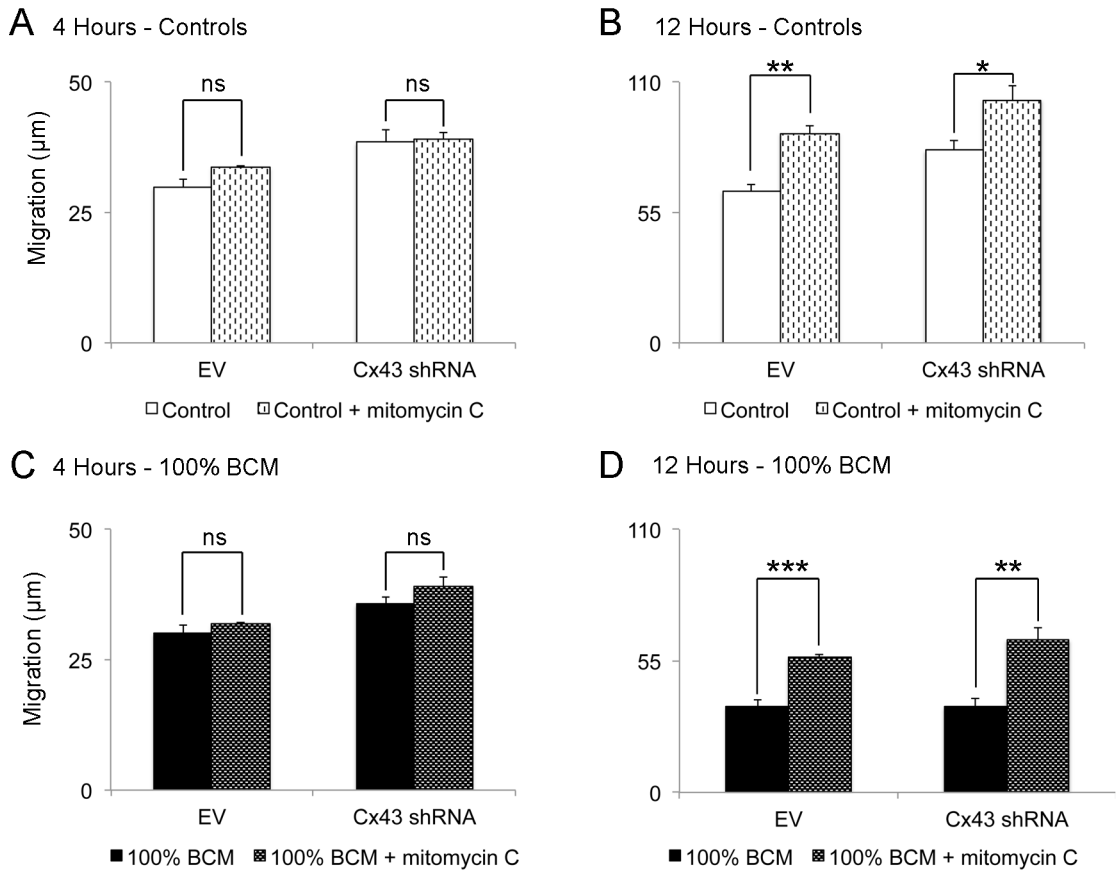

Figure 4.15. A comparison of the distance migrated by empty vector (EV) and Cx43 shRNA control and 100% biofilm conditioned medium (BCM) incubated fibroblasts, both with and without the proliferation blocker mitomycin C. Graphs illustrating the distance migrated at **(A and C)** 4 and **(B and D)** 12 hours by EV and Cx43 shRNA **(A and B)** controls and **(C and D)** cells incubated with 100% BCM. The indicated cells were treated with 10 µg ml-1 mitomycin-C for 2 hours prior to scratching to prevent proliferation. Independent Student's t tests showed that mitomycin-C had no significant effect at 4 hours, but at 12 hours it had stimulated migration in all groups. N=3. All error bars are SEM. ns = not significant, **p<0.01, ***p<0.001.

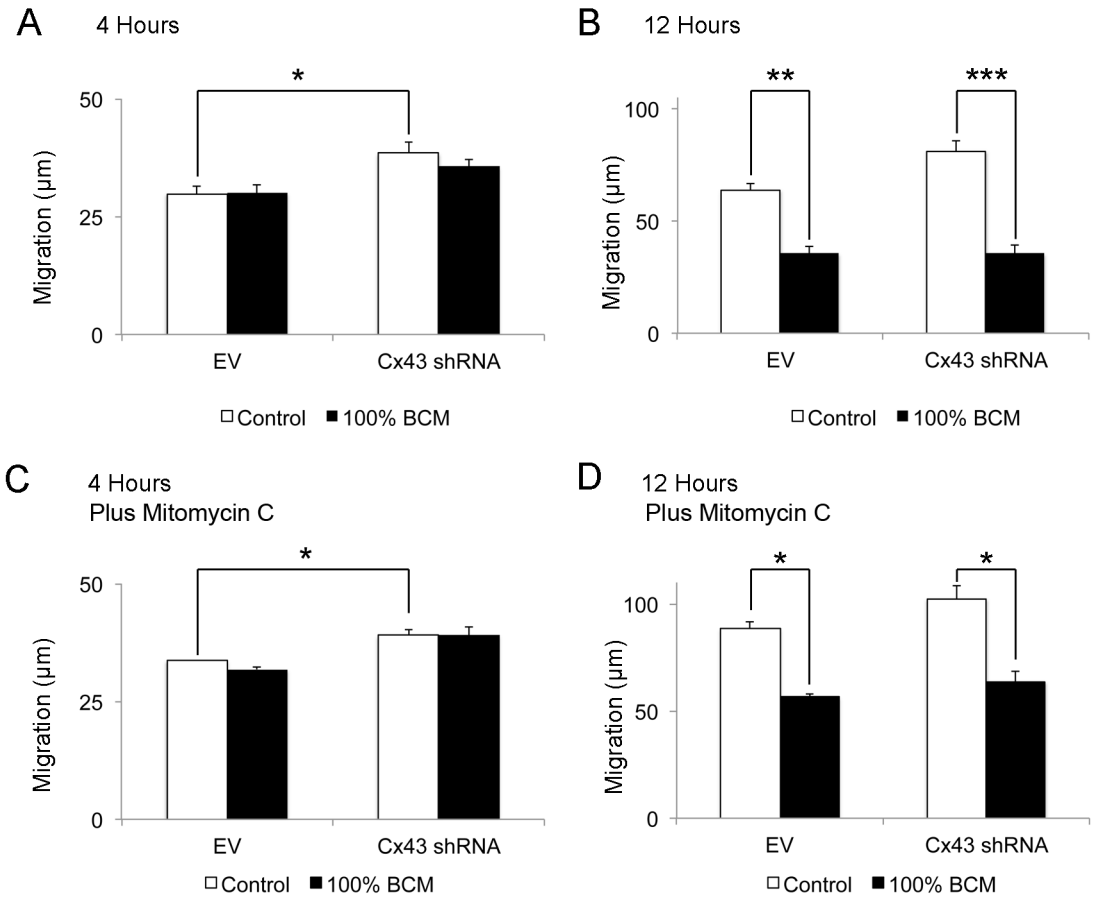

Figure 4.16. Incubation with 100% biofilm conditioned medium (BCM) impairs migration independently of Cx43 expression. Graphs illustrating the distance migrated at 4 **(A)** or 12 **(B)** hours by EV and Cx43 shRNA controls and cells incubated with 100% BCM. Graphs are also shown of migration over 4 **(C)** or 12 **(D)** hours when the cells were treated with 10 µg ml-1 mitomycin C for 2 hours prior to scratching to prevent proliferation. Independent Student' t-tests showed no significant differences at 4 hours with or without mitomycin C treatment. They did show significant differences at 12 hours where, both with and without mitomycin C, EV and Cx43 shRNA controls had migrated significantly further than their 100% BCM incubated counterparts. **(C and D)**. Student's t tests also showed that Cx43 shRNA control cells at 4 hours migrated significantly further than EV controls. N=3. All error bars are SEM. *p<0.05, **p<0.01, ***p<0.001.

4.4. Discussion

S.aureus is a pathogenic species of bacteria commonly found in wounds (Davies et al. 2004; Gjødsbøl & Christensen 2006) where the bacteria primarily exist within a biofilm (James et al. 2007). Biofilm *S.aureus* secrete a plethora of virulence factors, which differ when found in the planktonic and biofilm states (Resch & Rosenstein 2005; Secor et al. 2011). Cx43 expression is abnormal in chronic wounds (Brandner et al. 2004; Mendoza-Naranjo, Cormie, A. Serrano, et al. 2012; Mendoza-Naranjo, Cormie, A. E. Serrano, et al. 2012) and interestingly, studies have found that *S.aureus* derived peptidoglycan (PGN), a component of the cell wall, can alter Cx43 expression in astrocytes, microglia, keratinocytes and endothelial cells (Garg et al. 2005; Esen et al. 2001; Donnelly et al. 2012). However, no previous studies have characterised the effect of *S.aureus* biofilm exotoxins on Cx43 expression, which has been done here. The hypothesis investigated in this chapter was that one mechanism through which *S.aureus* exotoxins impair healing is by contributing to the abnormal Cx43 expression seen in dermal chronic wounds.

Initially, the effect BCM had on fibroblasts was characterised. Live imaging of PI uptake showed that *S.aureus* (ATCC® 29213™) BCM was not toxic to 3T3 fibroblasts. It was unexpected that BCM didn't increase PI uptake, as infection with live bacteria of this strain of *S.aureus* was previously found to be cytotoxic to fibroblasts (Krut et al. 2003). It is possible that the products secreted by the bacteria in the biofilm form are less toxic than those secreted when planktonic. However, a number of experiments from different groups, using various strains of *S.aureus,* have suggested that the bacteria's ability to induce apoptosis, but not necrosis, is dependent on internalisation into the host cell (Mempel et al. 2002; Krut et al. 2003; Haslinger-Löffler et al. 2005; Kubica et al. 2008). Nevertheless, Kirker et al found that BCM from a methicillin resistant *S.aureus* (MRSA) strain was toxic to fibroblasts, though they did not investigate whether the cells underwent apoptosis or necrosis (Kirker & James 2012). Nonetheless, differences in the toxicity of the two BCMs suggests that the virulence factors secreted by the two strains differ.

BCM incubation caused significant reduction in cell number compared to untreated controls, by impairing proliferation. Planktonic condition medium from

several strains of *S.aureus* has previously been reported to reduce proliferation in MAC-T cells (Zavizion et al. 1995). A few *S.aureus* secreted toxins have also been found to inhibit cell proliferation. Enterotoxin B, inhibited proliferation of nasal fibroblasts (Pérez-Novo et al. 2008), and the S component of Panton-Valentine leukocidin (LukS-PV), was reported to induce G0/G1 cell cycle arrest, although exposure was found to ultimately result in apoptosis (Bu et al. 2013). From these data it is not possible to determine at what phase of the cell cycle cells became arrested at, or whether LukS-PV or enterotoxin B were some of the secreted factors in the BCM. It is possible that these, or another as yet unknown secreted products, are responsible for the prevention of proliferation.

As BCM incubation reduced cell proliferation, it was investigated whether BCM induced premature senescence in fibroblasts. Cellular senescence is the state of irreversible cell cycle arrest in viable and metabolically active cells (Georgakopoulou et al. 2013). There is no single marker that can be used to confirm senescence, and instead a combination of several markers are required for verification (Kuilman et al. 2010). After 7 days incubation with BCM the fibroblasts displayed increased nuclear size, increased SA-β-gal activity and increased lipofuscin related autofluorescence, all markers of senescence (Kuilman et al. 2010; Zglinicki et al. 1995). This suggests that it is highly likely that incubation with BCM induced premature senescence, although it would be beneficial to ensure that returning the fibroblasts to normal culture conditions would not restore proliferation, which would confirm unequivocally that proliferative potential has been lost (Blagosklonny 2011). Unlike replicative senescence, premature senescence is not a result of telomere shortening, but a result of exposure to stresses. These stresses include loss of a tumour suppressor (Chen et al. 2005), activation of an oncogene (Serrano et al. 1997), oxidative stress (Liu et al. 2014), and impairment of autophagy (Kang et al. 2011). Evidence for the mechanism of BCM induced senescence could be gained through observing additional senescence markers, including detection of reactive oxygen species (ROS), the cell cycle markers p53 or $p16^{INK4A}$-RB, and DNA damage markers like γ-H2AX (Kuilman et al. 2010).

The induction of senescence in fibroblasts incubated with BCM is of particular interest because senescent fibroblasts have been reported in chronic wounds

(M. V Mendez et al. 1998; Ågren & Steenfos 1999; A. C. Stanley et al. 1997; Vande Berg et al. 1998; Wall et al. 2008). Fibroblasts isolated from venous leg ulcers showed increased characteristics of senescence compared to fibroblasts from the contralateral leg (M. V Mendez et al. 1998); it was further noted that this was more prominent in older chronic wounds, of 3 years or more, compared to younger wounds (Ågren & Steenfos 1999). Similar results were observed in fibroblasts isolated from pressure ulcers, where 60-70% of fibroblasts stained positive for terminin, another marker for senescence (Vande Berg et al. 1998). Wall et al showed that fibroblasts in venous leg ulcers became senescent independent of telomere length, providing evidence that senescence in chronic wound fibroblasts is not early onset of replicate senescence as previously thought, but premature stress induced senescence (Wall et al. 2008). Moreover, senescent fibroblasts have been observed *in vivo* in clusters in the wound beds by staining for terminin; of interest, the authors also observed a correlation between the extent of bacterial infection and the lack of proliferative potential of chronic wound fibroblasts (Vande Berg et al. 1998). However, premature senescence has not previously been reported in cells in direct response to *S.aureus*, although interestingly, it has been observed following challenge with toxins from two other bacterial species. *Escherichia coli* colibactin toxin induced senescence in both human lung fibroblasts and rat intestinal epithelial cells, and *Pseudomonas aeruginosa* pyocyanin toxin induced senescence in human epithelial like cells (Muller 2006; Secher et al. 2013). Both species, like *S.aureus,* are commonly found in chronic wounds (Davies et al. 2004; Gjødsbøl & Christensen 2006).

When observing lipofuscin autofluorescence and SA-β-gal activity, it was evident that there was variation in the extent of each marker between cells. The variation may reflect real variety in the population's sensitivity to BCM. This is potentially the case, as it is normal for some cells within a population to not express stress induced senescent markers when exposed to a stress stimuli (Kang et al. 2011; Chen et al. 2005). Similarly, variations in senescence were observed *in vivo* in pressure ulcer chronic wounds (Vande Berg et al. 1998). Alternatively, 7 days incubation with BCM may not be a sufficient period of time for all the cells to fully develop the markers used to access senescence. In some studies considerably longer time periods (up to 21 days) have been used

when inducing senescence, although shorter periods (3-4 days) have also been reported (Kang et al. 2011; Chen et al. 2005; Liu et al. 2014). Observation after incubating cells with BCM for 14 or more days may clarify which is the case.

As well as impairing proliferation and inducing senescence, incubation of fibroblasts with BCM impaired migration. Significant differences in the distances migrated were observed at 12 hours. This is close to the time point of 11 hours where proliferation was first significantly reduced by incubation with BCM. However, blocking proliferation with mitomycin C showed that the difference was a result of reduced migration, and not an artefact of reduced proliferation. Impaired scratch wound closure was similarly shown for human keratinocytes and fibroblasts incubated with BCM from a MRSA strain (Kirker et al. 2009; Kirker & James 2012). However, in both studies the BCM also significantly reduced cell viability, which would clearly have impacted the ability of the cells to close the wound. Of note, impaired migration has also been reported in fibroblasts isolated from chronic wounds (Brem et al. 2007). These fibroblasts exhibited an abnormal morphology, and are described as 'misshaped' with enlarged nuclei. Interestingly, the MRSA BCM also caused morphological changes in human keratinocytes, though those changes were not reported in fibroblasts, and did not occur when the keratinocytes were incubated with PCM (Kirker et al. 2009). The authors describe the formation of dendrite like extensions and abnormal nuclear morphology, both of which were apparent in the 3T3 fibroblasts incubated with BCM. In contrast though, Kirker et al observed changes in keratinocytes when simply cultured with MRSA BCM, but morphological changes in 3T3 fibroblasts were only apparent when scratched, and then only at the scratch wound edge. Interestingly, the fibroblast morphology closely resembled that of RhoA or ROCK1 depleted cells (Vega et al. 2011). RhoA is a member of the Rho family of GTPases that regulate cytoskeletal dynamics, and the authors describe RhoA depleted cells as elongated with narrow protrusions and defective migration. A similar phenotype was observed when RhoA was depleted in several different cell types, showing that this isn't specific to one cell type. Depletion of ROCK1, a Rho regulated kinase, also produced a similar cell morphology, as well as defective tail retraction during migration. These features closely mimic those seen in the migrating fibroblasts incubated with BCM. Furthermore, *S.aureus* can secrete

epidermal cell differentiation inhibitor (EDIN), a C3-like ADP-ribosyltransferase, which very selectively inactivates Rho(A/B/C/E); this has been shown to inhibit migration in endothelial cells and macrophages by abolishing the formation of actin stress fibres (Aepfelbacher et al. 1997; Rotsch et al. 2012). It too causes an elongated morphology in 3T3 fibroblasts (Rotsch et al. 2012), and it would be interesting to determine whether EDIN is present in BCM. It would also be worth investigating if actin dynamics, and RhoA and ROCK1 expression, were abnormal in migrating BCM incubated fibroblasts, to determine if this is the mechanism for BCM impaired migration.

Interestingly, incubation with BCM reduced the expression of α-tubulin, as observed by western blot, within 24 hours. Both α- and β-tubulin are components of microtubules, which are vital for polarised cell migration (Etienne-Manneville 2013). The microtubule cytoskeleton is controlled by RhoGTPases, in a bidirectional relationship. It will therefore be interesting to determine if the microtubule dynamics and microtubule organising centre (MTOC) are perturbed in the migrating scratched wounded fibroblasts that were incubated with BCM.

To investigate the hypothesis that *S.aureus* exotoxins impair healing through inducing abnormal Cx43 expression, it was first determined whether Cx43 expression is influenced by incubation with BCM. Incubation with *S.aureus* BCM was found to have no effect on Cx43 protein expression within 9.5 hours, and no changes were observed in the levels of each differentially phosphorylated protein band. However, after incubation with BCM for 7 days distinct changes in Cx43 were apparent, with a significant reduction in the Cx43 and Cx43-P1 bands. Each protein band represents Cx43 with different states of phosphorylation, which are thought to signify separate conformational states that are associated with particular cellular locations; both the Cx43-P1 and Cx43-P2 bands were reported to preferentially be found at the plasma membrane, with Cx43-P2 solely in gap junctions (Lampe et al. 2006; Solan et al. 2007). The reduction in the Cx43-P1 band in the western blot was reflected in the immunofluorescent images; Cx43 no longer appeared to be primarily at the plasma membrane, but diffusely through the cytoplasm. The reduction in Cx43 expression may be a direct influence of prolonged incubation with BCM.

Alternatively, there is growing evidence that Cx43 expression is reduced in senescent cells of multiple origins, including fibroblasts (Statuto et al. 2002; Stein et al. 2008; Zhao et al. 2004), and loss of Cx43 protein expression has even been suggested as a marker for senescence (Statuto et al. 2002). Immunofluorescent images showing loss of Cx43 expression in human fibroblasts with both replicative and premature senescence mimics the loss Cx43 expression seen after BCM incubation, with the remaining Cx43 present diffusely in the cytoplasm (Statuto et al. 2002; Zhao et al. 2004). It has also been shown that Cx43 can mediate the induction of senescence (Zhang et al. 2006; Taniguchi Ishikawa et al. 2012). In glomerular mesangial cells (GMCs) an increase in SA-β-gal positive cells was observed when exposed to the senescence inducing stress of high glucose levels; this was abrogated by overexpression of Cx43 (Zhang et al. 2006). Similar results were found using Cx43 deficient hematopoietic stem cells (Taniguchi Ishikawa et al. 2012).

Cx43 can influence a number of cellular responses, including proliferation, viability and migration (Matsuuchi & Naus 2013; Vinken, Decrock, Vanhaecke, et al. 2012), all of which are altered by incubation with BCM. It was investigated whether the effect BCM has on these processes was mediated by Cx43 expression using Cx43 shRNA cells. In agreement with previous findings control Cx43 shRNA fibroblasts migrated further than control EVs (Mendoza-Naranjo, Cormie, A. Serrano, et al. 2012; Pollok et al. 2011; Wright et al. 2012). However, when incubated with BCM, Cx43 expression did not appear to influence the cell viability, proliferation or migration of fibroblasts. Thus it was concluded that mechanisms behind the effects of BCM on fibroblasts were independent of Cx43.

Chapter 5. Cx43 Involvement in *Staphylococcus aureus* Internalisation and Virulence in Fibroblasts

5.1. Introduction

Fibroblasts are the most abundant cell type in the dermis. They are important during wound healing, as they must proliferate and migrate into the wound bed in order to lay down new extracellular matrix (Shaw & Martin 2009). Fibroblasts express the gap junction protein, Connexin43 (Cx43) (Guo et al. 1992). Changes in the expression of this protein play an important role during cutaneous wound healing (Mendoza-Naranjo, Cormie, A. Serrano, et al. 2012; Pollok et al. 2011). Cx43 expression in the dermis is reduced at the wound edge following injury, and further reducing it using Cx43 antisense has been shown to result in faster maturation of granulation tissue and improved healing (Mendoza-Naranjo, Cormie, A. Serrano, et al. 2012; Mori et al. 2008). In chronic wounds, wounds that remain open for 3 months or longer, Cx43 expression dynamics are abnormal, as they remain elevated at the dermal wound edge (Brandner et al. 2004; Mendoza-Naranjo, Cormie, A. Serrano, et al. 2012; Mendoza-Naranjo, Cormie, A. E. Serrano, et al. 2012). This is thought to contribute to the impaired healing of these wounds, but the reason for the high Cx43 expression is as yet unidentified.

Staphylococcus aureus is a bacterial pathogen. It frequently colonises skin as a commensal, but it is primarily pathogenic. As such it is one of the species most commonly isolated from skin wounds, particularly chronic wounds where it was detected in 89-95% of venous leg ulcers (Davies et al. 2004; Gjødsbøl & Christensen 2006).

There are now several studies showing that different bacterial species and their components can alter connexin expression and gap junction intercellular communication (GJIC) in a variety of mammalian cell types (Ceelen et al. 2011). This occurs either directly or by inducing cytokine production, which then influences connexin expression (Esen et al. 2007; Robertson et al. 2010). How connexin expression and GJIC is altered is dependent on both the bacterial species and the origin of the host cell. *S.aureus* derived peptidoglycan (10 μg ml^{-1}), a major component of the bacterial cell wall, increased Cx43 mRNA and protein expression and gap junction intercellular communication (GJIC) in human endothelial cells, but had no influence on human keratinocyte HaCaT

Cx43 expression (Donnelly et al. 2012). PGN (10 μg ml^{-1}) was also reported to increase Cx43 expression in mouse microglia, but decrease expression and GJIC in mouse astrocytes (Esen et al. 2007; Garg et al. 2005). Heat killed *S.aureus* similarly decreased Cx43 expression and GJIC in mouse astrocytes (Esen et al. 2007).

S.aureus is an opportunistic intracellular pathogen, and is able to invade cells, including fibroblasts (Sinha et al. 1999). Heat killed *S.aureus* are also internalised into cells (Kahl et al. 2000). *S.aureus* binds fibronectin and uses it as bridge to host expressed integrin α5β1. The bound *S.aureus* is then actively endocytosed by the cell (Sinha & Fraunholz 2010). The fate of internalised *S.aureus* is largely dependent on the bacterial strain (Krut et al. 2003). Some strains exert little effect and are destroyed by the host cells. Other strains can persist within the cell and influence cellular function, such as by reducing proliferation (Alekseeva et al. 2013). Alternatively, some strains are cytotoxic and induce apoptosis or necrosis of the host cells (Krut et al. 2003). In fact invasion is increasingly thought to be a necessity for *S.aureus* to induce apoptosis, but not necrosis (Sinha & Fraunholz 2010), and there is mounting evidence that cell invasion is a key part of *S.aureus* virulence and pathogenesis in a physiological setting (Colombo et al. 2013; Hamza et al. 2013; Edwards et al. 2010). Interestingly, connexins are reportedly involved in the internalisation of several bacterial species, including *Yersinia enterocolitica* and *Shigella flexneri* (Tran Van Nhieu et al. 2003; L. Velasquez Almonacid et al. 2009; Man et al. 2007). However, it is not currently known how infection with *S.aureus* influences Cx43 expression in fibroblasts, and whether Cx43 in turn influences *S.aureus* invasion.

It was hypothesised that Cx43 expression may regulate the internalisation of *S.aureus* into fibroblasts, and subsequently the response the cells have to the infection. Furthermore, it was hypothesised that *S.aureus,* or its surface proteins, in turn might influence Cx43 expression in fibroblasts, and be contributing to the abnormal dermal Cx43 expression seen in chronic wounds.

5.2. Materials and methods

See Chapter 2 for general materials and methods. Only the materials and methods specific to this section of work are described here.

5.2.1. Bacterial cytotoxicity assay

This protocol was adapted from others previously published (Krut et al. 2003; Mempel et al. 2002). Briefly, cells were grown in 6 well plates. They were washed to remove all antibiotics, and media replaced with DMEM supplemented with 10% DBS. *S.aureus* or HKSA were added per well. For groups testing the cytotoxicity of internalised bacteria a multiplicity of infection (MOI) of 500 was used: for groups where cells were incubated with the bacteria over night a MOI of 70 was used. A non-infected control group was always included. Cells were incubated at 37 °C and 5% CO_2. For groups testing the cytotoxicity of internalised bacteria the cells were washed after 90 minutes, and media supplemented with 200 ug ml^{-1} gentamicin sulphate added. Cells were incubated overnight, after which they were washed, trypsinised and re-suspended in media. All washes and media were kept and pooled with the re-suspended cells. An aliquot was diluted 1:2 with trypan blue solution (Sigma) and incubated for 5 minutes. An aliquot was introduced into a haemocytometer and the percentage of non-viable cells determined.

5.2.2. Bacterial internalisation assay

This protocol was adapted from others previously published, using a comparable MOI and incubation periods (Krut et al. 2003; Agerer et al. 2003; Agerer et al. 2005). Briefly, cells were grown on sterile glass coverslips. All washes were performed by dipping the coverslips in sterile PBS. DMEM supplemented with 10% DBS was added to cells and approximately 3.5 $x10^5$ CFU of *S.aureus* were added per well, resulting in an average MOI of 11. Cells were incubated with the bacteria at 37 °C and 5% CO_2 for 90 minutes to allow internalisation of the bacteria. The media was then removed and replaced with media containing 200 ug ml^{-1} gentamicin sulphate, which kills all extracellular bacteria but has no effect on internalised bacteria. This was left on the cells for 60 minutes. As a negative control, after the 60 minutes media was plated on LB agar and incubated overnight, to ensure all extracellular bacteria had been

killed. If any colonies grew from the lysate in this well the experiment was excluded.

After killing extracellular bacteria, cells were dip washed in sterile PBS before lysing in 0.5% Triton X-100 in PBS. Solutions of lysed cells were serial diluted and plated on LB agar. Plates were incubated at 37 °C overnight and colonies counted the following day. To ensure all colonies were from the *S.aureus* added during the experiment, a non-infected negative control was included. If any colonies grew from the negative control lysate then the experiment was discarded.

5.2.3. Bacterial infection cell counts

The total number of cells present in 8 mm^2 was counted using a haemocytometer. Total cell counts included both viable and non-viable cells (as determined by trypan blue exclusion). Cell counts were conducted on EV and Cx43 shRNA cells after 24 hours under the following conditions: uninfected cells, cells infected with HKSA (MOI of 70), cells infected with live *S.aureus* (MOI of 70), or cells incubated with internalised live *S.aureus* (MOI of 500 for 90 minutes-protocol described in more detail in 5.2.4). Cell counts were presented as a ratio of the largest count within the cell type in each experimental replicate.

5.2.4. Quantitative PCR

RNA extraction

Cells were grown in 6 well plates to 90-100% confluence before commencing experiments. They were incubated with *S.aureus* at a MOI of 5 for 24 hours. Following the incubation period, RNA was extracted using the RNeasy® mini kit (Qiagen) following the manufacturer's instructions. An on column DNA digestion was performed using the RNase-free DNase set (Qiagen), and the purified RNA re-suspended in 30 µl of RNase-free water (Qiagen). RNA was quantified using a NanoDrop® ND-1000 (NanoDrop Technologies). The A260/280 and A260/230 were determined and samples falling below a value of 2.0 were excluded. Samples were frozen at -80 °C until further use.

cDNA synthesis

RNA was reverse transcribed to cDNA using a TC-5000 thermal cycler (Techne) and the thermal cycling conditions in table 5.1. A master mix was made containing random primers (Invitrogen), Oligo dT15 (Promega), dNTP (Invitrogen), 5 X first strand buffer (Invitrogen), DTT (Invitrogen), RNase OUT™ ribonuclease inhibitor (Invitrogen) and Superscript® II Reverse Transcriptase (Invitrogen). 10 µl of master mix was added to 10 µl of RNase-free water (Qiagen) containing 2 µg of RNA. A no enzyme control was also included which did not contain reverse transcriptase.

Table 5.1. Thermal cycling conditions for cDNA synthesis.

Temperature (°C)	Duration (minutes)
65	5
25	10
42	60
70	15
4	hold

qPCR and primer efficiency

A master mix was made containing SYBR green™ JumpStart Taq Ready mix (Sigma-Aldrich), and 400 nM each of forward and reverse primers (see table 5.2. for primer information). Primers design was taken from (Mylvaganam et al. 2009). The optimal concentration of primers was determined by comparing cycle threshold (Ct) values from qPCR reactions using different combinations of forward and reverse primer concentrations. Efficiency of the primers was determined by creating four serial dilutions of cDNA, and performing qPCR as described below. The data was used to plot a standard curve and the following equation used:

$$\text{Efficiency \%} = (10^{(-1/\text{slope})}-1)*100$$

Table 5.2. Connexin43 primer information

	Cx43 Forward Primer (5')	Cx43 Reverse Primer (3')
Primer sequence	TCATGCTGGTGGTGTCCTTG	CCCTTCACGCGATCCTTAAC
Melting temperature	67 °C	65 °C
GC content	55%	55%
Optimal Concentration	400 nM	400 nM
Efficiency	105%	

5 µl of cDNA previously diluted 1:10 was added to 20 µl of master mix in a 96 well Hard Shell PCR plate (Bio-Rad). All samples were assayed in triplicate. A no template control (containing water instead of cDNA) and a no enzyme control (containing reverse transcription product from the cDNA no enzyme control) were run for each primer set to ensure there was no contamination or genomic amplification respectively. The data was not used if any amplification occurred in these wells. The plate was sealed with PCR Microseal® 'B' film (Bio-Rad) and run on a CFX Connect™ Real-Time 96 well PCR Detection System (Bio-Rad). See table 5.3. for thermal cycling conditions. A melt curve was performed at the end of each PCR to ensure that only a single product was present in each well.

Table 5.3. qPCR thermal cycling conditions.

Temperature (°C)	Duration	Cycles
94	2 minutes	
94	15 seconds	
60	30 seconds	X 49
72	30 seconds	
60-90	Melt curve	

Selecting a reference gene

A geNorm reference gene selection kit (PrimerDesign Ltd) was used to select a normalisation gene that was stable between control and *S.aureus* infected

samples. Five genes were tested for stability: 18S, GAPDH, EIF4A2, ACTB and SDHA. The manufacturer's instructions were followed and the stability of the genes between the groups determined using the geNorm analysis software, qbase^{PLUS} (PrimerDesign Ltd). The most stable gene as determined by the software, 18S, was used as a reference gene. PrimerDesign supplied all primers.

Analysis of qPCR results

Each sample was run in triplicate, and any outliers removed. Cycle thresholds (Cts) for each sample were averaged. The $2^{-\Delta\Delta C}{}_T$ method was used to analyse results, using 18S as a reference gene.

5.3. Results

5.3.1. Selecting optimal concentrations of live and heat killed *S.aureus*

S.aureus can be commensal, co-existing apparently harmlessly with mammalian cells. However many strains are cytotoxic, including the ATCC® 29213™ strain investigated here (Krut et al. 2003). Infection of 3T3 fibroblasts with ATCC® 29213™ *S.aureus* results in considerable cell death. In order to investigate the effect *S.aureus* infection has on Cx43 expression, a sublethal concentration of bacteria had to be determined. This was vital as Cx43 expression is influenced by cell confluence: cells at low cell density express less Cx43 than cells at high cell density. Substantial loss of viability in infected cells would reduce cell density, and thus could potentially reduce Cx43 expression, irrespective of any affect the bacterium may have.

To determine a sublethal concentration of *S.aureus* infection, 3T3 fibroblasts were incubated with a range of *S.aureus* inoculums. The nuclei of live fibroblasts were visualised by staining with Hoechst and then imaged hourly over a 24 hour incubation. Cell viability was assessed throughout the experiment by the addition of propidium iodide (PI) to the media. PI enters cells that have lost membrane integrity but is excluded by viable cells, and so it is frequently used to assess cell viability (Johnson et al. 2013). By imaging both Hoechst (total number of cells per image) and PI labelled cells (non-viable cells), any changes in the percentage of PI positive cells over the 24 hour incubation period could be determined. Additionally Hoechst labelling enabled the rate of cell proliferation to be assessed by comparing the total number of cells at each time point. This is an important control, as if infection reduced the proliferation of the fibroblasts there would also be an impact on cell density over time, and consequently on Cx43 expression. Differences were assessed using a mixed design ANOVA. This analysis determines the influence of both infection concentration and time on the dependent variable (fold change in cell number, or the percentage of PI positive cells). A Tukey's post hoc analysis was then used to compare the overall data from the time course for statistical differences, but not individual time points, as it was important to determine the overall influence of infection over the 24 hour time course. The highest concentration of

live *S.aureus* tested, 5.5 x10^5 CFU ml^{-1}, caused a significant increase in PI positive cells (figure 5.1.A). While lower concentrations caused a trend showing a marginal increase, this did not differ significantly from controls. While PI is normally used to assess viability, it has been reported that in circumstances where cells are stressed it can enter them through open hemichannels (Kondo et al. 2000). Bacterial infection could induce hemichannel opening, resulting in cells being incorrectly labelled as non-viable. However, as the lower concentrations of *S.aureus* do not significantly alter PI uptake compared to controls, mislabelled viable cells will have no significant impact on cell density. Proliferation, as assessed by determining the fold change in cell number, also didn't differ significantly between controls and infected samples (figure 5.1.B). As a concentration of 2 x10^5 CFU ml^{-1} of *S.aureus* didn't cause a significant loss of viability or decrease in proliferation rate it was determined that this concentration was sublethal over 24 hours. This concentration is equivalent to a multiplicity of infection (MOI) of 5, meaning that there were 5 bacteria per cell at the onset of infection. Therefore this concentration was used in all further experiments where a sublethal infection was required.

Heat killing *S.aureus* maintains many of the surface antigens intact, and infection of mouse astrocytes with heat killed *S.aureus* (HKSA) reduced Cx43 expression in astrocytes (Esen et al. 2007). As Cx43 expression is influenced by cell confluence, in order to investigate if ATCC® 29213™ HKSA alters Cx43 in 3T3 fibroblasts it was therefore necessary to first determine whether infection with HKSA altered cell density over a 24 hour incubation period, by looking at viability and proliferation. Fibroblasts were infected with increasing concentrations of HKSA and the proliferation rate investigated by live imaging Hoechst labelled nuclei and determining the fold change in total cell number. PI was included in the media, and the changing percentage of cells that took up PI was quantified in order to assess viability. None of the concentrations of HKSA tested had a significant effect on the percentage of cells that took up PI (figure 5.2.A). The fold change in cell number (figure 5.2.B) was similarly unaffected by HKSA infection, thus infection with HKSA had no impact on cell density. In further experiments a maximum HKSA concentrations of 1.2 x10^7 CFU ml^{-1} (an MOI of 400, and the highest concentration tested) was used.

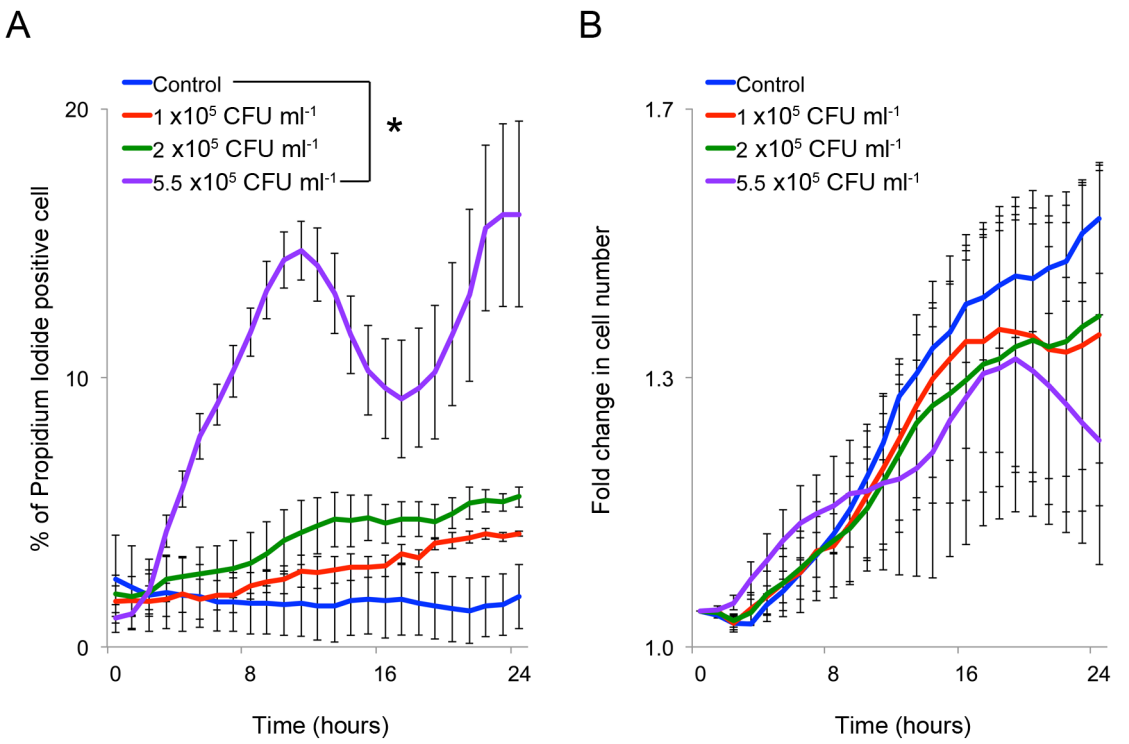

Figure 5.1. Determining a concentration of live *S.aureus* that does not cause significant loss of cell viability. (A) The number of propidium iodide positive cells, as a percentage of the population over 24 hours is shown for control 3T3 fibroblasts, and for fibroblasts incubated with increasing concentrations of *S.aureus*. A mixed design ANOVA showed there was a significant differences between the groups and a Tukey's post hoc revealed that only the highest concentration of 5.5 x 10^5 CFU ml^{-1} caused a significant increase in the percentage of propidium iodide positive cells ($p<0.05$). **(B)** The fold change in cell number over 24 hours is shown for cells incubated with the same concentrations of *S.aureus* as **(A).** A mixed design ANOVA showed that there were no significant differences in proliferation between the groups. N=3. All error bars are SEM. *$p<0.05$.

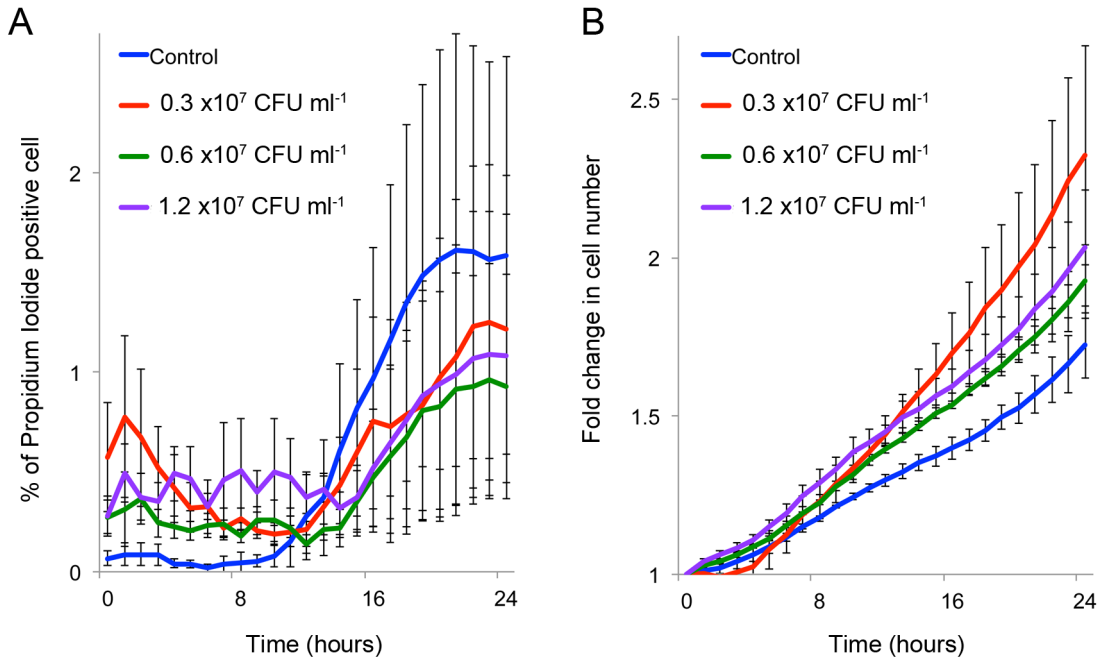

Figure 5.2. Determining a concentration of heat killed *S.aureus* (HKSA) that doesn't cause significant loss of cell viability. (A) The number of propidium iodide positive cells, as a percentage of the population over 24 hours is shown for control 3T3 fibroblasts, and for fibroblasts incubated with increasing concentrations of HKSA. **(B)** The fold change in cell number over 24 hours is shown for cells incubated with the same concentrations of HKSA as **(A).** Mixed design ANOVAs were used to compare the groups, and showed no significant differences in cell death or proliferation between controls and HKSA infected cells. N=3. All error bars are SEM.

5.3.2. Knockdown of Cx43 reduces the viability of fibroblasts when infected with live *S.aureus*

Infection of fibroblasts with live ATCC® 29213™ *S.aureus* is cytotoxic to 3T3 fibroblasts, and *S.aureus* can induce cell death through apoptotic mechanisms (Fraunholz & Sinha 2012). Importantly, Cx43 can regulate the induction of apoptosis. This is through both GJIC and non-junctional mechanisms, and can be through either pro- or anti-apoptotic, depending on the circumstances (Vinken, Decrock, Leybaert, et al. 2012). Furthermore, a reduction in Cx43 expression was recently reported to protect epithelial cells from apoptosis induced by the *Helicobacter pylori* VacA toxin (Radin et al. 2014). Therefore, it was investigated whether Cx43 expression influenced the viability of fibroblasts when infected with *S.aureus.* The live imaging technique described above, using Hoechst labelled nuclei and media containing PI, was again used as it enabled simultaneous analysis of both proliferation and viability. 3T3 empty vector controls (EVs: mixed design ANOVAs confirmed that there were no statistical differences between EVs and non-transfected 3T3s in any of the assays performed-data not shown) and fibroblasts with Cx43 constitutively knocked down (Cx43 shRNAs) were infected with sublethal concentrations of live *S.aureus* and imaged hourly for 24 hours. A sublethal concentration was used due to experimental constraints: higher concentrations caused extensive cell death, resulting in large numbers of dead cells detaching from the cell dish. Detachment of cells in infections with toxic concentrations would mean fallaciously low results were recorded when determining what percentage of the population had died. This problem did not occur with a sublethal concentration of *S.aureus.*

The fold change in cell number was compared (using a mixed design ANOVA) between all four groups: EV uninfected controls, EV infected cells, Cx43 shRNA uninfected controls and Cx43 shRNA infected cells (figure 5.3). Cx43 knockdown was previously shown to reduce the rate of fibroblast proliferation over 90 hours (Mendoza-Naranjo, Cormie, A. Serrano, et al. 2012). In line with previous evidence, uninfected Cx43 shRNA cells appeared to proliferate slower than EV controls, but there was no statistically significant difference over this time period. There were also no significant differences in the fold change

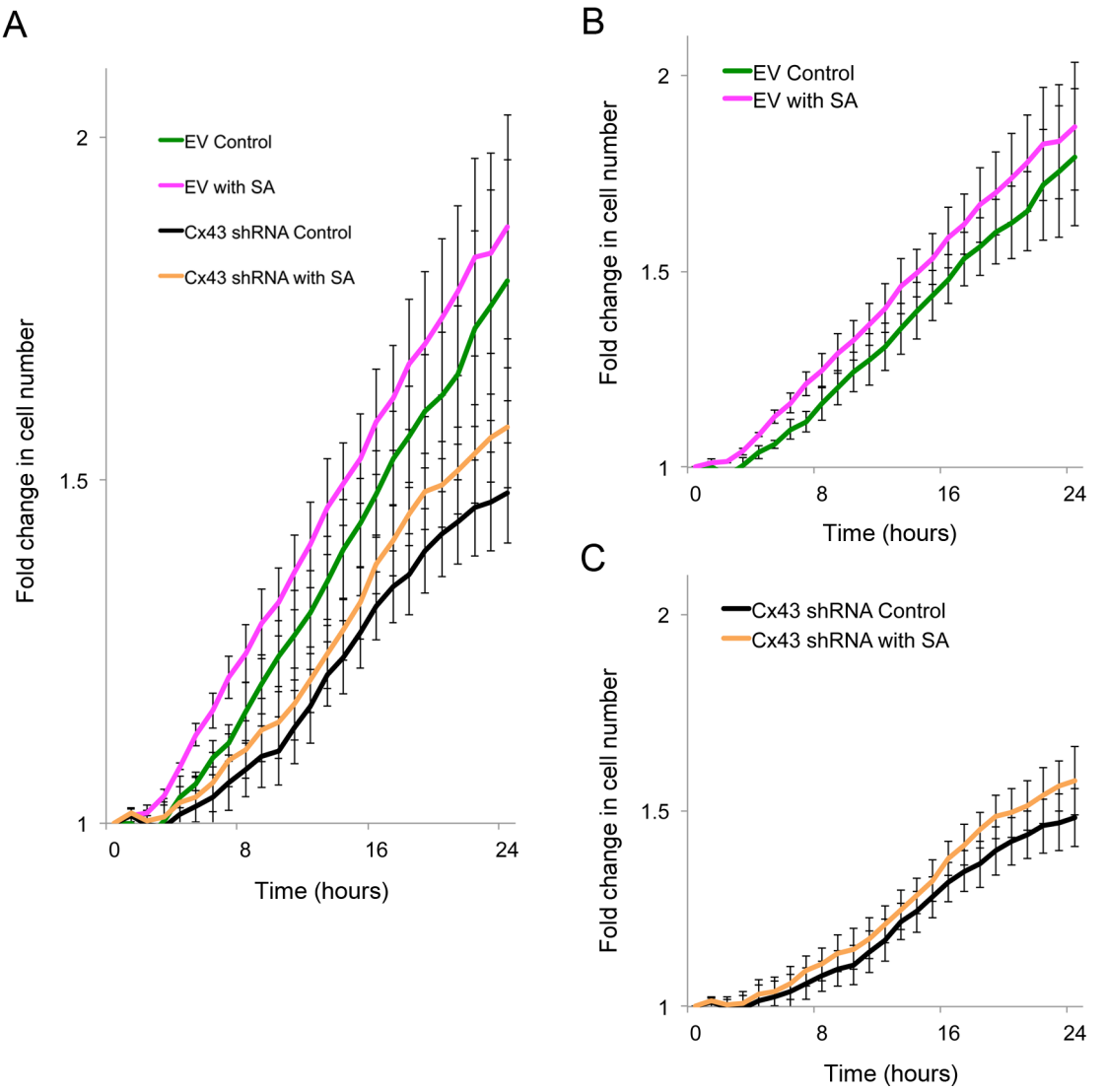

Figure 5.3. Knockdown of Cx43 does not alter the proliferation of fibroblasts when infected with a sublethal concentration of *S.aureus*. (A) The fold change in cell number over 24 hours is shown for EV and Cx43 shRNA fibroblast controls and cells infected with an average of 1.4 x10^5 CFU ml^{-1} of *S.aureus* (SA) (MOI of 4). Separate graphs for **(B)** EVs and **(C)** Cx43 shRNAs are shown for clarity. A mixed design ANOVA comparing the fold change for all groups revealed no significant differences. N=3 experiments. All error bars are SEM.

between any of the other groups. The percentage of cells that had taken up PI was also compared for all four groups (figure 5.4). Infection of EV fibroblasts did not cause a statistically significant overall increase in the percentage of PI positive cells over the time course (figure 5.4.A and B). However, infection of Cx43 shRNA fibroblasts did cause a significant increase in the percentage of PI positive cells compared to controls (figure 5.4.A and C). This shows that a reduction in Cx43 expression reduced the viability of fibroblasts when infected with *S.aureus*.

Previous analysis revealed that HKSA had no effect on viability in 3T3 fibroblasts. The response of Cx43 shRNA cells to the challenge was also investigated to determine whether Cx43 expression would influence this. There were no significant differences in the percentage of PI positive cells between EV and Cx43 shRNA control or HKSA infected cells (figure 5.5.A). Similarly, there were no significant differences in the fold changes in cell number (figure 5.5.B). From this it was concluded that knockdown of Cx43 expression had no effect on the viability or proliferation of fibroblasts infected with HKSA.

It has been reported that when cells are under stress, PI can enter a viable cell through connexin hemichannels (Kondo et al. 2000). It is therefore possible that infection with live *S.aureus* could be inducing hemichannel opening. However, it is highly unlikely that the increase in PI uptake observed in the infected Cx43 shRNA is a result of hemichannel opening, as Cx43 expression is significantly reduced in these cells (figure 4.3) and there are therefore fewer hemichannels. Nevertheless, to be certain that the increase in PI positive cells observed in Cx43 shRNA cells is predominantly due to a loss of viability and not hemichannel opening, trypan blue exclusion was also used to assess *S.aureus* toxicity. Trypan blue is excluded by viable cells (Johnson et al. 2013), but unlike PI, it is not able to pass through connexin hemichannels. The percentage of EV and Cx43 shRNA cells that had taken up trypan blue was assessed after 24 hours infection with *S.aureus* (figure 5.6). A toxic concentration was used (2.6 $x10^6$ CFU ml^{-1}, an MOI of 70), rather than a sublethal concentration, as very small differences in viability would be more difficult to accurately determine using this technique than the previous. Thus using a toxic concentration of *S.aureus* enabled differences between the groups to be determined with greater

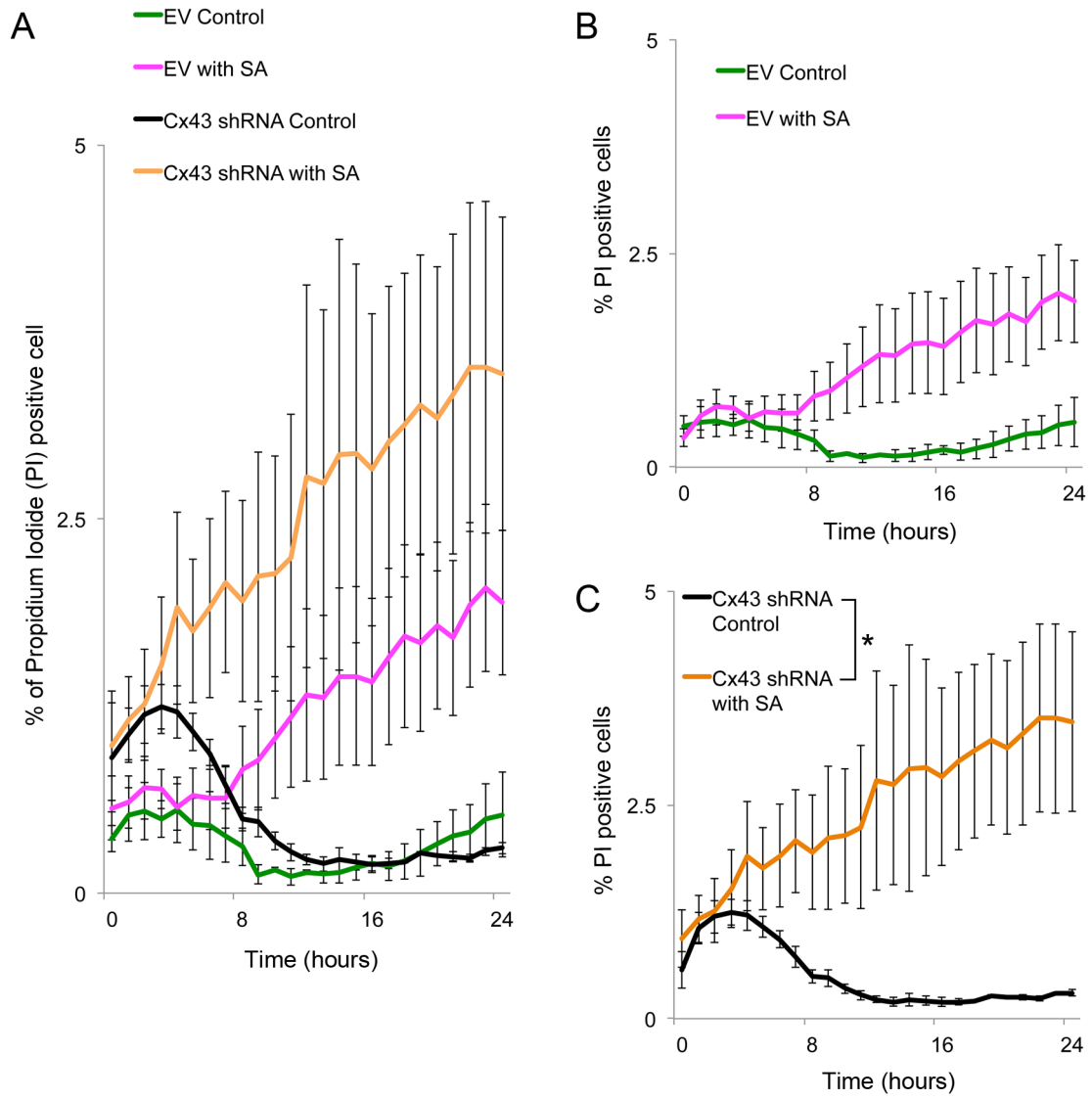

Figure 5.4. Knockdown of Cx43 reduces the viability of 3T3 fibroblasts when incubated with a sublethal concentration of *S.aureus*. (A) The number of propidium iodide positive cells, as a percentage of the whole population over 24 hours, is shown for controls and EVs and Cx43 shRNA fibroblast controls and cells infected with an average of 1.4 x10^5 CFU ml^{-1} of *S.aureus* (SA) (MOI of 4). Separate graphs for **(B)** EVs and **(C)** Cx43 shRNAs are shown for clarity. A mixed design ANOVA showed there was a significant differences between the groups and a Tukey's post hoc was conducted which showed that *S.aureus* infection only caused a significant increase in the percentage of propidium iodide positive cells in the Cx43 knockdown fibroblasts ($p<0.05$). N=3 experiments. All error bars are SEM.*$p<0.05$.

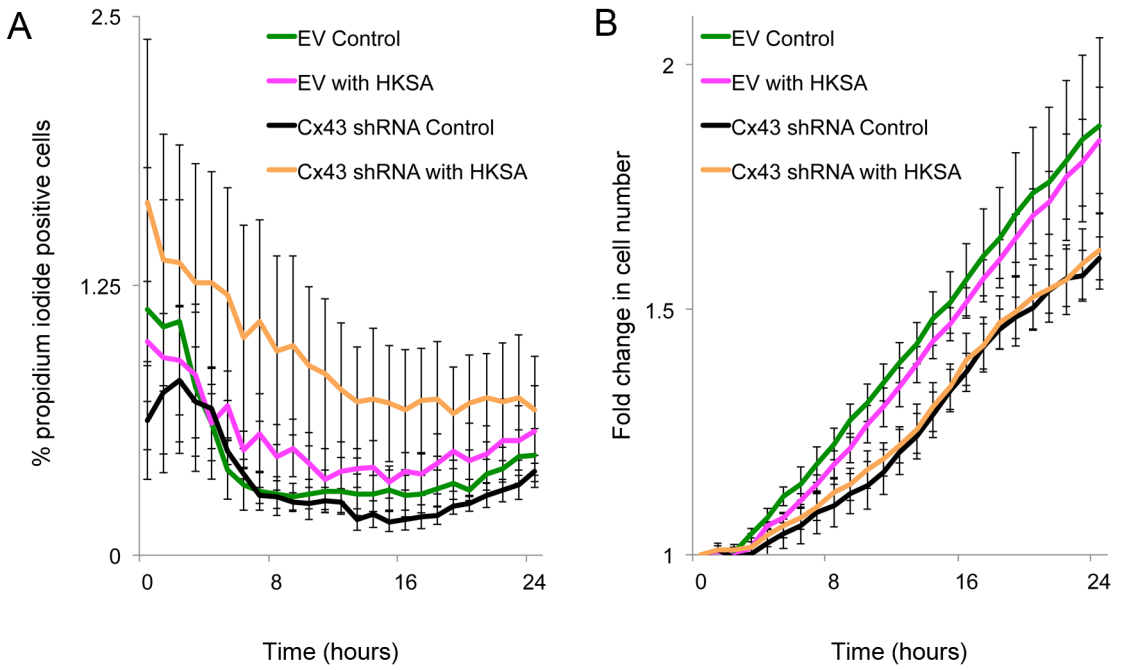

Figure 5.5. Knockdown of Cx43 does not alter the proliferation or viability of fibroblasts when infected with a sublethal concentration of heat killed *S.aureus* (HKSA). (A) The number of propidium iodide positive cells, as a percentage of the whole population over 24 hours, is shown for EV and Cx43 shRNA fibroblast controls and cells infected with an average of 7.5 x10^6 CFU ml^{-1} of HKSA (MOI of 170). **(B)** The fold change in cell number over 24 hours is also shown control and HKSA infected for EV and Cx43 shRNA fibroblast. Mixed design ANOVAs comparing all the groups revealed no significant differences. N=4 experiments. All error bars are SEM.

reliability. Pilot experiments determined that over a 24 hour period less than 20% of infected EV cells would be killed. There were no significant differences in the percentage of trypan blue cells between EV and Cx43 shRNA cells, in either the uninfected or HKSA infected groups (figure 5.6). Infection of EVs with live *S.aureus* resulted a small but significant increase in trypan blue positive cells compared to both uninfected and HKSA infected EV cells ($p<0.05$). Infection of Cx43 shRNA cells with live *S.aureus* also caused a significant increase in the percentage of trypan blue cells compared to both uninfected and HKSA infected Cx43 shRNA cells ($p<0.001$). Interestingly, the increase in the percentage of trypan blue cells compared to uninfected cells was much greater in the Cx43 shRNAs than EVs; 41.9% (±2.7%) of Cx43 shRNA cells were trypan blue positive compared to 14.7% (±4.4%) of EV cells. The percentage of trypan blue positive EV and Cx43 shRNA cells were also statistically compared for the *S.aureus* infected group; there was a significantly greater percentage of Cx43 shRNA cells infected with live *S.aureus* that took up trypan blue than infected EV cells (figure 5.6). This shows that knockdown of Cx43 increases the loss of cell viability when infected with live *S.aureus.* These data also supports the conclusion drawn from the PI uptake data, which was that *S.aureus* infection was reducing cell viability and not causing hemichannel opening (figure 5.4). Together these data show that knockdown of Cx43 expression in fibroblasts increases the cytotoxicity observed in these cells when infected with live *S.aureus.*

5.3.3. Knockdown of Cx43 increases the internalisation of live *S.aureus*

Although *S.aureus* has traditionally been thought of as an extracellular pathogen, there is a growing body of evidence showing that this bacterium is internalised by non-phagocytic cells (Fraunholz & Sinha 2012). Bacterial internalisation assays were performed to test whether Cx43 expression altered the rate of *S.aureus* invasion. EV and Cx43 shRNA fibroblasts were infected with a high concentration of live *S.aureus.* They were incubated for 90 minutes in order for the *S.aureus* to internalise into the fibroblasts, then all extracellular bacteria were killed. Intracellular *S.aureus* were grown from the lysed fibroblasts, and the colony forming units (CFU) counted (Figure 5.7.A).

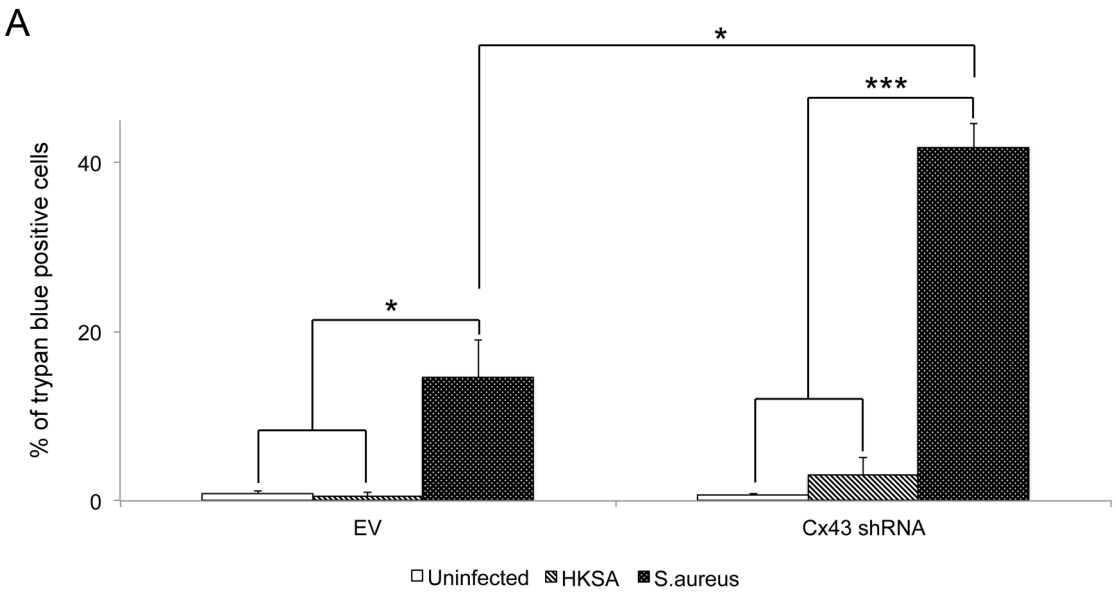

Figure 5.6. Knockdown of Cx43 reduces the viability of 3T3 fibroblasts when incubated with a toxic concentration of *S.aureus*. (A) Graph showing the percentage of EV or Cx43 shRNA cells that took up trypan blue dye, and were thus not viable, after incubation with 2.6 $x10^6$ CFU ml^{-1} of HKSA or *S.aureus* (MOI of 70) for 24 hours. Independent Student's t-tests were performed on uninfected, HKSA infected or *S.aureus* infected groups comparing the percentage of EV and Cx43 shRNA trypan blue positive cells. These revealed no statistical differences between EV and Cx43 shRNA cells in the control or HKSA infected groups. They showed that infection with *S.aureus* caused a significant increase in trypan blue positive Cx43 shRNA cells compared to EV cells ($p<0.05$). N=4. All error bars are SEM.*$p<0.05$.

The number of CFUs is equivalent to the number of bacteria internalised by the fibroblasts. Statistical analysis revealed that there was a significant increase in the CFUs grown from Cx43 shRNA cells compared to EV cells ($p<0.01$). These data demonstrate that a reduction in Cx43 expression increases *S.aureus* internalisation into 3T3 fibroblasts.

Previous experiments have shown that reducing Cx43 expression significantly increased the loss of cell viability when fibroblasts were infected with live *S.aureus.* In order to determine if an increase in internalised *S.aureus* is the cause of the reduction in viability, trypan blue experiments were again conducted on EV and Cx43 shRNA fibroblasts. However, instead of maintaining a constant infection in the medium throughout the 24 hour incubation, *S.aureus* were allowed to invade the fibroblasts for 90 minutes then all extracellular bacteria were destroyed using antibiotics, the same technique used in the internalisation assays. A higher concentration of the bacterium was used (1.8×10^7 CFU ml^{-1}, an MOI of 500) than in the previous trypan blue experiments in order to ensure that there was sufficient internalisation of bacteria over the incubation period to observe changes in viability. The fibroblasts were incubated for a further 22 hours with the internalised *S.aureus* before assessing viability (figure 5.7.B). As found previously in section 5.3.2, only a small percentage of uninfected and HKSA infected cells took up trypan blue, and there was no significant differences between EV and Cx43 shRNA cells in either condition. Under these conditions, internalised *S.aureus* also did not result in a significant increase in trypan blue positive EV fibroblasts compared to uninfected and HKSA infected EVs. A comparison between the percentage of trypan blue positive EV and Cx43 shRNA cells incubated with internalised *S.aureus* also showed no statistical differences between the groups, although there was an 8.6 fold increase in the percentage of trypan blue positive Cx43 shRNA cells compared to EV cells. In contrast though, Cx43 shRNA cells incubated with internalised live *S.aureus* had a significantly greater percentage of trypan blue positive cells, compared to uninfected and HKSA infected cells. Knockdown of Cx43 was previously shown to increase the internalisation of *S.aureus.* Thus, these data suggest that internalisation of *S.aureus* may be an important factor influencing the viability of fibroblasts when challenged by *S.aureus* infection,

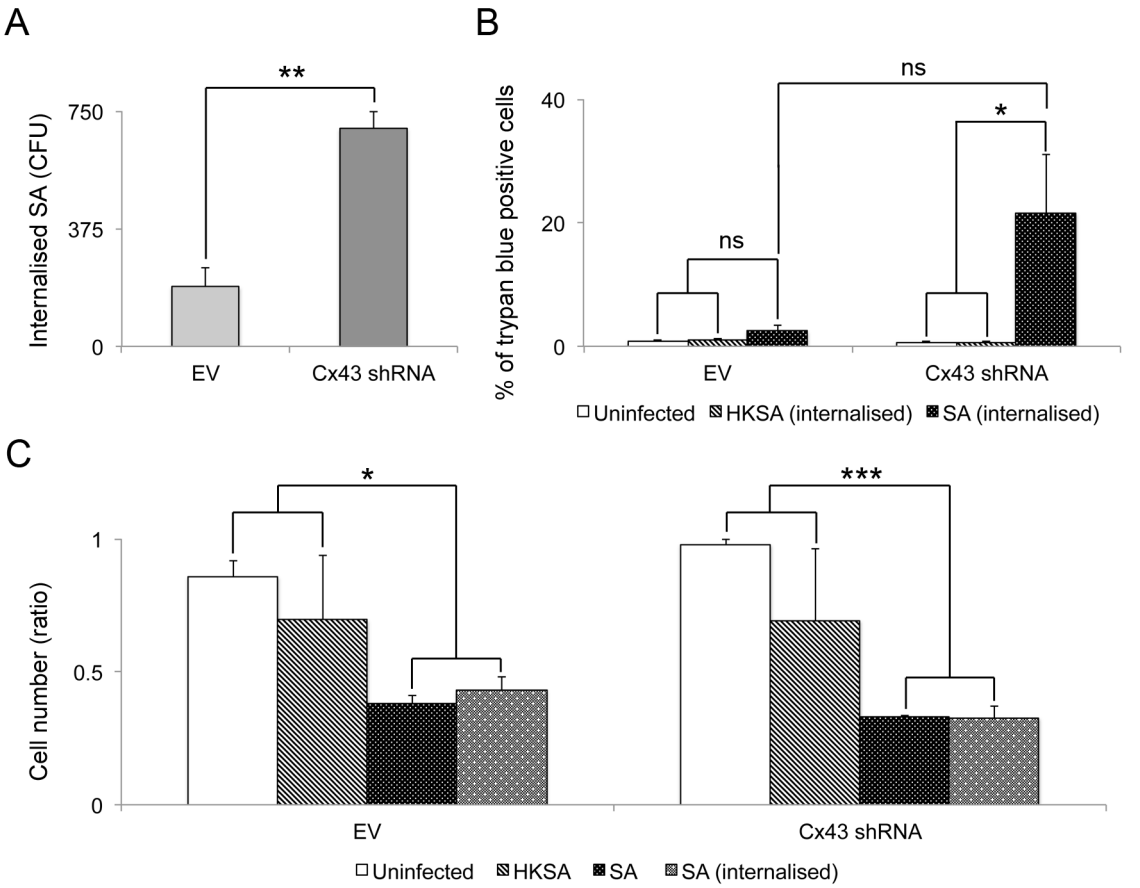

Figure 5.7. Knockdown of Cx43 expression increases the internalisation of *S.aureus* (SA), reducing viability and proliferation. (A) Graph showing the number of colony forming units (CFU) of *S.aureus* internalised by EV and Cx43 shRNA cells when inoculated with 3.8 x10^7 CFU ml^{-1} *S.aureus.* An independent Student's t-tests showed a statistical difference between the groups ($p<0.01$). **(B)** Graph showing the percentage of EV and Cx43 shRNA cells that took up trypan blue dye. Cells were incubated for 2 hours with 1.8 x10^7 CFU ml^{-1} of HKSA or SA (MOI of 500). External bacteria were then killed and the cells grown for a further 22 hours before assessing viability by trypan blue exclusion. Statistical differences were determined using one-way ANOVAs and independent Student's t tests as appropriate. **(C)** Graph demonstrating the fold in cell number when EV or Cx43 shRNA fibroblasts were infected with HKSA, *S.aureus*, or incubated with internalised *S.aureus*. The cell number is presented as a ratio of the largest cell count in each experimental replicate. Statistical differences were determined using one-way ANOVAs. A, N=4; B, N=4, C, N=4. All error bars are SEM. Ns=not significant, *$p<0.05$, **$p<0.01$, ***$p<0.001$.

and that increased internalisation of *S.aureus* is likely contributing to the reduction in cell viability when Cx43 is knocked down.

Of additional interest, whilst determining viability using trypan blue exclusion it was observed that there appeared to be fewer cells in the live *S.aureus* infected samples. To ascertain if this was the case, a comparison was made of the total number of cells (viable and non-viable cells) for the following groups: uninfected, infected with HKSA, infected with live *S.aureus*, or incubated with internalised *S.aureus* (figure 5.7.C). Cell numbers were presented as a ratio, relative to the highest number of cells counted in each experimental replicate. One-way ANOVAs showed that infection with live *S.aureus,* but not HKSA, reduced the total number of cells present after 24 hours in both EV and Cx43 shRNA cells. As the cell count included both viable and non-viable cells, this suggested that as well as reducing viability, infection with *S.aureus* retarded proliferation. Furthermore, the total cell number was also significantly reduced compared to uninfected and HKSA infected cells when EV or Cx43 shRNA cells incubated only with internalised *S.aureus*. There was no significant difference in total cell number between the *S.aureus* infected and internalised *S.aureus* only infected cells. This indicates that internalisation of the bacteria might be playing a role in the effect *S.aureus* has on fibroblast proliferation.

5.3.4. Infection with live *S.aureus* reduces Cx43 protein expression

Fibroblasts were infected with increasing concentrations of HKSA (MOI from 15 to 300), and total cell protein was harvested after 24 hours. As a control the same technique for protein extraction was used on an aliquot of HKSA, and the lysate run alongside cell protein. Neither the Cx43 or α-tubulin antibodies bound to protein in the HKSA lane, confirming that the antibodies used did not bind to the HKSA. Additionally, a comparison of the α-tubulin expression in each group validated this protein as a loading control, as its expression did not differ significantly between controls and HKSA infected cells ($p=0.31$; figure 5.8.F). The western blots showed that after 24 hours infection with varying concentrations of HKSA there was no change in total Cx43 expression compared to controls (figure 5.8.A and B). When analysed by SDS/PAGE Cx43

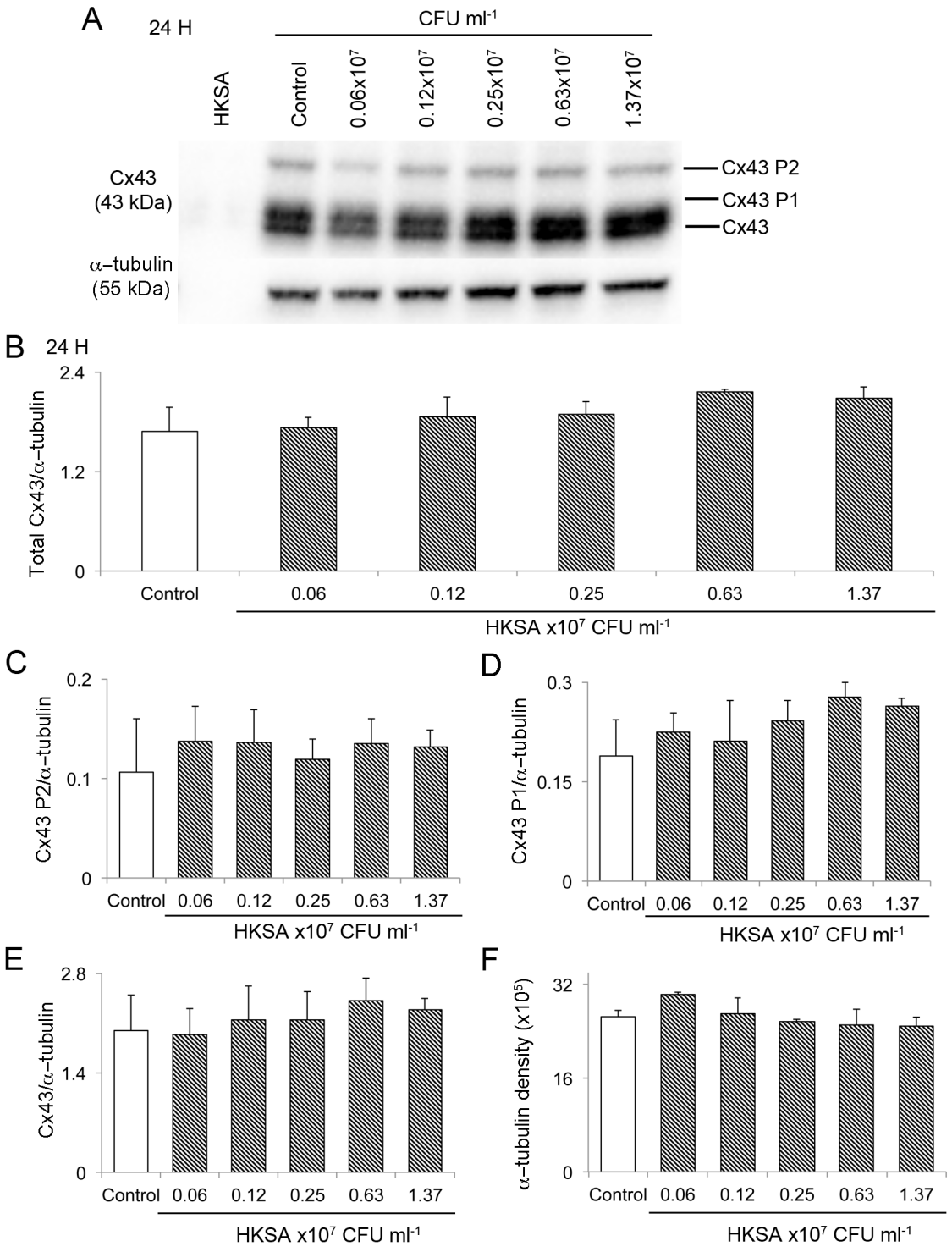

Figure 5.8. Infection with HKSA has no effect on Cx43 protein levels. (A) A western blot showing Cx43 protein expression in fibroblasts infected with increasing concentrations of HKSA for 24 hours (MOI ranged from 15 to 300). α-tubulin expression was used as a loading control. Protein extracted from HKSA using the same methods as for cells is shown as a negative control. **(B)** Graph quantifying the total Cx43 expression relative to α-tubulin expression. **(C-E)** Graphs showing the relative expression of the different bands of Cx43 seen on the western blot, which indicate the different phosphorylation states of Cx43. **(F)** Graph comparing the α-tubulin expression for each group. One-way ANOVAs were used to test statistical differences for graphs A-F. N=3. All error bars are SEM.

forms three distinct protein bands. The fastest migrating band is referred to as Cx43, and the two slower bands are commonly referred to as Cx43 P1 and Cx43 P2. The protein bands are known to be phosphorylated at different sites, and are thought to indicate conformational changes in Cx43 related to functional location within the cell (Solan & Lampe 2009). Densiometric analysis of the different bands showed that infection with HKSA also caused no detectable changes in phosphorylation (figure 5.8.C-E). Similar results were found when fibroblasts incubated with varying concentration of HKSA for 48 hours (data not shown). From this it was concluded that HKSA infection therefore does not influence Cx43 expression or phosphorylation in 3T3 fibroblasts.

There are few studies investigating the effect *S.aureus* has on Cx43 expression and the majority of these use either heat killed *S.aureus* or *S.aureus* derived peptidoglycan (Garg et al. 2005; Esen et al. 2007; Karpuk et al. 2011). However, metabolically active *S.aureus* do not always elicit the same response from cells as their isolated components or inactivated counterparts (Krut et al. 2003; Alekseeva et al. 2013). It was therefore interesting to establish whether infection with live *S.aureus* alters Cx43 expression in fibroblasts. The cells were infected with a sublethal concentration of *S.aureus* (MOI of 5) (figure 5.2), and after 24 hours the total protein was harvested. As with the HKSA western blots, the same technique for protein extraction was used on an aliquot of live *S.aureus*, and the lysate run alongside cell protein. Neither the Cx43 or α-tubulin antibody bound to protein in this lane either, again confirming the specificity of the antibodies for the murine antigen. A comparison of the α-tubulin expression in each group again validated this protein as a loading control, as its expression doesn't differ significantly between controls and *S.aureus* infected cells ($p=0.64$; figure 5.9.F). Interestingly, the western blots showed a significant reduction in Cx43 in the *S.aureus* infected samples (figure 5.9.A and B). Densiometric analysis of the different bands was also conducted. Analysis showed that the reduction was in the Cx43 and Cx43 PI protein bands, but not the Cx43 P2 band (figure 5.9.D). Heat killed *S.aureus* and its peptidoglycan derivative have been reported to attenuate Cx43 expression in astrocytes by both directly and indirectly reducing Cx43 mRNA expression (Esen et al. 2007). While western blots enable analysis of protein levels they cannot reveal whether the mRNA expression is similarly affected. qPCR was therefore performed in order to

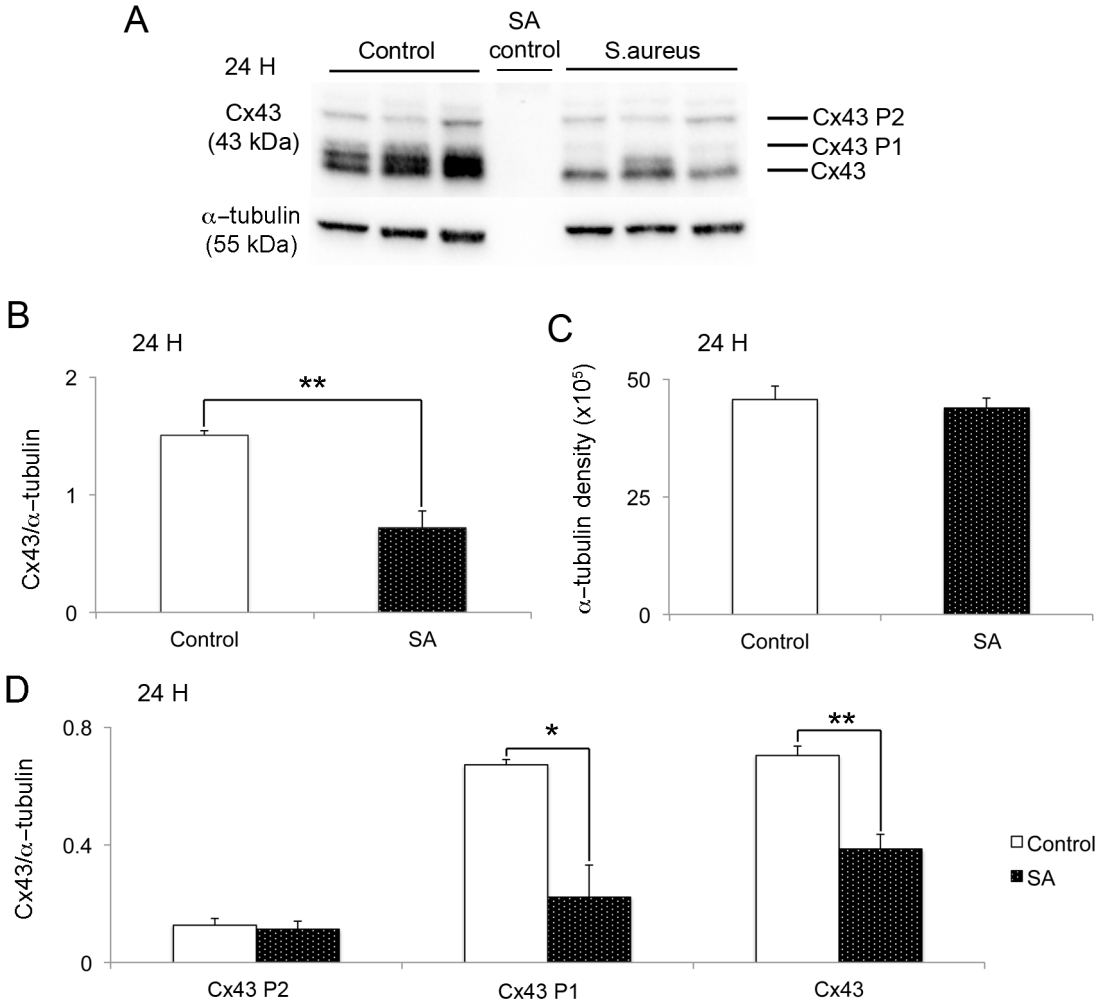

Figure 5.9. Infection with a sublethal concentration of *S.aureus* (SA) for 24 hours reduces Cx43 protein levels. (A) A western blot showing Cx43 protein expression in controls and in fibroblasts incubated with 1.4 x10^5 CFU ml^{-1} *S.aureus* for 24 hours (MOI of 5). α-tubulin expression was used as a loading control. **(B)** Graph quantifying the total Cx43 expression relative to α-tubulin expression. **(C)** Graph quantifying the α-tubulin expression for control samples, and samples incubated with SA. **(D)** Graph quantifying the different bands of Cx43 seen on the western blot, which indicate the different phosphorylation states of Cx43. Expression is relative to total α-tubulin expression. Independent Student's t tests were used to tests statistical differences. N=3. All error bars are SEM. *p<0.05, **p<0.01.

ascertain if the reduction in Cx43 protein expression caused by live *S.aureus* infection also correlated with a decline in mRNA expression. Interestingly, no difference was observed in Cx43 mRNA expression between control and *S.aureus* infected cells (figure 5.10). This shows that the bacteria are not altering the cell's transcription of Cx43. Instead the bacterium could be increasing the degradation of Cx43 protein, though further experiments are required to determine if this is the case.

5.3.5. Infection with live *S.aureus* alters Cx43 cellular location

Western blots demonstrated that Cx43 protein expression is reduced when infected with live *S.aureus* but not HKSA. However, this technique does not enable the visualisation of connexin distribution within the cells. Previous studies have shown that connexin distribution within the cell can be altered by various factors, including infections (Campos de Carvalho et al. 1998; Martínez & Sáez 2000), and so Cx43 protein was also visualised using immunofluorescence. Confocal images were taken of Cx43 immunofluorescence after 24 hours of infection with the highest HKSA concentration tested by western blot, 1.2 x 10^7 CFU ml^{-1} (MOI of 300: figure 5.11.A), or infection with 1.4 x 10^5 CFU ml-1 of *S.aureus* (MOI: figure 5.12.A). Quantification of Cx43 expression in the images confirmed the results seen by western blot, as no differences in Cx43 levels were found when infected with HKSA (figure 5.11.B), but a significant reduction observed when infected with *S.aureus* (figure 5.12.B). This analytical method normalises to the number of cells per image, so to validate this method it was confirmed that the number of cells per image didn't differ significantly between the groups in both the HKSA infected ($p=0.74$: figure 5.11.C) and live *S.aureus* infected experiments ($p=0.58$: figure 5.12.C). Observations of Cx43 distribution in control cells showed high expression in foci around the nuclei and at intercellular junctions, with some diffuse cytoplasmic expression. No differences in Cx43 distribution were observed in cells infected with HKSA (figure 5.11). In contrast, Cx43 expression was reduced throughout the cell in the *S.aureus* infected cells, with a slight change in distribution (figure 5.12). It was still present in some intercellular foci and somewhat in the cytoplasm, but appeared to be primarily lost from the nuclear foci.

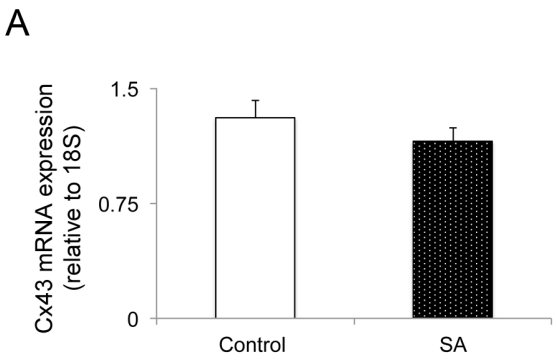

Figure 5.10. Infection with a sublethal concentration of *S.aureus* (SA) for 24 hours does not reduce Cx43 mRNA levels. (A) Graph showing Cx43 mRNA expression relative to 18S expression, in fibroblasts that had been infected with 1.4 $x10^5$ CFU ml^{-1} *S.aureus* for 24 hours (MOI of 5). A Student's t test revealed that there was no significant difference. N=3. All error bars are SEM.

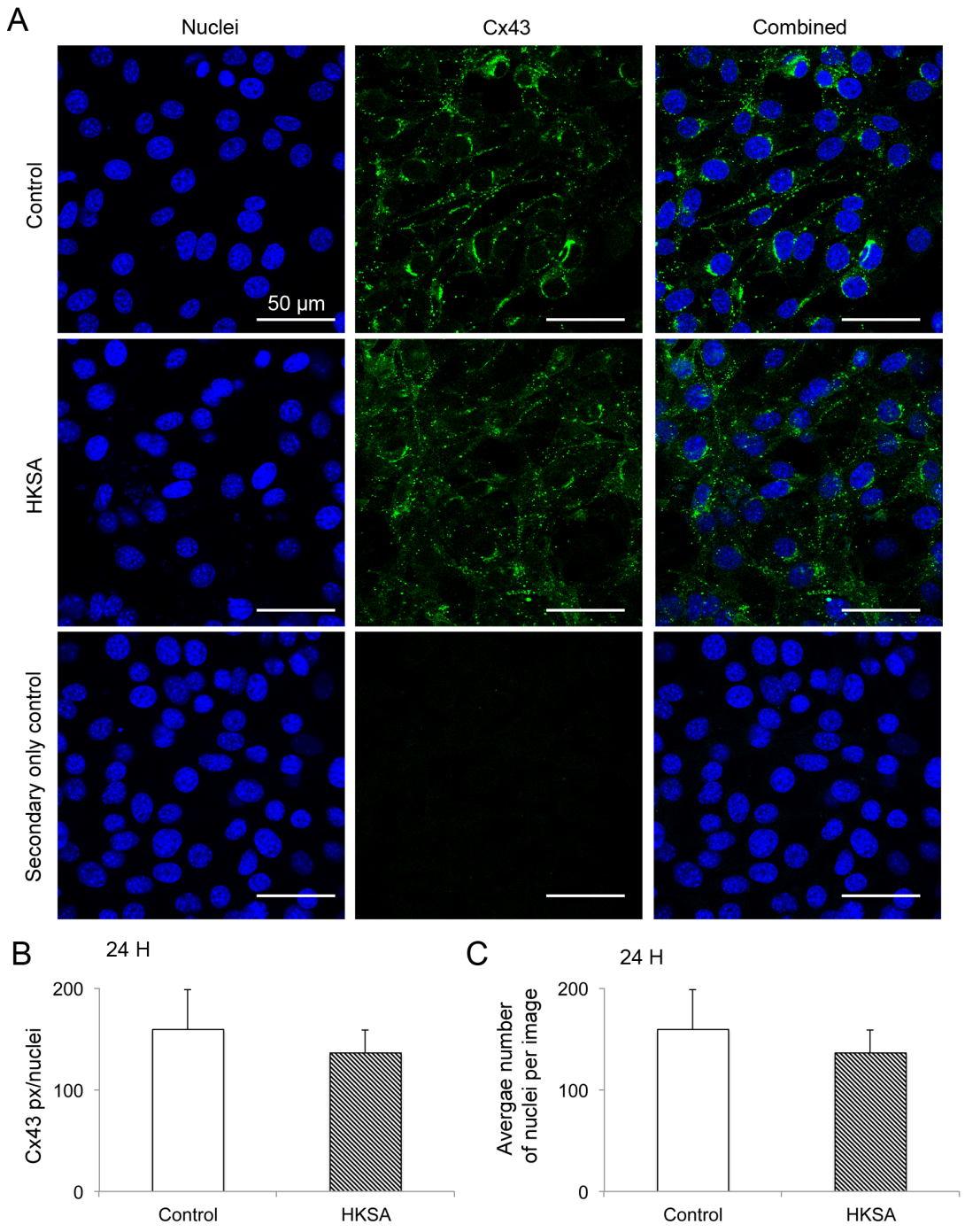

Figure 5.11. Infection with a sublethal concentration of heat killed *S.aureus* (HKSA) has no effect on Cx43 protein levels or cellular location. (A) Examples of immunofluorescent confocal images showing nuclei (blue) and Cx43 (green) in controls (top row) and in fibroblasts incubated with 1.2 x10^7 CFU ml^{-1} HKSA (MOI of 300) for 24 hours (middle row). A negative control using secondary antibody only is shown in the bottom panel. Scale bars indicate 50 µm. **(B)** Graph illustrating the Cx43 protein expression levels as quantified from confocal images, shown as Cx43 pixels per nuclei. **(C)** Graph showing the average number of nuclei in the Cx43 immunofluorescent images used to quantify Cx43 expression. Independent Student's t tests were used to test statistical differences. These showed there were no significant differences. N=3. All error bars are SEM.

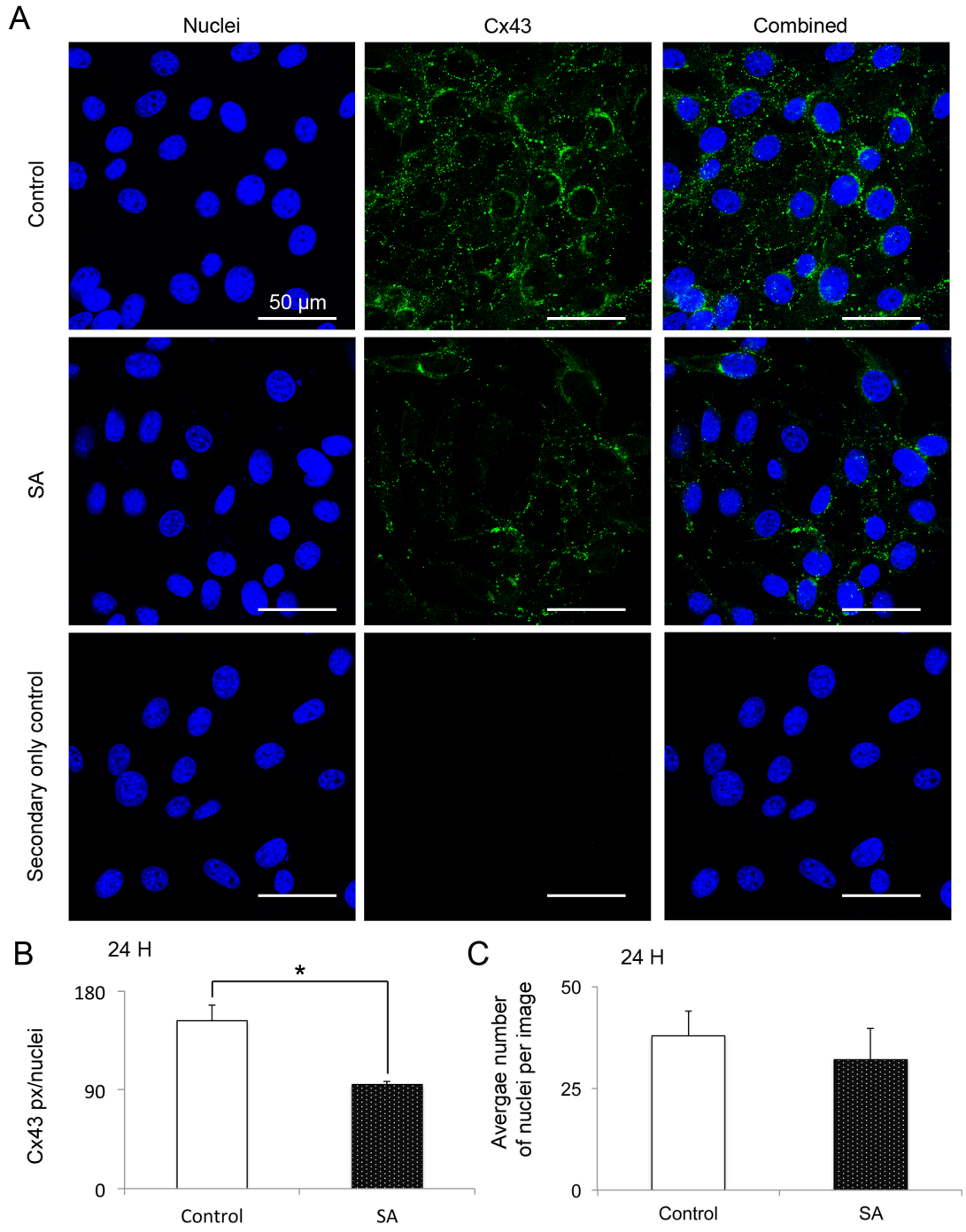

Figure 5.12. Infection with a sublethal concentration of *S.aureus* (SA) for 24 hours reduces Cx43 protein levels, but does not alter cellular location. (A) Examples of immunofluorescent confocal images showing nuclei (blue) and Cx43 (green) in controls (top row) and in fibroblasts incubated with 1.4 x10^5 CFU ml^{-1} *S.aureus* (MOI of 5) for 24 hours (middle row). A negative control using secondary antibody only is shown in the bottom panel. Scale bars indicate 50 µm. **(B)** Graph illustrating the Cx43 protein expression levels as quantified from confocal images, shown as Cx43 pixels per nuclei. **(C)** Graph showing the average number of nuclei in the Cx43 immunofluorescent images used to quantify Cx43 expression. Independent Student's t tests were used to test statistical differences. N=3. All error bars are SEM. *p<0.05.

5.4. Discussion

S.aureus is a pathogenic bacterium. It is internalised by host cells, and intracellular *S.aureus* are increasingly acknowledged to not only be physiologically relevant, but to also play an important role in *S.aureus* virulence and recurrent infections. A reduction in Cx43 expression was found to increase *S.aureus* internalisation, and *S.aureus* in turn was found to reduce Cx43 expression, thus facilitating its own internalisation.

In fibroblasts *S.aureus* becomes intracellular through adherence to fibronectin. Fibronectin forms a bridge between the bacteria and host cell as it is also adhered to by α5β1 integrins on host cells. Clustering of integrins causes the activation of several signalling pathways and a cytoskeletal reorganisation that results in active endocytosis of *S.aureus* by the cell (Fraunholz & Sinha 2012). Knockdown of Cx43 increases the number of intracellular *S.aureus* grown from a culture of fibroblasts, though at this point it has not been determined whether it increases the number of cells containing intercellular bacteria, or the number of bacteria per infected cell. FACS analysis of fibroblasts infected with immunofluorescent-labelled *S.aureus* may help to determine which is the case. Nevertheless, it is reasonable to presume that Cx43 is somehow involved in the process. Moreover, it appears to have a protective role during *S.aureus* infection as a decrease in expression increases intracellular *S.aureus*. However, determining whether overexpression of Cx43 significantly decreases *S.aureus* internalisation is required to show if Cx43 is protective against *S.aureus* internalisation. How Cx43 influences *S.aureus* internalisation is as yet unknown. It is possible that Cx43 might be influencing *S.aureus* internalisation by directly interacting with α5β1, as in osteocytes Cx43 was shown to directly interact with α5β1, which influenced hemichannel activity through its activation (Batra et al. 2012). Alternatively, Cx43 could be influencing *S.aureus* invasion through interactions with other binding partners that could potentially be mutual with α5β1. *S.aureus* is not the only bacterium that exploits α5β1 integrins in order to enter host cells. Other bacteria include *Bartonella bacilliformis, Myobacterium paratuberculosis, Neisseria* spp*, Porphyromonas gingivalis, Pseudomonas aeruginosa, Shigella, Streptococcus* spp *and Yersinia* spp (Scibelli et al. 2007). A functional link between connexin expression and bacterial invasion has already been established for *Yersinia enterocolitica* and *Shigella flexneri*

internalisation (L. Velasquez Almonacid et al. 2009; Tran Van Nhieu et al. 2003). For internalisation of these species, cellular connexin expression increased bacterial internalisation, through a mechanism that was dependent on opening of Cx43 and Cx26 hemichannels respectively. As Cx43 expression result in fewer intracellular *S.aureus,* it seems unlikely that the same mechanism is employed during *S.aureus* internalisation into fibroblasts, as Cx43 shRNA cells have lower gap junction activity (Mendoza-Naranjo, Cormie, A. Serrano, et al. 2012), and presumably also reduced hemichannel activity. Nevertheless, Cx43 may still be influencing internalisation through gap junction or hemichannel activity, but via a different mechanism. This is in fact a possibility that was investigated in the course of this research, but all gap junction blockers tested proved toxic to *S.aureus.* Further experimentation is thus required to shed light on the mechanisms behind Cx43 involvement in *S.aureus* internalisation, and it will be interesting to see whether connexins influence the internalisation of other bacterial species that exploit α5β1.

ATCC® 29213™ *S.aureus* is a toxic strain (Krut et al. 2003), and infection of 3T3 fibroblasts with it caused a loss of viability, as shown by PI and trypan blue uptake. Toxicity was not observed when infected with heat killed *S.aureus* (HKSA), in line with previous reports (Krut et al. 2003; Alekseeva et al. 2013), suggesting that the bacteria must be metabolically active in order to instigate cell death. Reduction in Cx43 expression increased the toxicity of the infection and resulted in increased cell death. Its possible that knockdown of Cx43 could have increased the susceptibility of the fibroblasts to *S.aureus* virulence, as reduced Cx43 expression in Cx43 heterozygous mice, or GJIC inhibition in mice by treatment with oleamide, increased mortality in an *Escherichia coli* peritonitis *in vivo* model (Anand et al. 2008). Cx43 expression was also recently related to the susceptibility of epithelial cells to the apoptotic effects of *Helicobacter pylori* VacA toxin, where a reduction in Cx43 decreased apoptosis (Radin et al. 2014). However, since Cx43 knockdown increased intracellular *S.aureus,* it seems likely that the increased bacterial load may be responsible for the increase in cell death. One way to test this would be to prevent *S.aureus* internalisation into Cx43 shRNA fibroblasts by depleting α5β1 expression, and then assessing the toxicity of the infection. This would also enable an assessment of whether internalisation of *S.aureus* in these cells is necessary for induction of cell death.

This has been found to be the case in a number of cell types infected with various *S.aureus* strains (Mempel et al. 2002; Krut et al. 2003; Haslinger-Löffler et al. 2005; Kubica et al. 2008), and is also supported by the finding here; internalised *S.aureus* did not cause a significant increase in trypan blue positive EV cells, but did in Cx43 shRNA cells, which were shown to have increased intracellular *S.aureus.* However, the notion that *S.aureus* must be intracellular to induce apoptosis is still considered to be somewhat controversial as toxins which are secreted by the bacteria can also cause cell death in isolation (Bronner et al. 2004).

Infection with toxic concentrations of *S.aureus* was also found to affect the proliferation of fibroblasts. Proliferation was significantly reduced compared to uninfected and HKSA infected cells both when the extracellular *S.aureus* were left in the culture media, and when only intracellular bacteria were allowed to persist, suggesting that internalised *S.aureus* are important for this effect. This was also observed by Alekseeva et al, who reported that only intracellular metabolically active *S.aureus* impaired proliferation of epithelial cells, by delaying the transition between G2 and M in the cell cycle (Alekseeva et al. 2013). They showed this using three different strains of *S.aureus* on both human and bovine epithelial cells. In agreement with their observations, it was similarly found here that heat killed *S.aureus* did not impair proliferation, again suggesting that the bacteria must be metabolically active to affect proliferation. *S.aureus* planktonic conditioned medium has also been shown to reduce proliferation in MAC-T cells (Zavizion et al. 1995), and a few specific *S.aureus* secreted toxins that inhibit cell proliferation have been identified; enterotoxin B, inhibited proliferation of nasal fibroblasts (Pérez-Novo et al. 2008), and the S component of Panton-Valentine leukocidin (LukS-PV), was reported to induce G0/G1 cell cycle arrest (Bu et al. 2013). From the experiments conducted here it is not possible to ascertain at what phase of the cell cycle cells underwent arrest, but it would be interesting to see whether it was also at the G2/M phase as previously shown by Alekseeva et al (Alekseeva et al. 2013). Infection of 3T3 fibroblasts with sublethal concentrations of *S.aureus* (MOI of 4) did not appear to reduce proliferation though, as assessed by live imaging of Hoechst labelled nuclei. Alekseeva et al similarly found that a low concentrations of *S.aureus* (MOI of 5) did not reduce proliferation, while MOIs of 10 or more did (Alekseeva

et al. 2013). The reason for this as yet unclear but may be to do with lower concentrations of the growth inhibiting toxins within the cells as a result of fewer intracellular *S.aureus.*

Infection of fibroblasts with *S.aureus* reduced the protein expression of Cx43. A reduction in Cx43 expression has previously been seen in astrocytes in culture following incubation with *S.aureus* peptidoglycan (PGN) (Esen et al. 2007). This also occurred when PGN was replaced with whole heat killed *S.aureus*, but here HKSA had no effect on either Cx43 expression levels or cellular location. Western blot analysis shows three Cx43 protein bands; each band represents Cx43 in different states of phosphorylation and conformation, and has also been related to cellular location (Solan & Lampe 2009). Both the Cx43-P1 and Cx43-P2 bands were reported to preferentially be found at the plasma membrane, with Cx43-P2 solely in gap junctions (Lampe et al. 2006; Solan et al. 2007). Live *S.aureus* reduced levels of the Cx43-P1 and Cx43 bands, but not the Cx43-P2 band, suggesting a reduction in Cx43 protein in all differentially phosphorylated bands except the one found preferentially in gap junctions. This is also suggested by observing the Cx43 immunofluorescent images, and it will be interesting to determine if there is still gap junction intracellular communication. Moreover, despite a reduction in Cx43 protein, *S.aureus* infection does not result in decreased Cx43 mRNA levels. This suggests that the infection might be increasing protein degradation, a theory that could be tested by chemically blocking proteasome activity during infection, or by imaging the turnover of fluorescently labelled Cx43. Interestingly, it is known that α5β1 can influence Cx43 expression. Culturing alveolar epithelial cells on fibronectin increases Cx43 expression, but antibodies against α5β1 reduced Cx43 abundance and results in its redistribution to the cytosol (Guo et al. 2002). Alternatively, activation of α5β1 was shown to increase Cx43 expression in rat cardiomyocytes, (Shanker et al. 2005). Thus it is possible that *S.aureus* may be influencing Cx43 expression through its interaction with α5β1.

In this chapter it was shown that *S.aureus* infection of fibroblasts decreased Cx43 protein expression, and that in turn, a reduction in Cx43 increased the internalisation of *S.aureus*, with consequences for the viability of the cell. Thus *S.aureus* influences the host cell in a manner that increases its own virulence. A

reduction in Cx43 expression in vivo was also shown to increase the virulence of another bacterial species, *E.coli*, although in contrast, reduced Cx43 was shown to protect cells from apoptosis induced by *helicobacter pylori* VacA toxin (Radin et al. 2014; Anand et al. 2008). Cx43 expression in chronic wounds is abnormally high at the dermal wound edge (Mendoza-Naranjo, Cormie, A. E. Serrano, et al. 2012; Mendoza-Naranjo, Cormie, A. Serrano, et al. 2012). It is feasible to speculate that high Cx43 expression could be a protective mechanism against *S.aureus* and other bacterial species commonly found in chronic wounds, including *E.coli* (Davies et al. 2004; Gjødsbøl & Christensen 2006). However, the clinical roles of intracellular S.aureus in in vivo wounds are as yet unknown. Nevertheless, intracellular *S.aureus* have been shown to have physiological relevance in several types of wounds; internalisation is thought to aid in the pathogen's evasion of the immune system, its virulence, persistence, and reoccurrence of infections (Kubica et al. 2008; Edwards et al. 2010; Hamza et al. 2013; Menzies et al. 2002). Although *S.aureus* is one of the most common pathogens in chronic skin wounds (Davies et al. 2004; Gjødsbøl & Christensen 2006), the presence of intracellular *S.aureus* specifically in this type of wound has not yet been established. This is the next step in establishing the relationship between intracellular *S.aureus* and Cx43 expression in wounds.

Chapter 6. Effects of *Staphylococcus aureus* Infection on Healing and Connexin Expression in an *In Vivo* Cutaneous Wound Model

6.1. Introduction

Healing an injury in the skin after wounding requires the coordination of numerous cell types (Shaw & Martin 2009). Primarily tissue haemostasis must be re-established, and leukocytes are recruited to clear the wound of debris and contaminants. Fibroblasts proliferate and migrate into the wound, laying down extracellular matrix. Some will terminally differentiate as myofibroblasts, which contract the wound. In addition, angiogenesis results in a dense network of blood vessels in the wound bed, and together these components form granulation tissue. Keratinocytes in the epidermis proliferate and migrate over the granulation tissue to reform the skin barrier. Lastly, after wound closure the new dermis is remodelled. Excessive blood vessels are retracted, remaining vessels mature, collagen type III is exchanged for type I, and myofibroblasts undergo apoptosis.

Unfortunately, healing does not always proceed smoothly, and wounds can become chronic. Chronic wounds typically have defective granulation tissue formation and remodelling (Herrick et al. 1992). They also have hyper-proliferation of keratinocytes at the wound edge, alongside a failure of migration and re-epithelialisation of the wound (Stojadinovic et al. 2005; Usui et al. 2008; Brem et al. 2007; Stojadinovic et al. 2008). Chronic wounds are thought to be a result of four underlying factors: ischaemic reperfusion, hypoxia, intrinsic host disease and bacterial infection (Mustoe et al. 2006). One bacterial species commonly isolated from skin wounds, and chronic wounds in particular, is *Staphylococcus aureus* (Davies et al. 2004; Gjødsbøl & Christensen 2006). It is thought to primarily exist in wounds in the form of a biofilm, a community of sessile bacteria encased in a self-produced matrix (James et al. 2007). *S.aureus* biofilms are formed naturally and rapidly, and mature biofilms have been shown in a mouse wound infection model by 24 hours (Akiyama et al. 1996). Manipulation of biofilm formation in *in vivo* models of *S.aureus* infected wounds suggest that the ability of *S.aureus* to form a biofilm is an important part of its impairment of wound healing (Gurjala et al. 2011; Schierle et al. 2009). Biofilm *S.aureus* secrete different toxins from their planktonic counterparts (Resch & Rosenstein 2005; Secor et al. 2011). Results from *in vitro* experiments using biofilm conditioned medium (BCM) have shown that these

exotoxins can impair viability and migration of both fibroblasts and keratinocytes (Kirker et al. 2009; Kirker & James 2012), although the toxicity of *S.aureus* is dependent on the particular strain (Krut et al. 2003). Furthermore, results from chapter four in this thesis showed that BCM from the ATCC 29213 strain of *S.aureus* could induce a senescence phenotype in fibroblasts *in vitro*, as well as also impairing migration.

Connexins are a group of proteins that form gap junction, and they are expressed throughout the skin. Gap junctions are tightly regulated, and appear to also have non-junctional roles in several cellular processes, including apoptosis, migration, proliferation and differentiation (Dbouk et al. 2009). Cx43 is expressed at reasonably high levels by fibroblasts in the dermis, and by keratinocytes in lower spinous and basal layers of the epidermis (Goliger & Paul 1994; Coutinho et al. 2003; Risek et al. 1992; Kretz et al. 2003). Cx26 and Cx30 are expressed at very low levels by keratinocytes in the granular layer of the epidermis. Expression of all three connexins changes dynamically during wound healing. Cx43 is down-regulated at the epidermal and dermal wound edge upon injury, but increased in epidermal hyperproliferative regions behind this and throughout the new epidermis following re-epithelialisation (Goliger & Paul 1995; Coutinho et al. 2003; Mendoza-Naranjo, Cormie, A. Serrano, et al. 2012). Cx26 and Cx30 behave like one another; they become up-regulated directly behind the wound edge, and remain elevated for some time in the hyperproliferative epidermis following re-epithelialisation, before returning to normal levels after complete restoration of barrier function (Goliger & Paul 1995; Coutinho et al. 2003). Cx26, Cx30 and Cx43 are all abnormally expressed in chronic wounds, where they become elevated at the wound edge and for several millimetres away (Brandner et al. 2004; Mendoza-Naranjo, Cormie, A. E. Serrano, et al. 2012; Mendoza-Naranjo, Cormie, A. Serrano, et al. 2012). Experimentally reducing Cx43 expression with Cx43 antisense in both normal and diabetic wounds (which heal slowly and have abnormal Cx43 expression) in mouse skin has shown to improve the rate of healing (Mori et al. 2006; Wang et al. 2007). Ectopic overexpression of Cx26 in the skin of mice impaired wound healing, whilst no differences have been observed in skin wound healing in Cx30 knockout mice (Djalilian et al. 2006; Kretz et al. 2003). Although there is

not yet a complete understanding of their role it is clear that connexins, and Cx43 in particular, have important roles during the process of wound healing.

Connexin expression and GJIC can be altered by exposure to several bacteria or their components; the effect is dependent on the bacterial species, the cell type, and the particular connexin (Ceelen et al. 2011). Peptidoglycan, a bacterial cell wall component, was found to increase Cx43 expression and GJIC in human endothelial cells. However, it had no influence on Cx43 in human keratinocyte HaCaTs, but instead increased Cx26 expression (Donnelly et al. 2012). In contrast, PGN and heat killed *S.aureus* (HKSA) were found to decrease Cx43 expression and GJIC in mouse astrocytes (Esen et al. 2007), whereas no effect on Cx43 expression was observed when 3T3 fibroblasts were exposed to HKSA (chapter 5 of this thesis, section 5.3.4-5). Alternatively, exposure to live *S.aureus* decreased Cx43 protein expression (chapter 5 of this thesis, 5.3.4), as did exposure to BCM for 7 days (chapter 4 of this thesis, 4.3.6-7). However, the effects of exposure to *S.aureus in vivo* can differ from the effect *in vitro* as the *in vivo* wound healing response involves multiple cell types from within the tissue, the recruitment of inflammatory cells, and the release of a plethora of cytokines and signals. It is not currently known how BCM, HKSA or live *S.aureus* influence the expression of connexins during the healing of skin wounds *in vivo*, or even whether BCM or HKSA impair healing at all.

It was hypothesised that the presence of *S.aureus* or its secreted exotoxins would impair cutaneous wound healing and cause abnormal connexin expression at the wound edges.

6.2. Materials and methods

See Chapter 2 for general materials and methods. Materials and methods used only in this chapter are described here.

6.2.1. Surgery

Six week old male imprinted control region (ICR) mice were anaesthetised with 4% isofluorane in oxygen at 2 L m^{-1} and nitric oxide at 1 L m^{-1}. They were then injected with 0.1 mg kg^{-1} of buprenorphine subcutaneously in the scruff of the neck. Hair was removed from the backs of mice by shaving. The remaining hair was removed by applying a thin layer of Nair® (Church and Dwight, Folkestone, UK). Nair and hair was removed using warm moist gauze, and the skin was sterilised by wiping with 70% ethanol. Mice were placed on a heated mat during the operation, and kept anaesthetised on a nose cone. Four full thickness excisional biopsy punch wounds were made in the dorsal skin, 2 on each side of the midline (see figure 2.1.C) using 6 mm medical biopsy punches (Kai Industries). Heat killed *S.aureus* (HKSA) and live *S.aureus* were suspended at the appropriate concentrations in DMEM supplemented with 10% DBS and containing 30% pluronic F127 (pluronic), and 30% pluronic F127 (pluronic) was added to biofilm conditioned medium (BCM) (see Chapter 2.2.3 for the protocol to make BCM). Wounds were treated with 20 µl of either HKSA, live *S.aureus* or BCM pluronic gel as indicated, and control wounds were treated with DMEM supplemented with 10% DBS and containing 30% pluronic F127 (pluronic) only. Pluronic gel is a liquid when cold, allowing delivery, but solidifies rapidly upon warming, ensuring that the substance is retained at the wound site as long as possible. Wounds were then covered in tegaderm™ (3M), to keep the substances in place and to prevent transfer of to the external environment for safety reasons. A separate sheet was used for control and infected wounds for *S.aureus* infected wounds, in order to prevent transfer bacteria between the wounds. Mice were then allowed to recover in a heated box and returned to their home cages. Pre-emptive analgesia was maintained throughout by administration of 1.6 mg ml^{-1} paracetamol, a nonsteroidal analgesic lacking anti-inflammatory properties in the water. They were weighed daily, and observed for signs of discomfort or systemic infection.

6.2.2. Tissue harvesting and processing

Mice were euthanised by a rising concentration of CO_2, and death confirmed by cervical dislocation. Mice were harvested at 3 or 7 days. Tissue was excised and fixed in 4% PFA in PBS overnight at room temperature, except for where tissue was to be used to determine senescence associated β-galactosidase (SA-β-gal) activity: This tissue was fixed for only 2 hours in 4% PFA. All tissue was then washed with PBS, then transferred to 20% sucrose in PBS with 0.1% sodium azide at 4 °C overnight. Tissue was frozen into O.C.T and stored at -80 °C until further processing, except for the tissue to be used for SA-β-gal staining which was sectioned immediately and stained that day. Cross sections of wounds were cut on a cryostat at 12 μm thicknesses. Serial sections were taken across slides, so each slide contained multiple sections spanning approximately 200 μm of the wound.

6.2.3. H&E

H&E staining

Fixed tissue sections were H&E stained as described in chapter 2 materials and methods. They were imaged on an AxioScan Z1 slide scanner (Zeiss) using a x20 objective. Images were opened in Zen 2012 software (Zeiss) and all measurements made using the tools in the software unless indicated otherwise.

Measuring re-epithelialisation

Re-epithelialisation was measured from the wound edge (where the incision was made and normal dermis was present) to the tip of the new growth. Re-epithelialisation was measured at both wound edges in a minimum of 2 sections, taken from different regions of the wound. The measurements were averaged.

Measuring granulation tissue area

Granulation tissue was measured from the site of incision at the edge of the undamaged dermis. The region encompassed all tissue under the new epithelium, with the bottom of the region in line with the layer of muscle beneath the adjacent undamaged dermis. Results were averaged from a minimum of 2 sections, taken from different regions of the wound.

Measuring wound width

Wound width was measured as a straight line from the left wound edge to the right wound edge at the epidermal level. An average from a minimum of 3 sections was taken, from different regions of the wound.

Calculating the wound closure percentage

The percentage of the wound width that the new epithelial tongue had covered (wound closure percentage) was determined by dividing the re-epithelialisation length by the wound width, and expressing the result as a percentage.

Measuring epidermal thickness

The thickness of the epidermis was measured in 3 randomly selected regions 0.5-1 mm from the wound edge. Both sides of the wound were measured, and the thickness averaged over a minimum of 2 sections, taken from different regions of the wound.

6.2.4. Counting the number of cells in a section of epidermis

Confocal images of regions of Hoechst stained distal epidermis in control and *S.aureus* infected wounds were opened in Image J (NIH) image analysis software. The number of cells in the epidermis within a 30-40 μm distance were counted, and presented as nuclei per μm of epidermis.

6.2.5. Senescence associated β-galactosidase activity stain

Immediately following sectioning, the tissue was washed in PBS for 10 minutes to remove O.C.T. The tissue was incubated in a humidified chamber with the senescence associated β-galactosidase (SA-βGal) staining solution (see table 2.1. for the recipe) in the dark at 37 °C for 24 hours. Slides were then washed in PBS, counter stained with nuclear fast red solution (Sigma-Aldrich) for 20 seconds, and washed again, before mounting in 70% glycerol. Slides were imaged on an AxioScan Z1 slide scanner (Zeiss).

6.3. Results

6.3.1. Wound healing is impaired by application of 100% BCM

Previous analysis showed that *in vitro* 100% BCM had a significant effect on cellular functions that are important in wound repair. It stopped proliferation of fibroblasts (figure 4.2), which, after prolonged incubation, became senescent (figure 4.3. and 4.4). It also retarded migration of these cells (figure 4.5–7). As proliferation and migration are both integral aspects of cellular behaviour during tissue repair it was investigated whether BCM also negatively impacted healing *in vivo.*

Full thickness punch biopsy wounds were made in the dorsal skin of mice, and 100% BCM in pluronic gel applied to the wounds. The wounds were then covered, and the tissue harvested after 3 or 7 days. A 7 day time point was included as *in vitro* experiments showed induction of senescence at 7 days when fibroblasts were incubated with 100% BCM in cell culture. A pilot experiment using 50%, 75% and 100% BCM in wounds showed a trend indicating that the higher the concentration of BCM the greater the effect it had on retarding re-epithelialisation. Thus for the purpose of this experiment 100% BCM was applied to experimental wounds. The extent of healing at 3 and 7 days was compared between control and BCM applied wounds (figure 6.1). Examples of typical wounds on day 7 are shown in figure 6.1.H-I. A technique commonly use to quantify the degree of healing is measurement of the re-epithelialisation length of the epidermis. This is the distance the keratinocytes have migrated from the original wound edge into the wound bed as indicated in the inset in figure 6.1. Measuring re-epithelialisation at 3 days showed no difference between control and BCM applied wounds (figure 6.1.A). Additionally, mice heal partly through contraction of their wounds, so to determine if wound contraction differed between control and BCM applied wounds the wound width was measured. This is a measurement taken from one wound edge to the other at the height of the epidermis. The wound width of BCM applied wounds did not differ from that of controls at 3 days (figure 6.1.B). While independently useful the wound width and re-epithelialisation length measurements can also used to assess the percentage of the wound that is closed (figure 6.1.C). At 3 days control wounds were 19% (± 4%) closed. This did not differ significantly from

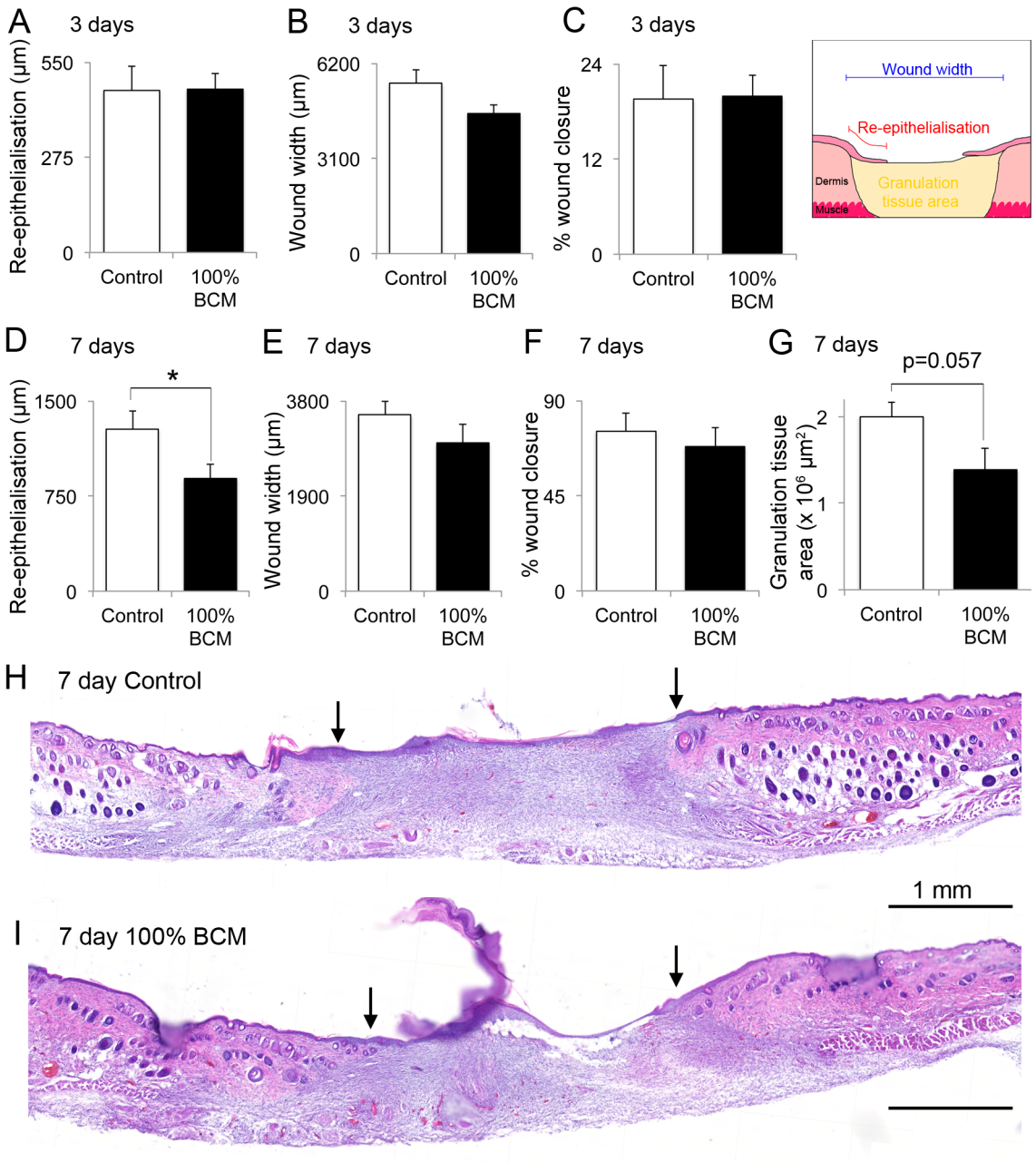

Figure 6.1. A single application of 100% biofilm conditioned medium (BCM) to wounds inhibits healing at 7 days. (A-C) Graphs showing the **(A)** length of the re-epithelialisation, **(B)** the wound width (as indicated on the inset) and the **(C)** percentage of wound closure at 3 days after wounding, in controls and wounds where 100% BCM was applied straight after wounding. **(D-G)** Graphs illustrating the **(D)** length of the re-epithelialisation, **(E)** the wound width, **(F)** the percentage of wound closure, and **(G)** the area of granulation tissue at 7 days after wounding in control and 100% BCM applied wounds. **(H-I)** H&E example images of a matched control wound **(H)** and wound where 100% BCM was applied at the time of wounding **(I)**. Statistical differences were tested using independent Student's t tests. Arrows indicate the wound edges. 3 day, N=10; 7 day, n=12. Scale bars indicate 1 mm. All error bars are SEM. *p<0.05.

the BCM applied wounds which were also 19% (± 3%) closed. Therefore it was concluded that a single topical application of 100% BCM has no significant impact at 3 days on any of the aspects of wound closure assessed here.

The analysis used to assess healing at 3 days was also used to assess healing at 7 days after application of 100% BCM. At 7 days there was a small but significant reduction in the re-epithelialisation length in the wounds where BCM was applied (figure 6.1.D). In contrast, a comparison of the wound width confirmed that this did not differ significantly, showing that contraction of the wounds did not differ (figure 6.1.E). As there was no difference in the average wound width it is unlikely that the small reduction observed in the epithelial tongue length was caused by contraction of the wounds making the BCM wounds smaller. Re-epithelialisation length and wound width were also used to determine the percentage of wound closure (figure 6.1.F). Control wounds were 75% (± 9%) closed, while BCM applied wounds were 68% (± 9%) closed; a Mann Whitney U test showed that the difference was not significant. Interestingly, despite wound width not differing, there was a clear trend ($p=0.057$) for less granulation tissue in the BCM applied wounds (figure 6.1.G). Therefore it was concluded that a single topical application of 100% BCM reduced the length of re-epithelialisation at 7 days, and could potentially be reducing granulation formation. Wound closure was consequently somewhat impaired, but a single application of BCM was not sufficient to cause significant differences in the percentage wound closure.

In addition to impairing proliferation and migration *in vitro*, prolonged incubation with 100% BCM was previously shown to induce a senescent phenotype in fibroblasts (section 4.3.3). To investigate whether a single topical application of 100% BCM to wounds induced a senescence phenotype *in vivo,* senescence associated β-galactosidase (SA-βGal) activity was observed in tissue harvested 7 days after wounding (figure 6.2). This was highly variable between animals, with some exhibiting almost no SA-βGal activity, as shown in figure 6.2.C-D, and others having large amounts of staining, as shown in the example in figure 6.2.A-B. In most animals though, there appeared to be a small increase in SA-βGal activity in the wounds where 100% BCM was applied compared to the animal matched controls. Staining was particularly apparent in the wound bed

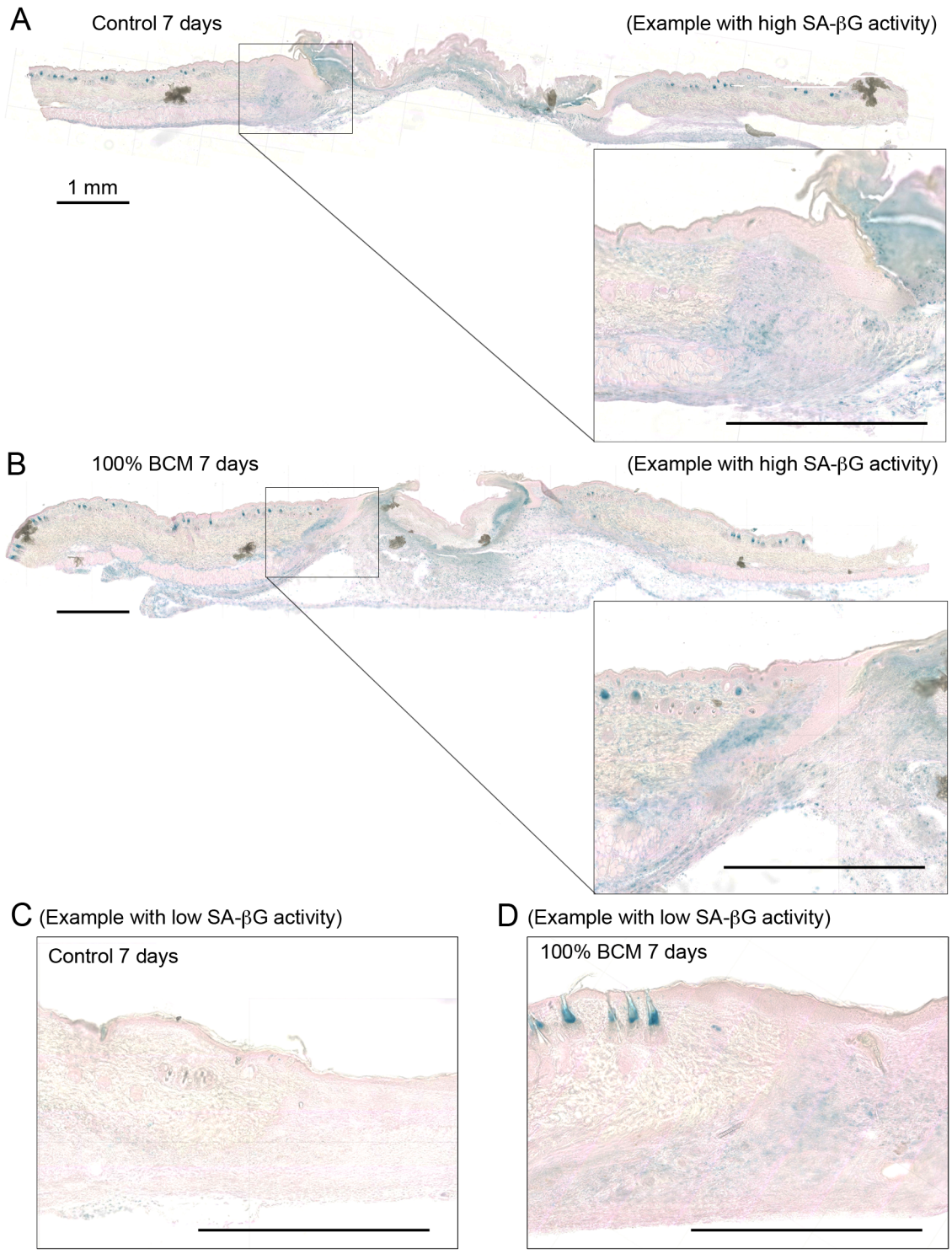

Figure 6.2. Application of 100% biofilm conditioned medium (BCM) to wounds appears to increase senescence associated β-galactosidase activity at 7 days. (A-D) Images are shown of 7 day wounds tested for senescence associated β-galactosidase (SA-β-Gal) activity (blue) and counterstained with nuclear fast red (pink). Examples with **(A-B)** high and **(C-D)** low SA-β-Gal activity are shown. Animal matched controls **(A and C)** and 100% BCM **(B and D)** wounds are shown. The whole wound is shown for the high SA-βG activity example, with enlarged insets of the wound edge. Enlarged images of the wound edge only are shown for the low example. All scale bars indicate 1 mm.

and in the dermis at the wound edge. It is not possible to be conclusive in the finding here, but if this observed trend is correct then this is potentially a plausible reason for the slight impairment of healing observed in wounds where 100% BCM was applied.

6.3.2. Wound healing is impaired by infection with live *S.aureus* but not HKSA

In vitro infection with *S.aureus* significantly reduced cell viability (figures 5.1, 5.6) and proliferation (figure 5.7.C), both of which are vitally important during the healing process. Whilst infection with HKSA had no effect on viability or proliferation of fibroblasts in the *in vitro* experiments conducted (figures 5.2, 5.6), *in vivo* healing is complex, involving the coordination of many signals and cell types. Therefore it is feasible that HKSA may have an effect on healing *in vivo*. Thus it was investigated whether infection of wounds with either HKSA or live *S.aureus* retarded healing. Only a day 3 time point was included as infection with live *S.aureus* beyond this time point resulted in a spreading infection.

Healing was compared at 3 days for wounds infected with HKSA (figure 6.3). Pilots using several concentrations of HKSA revealed no trend, so the highest concentration tested in the pilots was selected for proceeding experiments (6 x 10^6 CFU ml^{-1}). Typical examples of HKSA day 3 wounds are shown in figure 6.3.D-E). Infecting wounds with HKSA did not impair re-epithelialisation, as the length of the epithelial tongue did not differ between controls and infected wounds (figure 6.3.A). Similarly HKSA infection did not alter contraction, as the width of the wounds also did not differ (figure 6.3.B). Assessment of wound closure showed 15% (± 2%) closure in controls and 16% (±2 %) in HKSA wounds (figure 6.3.C). Thus it was concluded that infection with HKSA did not impair wound healing at 3 days after infection.

Several pilot experiments were also conducted to select a concentration of live *S.aureus*. This was particularly important as most concentrations tested resulted in extensive damage to the surrounding tissue; there was often complete loss of the epidermis and de-cellularisation of the dermis for several millimetres away from the wound, with no indications of healing. The

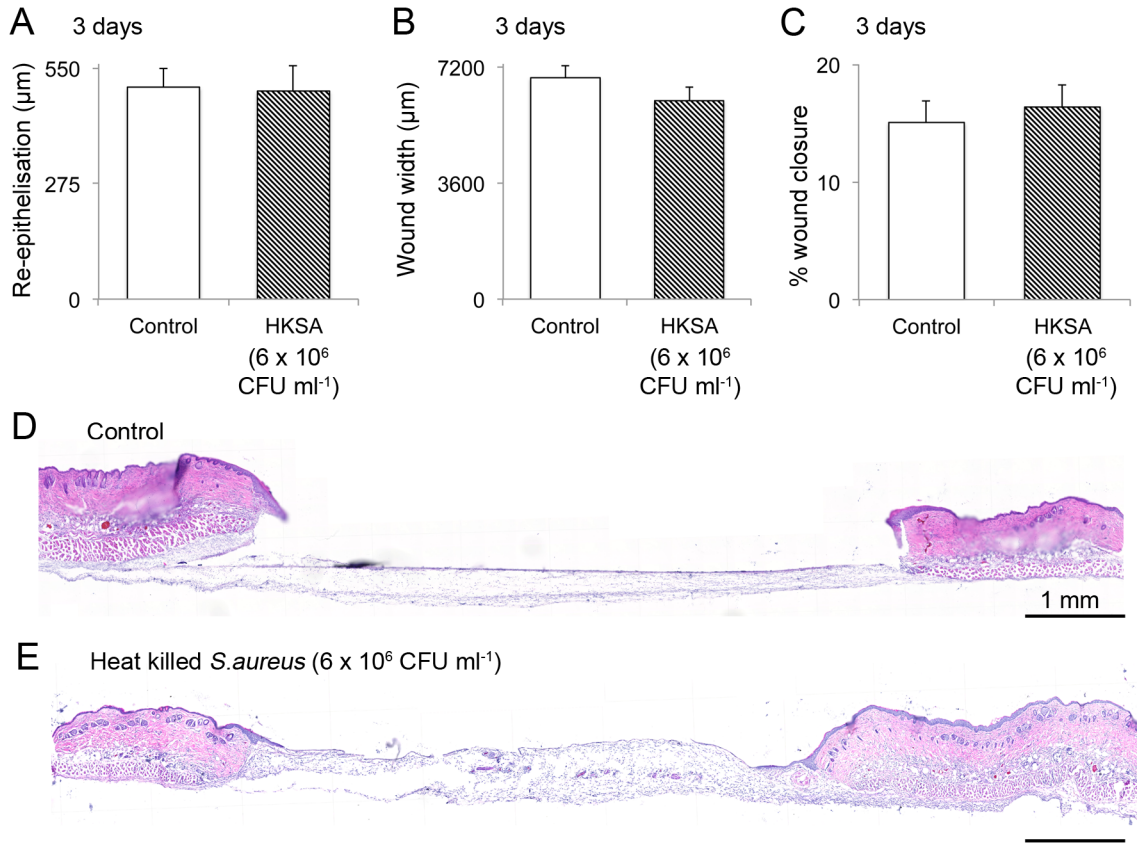

Figure 6.3. Infection of wounds with heat killed *S.aureus* does not delay healing at 3 days. **(A-C)** Graphs showing the **(A)** length of the re-epithelialisation measured from the wound edge to the tip of the new growth, **(B)** the wound width, and **(C)** the percentage of wound closure at 3 days after wounding for animals infected with 6 x10^6 CFU ml^{-1} of heat killed *S.aureus* (HKSA). **(D-E)** Representative images are shown of control and *HKSA* infected wounds at 3 days. Scale bars indicate 1 mm. Statistical differences were tested using independent Student's t tests. N=7. All error bars are SEM.

concentration finally selected for this experiment was 9 x 10^4 CFU ml^{-1}. Observations of H&E images of the 3 days wounds infected with this concentration of *S.aureus* show clear signs of infection, alongside some signs of healing. Typical examples of these 3 day wounds are shown in figure 6.4.D-E. Infection was evident in the wound bed, where there was abundant material, and the skin often became attached to the underlying fascia (see figure 6.4.E for an example). There was re-epithelialisation, although there were indications of tissue damage; the re-epithelialising tongue often contained lesions (see red arrow in the inset of figure 6.4.E), and some rounded nuclei, indicating potential loss of viability. There was also hyperkeratosis (thickened stratum corneum), particularly around the wound edge (this is indicated by the black arrow in figure 6.4.E inset). In order to quantitatively compare healing in control and infected wounds, measurements of re-epithelialisation, wound width, and percentage wound closure were made. Infection with *S.aureus* impaired re-epithelialisation as the length of the epithelial tongue in infected wounds was significantly shorter than in control wounds (figure 6.4.A). Sometimes, but not always, this was accompanied by an increase in epidermal thickness of the re-epithelialising tongue, as in the example in figure 6.4.E. Interestingly the wound width was also significantly reduced by infection with *S.aureus* (figure 6.4.B), suggesting that bacterial infection may increase contraction of the wound. Although the wound width of infected wounds was less than in control wounds, the wound closure was only 9% (± 1%) in infected wounds compared to 20% (± 2%) in control wounds (figure 6.4.C). From this it was concluded that infection with a low concentration of *S.aureus* impairs wound closure by hindering re-epithelialisation, despite also increasing contraction of the wound.

S.aureus rapidly develop into a biofilm, and previous *in vivo* wound healing models have shown *S.aureus* biofilms to develop within 24 hours (Akiyama et al. 1996; Gurjala et al. 2011). It is therefore probable that *S.aureus* in the wound beds of the infected mice would have formed a biofilm. As *S.aureus* biofilm conditioned medium (BCM) induces a senescent phenotype *in vitro* (section 4.3.3), and a single topical application appears to increase SA-βGal activity *in vivo* (figure 6.2), it is feasible that infection with *S.aureus* may also affect senescence. This was tested using SA-βGal activity (figure 6.5). At 3 days there appeared to be less SA-β-Gal activity than seen at 7 days in the BCM *in vivo*

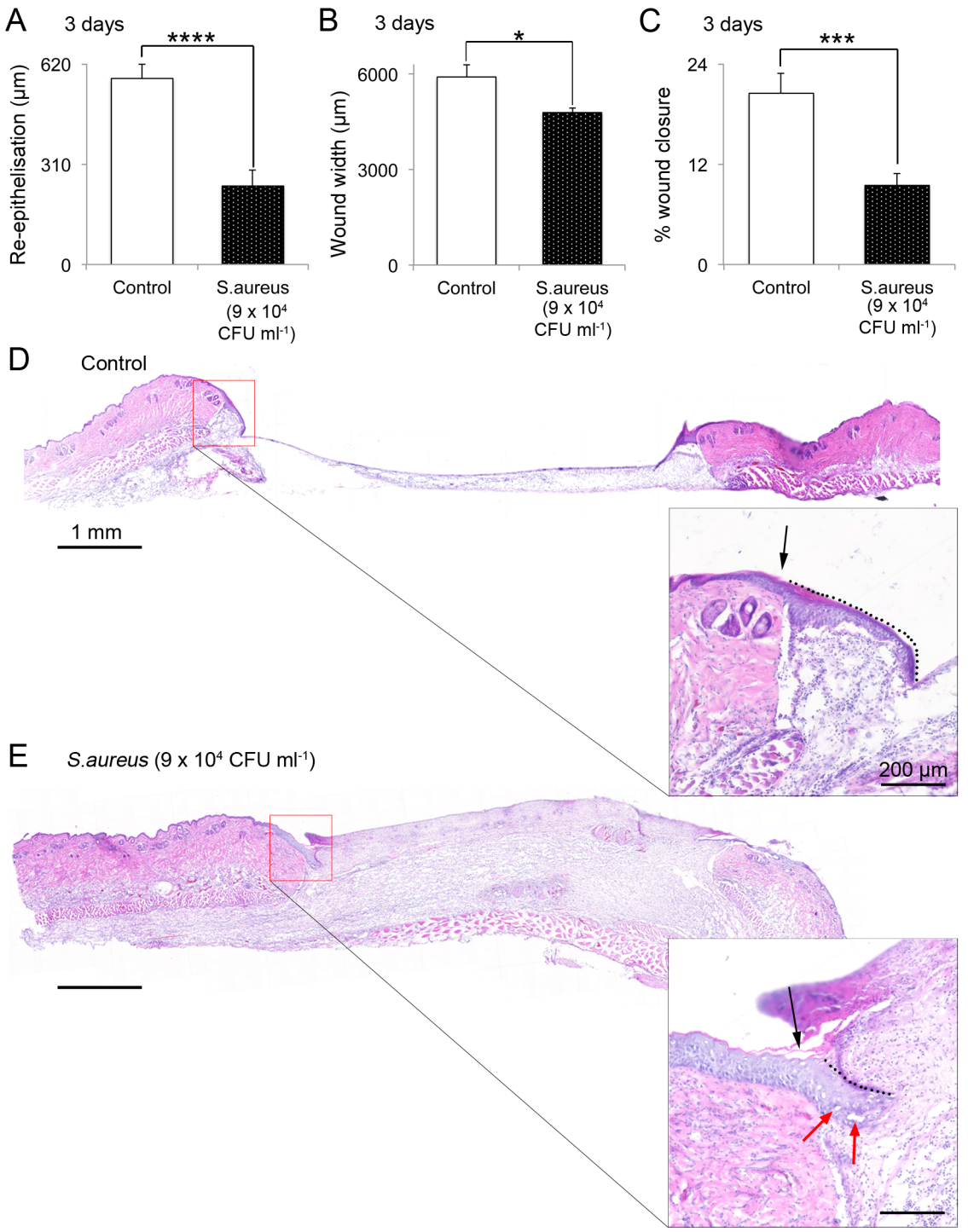

Figure 6.4. Infection of wounds with live *S.aureus* inhibits healing at 3 days. (A-C) Graphs showing **(A)** the length of the re-epithelialisation measured from the wound edge to the tip of the new growth, **(B)** the wound width, and **(C)** the percentage of wound closure at 3 days after wounding for animals infected with 9 x10^4 CFU ml^{-1} of live *S.aureus* (SA). **(D-E)** Representative images are shown of control and *S.aureus* infected wounds at 3 days. The region in the red square is inset. The wound edges are indicated by black arrows, and the re-epithelialised region by the black dotted line. Red arrows indicate lesions in the epithelial tongue. Scale bars indicate 200 µm (insets) or 1 mm as indicated. Statistical differences were tested using independent Student's t tests. N=12. All error bars are SEM. *p<0.05, ***p<0.001, ****p<0.0001.

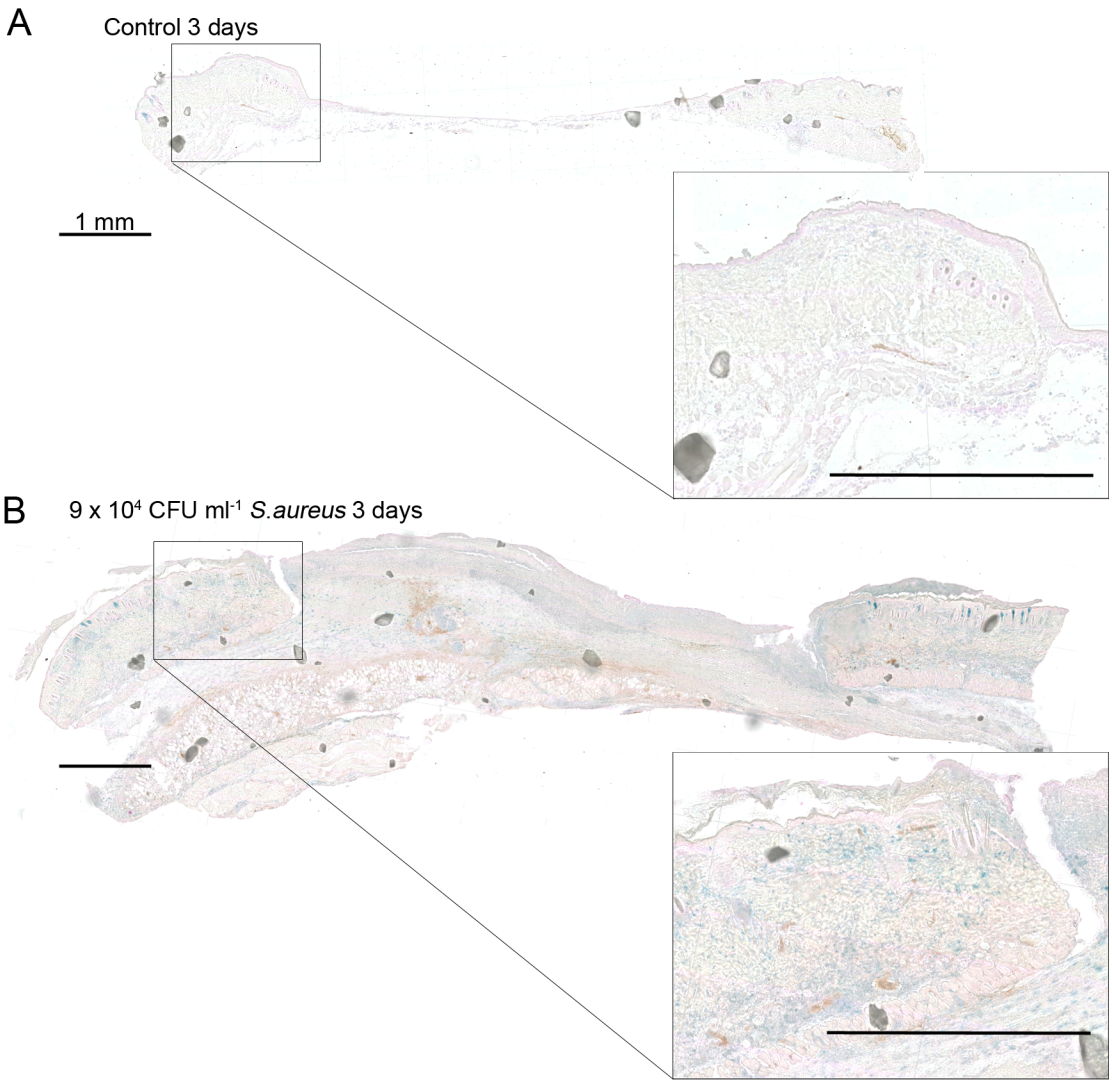

Figure 6.5. Infection of wounds with *S.aureus* appears to increase senescence associated β-galactosidase activity at 3 days. (A-B) Images are shown of 3 day wounds tested for senescence associated β-galactosidase activity (blue) and counterstained with nuclear fast red (pink). An animal matched control **(A)** and wound infected with 9 x10^4 CFU ml^{-1} *S.aureus* **(B)** are shown, with enlarged insets of the wound edge. All scale bars indicate 1 mm.

samples (figure 6.2), and there was again high variability between animals. However, there was generally appeared to be more SA-β-Gal activity in infected than control wounds (an example with relatively high SA-β-Gal activity is shown in figure 6.5). This was most visible in the dermis at the wound edge and in the wound bed, but there also appeared to be increased staining in the epidermis and in the dermis extending away from the wound edge. It is not possible to be conclusive in the finding here, but if this observed trend is correct then potentially an increase in senescence could have contributed to the impairment of healing observed in wounds infected with *S.aureus*. There was insufficient time to conduct the experiment, but it would be interesting to compare the extent of senescence in control and infected wounds at a later time point, such as 7 or 10 days.

6.3.3. A comparison of the effect of BCM, HKSA and *S.aureus* on Cx43 expression in the dermis

Cx43 is expressed in the dermis of skin, where fibroblasts are the predominant cell type. After wounding, Cx43 becomes down-regulated at the dermal wound edge, a change that has been suggested to be necessary for fibroblasts to migrate into the wound bed (Mendoza-Naranjo, Cormie, A. Serrano, et al. 2012). Previous analysis showed that incubation of fibroblasts *in vitro* with 100% BCM for 7 days caused a reduction in Cx43 expression (figure 4.10 and figure 4.12), though a shorter incubation of 9.5 hours did not (figure 4.9 and figure 4.11). To see if application of 100% BCM to cutaneous wounds also reduced Cx43 expression in the dermis, immunofluorescence staining was conducted on sectioned tissue from these wounds. Cx43 expression was examined at both day 3 and day 7. The dermis was imaged and single optical sections taken of a distal region (up to 1 mm from the wound edge) and at the wound edge, as indicated in the inset in figure 6.5. The Cx43 expression in each image was quantified (figure 6.6) and expression in control wounds compared to BCM treated wounds. In all wounds, both controls and where BCM was applied, Cx43 expression reduced at the dermal wound edge compared to the distal region. Distal Cx43 expression was compared for control and BCM applied wounds at both 3 and 7 days, and there were no significant differences in

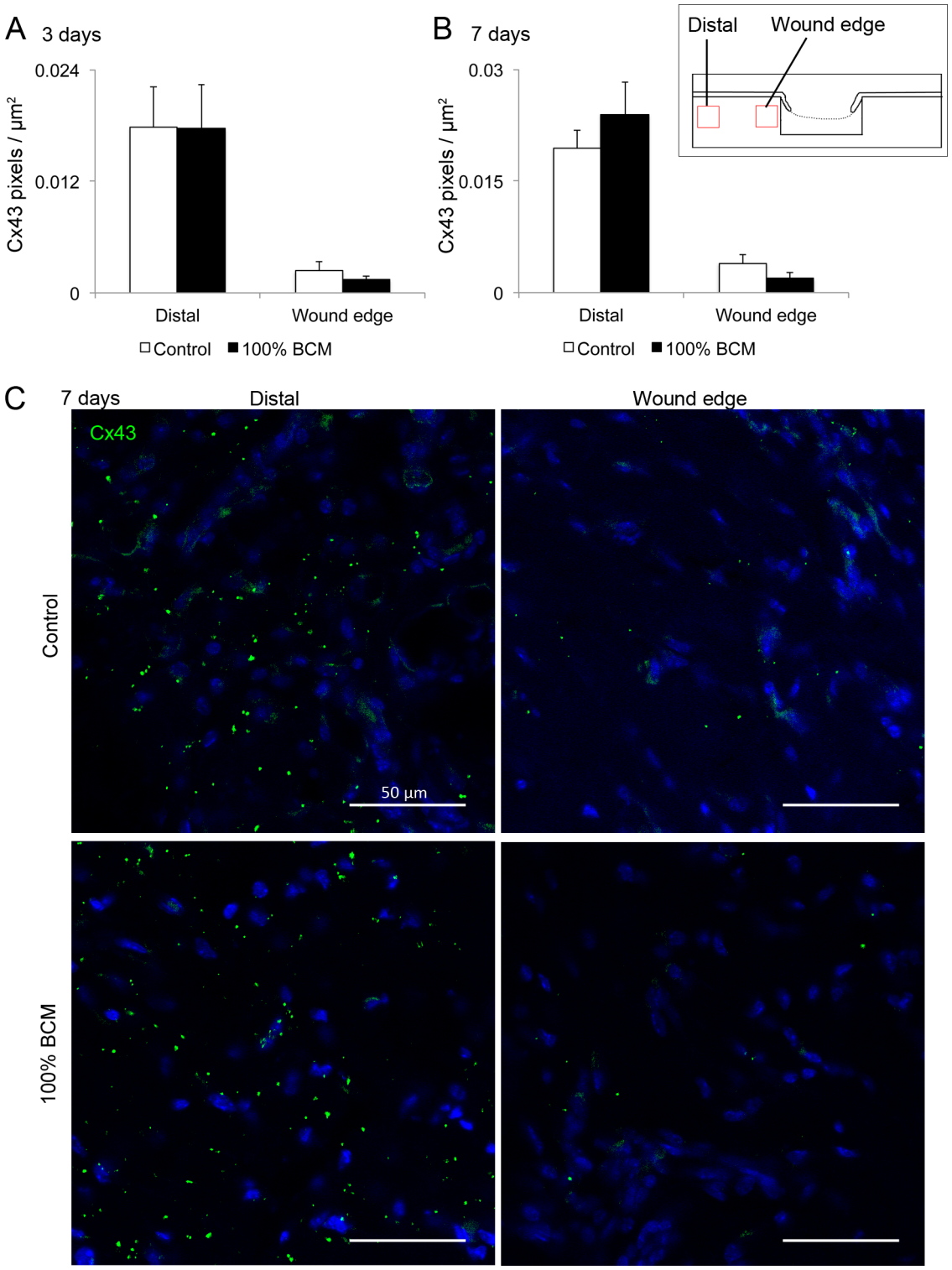

Figure 6.6. Application of 100% biofilm conditioned medium (BCM) has no effect on dermal Cx43 expression at 3 or 7 days. (A-B) Graphs illustrating the Cx43 pixels/µm^2 in the dermis of skin wounds from controls and wounds where 100% BCM had been applied at 3 days **(A)** and 7 days **(B)**. Images were taken of the dermis in regions as indicated by the inset diagram. Distal regions are up to 1 mm from the wound edge. **(C)** Representative confocal images are shown of Cx43 expression (green) in the dermis in a distal region and at the wound edge at 7 days after wounding. Nuclei are counterstained with Hoechst (blue). Scale bars

indicate 50 μm. Statistical differences were tested using independent Student's t tests, but were not significant. 3 days, n=7: 7 days, n=9. All error bars are SEM.

expression. Similarly, dermal wound edge Cx43 expression was compared for control and BCM applied wounds at both 3 and 7 days, and there were no significant differences in expression. Thus it was concluded that a single topical application of 100% BCM did not alter dermal Cx43 at the wound edge or distally at 3 or 7 days after wounding.

In addition to BCM, infection with a low concentration of live *S.aureus in vitro* also caused a down-regulation of Cx43 protein expression (figure 5.9), whereas infection with HKSA did not (figure 5.8). To see if infection of wounds *in vivo* with live *S.aureus* or HKSA reduced Cx43 expression in the dermis immunofluorescence staining was conducted on sectioned tissue from these 3 day wounds. As with the wounds where BCM was applied, the dermis was imaged in a distal region and at the wound edge. The Cx43 expression in each image was quantified (figures 6.7 and 6.8) and expression in control wounds compared to HKSA or *S.aureus* infected wounds. In all wounds, both controls and infected wounds, Cx43 expression reduced at the dermal wound edge compared to the distal region. Surprisingly though, infection of wounds *in vivo* for 3 days with HKSA caused a significant down-regulation of Cx43 expression at the dermal wound edge compared to controls (figure 6.7.A: $p<0.001$). Distal Cx43 expression did not vary significantly between controls and HKSA infected wounds. In contrast, infection with live *S.aureus* did not cause a significant difference in Cx43 dermal expression at the wound edge (figure 6.7.A). Interestingly though, there was a trend ($p=0.09$) towards increased distal dermal Cx43 expression in *S.aureus* infected wounds compared to controls (figure 6.8.A).

6.3.4. A comparison of the effect of BCM, HKSA and *S.aureus* on Cx43 expression in the epidermis

Cx43 is expressed not only in the dermis of skin but in the epidermis as well. Its expression changes dynamically during the healing process, becoming down-regulated initially at the growth tip of the epithelial tongue, and only returning to normal levels once re-epithelialisation is complete (Goliger & Paul 1995; Coutinho et al. 2003). Thus changes in Cx43 expression were observed in the epidermis in response to the application of BCM, HKSA and *S.aureus* to

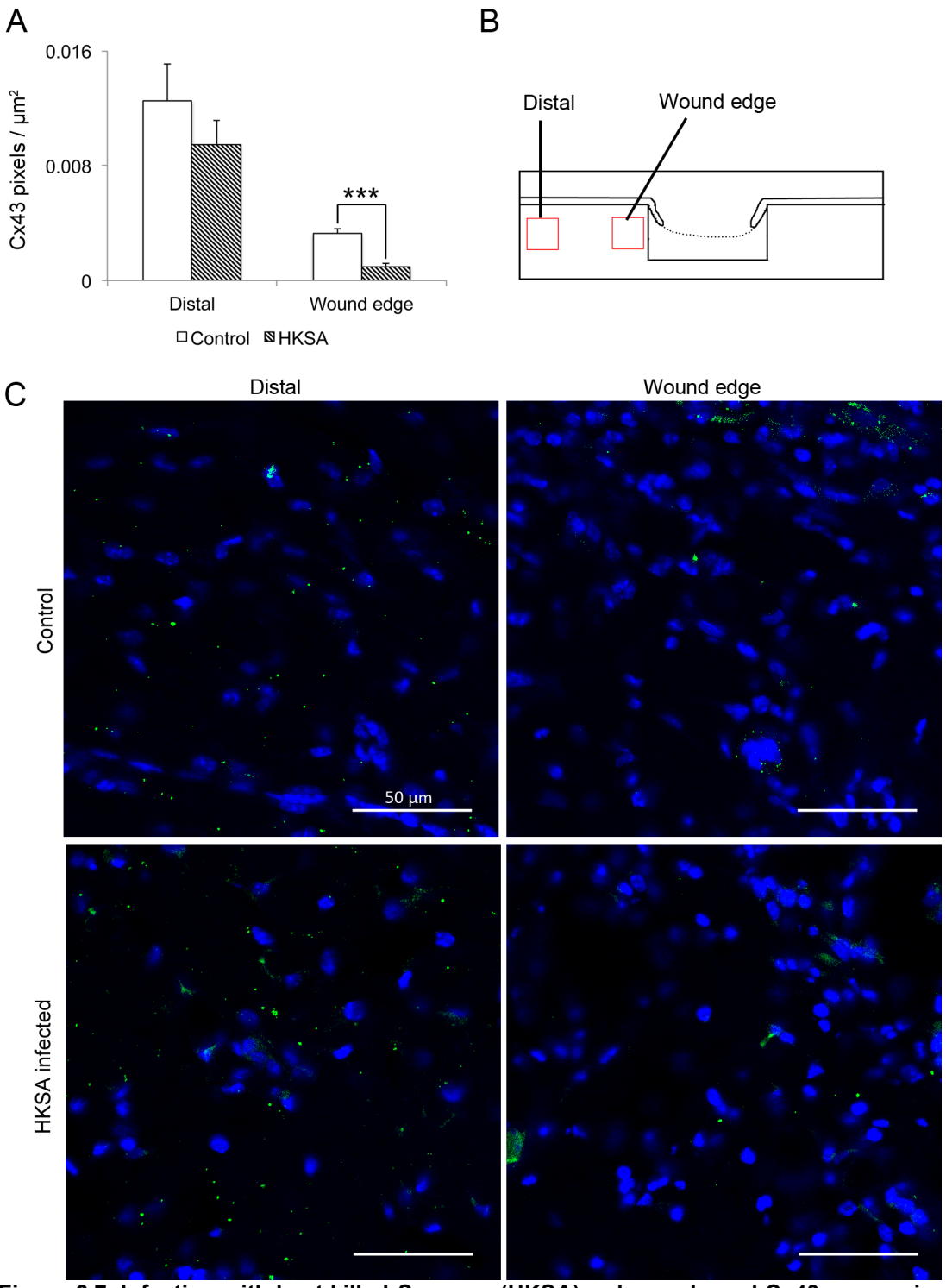

Figure 6.7. Infection with heat killed *S.aureus* (HKSA) reduces dermal Cx43 expression at the wound edge at 3 days. (A) Graph showing the Cx43 pixels/µm^2 in the dermis of skin wounds from controls and wounds infected with 6 x 10^6 CFU ml^{-1} of heat killed *S.aureus* (HKSA). Images were taken of the dermis in regions as indicated by the diagram in **(B)**. Distal regions are up to 1 mm from the wound edge. **(C)** Representative confocal images are shown of Cx43 expression (green) in the dermis in a distal region and at the wound edge. Nuclei are counterstained with Hoechst (blue). Scale bars indicate 50 µm. Statistical differences were tested using independent Student's t tests. N=7. All error bars are SEM. ***p<0.001.

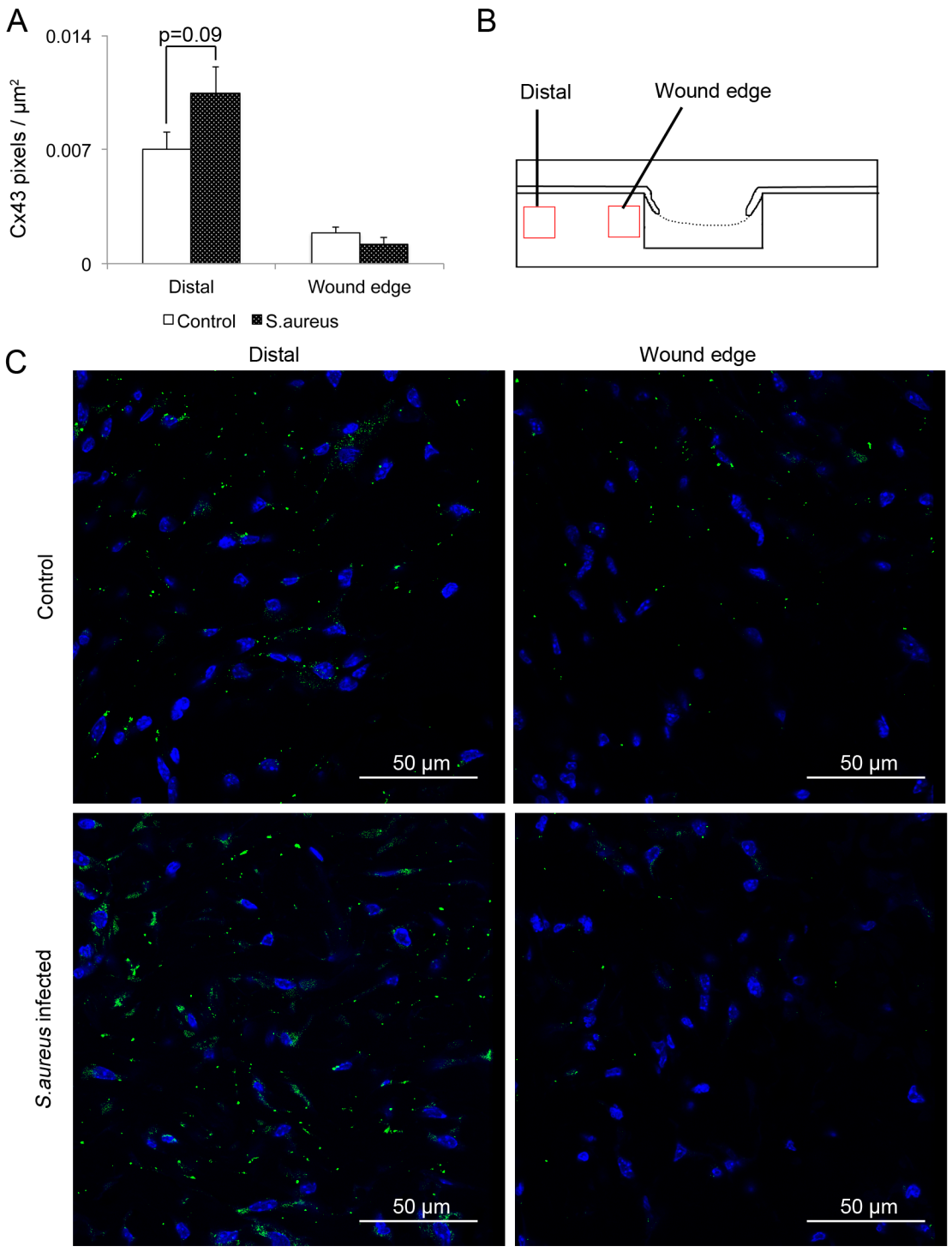

Figure 6.8. Infection with *S.aureus* has no significant effect on dermal Cx43 expression at 3 days. (A) Graph showing the Cx43 pixels/µm^2 in the dermis of skin wounds from controls and wounds infected with 9 x 10^4 CFU ml^{-1} of *S.aureus*. Images were taken of the dermis in regions as indicated by the diagram in **(B)**. Distal regions are up to 1 mm from the wound edge. **(C)** Representative confocal images are shown of Cx43 expression (green) in the dermis in a distal region and at the wound edge. Nuclei are counterstained with Hoechst (blue). Scale bars indicate 50 µm. Statistical differences were tested using independent Student's t tests but were not significant. N=9. All error bars are SEM.

wounds. In all 3 day wounds (BCM, HKSA and *S.aureus* infected) expression of Cx43 was observed at a distal region up to 1 mm from the wound edge, at the original wound edge itself, and at the tip of nascent epithelial growth. In the 7 day wounds Cx43 expression was measured distally and at the original wound edge, but not at the growth tip at 7 days as many wounds had completed the process of re-epithelialisation. In all 3 day control wounds Cx43 expression reduced at the epidermal growth tip compared to distal expression, consistent with previous reports (Goliger & Paul 1995; Coutinho et al. 2003). Epidermal Cx43 expression was compared at each location between control and BCM applied wounds at both 3 (figure 6.9) and 7 (figure 6.10) days; there were no statistically significant differences in any epidermal location or at either time point. There were also no differences observed in the epidermal layers Cx43 was normally expressed in. Epidermal Cx43 expression was also compared at each location between control and HKSA infected 3 day wounds (figure 6.11). Unlike in the dermis, infection with HKSA had no significant effect on epidermal Cx43 expression compared to controls at any of the epidermal locations. There were also no differences observed in the epidermal layers Cx43 was expressed in. In contrast, comparison of epidermal Cx43 expression in wounds infected with *S.aureus* showed significant increases in distal epidermal expression (figure 6.12). Cx43 also became expressed throughout all layers except the most superficial, the stratum corneum. As with BCM and HKSA, no differences were observed in Cx43 expression at the wound edge or in the growth tip.

6.3.5. *S.aureus* infection increases distal epidermal thickness as well as Cx26 and Cx30 expression

Infection with *S.aureus* caused a significant increase in Cx43 expression in distal regions of the epidermis in infected wounds (figure 6.12). Observing these images suggested that the thickness of the epidermis might also be increased. Measurements were taken of the epidermis thickness using H&Es, at a distance of 0.5-1 mm from the wound edge (figure 6.13.A). These showed that epidermal thickness was significantly increased ($p<0.0001$) from a thickness of 17±1 μm in controls to 45±4 μm in infected samples, more than 2.6 fold the thickness. The epidermal thickening was present for an average of 2.3 mm (± 0.3 mm) from the wound edge. However, the epidermal thickening was apparent throughout the

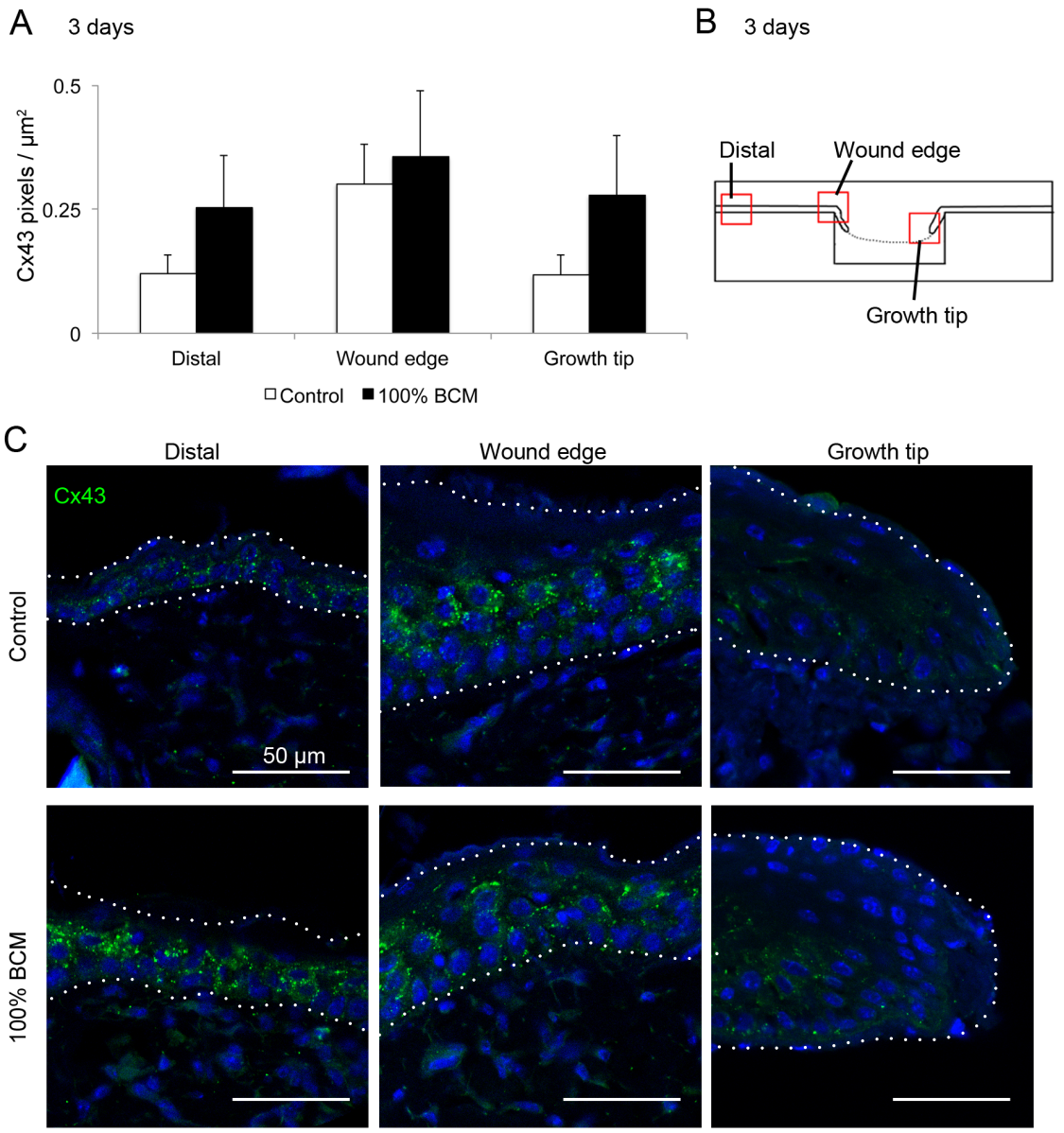

Figure 6.9. Application of 100% biofilm conditioned medium (BCM) has no effect on epidermal Cx43 expression at 3 days. (A) Graph showing the Cx43 pixels/µm^2 after 3 days in the epidermis of skin from controls and wounds where 100% BCM was applied. Images were taken of the epidermis in three regions, as indicated by the diagram in **(B)**. Distal regions are up to 1 mm from the wound edge. **(C)** Representative confocal images are shown of Cx43 expression (green) in the epidermis in a distal region, at the wound edge, and at the growth tip. Nuclei are counterstained with Hoechst (blue), and white dotted lines delineate the area measured to quantify expression. Scale bars indicate 50 µm. Statistical differences were tested using independent Student's t tests but were not significant. N=7. All error bars are SEM.

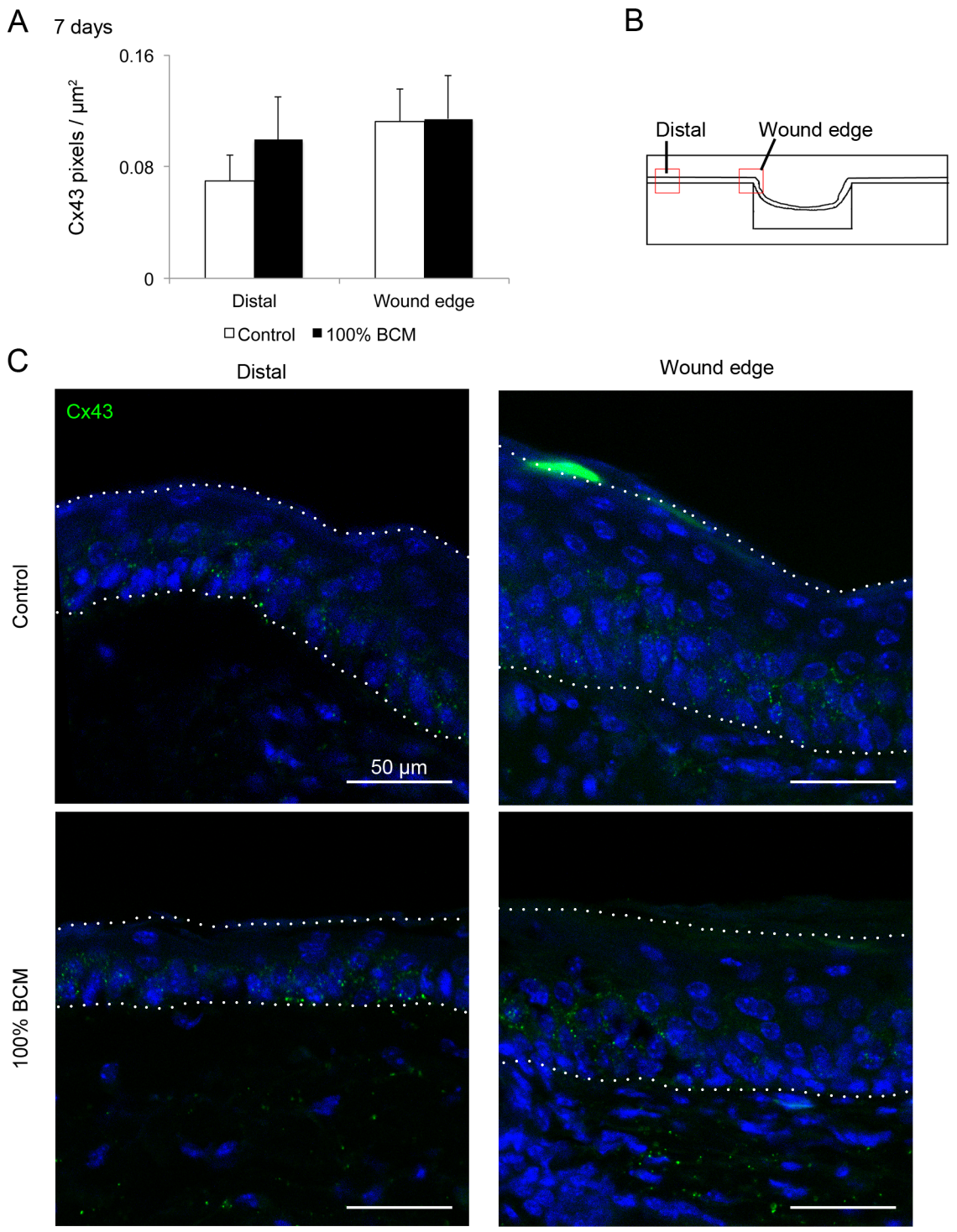

Figure 6.10. Application of 100% biofilm conditioned medium (BCM) has no effect on epidermal Cx43 expression at 7 days. (A) Graph showing the Cx43 pixels/µm^2 after 7 days in the epidermis of skin from controls and wounds where 100% BCM was applied. Images were taken of the epidermis in two regions, as indicated by the diagram in **(B)**. Distal regions are up to 1 mm from the wound edge. **(C)** Representative confocal images are shown of Cx43 expression (green) in the epidermis in a distal region AND at the wound edge. Nuclei are counterstained with Hoechst (blue), and white dotted lines delineate the area measured to quantify expression. Scale bars indicate 50 µm. Statistical differences were tested using independent Student's t tests, but were not significant. N=9. All error bars are SEM.

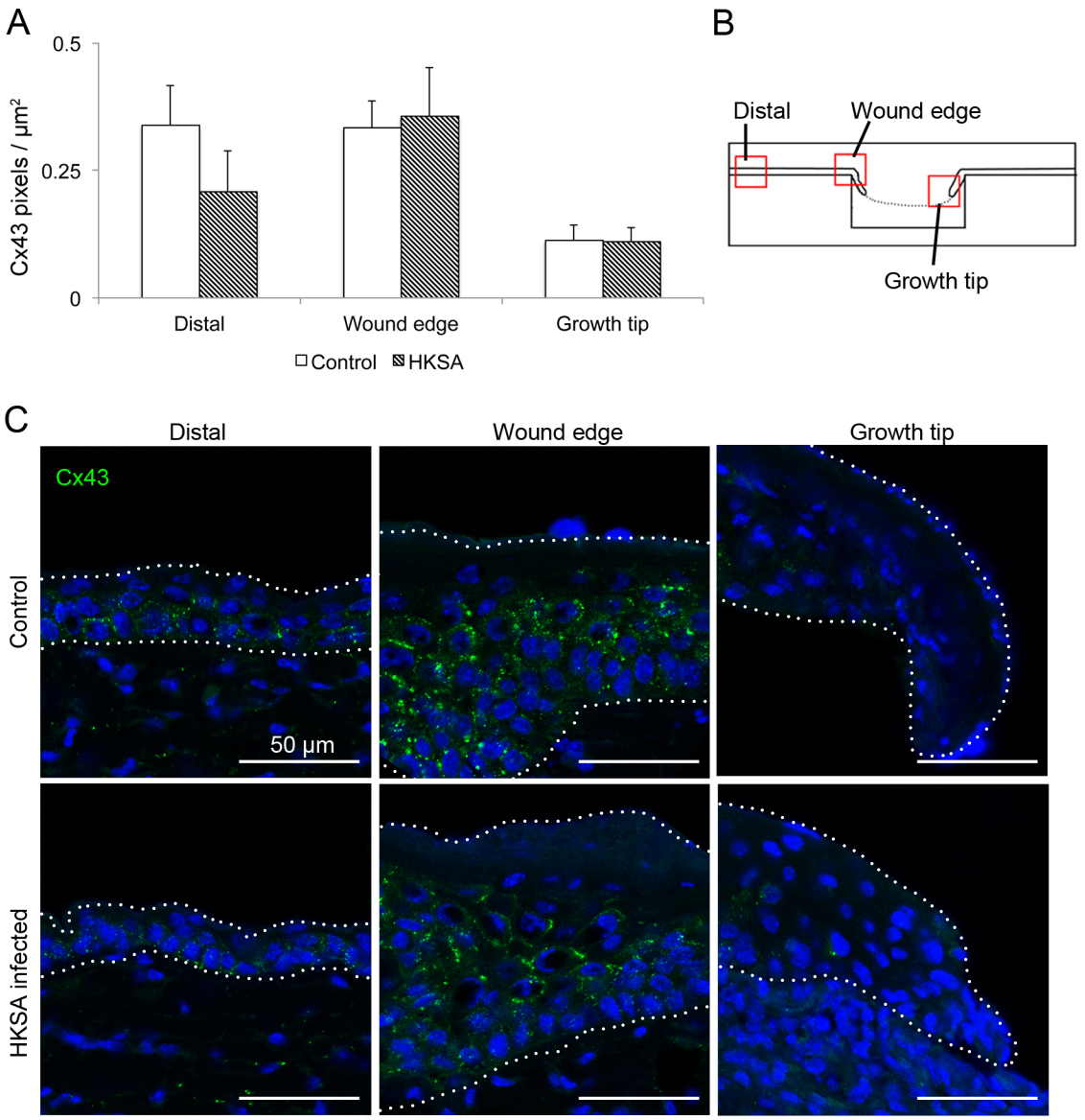

Figure 6.11. Infection with heat killed *S.aureus* (HKSA) has no effect on epidermal Cx43 expression at 3 days. (A) Graph showing the Cx43 pixels/µm^2 in the epidermis of skin from controls and wounds infected with 6 x 10^6 CFU ml^{-1} of heat killed *S.aureus* (HKSA). Images were taken of the epidermis in three regions, as indicated by the diagram in **(B)**. Distal regions are up to 1 mm from the wound edge. **(C)** Representative confocal images are shown of Cx43 expression (green) in the epidermis in a distal region, at the wound edge, and at the growth tip. Nuclei are counterstained with Hoechst (blue), and white dotted lines delineate the area measured to quantify expression. Scale bars indicate 50 µm. Statistical differences were tested using independent Student's t tests, but were not significant. N=7. All error bars are SEM.

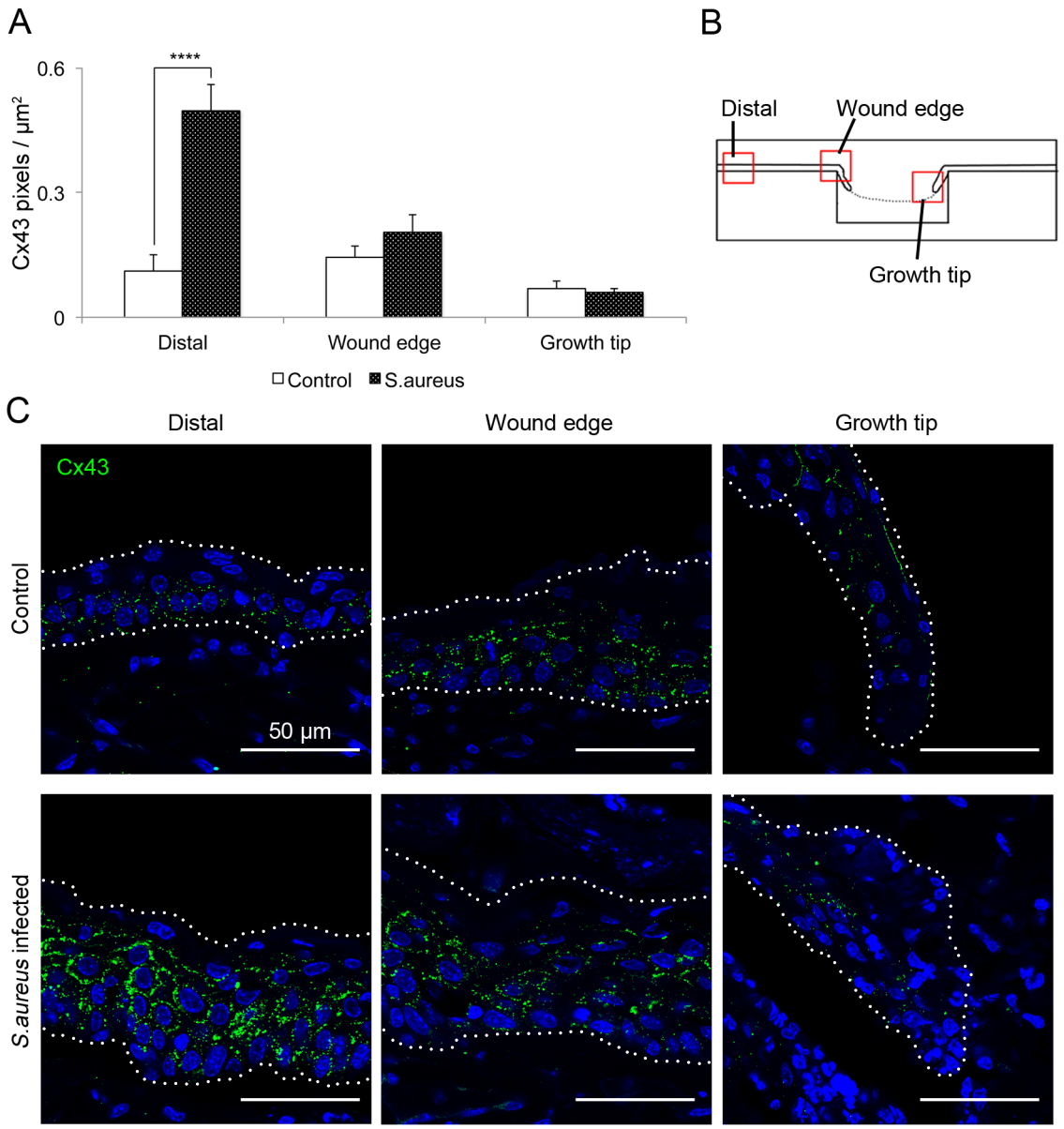

Figure 6.12. Infection with *S.aureus* (SA) increases distal epidermal Cx43 expression at 3 days. (A) Graph showing the Cx43 pixels/µm^2 in the epidermis of skin from controls and wounds infected with 9 x 10^4 CFU ml^{-1} of *S.aureus*. Images were taken of the epidermis in three regions, as indicated by the diagram in **(B)**. Distal regions are up to 1 mm from the wound edge. **(C)** Representative confocal images are shown of Cx43 expression (green) in the epidermis in a distal region, at the wound edge, and at the growth tip. Nuclei are counterstained with Hoechst (blue), and white dotted lines delineate the area measured to quantify expression. Scale bars indicate 50 µm. Statistical differences were tested using independent Student's t tests. N=9. All error bars are SEM. ****p<0.0001.

entire length of many of the biopsies, so may in fact extend further than this. There were also signs of hyperkeratosis (thickened stratum corneum) in many samples, as indicated by the arrow in figure 6.13.C. The number of cells in the epidermis within a 30-40 μm distance were counted, and presented as nuclei per μm of epidermis (figure 6.13.D). Statistical analysis confirmed that the observed hyper-thickening was in conjunction with a significant increase in the number of cells within the epidermis. Interestingly, HKSA had no effect on epidermal thickness, suggesting that metabolically active *S.aureus* are required for this response to occur.

Hyperproliferative, or hyper-thickened, epidermis is frequently associated with high expression of Cx26 and Cx30 by keratinocytes in a number of human skin conditions: high levels of Cx26 have been reported in viral warts, psoriasis (Lucke et al. 1999; Labarthe et al. 1998) and porokeratosis (Hivnor et al. 2004), and high levels of Cx30 in psoriatic and porokeratotic skin (Lemaître et al. 2006). As *S.aureus* infection resulted in a hyper-thickened epidermis up to 2.3 mm from the wound, with elevated Cx43 expression, it was investigated whether Cx26 and Cx30 expression were similarly increased. Expression of both connexins was measured at the original wound edge and in a distal region of the epidermis. Expression in these regions in controls was compared to expression in wounds treated with BCM, or infected with HKSA or *S.aureus.* In all wounds both connexins became elevated at the wound edge compared to distal regions, in agreement with previous reports (Coutinho et al. 2003; Goliger & Paul 1995). Application of neither BCM nor HKSA had a significant effect on distal or wound edge Cx26 or Cx30 expression at 3 days compared to controls (figure 6.14). Similarly infection with live *S.aureus* had no significant effect on either Cx26 or Cx30 expression at the wound edge of day 3 wounds compared to controls. In contrast, live *S.aureus* infection caused a significant increase in distal Cx26 (figure 6.15) and Cx30 (figure 6.16) expression in all but the basal layer of the epidermis.

Thus is was concluded that infection with live *S.aureus* results in changes in the expression patterns of three connexins that normally change dynamically during the healing of cutaneous wounds, and are thought to be important for the healing process. In particular infection results in abnormally elevated

expression of Cx26, Cx30 and Cx43 in the epidermis for up to 1 mm from the wound edge. The mechanism of this change is as yet unknown, and the full implications of it require further exploration.

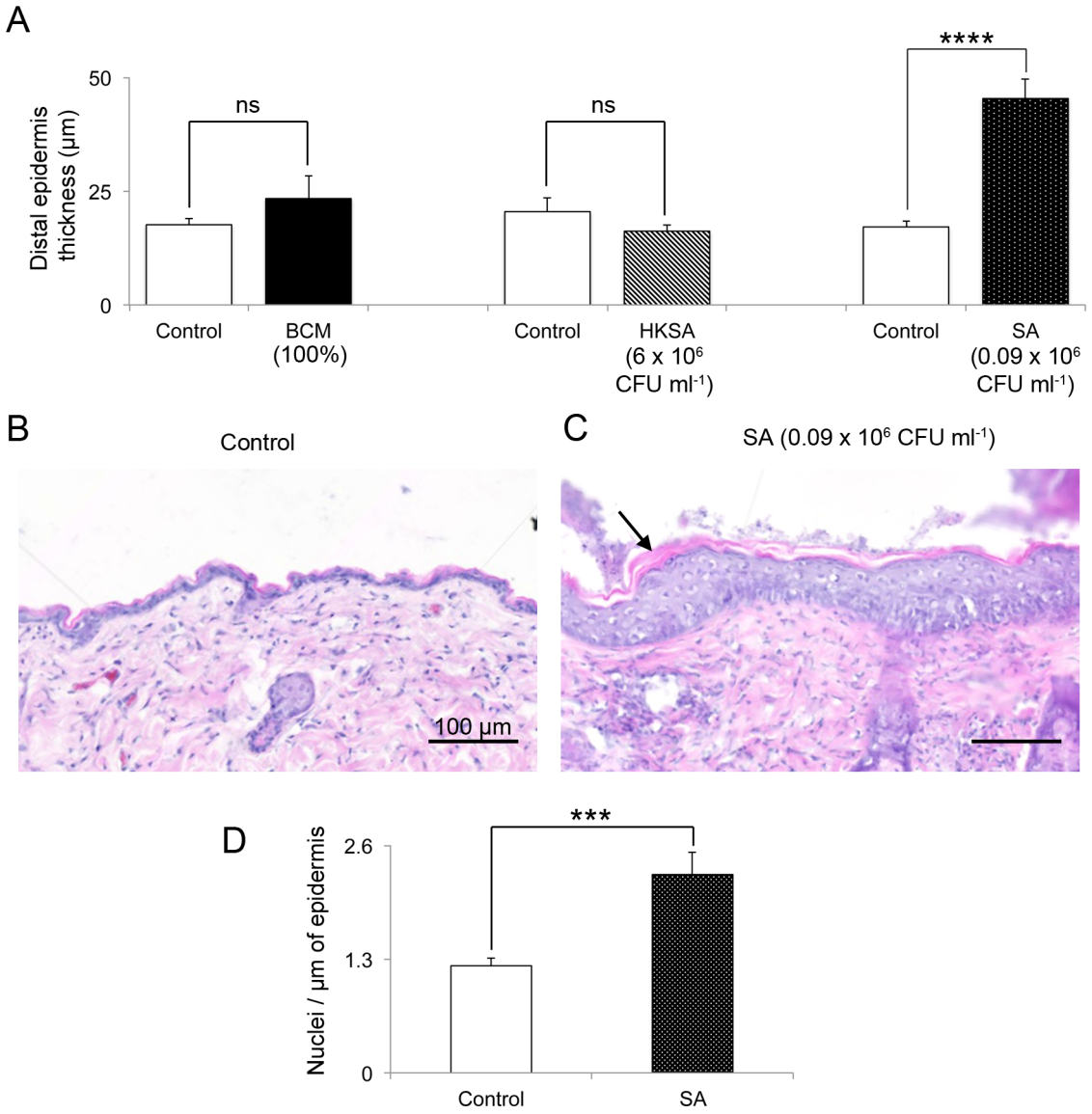

Figure 6.13. Infection with *S.aureus* (SA) causes distal epidermal hyper-thickening. (A) Graphs showing the average thickness of the epidermis 3 days after wounding, in a region 0.5-1 mm from the wound edge. Different animals were used for each experimental condition (BCM, HKSA and SA) with matched controls. **(B-C)** Representative images are shown of the epidermis in a region 0.5-1 mm from the wound edge. Images are of mice whose wounds were initially infected with 9 x 10^4 CFU ml^{-1} of *S.aureus*. The arrow on C indicates the stratum corneum, which appears hyperkeratotic in many infected wounds. **(D)** Graph illustrating the number of nuclei per µm of the epidermis, as measured along the bottom of the epidermis. Scale bars indicate 100 µm. Statistical differences were tested using independent Student's t tests. BCM, N=7; HKSA, N=7; SA, N=12. All error bars are SEM. ns = not significant. ***p<0.001, ****p<0.0001.

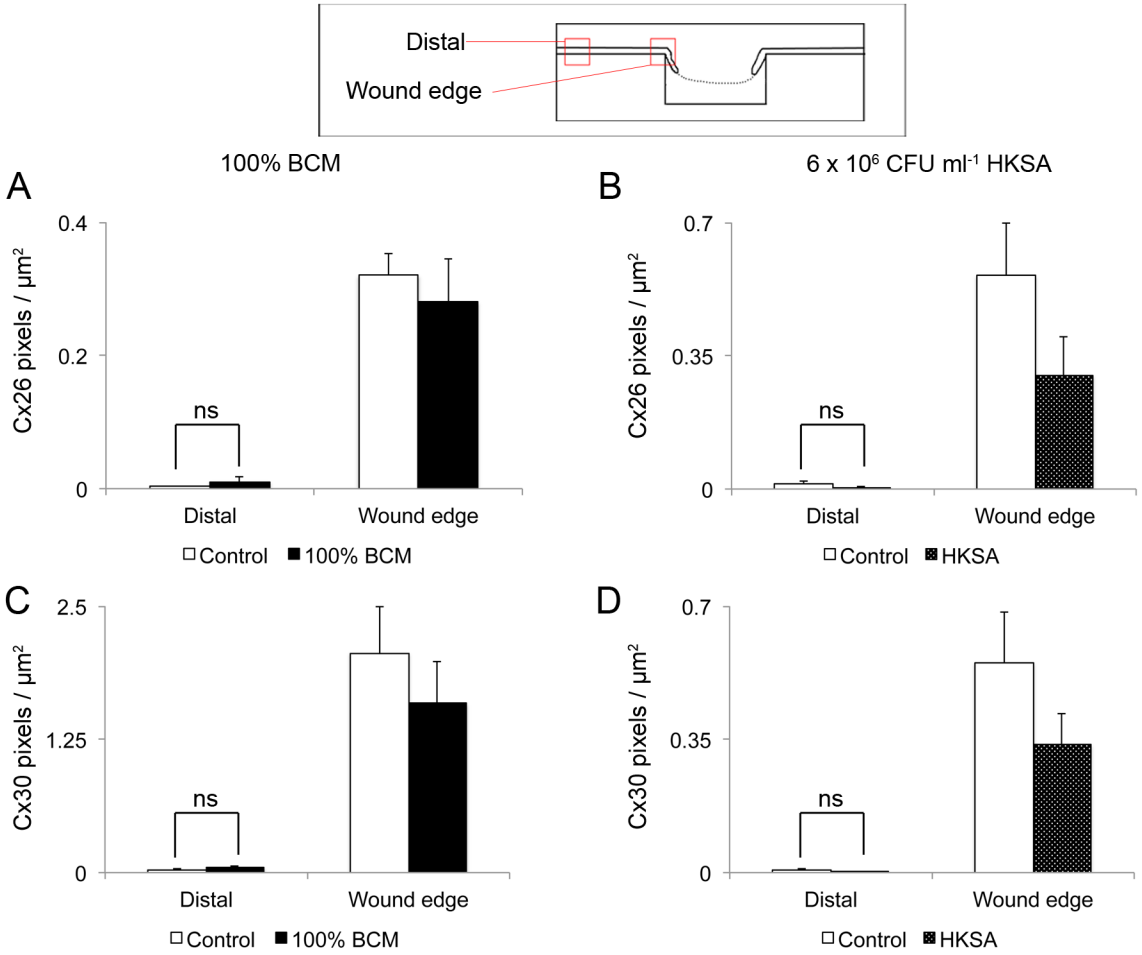

Figure 6.14. Application of BCM and HKSA has no effect on Cx26 or Cx30 expression. A schematic is shown of the regions imaged. Distal regions are up to 1 mm from the wound edge. **(A-D)** Graphs illustrating the Cx26 pixels/µm^2 **(A and B)** or Cx30 pixels/µm^2 **(C and D)** in the epidermis of skin from controls and wounds where 100% was applied **(A and C)** or were infected with 6 x 10^6 CFU ml^{-1} of heat killed *S.aureus* (HKSA) **(B and D)**. Statistical differences were tested using independent Student's t tests, but none were significant (ns). A, B and D, n=7; C, n=6. All error bars are SEM.

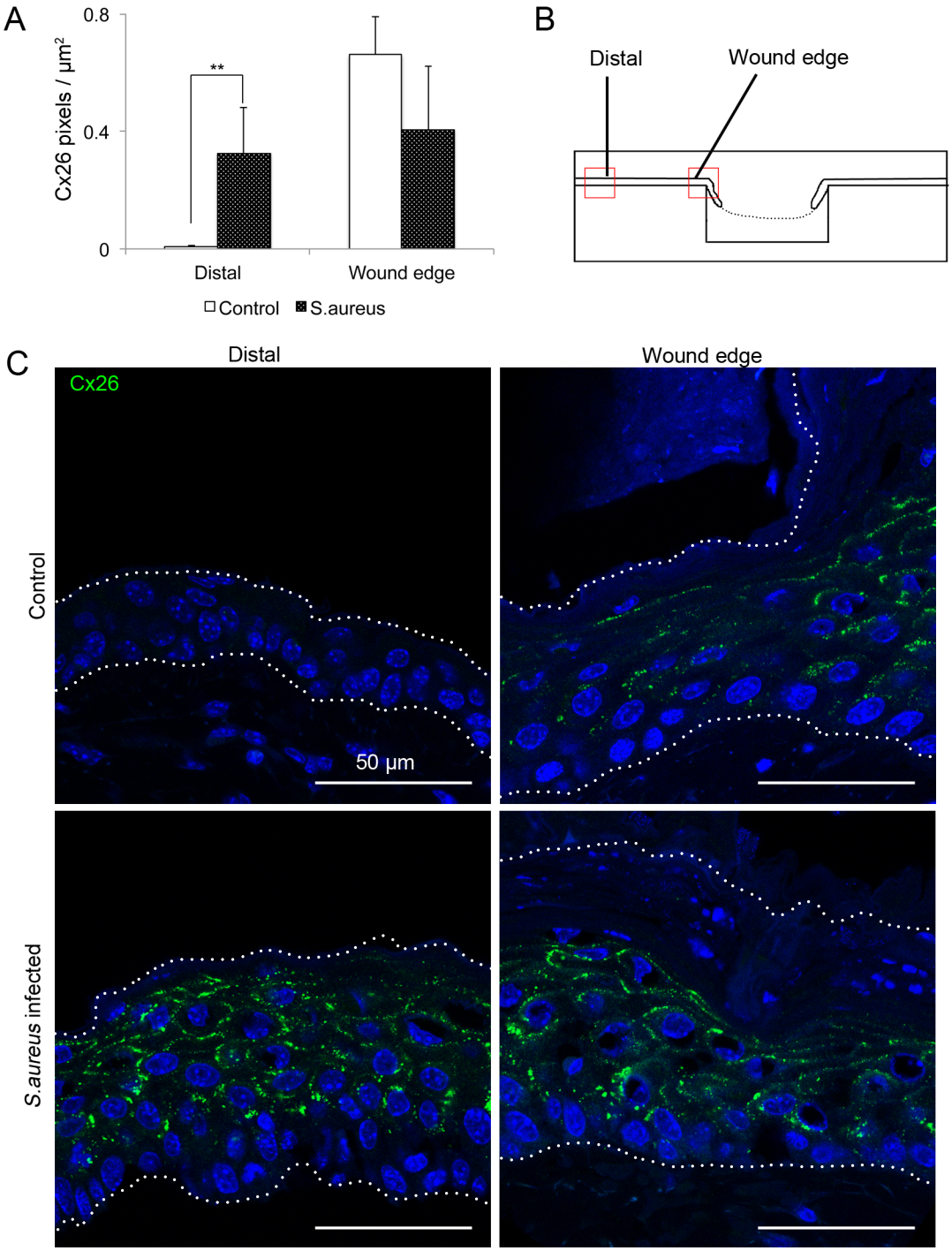

Figure 6.15. Infection with *S.aureus* increases distal Cx26 expression. (A) Graph showing the Cx26 pixels/µm^2 in the epidermis of skin from controls and wounds infected with 9 x 10^4 CFU ml^{-1} of *S.aureus*. Images were taken of the epidermis in regions as indicated by the diagram in **(B)**. Distal regions are up to 1 mm from the wound edge. **(C)** Representative confocal images are shown of Cx26 expression (green) in the epidermis in a distal region and at the wound edge. Nuclei are counterstained with Hoechst (blue), and white dotted lines delineate the area measured to quantify expression. Scale bars indicate 50 µm. Statistical differences were tested using independent Student's t tests. N=6. All error bars are SEM. **p<0.01.

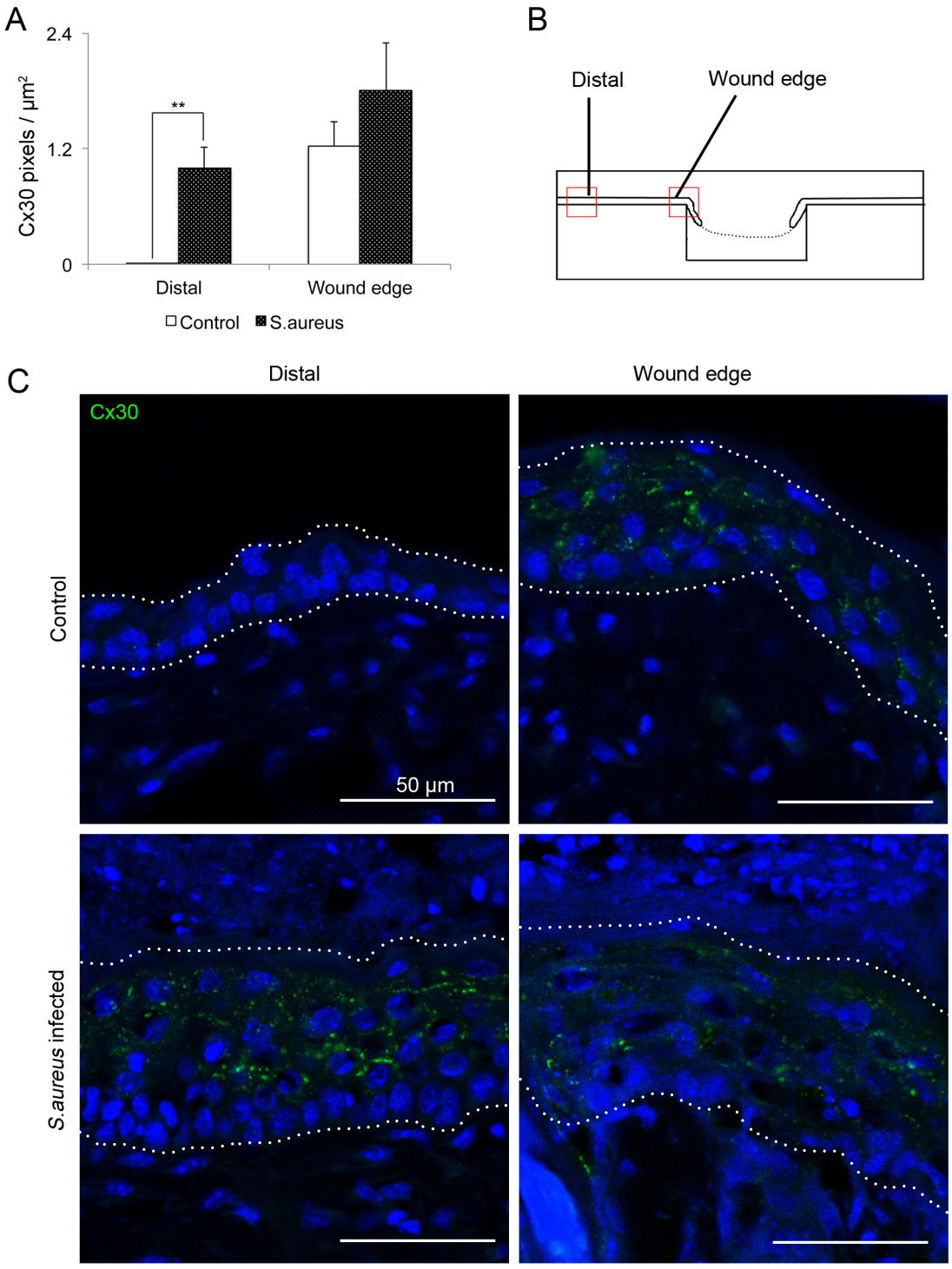

Figure 6.16. Infection with *S.aureus* increases distal Cx30 expression. (A) Graph showing the Cx30 pixels/µm^2 in the epidermis of skin from controls and wounds infected with 9 x 10^4 CFU ml^{-1} of *S.aureus*. Images were taken of the epidermis in regions as indicated by the diagram in **(B)**. Distal regions are up to 1 mm from the wound edge. **(C)** Representative confocal images are shown of Cx30 expression (green) in the epidermis in a distal region and at the wound edge. Nuclei are counterstained with Hoechst (blue), and white dotted lines delineate the area measured to quantify expression. Scale bars indicate 50 µm. Statistical differences were tested using independent Student's t tests. N=7. All error bars are SEM. **p=0.01.

6.4. Discussion

S.aureus is a pathogenic species and is commonly found in wounds, particularly chronic wounds (Davies et al. 2004; Gjødsbøl & Christensen 2006). Moreover, in chronic wounds it is usually found within a biofilm (James et al. 2007). Infection with *S.aureus* or its products have previously been shown to alter the connexin expression in several cell types including keratinocytes (Donnelly et al. 2012; Esen et al. 2007; Garg et al. 2005) and experiments in previous chapters of this thesis showed an effect on fibroblasts. Connexin expression is also abnormal in chronic wounds (Brandner et al. 2004; Mendoza-Naranjo, Cormie, A. E. Serrano, et al. 2012; Mendoza-Naranjo, Cormie, A. Serrano, et al. 2012), but it is not known if *S.aureus* is responsible for this abnormal expression. Mouse wounds were infected with *S.aureus,* in either an alive or heat killed state. Wounds on additional mice were treated with media conditioned with the toxins secreted by *S.aureus* when in a biofilm state (BCM). The effect they had on healing and expression of Cx43, Cx26 and Cx30 were investigated.

In agreement with previous findings, live *S.aureus* significantly impaired healing, by retarding re-epithelialisation (Schierle et al. 2009; Gurjala et al. 2011; Akhil K. Seth et al. 2012; A. Seth et al. 2012; Pastar et al. 2013). Interestingly, *S.aureus* infection decreased the width of the wound compared to controls. This is in contrast to findings in both pig and rabbits ear wounds, where *S.aureus* infection significantly increased the granulation gap (Gurjala et al. 2011; Akhil K Seth et al. 2012). This could be a reflection of the different time points examined, as both Gurajala et al and Seth et al examined the wounds 12 days post wounding, whereas I examined the wounds after 3 days. Alternatively, it may be a reflection of the differences in healing mechanisms between the model species, as unlike rabbits and pigs, mice heal partly through contraction of the wound. Nevertheless, it was unexpected that the wound width was significantly smaller in infected wounds. It would be interesting to ascertain whether there was also an increase in myofibroblasts in the wound, the fibroblast derived contractile cells found in granulation tissue. Like live *S.aureus*, application of 100% BCM to wounds similarly impaired re-epithelialisation, although to a lesser extent, as a difference in the length of re-epithelialisation compared to controls wasn't apparent at day 3, only day 7. A single application

was sufficient to result in a small but significant reduction in re-epithelialisation. It would be interesting to see whether repeated application would more closely resemble the phenotype of live *S.aureus* infected wounds, as the lesser effects might be due to less exposure of the cells to the toxins. At 7 days after wounding there was also a trend towards less granulation tissue in the wounds where BCM was applied. This reflects the *in vitro* experimental data with BCM, where there was a reduction in fibroblast migration. However, in that instance the cells were incubated continuously in BCM, whereas *in vivo* BCM was only applied once (immediately after wounding). Thus *in vivo,* delivery of the toxins were restricted to the period of time the pluronic gel remained in place, which may be the reason why the impairment was not as severe. On the other hand heat killed *S.aureus* did not significantly affect healing compared to controls, which is also in agreement with *in vitro* data, where HKSA had no effect on the viability or proliferation of cells (although its effect on migration was not tested). As no effect on healing was observed when HKSA was applied, it suggests that the coat proteins in *S.aureus* are not responsible for the impaired healing observed in the live *S.aureus* infection.

In future experiments it would be informative to look at proliferation in the BCM and *S.aureus* challenged wounds, through incorporation of BrdU or using proliferative markers such as Ki67. *In vitro* experiments indicated that live *S.aureus* reduced proliferation, and showed that BCM induced senescence in fibroblasts. Visual observations of SA-βGal activity in wounds where BCM was applied or were infected with live *S.aureus* suggested that both might increase SA-β-Gal activity. This suggests that there may be an increase in senescence in the bacteria challenged wounds, but to determine this for certain several senescence markers should be used, such as the cell cycle inhibitor markers p53 and $p16^{INK4A}$ (Kuilman et al. 2010). Senescence has been associated with poor healing in chronic wounds (Clark 2008). Increased senescence has previously been noted in the dermis of pressure sores using the senescent marker, terminin (Vande Berg et al. 1998), but has most frequently been observed in fibroblasts isolated from chronic wounds (Ågren & Steenfos 1999; M. V Mendez et al. 1998; A. C. Stanley et al. 1997; Vande Berg et al. 1998). In fact, a correlation was established whereby difficult to heal ulcers were associated with more than 15% senescence in the population of *in vitro* grown

fibroblasts isolated from the chronic wound (Stanley & Osler 2001). Senescence in cell culture has also been shown in response to challenge by *Escherichia coli* colibactin toxin and *Pseudomonas aeruginosa* pyocyanin toxin (Muller 2006; Secher et al. 2013), although neither has been tested *in vivo*. Interestingly, like *S.aureus*, both these species are common in chronic wounds (Davies et al. 2004; Gjødsbøl & Christensen 2006).

Infection of wounds with live *S.aureus* caused a significant hyper-thickening of the epidermis for several millimetres from the wound. This was in conjunction with an increased number of nuclei, indicating increased proliferation although this was not confirmed with a proliferative marker. Interestingly, epidermal hyperplasia is also a feature of chronic wounds: increased epidermal thickness is associated with hyper-proliferation of keratinocytes (Brem et al. 2007). Moreover, in chronic wounds the epidermis is also frequently hyperkeratotic (thickened cornified layer), parakeratotic (nuclei present in the cornified layer), and fails to differentiate properly (Stojadinovic et al. 2005; Usui et al. 2008; Brem et al. 2007; Stojadinovic et al. 2008). The epidermis surrounding *S.aureus* infected wounds was similarly hyperkeratotic, and so it would be interesting to ascertain whether keratinocyte differentiation is also abnormal. Epidermal hyperplasia also occurs in a number of skin diseases, including psoriasis and atopic dermatitis, both of which have been associated with *S.aureus* (Balci et al. 2009; Hong et al. 2014). When α-haemolysin from *S.aureus* was injected subcutaneously in mice it resulted in atopic dermatitis-like symptoms, including increased inflammation and epidermal hyperplasia (Hong et al. 2014). *S.aureus* infection, particularly toxic strains, was also found to be correlated with patients who had psoriasis, but not with healthy controls (Balci et al. 2009). Interestingly, *S.aureus* peptidoglycan (PGN) was found to have anti-apoptotic effects on keratinocytes *in vitro*, and the authors suggest that it could favour proliferation in psoriasis (Vázquez-Sánchez et al. 2014). Moreover, increased proliferation was shown *in vitro* when keratinocytes were exposed to *S.aureus* α-toxin or protein A (SpA), associated with increased epidermal growth factor (EGF) and EGF receptor activation respectively (Haugwitz et al. 2006; Soong et al. 2011). Increased proliferation was similarly shown in keratinocytes challenged with *S.aureus* epidermal cell differentiation inhibitor (EDIN) (Sugai et al. 1992). As well as promoting proliferation EDIN prevented differentiation, and injection into

mouse skin resulted in extreme hyperplasia. It is therefore apparent that *S.aureus* infection is capable of causing hyperplasia. Whether this is in direct response to the bacteria and its toxins, or predominantly a consequence of inflammation elicited by the bacteria, is currently unknown. It has been shown though, that inflammation is sufficient to cause hyperplasia. For example, IL-17C is a pro-inflammatory cytokine found expressed abundantly in psoriasis; its ectopic overexpression in keratinocytes in mice resulted in epidermal hyperplasia (Johnston et al. 2013). Moreover, both psoriasis and atopic dermatitis are chronic inflammatory skin diseases in which the cytokine IL-22 has been shown to play a critical role (Swindell et al. 2013; Hong et al. 2014; Fujita 2013).

Hyperproliferative or hyperplasic epidermis is frequently associated with an increase in Cx26, and to a lesser extent Cx30, expression; high levels of Cx26 and Cx30 are frequently reported in hyperproliferative skin conditions including viral warts, psoriasis and porokeratosis (Hivnor et al. 2004; Lemaître et al. 2006; Lucke et al. 1999; Labarthe et al. 1998). Skin surrounding chronic wounds is also typically hyperplastic (Brem et al. 2007), and recently, the Becker lab has identified significantly elevated levels of Cx26 and Cx30 in the epidermis of human chronic wounds for up to 4 mm from the wound edge (Sutcliffe et al-manuscript submitted). Both Cx26 and Cx30 have been proposed as markers of hyper-thickened epidermis, and both are expressed at significantly elevated levels in the hyper-thickened epidermis of *S.aureus* infected wounds. The relationship between these connexins and proliferation of keratinocytes is somewhat confusing, with conflicting results. *In vivo* Cx26 and Cx30 expressing cells are often not associated with proliferation markers (Goliger & Paul 1995; Lucke et al. 1999; Coutinho et al. 2003). However, ectopic overexpression of Cx26 in keratinocytes caused hyperplasia in transgenic mice, and overexpression of mutant Cx30 caused mild hyperkeratosis (Djalilian et al. 2006; Bosen et al. 2014). Conversely, manipulating Cx26 and Cx30 expression in keratinocytes *in vitro* has been found to have no effect on proliferation in some circumstances, but over expression increased proliferation in other reports (Man et al. 2007; Wiszniewski et al. 2001; Thomas et al. 2007). Thus it is unclear whether increased Cx26 or Cx30 expression is a cause of epidermal hyperplasia, or a consequence of it. Interestingly, it has been shown *S.aureus*

can increase the expression of Cx26 and Cx30; exposure of astrocytes and keratinocytes to *S.aureus* derived PGN increased Cx26 expression, though PGN decreased Cx30 expression in astrocytes (Esen et al. 2007; Donnelly et al. 2012). Expression of Cx26 was also recently linked to the invasion of epithelial cells and keratinocytes by the pathogen *Shigella flexneri* (Tran Van Nhieu et al. 2003; Man et al. 2007). Furthermore, tape stripping (repeated epidermal trauma from application and removal of sticky tape) increased Cx26 expression in the epidermis of humans (Lucke et al. 1999), and tape stripping was also found to increase the colonisation of *S.aureus* in mice (Wanke et al. 2013). Thus it is possible to postulate that *S.aureus* infection might directly, or perhaps through inflammation, be influencing Cx26, and perhaps also Cx30, expression in the epidermis. Of note, there was no increase in either connexin at the wound edge in the *S.aureus* infected wounds compared to controls. It is possible that this is because both Cx26 and Cx30 are already elevated in this region, as both normally become elevated behind the re-epithelising growth tip (Goliger & Paul 1995; Coutinho et al. 2003).

As well as high levels of Cx26 and Cx30, the Cx43 expression was also elevated in the hyper-thickened epidermis of the *S.aureus* infected wounds. Cx43 is also reported to be highly expressed in hyperproliferative psoriatic epidermis, and viral warts (Lucke et al. 1999; Labarthe et al. 1998), and in the epidermis of non-healing chronic wounds, which usually have epidermal hyperplasia (Brandner et al. 2004; Mendoza-Naranjo, Cormie, A. E. Serrano, et al. 2012; Mendoza-Naranjo, Cormie, A. Serrano, et al. 2012). High Cx43 expression in the epidermis is similarly reported in hyperproliferative regions during wound healing, where its expression was found to correlate with Ki67, a proliferative marker (Goliger & Paul 1995; Coutinho et al. 2003). There are, though, conflicting reports about the role of Cx43 in cell proliferation, where it has been reported to both stimulate and prevent proliferation (Vinken, Decrock, Leybaert, et al. 2012). High Cx43 epidermal is also associated with poor healing, as it is highly expressed in the wound edge of streptozotocin (STZ) diabetic rats, which have delayed healing (Wang et al. 2007). Reducing Cx43 expression in the epidermis also improves healing (Mori et al. 2006; Coutinho et al. 2005). Although Cx43 is elevated in distal epidermis, *S.aureus* derived PGN was found not to alter Cx43 expression in the HaCaT keratinocyte cell line (Donnelly et al.

2012). There is similarly a trend for increased distal expression in the dermis, although *S.aureus* infection was shown in the previous chapter to decrease Cx43 expression in fibroblasts (chapter 4.3.6). However, the effect of other *S.aureus* products on Cx43 expression in keratinocytes and fibroblasts has not been explored. Moreover, it is possible that Cx43 may be up-regulated in keratinocytes or fibroblasts by inflammation, although TNF-α, a pro-inflammatory cytokine, was found instead to reduce Cx43 in both corneal fibroblasts and HaCaT keratinocytes (Kimura et al. 2013; Tacheau et al. 2008). For now, why Cx43 becomes elevated is not known. However, in fibroblasts *in vitro* low Cx43 expression facilitated *S.aureus* internalisation. If the same is true of keratinocytes, then perhaps increased Cx43 expression may be a protective mechanism against the bacterium.

In the previous chapter it was shown that *S.aureus* infection decreased Cx43 expression in 3T3 fibroblasts (chapter 5.3.4). However, a significant decrease in Cx43 at the dermal wound edge was not found in *S.aureus* infected mice. Similarly, *in vitro* prolonged incubation with BCM decreased fibroblast Cx43 expression (chapter 4.3.6), but BCM did not decrease dermal wound edge Cx43 expression at 3 or 7 days post wounding. Fibroblasts are not the only cell type in the dermis though, and it was previously found that Cx43 expression increased in endothelial cells when exposed to *S.aureus* PGN (Donnelly et al. 2012). Furthermore, it has been demonstrated that Cx43 expression is turned on in activated neutrophils, and presumably there was an increased influx of neutrophils into infected wounds (Zahler & Hoffmann 2003; Jara et al. 1995). Thus any decrease in Cx43 expression in dermal wound edge fibroblasts could be masked by the expected increased expression in neutrophils and endothelial cells. Interestingly, HKSA caused a significant decrease in dermal Cx43 expression. HKSA had no effect on fibroblast Cx43 expression *in vitro* (chapter 5.3.4) so this was unexpected, and the reason for it is unknown. Perhaps it would be worth ascertaining if HKSA reduces angiogenesis or the expression of Cx43 in endothelial cells; either could result in lower Cx43 expression at the dermal wound edge. For now though, the reason for this cannot be explained.

In this chapter it was shown that infection with *S.aureus* impaired healing of mouse skin wounds, as did BCM, but to a lesser extent. *S.aureus* infection also

resulted in hyper-thickening of the epidermis for several millimetres around the wound, which was in conjunction with increased expression of Cx26, Cx30 and Cx43. This response was only caused by infection with the live bacteria, and was a phenotype very similar to that of chronic wounds, which also have elevated Cx26, Cx30 and Cx43 in hyperplasic epidermis surrounding the wound (Brandner et al. 2004; Mendoza-Naranjo, Cormie, A. E. Serrano, et al. 2012; Mendoza-Naranjo, Cormie, A. Serrano, et al. 2012). Whether the increased connexin expression was due to inflammation or in direct response to interaction with *S.aureus* or its secreted toxins remains to be determined, but these experiments suggest a new role for *S.aureus* infection in the aetiology of chronic wounds.

Chapter 7. General Discussion

7.1. Introduction

Both biofilm conditioned medium (BCM) and infection with live *S.aureus* decreased Cx43 expression in fibroblasts. Although exceptions exist, the majority of bacteria, or components derived from them, decrease connexin expression and gap junction intercellular communication (GJIC) in non-professional phagocytic cells in cell culture (Ceelen et al. 2011). In contrast though, the expression of three connexins, Cx26, Cx30 and Cx43, is increased in chronic wounds (Brandner et al. 2004; Mendoza-Naranjo, Cormie, A. Serrano, et al. 2012; Mendoza-Naranjo, Cormie, A. E. Serrano, et al. 2012), wounds which typically are infected with bacteria, including *S.aureus* (Davies et al. 2004; Gjødsbøl & Christensen 2006). Moreover, it was demonstrated in this thesis that infection of skin wounds in mice with live *S.aureus* resulted in a phenotype that closely mimics several aspects of chronic wounds; impaired re-epithelialisation, hyperplasia of the epidermis surrounding the wound and hyperkeratosis (Brem et al. 2007; Herrick et al. 1992). In particular, the hyperproliferative epidermis also expressed high levels of Cx26, Cx30 and Cx43, suggesting that *S.aureus* infection is involved in the abnormal connexin expression in chronic wounds. This is despite *S.aureus* causing a decrease in Cx43 expression in fibroblasts *in vitro*, although the effect on connexins in keratinocytes wasn't investigated. High levels of Cx43 expression in the epidermis have previously been shown to impair re-epithelialisation (Wang et al. 2007). Interestingly, the high connexin expression and thickened epithelium also resembles buccal mucosa, although this tissue exhibits privileged healing rather than impaired healing, potentially due to its ability to rapidly down-regulate connexin expression at the wound edge. The relationship between *S.aureus,* healing, and connexins are discussed here.

7.2. Parallels between *S.aureus* biofilms in oral inflammatory disease and chronic skin wounds

Bacterial biofilms have only relatively recently been established as major contributors to impaired healing in chronic wounds (James et al. 2007). Oral biofilms, though, have been studied for considerably longer. Comparisons have been drawn between bacterial biofilms in chronic wounds and oral mucosa biofilms, and it has been suggested that our understanding of oral biofilms may

aid our understanding of chronic wounds (Mancl et al. 2013). Despite oral mucosa normally healing both rapidly and with minimal or no scarring (Enoch & Stephens 2009), oral biofilms, in the form of dental plaques, have long been established as the cause behind inflammatory periodontal diseases (Mancl et al. 2013). Parallels can be drawn between chronic inflammation in periodontal disease and persistent inflammation in chronic skin wounds. Although not generally considered an oral pathogen, *S.aureus* oral mucosa biofilms particularly have been associated with aggressive periodontitis (Fritschi et al. 2008; Souto & Andrade 2006). *S.aureus* is also one of the most commonly recovered species in chronic wounds, where it was found to be associated with approximately 90% of ulcers (Davies et al. 2004; Gjødsbøl & Christensen 2006). It has been suggested that pockets of oral *S.aureus* biofilms may provide a reservoir responsible for airway and systemic infections, as well as preventing the removal of infection in both chronic wounds and oral disease.

7.3. The relationship between intracellular and biofilm *S.aureus* in inflammatory diseases

7.3.1. Correlations between biofilms and intracellular *S.aureus* and their roles in pathogenicity and virulence

It has been shown that, despite being healthy, human buccal epithelial cells contain and tolerate intracellular oral bacteria, without apparently causing inflammation (Rudney et al. 2001; Rudney & Chen 2006). Although it is not considered a normal oral pathogen *S.aureus* was demonstrated to be intracellular in buccal and gingival epithelial cells (Colombo et al. 2013). In this study it was reported that *S.aureus* was present in a significantly higher proportion in cells from patients with periodontitis compared to healthy controls, suggesting a role for the intracellular pathogen in the disease. Intracellular *S.aureus* have also been identified *in vivo* in a number of other chronic infections and inflammatory diseases caused by *S.aureus* infections; these include chronic rhinosinusitis, bovine chronic mastitis, recurrent tonsillitis and cystic fibrosis lung infections (Clement et al. 2005; Plouin-Gaudon et al. 2006; Hébert et al. 2000; Jarry & Cheung 2006). The intracellular location is considered to be involved in the persistence and reoccurrence of the infections. Interestingly though, *S.aureus* surface biofilm formation has also been linked to

persistence and reoccurrence in all these diseases (Cucarella et al. 2004; Madeo & Frieri 2014; Torretta et al. 2013; Davies & Bilton 2009). Despite both biofilm and intracellular *S.aureus* being associated with the same diseases there has been little examination of the association between the intracellular and biofilm state of *S.aureus*. It was reported, though, that in patients with chronic rhinosinusitis all incidences of intracellular *S.aureus* were associated with surface biofilms, and the authors suggested a link between the two (Tan et al. 2012). Also, in an *in vivo* rat model of *S.aureus* biofilm infection, significantly higher levels of intracellular (within leukocytes) than extracellular *S.aureus* were found in the wound fluid (Murillo et al. 2009). *S.aureus* can survive within leukocytes for several days, and the invasion of macrophages, mast cells and neutrophils has been suggested to be a virulence mechanism related to the pathogenicity and dissemination of the bacteria (Kubica et al. 2008; Gresham et al. 2000; Abel et al. 2011). Although the relationship between *S.aureus* biofilms and intracellular persistence is not clear, both have been shown to relate to the bacteria's virulence. Preventing internalisation of *S.aureus* through either pre-treatment with mimetic peptides or use of mutant *S.aureus* lacking certain copies of the fibronectin binding protein (FnBP), significantly decreased infection and mortality in guinea pig and murine *in vivo* models respectively (Menzies et al. 2002; Edwards et al. 2010). Similarly, disrupting *S.aureus* biofilm formation in a murine *in vivo* skin wound model using RNAIII inhibiting peptide (RIP), which disrupts biofilms but has no effect on *S.aureus* viability, restored normal healing in a mouse model (Schierle et al. 2009). Normal healing was also recovered by preventing biofilm formation using bacteria mutants unable to form biofilms. Thus for now both biofilm formation and intracellular persistence appear to be involved in recurrent infections, and it is highly feasible that both strategies are used by *S.aureus*; this bacterium is highly adaptable and mutable, and the predominant strategy used could well depend on the host environment and interactions with other bacteria (Goerke & Wolz 2010).

7.3.2. *S.aureus* biofilm formation and its influence on the internalisation of the bacterium

Interestingly, the ability of some bacteria, such as *Salmonella enterica,* to invade host cells has been shown to be related directly to the particular strain's

ability to form biofilms (Latasa et al. 2005). The biofilm associated protein (Bap) A gene was found to be necessary for *S.enterica* biofilm formation, and its loss significantly decreased the ability of the bacteria to invade intestinal epithelial cells. In contrast though, *S.aureus* expression of Bap (a functionally related homologue to BapA) increased adhesion to epithelial cells, but inhibited the internalisation of the bacterium (Valle et al. 2012). Moreover, using bovine mammary cells no direct correlation was found between the ability of different *S.aureus* strains to form a biofilm and their invasiveness into host cells (Oliveira et al. 2011).

It is also not known if the presence of biofilm *S.aureus* influences the invasiveness of planktonic *S.aureus*. Interestingly, migrating fibroblasts incubated with *S.aureus* BCM closely resemble RhoA depleted mutants in both morphology and impaired migration (Vega et al. 2011). Clinical isolates of *S.aureus* highly express the virulence factor epidermal cell differentiation inhibitor (EDIN), a very selective ADP-ribosyltransferase, which inactivates Rho(A/B/C/E) GTPases (Munro et al. 2011). Although not yet determined, it is highly possible that EDIN is secreted by *S.aureus* in biofilms. Rho GTPases are part of the integrin signalling pathway, and RhoA is a activated by α5β1 (Danen et al. 2002), the same integrin through which *S.aureus* are internalised (Sinha et al. 1999). Internalisation of *S.aureus* also requires RhoA activation by the bacterium's surface protein, Protein A (Soong et al. 2011), which when removed severely impaired the invasion of the null mutants into oral keratinocytes (Jung et al. 2001). Thus it would be interesting to determine if incubation with *S.aureus* biofilm toxins alters the internalisation of *S.aureus*, or other bacteria that utilise α5β1 to invade cells.

7.3.3. Intracellular biofilms

Intriguingly, it was discovered that both *Escherichia coli* and *Klebsiella pneumoniae* can form largely quiescent biofilm-like communities within the cytoplasm of host urinary tract epithelial cells and airway epithelial cells (Justice et al. 2006; Rosen et al. 2008; Garcia-medina et al. 2005). This ability has been shown using *in vivo* murine models but similar biofilm aggregates have also been observed in human urinary tract epithelial cells (Rosen et al. 2007). It is

not yet known whether other bacteria, such as *S.aureus,* also form intracellular biofilms, or what role these bacterial communities perform.

7.3.4. Intracellular *S.aureus* in chronic wounds

Thus far, intracellular *S.aureus* have not been demonstrated in cells isolated from chronic wounds, although their identification has not been the particular focus of any published research to date. Nevertheless, it was recently demonstrated that healthy human skin not only has a surface microbiome but also a subcutaneous microflora (Nakatsuji et al. 2013). Multiple species of bacteria were found within both the epidermis and dermis in healthy intact skin, though it wasn't determined if they were intra- or extra-cellular. *S.aureus* is known to commonly colonise the surface of human skin, though the study did not state if this was one of the species found under the surface. *S.aureus* though is able to invade many of the cell types present in wounded skin, including keratinocytes, fibroblasts, endothelial cells and leukocytes (Kubica et al. 2008; Gresham et al. 2000; Sinha et al. 1999; Kintarak et al. 2004). Moreover, another pathogenic bacteria, *Chlamydia pneumonia*, an obligate intracellular species, has been found in intracellular locations in chronic skin ulcers (King et al. 2001). It is therefore plausible that intracellular *S.aureus* could, in the future, be found in chronic wounds.

7.4. The relationship between *S.aureus* and connexins in wounds

7.4.1. The relationship between α5β1 and Cx43 expression

S.aureus predominantly enters cells through the host integrin α5β1, bridged by fibronectin (Sinha et al. 1999). A5β1 is a component of focal adhesions, forming the attachment between cells and the extracellular matrix component fibronectin. Its expression is required for the migration of keratinocytes, fibroblasts and endothelial cells (Watson et al. 2009; Xu & Clark 1996; Collo & Pepper 1999). *In vivo* it is expressed at low levels by keratinocytes and becomes up-regulated during re-epithelialisation, as the cells migrate over fibronectin in the wound bed (Larjava et al. 1993). Similarly, α5β1 expression increases in fibroblasts during wound healing, and endothelial cells during angiogenesis (Xu & Clark 1996; Boudreau & Varner 2004). Epidermal keratinocytes in chronic wounds do not

have increased α5 expression at the wound edge, unlike their acute wound counterparts (Ongenae et al. 2000). Currently, the α5β1 expression in chronic wound fibroblasts and endothelial cells is not known. However, we hypothesise that reduced wound edge α5β1 expression may protect cells in chronic wounds from invasion by *S.aureus*, and other bacteria that use α5β1 for internalisation, such as *P.aeruginosa* and *E.coli*, both also commonly found in chronic wounds (Scibelli et al. 2007; Gjødsbøl & Christensen 2006; Davies et al. 2004).

Moreover, α5β1 can regulate Cx43 expression (Guo et al. 2002; Shanker et al. 2005; Czyz et al. 2005). Interestingly, loss of the β1 component has been shown to result in an increase in Cx43 expression in embryonic stem cell derived cardiomyocytes (Czyz et al. 2005), although in contrast, activation of α5β1 has also been reported to increase Cx43 in cardiomyocytes and alveolar epithelial cells (Guo et al. 2002; Shanker et al. 2005). Cx43 expression is elevated in chronic wounds, which fail to increase α5 expression (Brandner et al. 2004; Mendoza-Naranjo, Cormie, A. Serrano, et al. 2012; Mendoza-Naranjo, Cormie, A. E. Serrano, et al. 2012; Ongenae et al. 2000). However, the relationship between α5β1 and Cx43 in both acute and chronic wounds remains to be determined. In this thesis it was demonstrated that Cx43 expression was significantly elevated in the distal epidermis of *S.aureus* infected wounds, and there was a trend for increased distal dermal Cx43 expression. Due to the phenotypic similarities between the *S.aureus* infected *in vivo* model and chronic wounds, we hypothesise that the infected wounds may too have aberrant or depleted α5β1 expression or activation.

7.4.2. The causes and consequences of increased epidermal connexin expression

S.aureus infection resulted in a significant increase in the expression of Cx26, Cx30 and Cx43 in the epidermis for several millimetres surrounding the wound edge (chapter 6). It also caused a trend for increased Cx43 expression in the dermis away from the wound edge (chapter 6). However, *in vitro S.aureus* infection, and *S.aureus* biofilm toxins, decreased Cx43 expression in fibroblasts (chapter 5 and 4 respectively). In keratinocyte HaCaT cells, *S.aureus* derived peptidoglycan (PGN) was found to have no effect on Cx43 expression, although

it did increase Cx26 expression (Donnelly et al. 2012). It is possible that *S.aureus* might have directly increased Cx26 expression in the epidermis, but it seems less plausible that the high Cx43 expression observed was in direct response to infection with the bacteria. Instead, increased Cx43 in the distal epidermis and dermis could perhaps be mediated through an as yet unknown mechanism, which may or may not involve the inflammatory response. Alternatively, increased Cx43 expression in the epidermis of infected wounds might not be in response to the infection, but be related to the hyperproliferative nature of the tissue during the infection, as could Cx26 and Cx30. All three connexins have been reported in hyperproliferative epitheliums such as viral warts and psoriasis (Hivnor et al. 2004; Lemaître et al. 2006; Lucke et al. 1999; Labarthe et al. 1998; Goliger & Paul 1995; Djalilian et al. 2006), and are also strongly expressed in the highly proliferative epidermis of buccal mucosa (chapter 3). Cx26 and Cx30 in particular have been suggested to be markers of proliferative epithelia, although their expression is often reported *in vivo* not to correlate with cells positive for proliferative markers (Goliger & Paul 1995; Lucke et al. 1999; Coutinho et al. 2003). However, overexpression of Cx26 in keratinocytes *in vitro* was found to increase proliferation, and ectopic overexpression in the skin of transgenic mice resulted in a hyperplasic epidermis (Djalilian et al. 2006; Man et al. 2007). So it is possible that increased Cx26 in keratinocytes exposed to *S.aureus* might be involved in the epidermal hyperplasia. The effect of infection with live *S.aureus* on Cx26 expression in keratinocytes in culture has yet to be determined, but it will be interesting to ascertain if it increases or decreases proliferation.

High levels of Cx43 expression impairs cell migration during wound healing, and decreasing the expression improves the rate of healing (Mori et al. 2006; Wang et al. 2007; Mendoza-Naranjo, Cormie, A. Serrano, et al. 2012). For example, abnormally elevated Cx43 was found in diabetic skin wounds and contributed to retarded healing; this was overcome by decreasing Cx43 expression with Cx43 asODN (Wang et al. 2007). Although Cx43 expression was elevated by *S.aureus* infection, it was elevated distally, not at the wound edge where migration primarily occurs. Consequently, the abnormally elevated Cx43 expression induced by the infection is unlikely to underlie the impaired healing. However, the change in Cx43 expression may have functional

consequences for the host's response to the bacterial infection. Reducing Cx43 expression in fibroblasts increased internalisation of *S.aureus* (chapter 5). Similarly, reducing Cx43 expression was found to result in increased mortality in an infected peritonitis murine model (Anand et al. 2008), where mice were infected with *E.coli*, another bacterium that is internalised into cells through integrin α5β1 and commonly found in chronic wounds (Scibelli et al. 2007; Davies et al. 2004; Gjødsbøl & Christensen 2006). Thus it is feasible to speculate that increased Cx43 expression could reduce internalisation of some species of bacteria, and so be protective. However, high Cx43 expression is not protective against all infections. Reducing Cx43 expression instead protected epithelial cells challenged with *Helicobacter pylori* VacA toxin (Radin et al. 2014), and inducing Cx43 expression in HeLa cells increased the invasion of *Yersinia enterocolitica* (L. A. Velasquez Almonacid et al. 2009). However, both *H.pylori* and *Y.enterocolitica* are primarily gastrointestinal pathogens, and are not commonly associated with skin or chronic wounds (Ceelen et al. 2011).

It is not currently known if the increased epidermal connexin expression seen in the infected mice is a specific response to *S.aureus* infection, or whether it is a more general response to infection with any bacteria. Determining this might shed some light on both the cause of the connexin increase, and its role in infected wounds.

7.5. Polymicrobial infections

Formerly it was thought that the bacterial load in a wound was a determinant for the healing outcome, with high bacterial counts indicative of poor healing. Increasingly though it is thought that it is actually the number of different species that may be more important. Using traditional culture techniques one study found that 76% of venous leg ulcers were simultaneously infected with multiple bacterial species, up to 5 different species at a time (Gjødsbøl & Christensen 2006). However, the number of species in each may actually be even higher, as another study, this time using PCR, found 40% more species in wounds compared to normal culture techniques (Davies et al. 2004). *In vivo* infected wound models similarly indicate that polymicrobial wounds impair healing to a significantly greater extent than single species infections (A. Seth et

al. 2012; Pastar et al. 2013). In a porcine model re-epithelialisation was significantly delayed in polymicrobial infections over single microbial wounds (Pastar et al. 2013). The same was found using different strains in a rabbit ear model, alongside an increase in IL-1β and TNF-α expression (A. Seth et al. 2012). Both studies focused on infections with *P.aeruginosa* and *S.aureus*, as both have been shown in approximately 90% of chronic wounds (Gjødsbøl & Christensen 2006; Davies et al. 2004). Another murine wound model found that a polymicrobial biofilm containing four species (*P.aeruginosa, S.aureus, Enterococcus faecalis* and *Finegoldia magna*) only significantly impaired healing at one time point compared to planktonic applied *P.aeruginosa* (A. Seth et al. 2012). The difference might be due to the fact that comparisons were made to *P.aeruginosa* infected wounds; *P.aeruginosa* was found to impair healing significantly more than infections with several other single species in a rabbit wound model (Akhil K. Seth et al. 2012), and its presence in is indicative of poor healing outcome in chronic wounds (Gjødsbøl & Christensen 2006). Alternatively, it might due to interactions between the bacterial species, as bacteria in polymicrobial biofilms can influence the behaviour of one another (A. Seth et al. 2012; Pastar et al. 2013; Dalton et al. 2011). Over 12 days Seth et al found that *in vitro* and in a rabbit *in vivo* model *P.aeruginosa* came to dominate *S.aureus* (A. Seth et al. 2012). Pastar et al further established that in their porcine model *P.aeruginosa* suppressed the growth of *S.aureus,* and altered the expression of several *S.aureus* virulence factors, reducing some and inducing others (Pastar et al. 2013). Likewise, *P.aeruginosa* outcompeted and reduced the virulence of *S.aureus* in cystic fibrosis polymicrobial biofilms (Baldan et al. 2014), and there is evidence that *P.aeruginosa* may even use *S.aureus* as a source of iron during co-culture (Mashburn et al. 2005). Furthermore, distinct 'pockets' of homogenous bacteria were observed in a polymicrobial wound biofilm containing four different species, with *P.aeruginosa* preferentially locating to the leading edge of the infection (Dalton et al. 2011). Biofilms in nature, and specifically in chronic wounds, are typically polymicrobial. Interestingly, it appears that intracellular populations may also be polymicrobial, at least in oral mucosa, where polymicrobial populations were identified in both buccal and gingival epithelial cells (Rudney et al. 2005; Colombo et al. 2013). As there may be an association between the presence of biofilms and intracellular bacteria in chronic rhinosinusitis (Tan et al. 2013) it would be

interesting to see if the same species are found in both locations, and whether this extend to other regions and diseases, including chronic wounds.

7.6. Concluding remarks

Connexins, and Cx43 in particular, are clearly important during the wound healing process. The exact roles played by each connexin is as yet uncertain though, and it is not known how much the expression patterns and changes in expression contribute to the healing ability of different tissues. The abnormal connexin expression in chronic wounds seems likely to contribute to their poor healing. Although a role for *S.aureus* in chronic wounds is acknowledged, it is evident that our understanding of the parts played by biofilm and intracellular bacteria is still rudimentary. Moreover, prior investigations into the relationship between *S.aureus* and connexins are very limited. From the investigations in this thesis, it is clear that live *S.aureus,* and its biofilm-secreted products, can reduce Cx43 expression in fibroblasts. Cx43 expression can also determine the internalisation of live *S.aureus* and thus influence the cell's viability in response to the pathogen, though it does not influence the cell's response to biofilm exotoxins. Both biofilm exotoxins and live *S.aureus* impaired healing in an *in vivo* cutaneous wound model, but only the live bacterium altered connexin expression, albeit by increasing the expression of Cx43, Cx26 and Cx30 away from the wound edge. However, it is not yet established how *S.aureus* infection results in abnormal connexin expression *in vivo*, and whether this contributes to the infection's impairment of healing. There is much still to be learnt about *S.aureus* and wound healing, and the relationship between the bacterium and connexin expression.

Appendix

Appendix Table 1. Summary of results related to connexin expression changes due to exposure to bacteria or bacterial components.

		BCM	HKSA	Live SA
***In vitro* (fibroblasts)**	Cx43	No effects at 24 hours, decreased at 7 days	No effect	Decreased at 24 hours
***In vivo* (dermis)**	Cx43	No effect at the wound edge or distally at 3 or 7 days	Decreased at wound edge at 3 days, no effect distally	No effect at the wound edge or distally at 3 days
***In vivo* (epidermis)**	Cx43	No effect at the growth tip, wound edge or distally at 3 or 7 days	No effect at the growth tip, wound edge or distally at 3 days	Increased distally at 3 days, no effect at the growth tip or wound edge
	Cx26	No effect at the wound edge or distally at 3 days	No effect at the wound edge or distally at 3 days	Increased distally at 3 days, no effect at the wound edge
	Cx30	No effect at the wound edge or distally at 3 days	No effect at the wound edge or distally at 3 days	Increased distally at 3 days, no effect at the wound edge

References

Abel, J., Goldmann, O., Ziegler, C., Höltje, C., Smeltzer, M.S., Cheung, A.L., Bruhn, D., Rohde, M. & Medina, E., 2011. Staphylococcus aureus evades the extracellular antimicrobial activity of mast cells by promoting its own uptake. *Journal of innate immunity*, 3(5), pp.495–507.

Abiko, Y. & Selimovic, D., 2010. The mechanism of protracted wound healing on oral mucosa in diabetes. Review. *Bosnian Journal of Basic Medical Sciences / Udruženje Basičnih Mediciniskih Znanosti = Association of Basic Medical Sciences*, 10(3), pp.186–191.

Van Acker, H., Van Dijck, P. & Coenye, T., 2014. Molecular mechanisms of antimicrobial tolerance and resistance in bacterial and fungal biofilms. *Trends in microbiology*, 22(6), pp.326–33.

Aepfelbacher, M., Essler, M., Huber, E., Sugai, M. & Weber, P.C., 1997. Bacterial Toxins Block Endothelial Wound Repair: Evidence That Rho GTPases Control Cytoskeletal Rearrangements in Migrating Endothelial Cells . *Arteriosclerosis, Thrombosis, and Vascular Biology* , 17 (9), pp.1623–1629.

Agerer, F., Lux, S., Michel, A., Rohde, M., Ohlsen, K. & Hauck, C.R., 2005. Cellular invasion by Staphylococcus aureus reveals a functional link between focal adhesion kinase and cortactin in integrin-mediated internalisation. *Journal of cell science*, 118(Pt 10), pp.2189–200.

Agerer, F., Michel, A., Ohlsen, K. & Hauck, C.R., 2003. Integrin-mediated invasion of Staphylococcus aureus into human cells requires Src family protein-tyrosine kinases. *The Journal of biological chemistry*, 278(43), pp.42524–42531.

Ågren, M. & Steenfos, H., 1999. Proliferation and Mitogenic Response to PDGF-BB of Fibroblasts Isolated from Chronic Venous Leg Ulcers is Ulcer-Age Dependent1. *Journal of Investigative Dermatology*, 112(4), pp.463–469.

Akiyama, H., Kanzaki, H., Tada, J. & Arata, J., 1996. Staphylococcus aureus infection on cut wounds in the mouse skin: experimental staphylococcal botryomycosis. *Journal of dermatological science*, 11(3), pp.234–8.

Alekseeva, L., Rault, L., Almeida, S., Legembre, P., Edmond, V., Azevedo, V., Miyoshi, A., Even, S., Taieb, F., Arlot-Bonnemains, Y., Le Loir, Y. & Berkova, N., 2013. Staphylococcus aureus-induced G2/M phase transition delay in host epithelial cells increases bacterial infective efficiency. *PloS one*, 8(5), p.e63279.

Amorena, B. & Gracia, E., 1999. Antibiotic susceptibility assay for Staphylococcus aureus in biofilms developed in vitro. *Journal of antimicorbial chemotherapy*, 44, pp.43–55.

Anand, R.J., Dai, S., Gribar, S.C., Richardson, W., Kohler, J.W., Hoffman, R. a., Branca, M.F., Li, J., Shi, X.-H., Sodhi, C.P. & Hackam, D.J., 2008. A Role for Connexin43 in Macrophage Phagocytosis and Host Survival after Bacterial Peritoneal Infection. *The Journal of Immunology*, 181(12), pp.8534–8543.

Anwar, H., Strap, J.L., Chen, K. & Costerton, J.W., 1992. Dynamic interactions of biofilms of mucoid Pseudomonas aeruginosa with tobramycin and piperacillin. *Antimicrobial agents and chemotherapy*, 36(6), pp.1208–14.

Artuc, M., Hermes, B., Steckelings, U.M., Grützkau, A. & Henz, B.M., 1999. Mast cells and their mediators in cutaneous wound healing--active participants or innocent bystanders? *Experimental dermatology*, 8(1), pp.1–16.

Balci, D., Duran, N., Ozer, B., Gunesacar, R., Onlen, Y. & Yenin, J., 2009. High prevalence of Staphylococcus aureus cultivation and superantigen production in patients with psoriasis. *European journal of dermatology*, 10(3), pp.238–42.

Baldan, R., Cigana, C., Testa, F., Bianconi, I., De Simone, M., Pellin, D., Di Serio, C., Bragonzi, A. & Cirillo, D.M., 2014. Adaptation of Pseudomonas aeruginosa in Cystic Fibrosis airways influences virulence of Staphylococcus aureus in vitro and murine models of co-infection. *PloS one*, 9(3), p.e89614.

Bao, X., Lee, S.C., Reuss, L. & Altenberg, G.A., 2007. Change in permeant size selectivity by phosphorylation of connexin 43 gap-junctional hemichannels by PKC. *Proceedings of the National Academy of Sciences of the United States of America*, 104(12), pp.4919–4924.

Batra, N., Burra, S., Siller-Jackson, A.J., Gu, S., Xia, X., Weber, G.F., DeSimone, D., Bonewald, L.F., Lafer, E.M., Sprague, E., Schwartz, M.A. & Jiang, J.X., 2012. Mechanical stress-activated integrin α5β1 induces opening of connexin 43 hemichannels. *Proceedings of the National Academy of Sciences of the United States of America*, 109(9), pp.3359–3364.

Beanes, S.R., Dang, C., Soo, C. & Ting, K., 2004. Skin repair and scar formation: the central role of TGF-[beta]. *Expert Reviews in Molecular Medicine*, 5(08), pp.1–11.

Beaudoin, T., Zhang, L., Hinz, A.J., Parr, C.J. & Mah, T.-F., 2012. The biofilm-specific antibiotic resistance gene ndvB is important for expression of ethanol oxidation genes in Pseudomonas aeruginosa biofilms. *Journal of bacteriology*, 194(12), pp.3128–36.

De Beer, D., Stoodley, P., Roe, F. & Lewandowski, Z., 1994. Effects of biofilm structures on oxygen distribution and mass transport. *Biotechnology and bioengineering*, 43(11), pp.1131–8.

Vande Berg, J., Rudolph, R., Carol, H. & Haywood-Reid, P., 1998. Fibroblast senescence in pressure ulcers. *Wound Repair and …*, 6(1), pp.38–49.

Bevans, C.G., Kordel, M., Rhee, S.K. & Harris, A.L., 1998. Isoform composition of connexin channels determines selectivity among second messengers and uncharged molecules. *The Journal of biological chemistry*, 273(5), pp.2808–2816.

Bhattacharyya, S., Tamaki, Z., Wang, W., Hinchcliff, M., Hoover, P., Getsios, S., White, E.S. & Varga, J., 2014. FibronectinEDA promotes chronic cutaneous fibrosis through Toll-like receptor signaling. *Science translational medicine*, 6(232), p.232ra50.

Bjarnsholt, T., 2013. The role of bacterial biofilms in chronic infections. *Acta Pathologica Microbiologica et Immunologica Scandinavica. Supplementum*, 121(136), pp.1–51.

Bjarnsholt, T., Alhede, M., Alhede, M., Eickhardt-Sørensen, S.R., Moser, C., Kühl, M., Jensen, P.Ø. & Høiby, N., 2013. The in vivo biofilm. *Trends in microbiology*, 21(9), pp.466–74.

Bjarnsholt, T., Kirketerp-Møller, K., Jensen, P.Ø., Madsen, K.G., Phipps, R., Krogfelt, K., Høiby, N. & Givskov, M., 2008. Why chronic wounds will not heal: a novel hypothesis. *Wound repair and regeneration : official publication of the Wound Healing Society [and] the European Tissue Repair Society*, 16(1), pp.2–10.

Blagosklonny, M. V, 2011. Cell cycle arrest is not senescence. *Aging*, 3(2), pp.94–101.

Blanc, E.M., Bruce-Keller, a J. & Mattson, M.P., 1998. Astrocytic gap junctional communication decreases neuronal vulnerability to oxidative stress-induced disruption of Ca2+ homeostasis and cell death. *Journal of neurochemistry*, 70(3), pp.958–70.

Bloch, W., Huggel, K., Sasaki, T. & Grose, R., 2000. The angiogenesis inhibitor endostatin impairs blood vessel maturation during wound healing. *The FASEB Journal*, 14(15), pp.2373–2376.

Bosen, F., Schütz, M., Beinhauer, A., Strenzke, N., Franz, T. & Willecke, K., 2014. The Clouston syndrome mutation connexin30 A88V leads to hyperproliferation of sebaceous glands and hearing impairments in mice. *FEBS letters*, 588(9), pp.1795–801.

Boudreau, N.J. & Varner, J. a, 2004. The homeobox transcription factor Hox D3 promotes integrin alpha5beta1 expression and function during angiogenesis. *The Journal of biological chemistry*, 279(6), pp.4862–8.

Brandner, J.M., Houdek, P., Husing, B., Kaiser, C. & Moll, I., 2004. Connexins 26, 30, and 43: Differences Among Spontaneous, Chronic, and Accelerated Human Wound Healing. *Journal of Investigative Dermatology*, 122(5), pp.1310–1320.

Brem, H., Stojadinovic, O., Diegelmann, R.F., Entero, H., Lee, B., Pastar, I., Golinko, M., Rosenberg, H. & Tomic-canic, M., 2007. Molecular Markers in Patients with Chronic Wounds to Guide Surgical Debridement. *Molecular Medicine*, 3(9), pp.1–10.

Brissette, J.L., Kumar, N.M., Gilula, N.B., Hall, J.E. & Dotto, G.P., 1994. Switch in gap junction protein expression is associated with selective changes in junctional permeability during keratinocyte differentiation. *Proceedings of the National Academy of Sciences of the United States of America*, 91(14), pp.6453–6457.

Bronner, S., Monteil, H. & Prévost, G., 2004. Regulation of virulence determinants in Staphylococcus aureus: complexity and applications. *FEMS microbiology reviews*, 28(2), pp.183–200.

Bu, S., Xie, Q., Chang, W., Huo, X., Chen, F. & Ma, X., 2013. LukS-PV induces mitochondrial-mediated apoptosis and G0/G1 cell cycle arrest in human acute myeloid leukemia THP-1 cells. *The international journal of biochemistry & cell biology*, 45(8), pp.1531–7.

Bur, S., Preissner, K.T., Herrmann, M. & Bischoff, M., 2013. The Staphylococcus aureus extracellular adherence protein promotes bacterial internalization by keratinocytes independent of fibronectin-binding proteins. *The Journal of investigative dermatology*, 133(8), pp.2004–12.

Campos de Carvalho, a C., Roy, C., Hertzberg, E.L., Tanowitz, H.B., Kessler, J. a, Weiss, L.M., Wittner, M., Dermietzel, R., Gao, Y. & Spray, D.C., 1998. Gap junction disappearance in astrocytes and leptomeningeal cells as a consequence of protozoan infection. *Brain research*, 790(1-2), pp.304–14.

Ceelen, L., Haesebrouck, F., Vanhaecke, T., Rogiers, V. & Vinken, M., 2011. Modulation of connexin signaling by bacterial pathogens and their toxins. *Cellular and molecular life sciences : CMLS*, 68(18), pp.3047–64.

Chen, L., Arbieva, Z. & Guo, S., 2010. Positional differences in the wound transcriptome of skin and oral mucosa. *BMC Genomics*, 11, p.471.

Chen, Z., Trotman, L.C., Shaffer, D., Lin, H.-K., Dotan, Z. a, Niki, M., Koutcher, J. a, Scher, H.I., Ludwig, T., Gerald, W., Cordon-Cardo, C. & Pandolfi, P.P., 2005. Crucial role of p53-dependent cellular senescence in suppression of Pten-deficient tumorigenesis. *Nature*, 436(7051), pp.725–30.

Cheon, S.S., Wei, Q., Gurung, A., Youn, A., Bright, T., Poon, R., Whetstone, H., Guha, A. & Alman, B. a, 2006. Beta-catenin regulates wound size and mediates the effect of TGF-beta in cutaneous healing. *FASEB journal : official publication of the Federation of American Societies for Experimental Biology*, 20(6), pp.692–701.

Cherian, P.P., Siller-Jackson, A.J., Gu, S., Wang, X., Bonewald, L.F., Sprague, E. & Jiang, J.X., 2005. Mechanical strain opens connexin 43 hemichannels in osteocytes: a novel mechanism for the release of prostaglandin. *Molecular biology of the cell*, 16(7), pp.3100–3106.

Churko, J.M., Kelly, J.J., Macdonald, A., Lee, J., Sampson, J., Bai, D. & Laird, D.W., 2012. The G60S Cx43 mutant enhances keratinocyte proliferation and differentiation. *Experimental dermatology*, 21(8), pp.612–618.

Churko, J.M. & Laird, D.W., 2013. Gap junction remodeling in skin repair following wounding and disease. *Physiology (Bethesda, Md.)*, 28(3), pp.190–8.

Churko, J.M., Shao, Q., Gong, X., Swoboda, K.J., Bai, D., Sampson, J. & Laird, D.W., 2011. Human dermal fibroblasts derived from oculodentodigital dysplasia patients suggest that patients may have wound-healing defects. *Human mutation*, 32(4), pp.456–66.

Clark, R. a F., 2008. Oxidative stress and "senescent" fibroblasts in non-healing wounds as potential therapeutic targets. *The Journal of investigative dermatology*, 128(10), pp.2361–4.

Clement, S., Vaudaux, P., Francois, P., Schrenzel, J., Huggler, E., Kampf, S., Chaponnier, C., Lew, D. & Lacroix, J.-S., 2005. Evidence of an intracellular reservoir in the nasal mucosa of patients with recurrent Staphylococcus aureus rhinosinusitis. *The Journal of infectious diseases*, 192(6), pp.1023–1028.

Collo, G. & Pepper, M.S., 1999. Endothelial cell integrin alpha5beta1 expression is modulated by cytokines and during migration in vitro. *Journal of cell science*, 112 (Pt 4, pp.569–578.

Colombo, A. V, Barbosa, G.M., Higashi, D., di Micheli, G., Rodrigues, P.H. & Simionato, M.R.L., 2013. Quantitative detection of Staphylococcus aureus, Enterococcus faecalis and Pseudomonas aeruginosa in human oral epithelial cells from subjects with periodontitis and periodontal health. *Journal of medical microbiology*, 62(Pt 10), pp.1592–600.

Contreras, J.E., Sánchez, H.A., Eugenin, E.A., Speidel, D., Theis, M., Willecke, K., Bukauskas, F.F., Bennett, M.V.L. & Sáez, J.C., 2002. Metabolic inhibition induces opening of unapposed connexin 43 gap junction hemichannels and reduces gap junctional communication in cortical astrocytes in culture. *Proceedings of the National Academy of Sciences of the United States of America*, 99(1), pp.495–500.

Costerton, J.W., Stewart, P.S. & Greenberg, E.P., 1999. Bacterial Biofilms: A Common Cause of Persistent Infections. *Science*, 284(5418), pp.1318 – 1322.

Cotrina, M.L., Lin, J.H., López-García, J.C., Naus, C.C. & Nedergaard, M., 2000. ATP-mediated glia signaling. *The Journal of neuroscience: the official journal of the Society for Neuroscience*, 20(8), pp.2835–2844.

Coutinho, P., Qiu, C., Frank, S., Tamber, K. & Becker, D., 2003. Dynamic changes in connexin expression correlate with key events in the wound healing process. *Cell Biology International*, 27(7), pp.525–541.

Coutinho, P., Qiu, C., Frank, S., Wang, C.M., Brown, T., Green, C.R. & Becker, D.L., 2005. Limiting burn extension by transient inhibition of Connexin43 expression at the site of injury. *British journal of plastic surgery*, 58(5), pp.658–67.

Cucarella, C., Tormo, M., Ubeda, C., Trotonda, P., Monzon, M., Peris, C., Amorena, B., Lasa, I. & Penades, J., 2004. Role of biofilm-associated protein bap in the pathogenesis of bovine Staphylococcus aureus. *Infection and immunity*, 72(4), pp.2177–2185.

Czyz, J., Guan, K., Zeng, Q. & Wobus, A.M., 2005. Loss of beta 1 integrin function results in upregulation of connexin expression in embryonic stem cell-derived cardiomyocytes. *The International journal of developmental biology*, 49(1), pp.33–41.

Dahl, E., Manthey, D., Chen, Y., Schwarz, H.-J., Chang, Y.S., Lalley, P. a., Nicholson, B.J. & Willecke, K., 1996. Molecular Cloning and Functional Expression of Mouse Connexin-30,a Gap Junction Gene Highly Expressed in Adult Brain and Skin. *Journal of Biological Chemistry*, 271(30), pp.17903–17910.

Dalton, T., Dowd, S.E., Wolcott, R.D., Sun, Y., Watters, C., Griswold, J.A. & Rumbaugh, K.P., 2011. An In Vivo Polymicrobial Biofilm Wound Infection Model to Study Interspecies Interactions J. L. Herrmann, ed. *PLoS ONE*, 6(11), p.e27317.

Danen, E.H.J., Sonneveld, P., Brakebusch, C., Fassler, R. & Sonnenberg, A., 2002. The fibronectin-binding integrins alpha5beta1 and alphavbeta3 differentially modulate RhoA-GTP loading, organization of cell matrix adhesions, and fibronectin fibrillogenesis. *The Journal of cell biology*, 159(6), pp.1071–86.

Darrow, B.J., Laing, J.G., Lampe, P.D., Saffitz, J.E. & Beyer, E.C., 1995. Expression of Multiple Connexins in Cultured Neonatal Rat Ventricular Myocytes. *Circulation Research* , 76 (3), pp.381–387.

Davies, C.E., Hill, K.E., Wilson, M.J., Stephens, P., Hill, C.M., Harding, K.G. & Thomas, D.W., 2004. Use of 16S Ribosomal DNA PCR and Denaturing Gradient Gel Electrophoresis for Analysis of the Microfloras of Healing and Nonhealing Chronic Venous Leg Ulcers. *Journal of Clinical Microbiology*, 42(8), pp.3549 –3557.

Davies, J.C. & Bilton, D., 2009. Bugs, biofilms, and resistance in cystic fibrosis. *Respiratory care*, 54(5), pp.628–40.

Davis, N.G., Phillips, A. & Becker, D.L., 2013. Connexin dynamics in the privileged wound healing of the buccal mucosa. *Wound repair and*

regeneration : official publication of the Wound Healing Society [and] the European Tissue Repair Society, 21(4), pp.571–8.

Davis, S.C., Ricotti, C., Cazzaniga, A., Welsh, E., Eaglstein, W.H. & Mertz, P.M., 2008. Microscopic and physiologic evidence for biofilm-associated wound colonization in vivo. *Wound repair and regeneration: official publication of the Wound Healing Society [and] the European Tissue Repair Society*, 16(1), pp.23–29.

Dbouk, H. a, Mroue, R.M., El-Sabban, M.E. & Talhouk, R.S., 2009. Connexins: a myriad of functions extending beyond assembly of gap junction channels. *Cell communication and signaling : CCS*, 7(4), pp.doi: 10.1186/1478–811X–7–4.

Decrock, E., De Vuyst, E., Vinken, M., Van Moorhem, M., Vranckx, K., Wang, N., Van Laeken, L., De Bock, M., D'Herde, K., Lai, C.P., Rogiers, V., Evans, W.H., Naus, C.C. & Leybaert, L., 2009. Connexin 43 hemichannels contribute to the propagation of apoptotic cell death in a rat C6 glioma cell model. *Cell Death and Differentiation*, 16(1), pp.151–163.

Degen, K.E. & Gourdie, R.G., 2012. Embryonic wound healing: a primer for engineering novel therapies for tissue repair. *Birth defects research. Part C, Embryo today : reviews*, 96(3), pp.258–70.

Derangeon, M., Bourmeyster, N., Plaisance, I., Pinet-Charvet, C., Chen, Q., Duthe, F., Popoff, M.R., Sarrouilhe, D. & Hervé, J.-C., 2008. RhoA GTPase and F-actin dynamically regulate the permeability of Cx43-made channels in rat cardiac myocytes. *The Journal of biological chemistry*, 283(45), pp.30754–30765.

Di, W.L., Rugg, E.L., Leigh, I.M. & Kelsell, D.P., 2001. Multiple epidermal connexins are expressed in different keratinocyte subpopulations including connexin 31. *The Journal of investigative dermatology*, 117(4), pp.958–64.

Diegelmann, R.F., 2003. Excessive neutrophils characterize chronic pressure ulcers. *Wound repair and regeneration: official publication of the Wound Healing Society [and] the European Tissue Repair Society*, 11(6), pp.490–495.

Diegelmann, R.F. & Evans, M.C., 2004. Wound healing: an overview of acute, fibrotic and delayed healing. *Frontiers in Bioscience: A Journal and Virtual Library*, 9, pp.283–289.

Diez, J.A., Ahmad, S. & Evans, W.H., 1999. Assembly of heteromeric connexons in guinea-pig liver en route to the Golgi apparatus, plasma membrane and gap junctions. *European journal of biochemistry / FEBS*, 262(1), pp.142–148.

Dimri, G.P., Lee, X., Basile, G., Acosta, M., Scott, G., Roskelley, C., Medrano, E.E., Linskens, M., Rubelj, I. & Pereira-Smith, O., 1995. A biomarker that identifies senescent human cells in culture and in aging skin in vivo.

Proceedings of the National Academy of Sciences of the United States of America, 92(20), pp.9363–7.

Djalilian, A.R., McGaughey, D., Patel, S., Seo, E.Y., Yang, C., Cheng, J., Tomic, M., Sinha, S., Ishida-Yamamoto, A. & Segre, J.A., 2006. Connexin 26 regulates epidermal barrier and wound remodeling and promotes psoriasiform response. *The Journal of clinical investigation*, 116(5), pp.1243–1253.

Donlan, R. & Costerton, J., 2002. Biofilms: survival mechanisms of clinically relevant microorganisms. *Clinical microbiology reviews*, 15(2), pp.167–193.

Donnelly, S., English, G., de Zwart-Storm, E.A., Lang, S., van Steensel, M.A.M. & Martin, P.E., 2012. Differential susceptibility of Cx26 mutations associated with epidermal dysplasias to peptidoglycan derived from Staphylococcus aureus and Staphylococcus epidermidis. *Experimental dermatology*, 21(8), pp.592–598.

Driffield, K., Miller, K., Bostock, J.M., O'Neill, a J. & Chopra, I., 2008. Increased mutability of Pseudomonas aeruginosa in biofilms. *The Journal of antimicrobial chemotherapy*, 61(5), pp.1053–6.

Dziewanowska, K., Patti, J.M., Claudia, F., Bayles, K.W., Trumble, W.R., Bohach, G.A. & Deobald, C.F., 1999. Fibronectin Binding Protein and Host Cell Tyrosine Kinase Are Required for Internalization of Staphylococcus aureus by Epithelial Cells Fibronectin Binding Protein and Host Cell Tyrosine Kinase Are Required for Internalization of Staphylococcus aureus by. *Infection and Immunity*, 67(9), pp.4673–4678.

Ebisawa, K., Kato, R., Okada, M., Sugimura, T., Latif, M.A., Hori, Y., Narita, Y., Ueda, M., Honda, H. & Kagami, H., 2011. Gingival and dermal fibroblasts: their similarities and differences revealed from gene expression. *Journal of bioscience and bioengineering*, 111(3), pp.255–8.

Edwards, A.M., Potts, J.R., Josefsson, E. & Massey, R.C., 2010. Staphylococcus aureus host cell invasion and virulence in sepsis is facilitated by the multiple repeats within FnBPA. *PLoS pathogens*, 6(6), p.e1000964.

Ehlers, L. & Bouwer, E., 1999. RP4 plasmid transfer among species of in a biofilm reactor. *Water Science and Technology*, 39(7), pp.163–171.

Elfgang, C., Eckert, R., Lichtenberg-Fraté, H., Butterweck, a, Traub, O., Klein, R. a, Hülser, D.F. & Willecke, K., 1995. Specific permeability and selective formation of gap junction channels in connexin-transfected HeLa cells. *The Journal of cell biology*, 129(3), pp.805–17.

Ellington, J.K., Harris, M., Webb, L., Smith, B., Smith, T., Tan, K. & Hudson, M., 2003. A mechanism for the indolence of osteomyelitis. *The journal of bone and joint surgery*, 85-B(6), pp.918–921.

Ellington, J.K., Reilly, S.S., Ramp, W.K., Smeltzer, M.S., Kellam, J.F. & Hudson, M.C., 1999. Mechanisms of Staphylococcus aureus invasion of cultured osteoblasts. *Microbial pathogenesis*, 26(6), pp.317–23.

Enoch, S. & Stephens, P., 2009. Scarless healing: oral mucosa as a scientific model. *Wounds UK*, 5(1), pp.42–48.

Enoch, S., Wall, I., Peake, M., Davies, L., Farrier, J., Giles, P., Baird, D., Kipling, D., Price, P., Moseley, R., Thomas, D. & Stephens, P., 2009. Increased Oral Fibroblast Lifespan Is Telomerase-independent. *Journal of Dental Research*, 88(10), pp.916 –921.

Esen, M., Schreiner, B., Jendrossek, V., Lang, F., Fassbender, K., Grassmé, H. & Gulbins, E., 2001. Mechanisms of Staphylococcus aureus induced apoptosis of human endothelial cells. *Apoptosis: An International Journal on Programmed Cell Death*, 6(6), pp.431–439.

Esen, N., Shuffield, D., Syed, M.M.D. & Kielian, T., 2007. Modulation of connexin expression and gap junction communication in astrocytes by the gram-positive bacterium S. aureus. *Glia*, 55(1), pp.104–117.

Eslami, A., Gallant-Behm, C.L., Hart, D. a, Wiebe, C., Honardoust, D., Gardner, H., Häkkinen, L. & Larjava, H.S., 2009. Expression of integrin alphavbeta6 and TGF-beta in scarless vs scar-forming wound healing. *The journal of histochemistry and cytochemistry : official journal of the Histochemistry Society*, 57(6), pp.543–57.

Etienne-Manneville, S., 2013. Microtubules in cell migration. *Annual review of cell and developmental biology*, 29, pp.471–99.

Eugenin, E., 2014. Role of connexin/pannexin containing channels in infectious diseases. *FEBS letters*, 588(8), pp.1389–95.

Eugenin, E. a., Branes, M.C., Berman, J.W. & Saez, J.C., 2003. TNF- Plus IFN- Induce Connexin43 Expression and Formation of Gap Junctions Between Human Monocytes/Macrophages That Enhance Physiological Responses. *The Journal of Immunology*, 170(3), pp.1320–1328.

Eugenín, E., González, H. & Sánchez, H., 2007. Inflammatory conditions induce gap junctional communication between rat Kupffer cells both in vivo and in vitro. *Cellular Immunology*, 247(2), pp.103–110.

Evans, D.J., Allison, D.G., Brown, M.R. & Gilbert, P., 1990. Effect of growth-rate on resistance of gram-negative biofilms to cetrimide. *The Journal of antimicrobial chemotherapy*, 26(4), pp.473–8.

Evans, W.H. & Martin, P.E.M., 2002. Gap junctions: structure and function (Review). *Molecular membrane biology*, 19(2), pp.121–36.

Evans, W.H., De Vuyst, E. & Leybaert, L., 2006. The gap junction cellular internet: connexin hemichannels enter the signalling limelight. *The Biochemical journal*, 397(1), pp.1–14.

Falanga, V., 1993. Chronic Wounds: Pathophysiologic and Experimental Considerations. *Journal of Investigative Dermatology*, 100(5), pp.721–725.

Fallon, R.F. & Goodenough, D. a, 1981. Five-hour half-life of mouse liver gap-junction protein. *The Journal of cell biology*, 90(2), pp.521–6.

Fazli, M., Bjarnsholt, T., Kirketerp-Møller, K., Jørgensen, A., Andersen, C.B., Givskov, M. & Tolker-Nielsen, T., 2011. Quantitative analysis of the cellular inflammatory response against biofilm bacteria in chronic wounds. *Wound repair and regeneration : official publication of the Wound Healing Society [and] the European Tissue Repair Society*, 19(3), pp.387–91.

Ferguson, M.W.J. & O'Kane, S., 2004. Scar-free healing: from embryonic mechanisms to adult therapeutic intervention. *Philosophical transactions of the Royal Society of London. Series B, Biological sciences*, 359(1445), pp.839–50.

Fernandez-Cobo, M., Gingalewski, C. & De Maio, A., 1998. Expression of the connexin 43 gene is increased in the kidneys and the lungs of rats injected with bacterial lipopolysaccharide. *Shock (Augusta, Ga.)*, 10(2), pp.97–102.

Fiorini, C., Decrouy, X., Defamie, N., Segretain, D. & Pointis, G., 2006. Opposite regulation of connexin33 and connexin43 by LPS and IL-1alpha in spermatogenesis. *American journal of physiology. Cell physiology*, 290(3), pp.C733–740.

Fournier, B. & Philpott, D., 2005. Recognition of Staphylococcus aureus by the innate immune system. *Clinical microbiology reviews*, 18(3), pp.521–540.

Frank, S., Stallmeyer, B., Kämpfer, H., Kolb, N. & Pfeilschifter, J., 2000. Leptin enhances wound re-epithelialization and constitutes a direct function of leptin in skin repair. *The Journal of clinical investigation*, 106(4), pp.501–9.

Fraunholz, M. & Sinha, B., 2012. Intracellular Staphylococcus aureus: live-in and let die. *Frontiers in cellular and infection microbiology*, 2(April), p.43.

Fritschi, B.Z., Albert-Kiszely, a. & Persson, G.R., 2008. Staphylococcus aureus and Other Bacteria in Untreated Periodontitis. *Journal of Dental Research*, 87(6), pp.589–593.

Fujita, H., 2013. The role of IL-22 and Th22 cells in human skin diseases. *Journal of dermatological science*, 72(1), pp.3–8.

Fushiki, S., Perez Velazquez, J.L., Zhang, L., Bechberger, J.F., Carlen, P.L. & Naus, C.C.G., 2003. Changes in neuronal migration in neocortex of connexin43 null mutant mice. *Journal of neuropathology and experimental neurology*, 62(3), pp.304–14.

Galkowska, H., 2006. Chemokines, cytokines, and growth factors in keratinocytes and dermal endothelial cells in the margin of chronic diabetic foot ulcers. *Wound repair and …*, 14(5), pp.558–565.

Galkowska, H., Wojewodzka, U. & Olszewski, W.L., 2006. Chemokines, cytokines, and growth factors in keratinocytes and dermal endothelial cells in the margin of chronic diabetic foot ulcers. *Wound repair and regeneration : official publication of the Wound Healing Society [and] the European Tissue Repair Society*, 14(5), pp.558–65.

Garcia-medina, R., Dunne, W.M., Singh, P.K. & Brody, S.L., 2005. Pseudomonas aeruginosa Acquires Biofilm-Like Properties within Airway Epithelial Cells Pseudomonas aeruginosa Acquires Biofilm-Like Properties within Airway Epithelial Cells. *Infection and Immunity*, 73(12), pp.8298–8305.

Garg, S., Md Syed, M. & Kielian, T., 2005. Staphylococcus aureus-derived peptidoglycan induces Cx43 expression and functional gap junction intercellular communication in microglia. *Journal of neurochemistry*, 95(2), pp.475–483.

Garzoni, C., Francois, P., Huyghe, A., Couzinet, S., Tapparel, C., Charbonnier, Y., Renzoni, A., Lucchini, S., Lew, D.P., Vaudaux, P., Kelley, W.L. & Schrenzel, J., 2007. A global view of Staphylococcus aureus whole genome expression upon internalization in human epithelial cells. *BMC genomics*, 8, p.171.

Garzoni, C. & Kelley, W.L., 2009. Staphylococcus aureus: new evidence for intracellular persistence. *Trends in microbiology*, 17(2), pp.59–65.

Georgakopoulou, E. a, Tsimaratou, K., Evangelou, K., Fernandez Marcos, P.J., Zoumpourlis, V., Trougakos, I.P., Kletsas, D., Bartek, J., Serrano, M. & Gorgoulis, V.G., 2013. Specific lipofuscin staining as a novel biomarker to detect replicative and stress-induced senescence. A method applicable in cryo-preserved and archival tissues. *Aging*, 5(1), pp.37–50.

Ghatnekar, G., O'Quinn, M., Jourdan, L.J., Gurjarpadhye, A.A., Draughn, R.L. & Gourdie, R.G., 2009. Connexin43 carboxyl-terminal peptides reduce scar progenitor and promote regenerative healing following skin wounding. *Regenerative medicine*, 4(2), pp.205–223.

Gillitzer, R. & Goebeler, M., 2001. Chemokines in cutaneous wound healing. *Journal of leukocyte biology*, 69(4), pp.513–21.

Gingalewski, C., Wang, K., Clemens, M.G. & De Maio, A., 1996. Posttranscriptional regulation of connexin 32 expression in liver during acute inflammation. *Journal of cellular physiology*, 166(2), pp.461–467.

Gjødsbøl, K. & Christensen, J., 2006. Multiple bacterial species reside in chronic wounds: a longitudinal study. *International wound journal*, 3(3), pp.225–231.

Glim, J.E., van Egmond, M., Niessen, F.B., Everts, V. & Beelen, R.H.J., 2013. Detrimental dermal wound healing: what can we learn from the oral mucosa? *Wound repair and regeneration : official publication of the Wound*

Healing Society [and] the European Tissue Repair Society, 21(5), pp.648–60.

Glim, J.E., Everts, V., Niessen, F.B., Ulrich, M.M. & Beelen, R.H.J., 2014. Extracellular matrix components of oral mucosa differ from skin and resemble that of foetal skin. *Archives of oral biology*, 59(10), pp.1048–1055.

Goerke, C. & Wolz, C., 2010. Adaptation of Staphylococcus aureus to the cystic fibrosis lung. *International journal of medical microbiology : IJMM*, 300(8), pp.520–5.

Goliger, J.A. & Paul, D.L., 1994. Expression of Gap Junction Proteins Cx26, Cx31.1, Cx37 and Cx43 in Developing and Mature Rat. *Developmental Dynamics: An Official Publication of the American Association of Anatomists*, 13, pp.1–13.

Goliger, J.A. & Paul, D.L., 1995. Wounding alters epidermal connexin expression and gap junction-mediated intercellular communication. *Molecular Biology of the Cell*, 6(11), pp.1491–1501.

Gomes, P., Srinivas, S.P., Van Driessche, W., Vereecke, J. & Himpens, B., 2005. ATP release through connexin hemichannels in corneal endothelial cells. *Investigative ophthalmology & visual science*, 46(4), pp.1208–1218.

Gottfried, I., Landau, M., Glaser, F., Di, W.-L., Ophir, J., Mevorah, B., Ben-Tal, N., Kelsell, D.P. & Avraham, K.B., 2002. A mutation in GJB3 is associated with recessive erythrokeratodermia variabilis (EKV) and leads to defective trafficking of the connexin 31 protein. *Human molecular genetics*, 11(11), pp.1311–6.

Graves, D.T., Nooh, N., Gillen, T., Davey, M., Patel, S., Cottrell, D. & Amar, S., 2001. IL-1 Plays a Critical Role in Oral, But Not Dermal, Wound Healing. *The Journal of Immunology*, 167(9), pp.5316–5320.

Gresham, H.D., Lowrance, J.H., Caver, T.E., Wilson, B.S., Cheung, a. L. & Lindberg, F.P., 2000. Survival of Staphylococcus aureus Inside Neutrophils Contributes to Infection. *The Journal of Immunology*, 164(7), pp.3713–3722.

Gröschl, M., Topf, H.-G., Kratzsch, J., Dötsch, J., Rascher, W. & Rauh, M., 2005. Salivary leptin induces increased expression of growth factors in oral keratinocytes. *Journal of molecular endocrinology*, 34(2), pp.353–66.

Grose, R. & Werner, S., 2004. Wound-healing studies in transgenic and knockout mice. *Molecular biotechnology*, 28(2), pp.147–66.

Guerrier, A., Fonlupt, P., Morand, I., Rabilloud, R., Audebet, C., Krutovskikh, V., Gros, D., Rousset, B. & Munari-Silem, Y., 1995. Gap junctions and cell polarity: connexin32 and connexin43 expressed in polarized thyroid epithelial cells assemble into separate gap junctions, which are located in

distinct regions of the lateral plasma membrane domain. *Journal of cell science*, 108, pp.2609–2617.

Günther, F., Wabnitz, G.H., Stroh, P., Prior, B., Obst, U., Samstag, Y., Wagner, C. & Hänsch, G.M., 2009. Host defence against Staphylococcus aureus biofilms infection: phagocytosis of biofilms by polymorphonuclear neutrophils (PMN). *Molecular immunology*, 46(8-9), pp.1805–13.

Guo, H., Acevedo, P., Parsa, F. & Bertram, J., 1992. Gap junction protein connexin 43 is expressed in dermis and epidermis of human skin: differential modulation of retinoids. *Journal of Investigative Dermatology*, 99(4), pp.460–467.

Guo, Y., Martinez-Williams, C. & Rannels, D.E., 2002. Integrin-Mediated Regulation of Connexin 43 Expression by Alveolar Epithelial Cells*. *CHEST Journal*, 121(3_suppl), p.30S–31S.

Gurjala, A.N., Geringer, M.R., Seth, A.K., Hong, S.J., Smeltzer, M.S., Galiano, R.D., Leung, K.P. & Mustoe, T.A., 2011. Development of a novel, highly quantitative in vivo model for the study of biofilm-impaired cutaneous wound healing. *Wound repair and regeneration: official publication of the Wound Healing Society [and] the European Tissue Repair Society*, 19(3), pp.400–410.

Guttman, J.A., Lin, A.E.-J., Li, Y., Bechberger, J., Naus, C.C., Vogl, A.W. & Finlay, B.B., 2010. Gap junction hemichannels contribute to the generation of diarrhoea during infectious enteric disease. *Gut*, 59(2), pp.218–226.

Häkkinen, L., Uitto, V.-J. & Larjava, H., 2000. Cell biology of gingival wound healing. *Periodontology 2000*, 24(1), p.127.

Hamza, T., Dietz, M., Pham, D., Clovis, N., Danley, S. & Li, B., 2013. Intra-cellular staphylococcus aureus alone causes infection in vivo. *European cells and materials*, 25, pp.341–350.

Han, A., Zenilman, J.M., Melendez, J.H., Shirtliff, M.E., Agostinho, A., James, G., Stewart, P.S., Mongodin, E.F., Rao, D., Rickard, A.H. & Lazarus, G.S., 2011. The importance of a multifaceted approach to characterizing the microbial flora of chronic wounds. *Wound repair and regeneration : official publication of the Wound Healing Society [and] the European Tissue Repair Society*, 19(5), pp.532–41.

Han, G., Li, F., Singh, T.P., Wolf, P. & Wang, X.-J., 2012. The pro-inflammatory role of TGFβ1: a paradox? *International journal of biological sciences*, 8(2), pp.228–35.

Hara, A., Murata, T., Uemura, R., Miura, T., Fukui, K., Matsukawa, H., Kasiwagi, K., Ito, T., Yoshioka, M. & Hibi, T., 1999. Identification of connexins in human oral mucosa and therapeutic effect of irsogladine maleate on aphthous stomatitis. *Journal of Gastroenterology*, 34, pp.1–6.

Hasan, A., Murata, H., Falabella, A., Ochoa, S., Zhou, L., Badiavas, E. & Falanga, V., 1997. Dermal fibroblasts from venous ulcers are unresponsive to the action of transforming growth factor-β 1. *Journal of Dermatological Science*, 16(1), pp.59–66.

Haslinger-Löffler, B., Kahl, B.C., Grundmeier, M., Strangfeld, K., Wagner, B., Fischer, U., Cheung, A.L., Peters, G., Schulze-Osthoff, K. & Sinha, B., 2005. Multiple virulence factors are required for Staphylococcus aureus-induced apoptosis in endothelial cells. *Cellular microbiology*, 7(8), pp.1087–97.

Hatakeyama, S., Mikami, T., Habano, W. & Takeda, Y., 2011. Expression of connexins and the effect of retinoic acid in oral keratinocytes. *Journal of Oral Science*, 53(3), pp.327–332.

Hatakeyama, S., Yaegashi, T., Oikawa, Y., Fujiwara, H., Mikami, T., Takeda, Y. & Satoh, M., 2006. Expression pattern of adhesion molecules in junctional epithelium differs from that in other gingival epithelia. *Journal of periodontal research*, 41(4), pp.322–328.

Haugwitz, U., Bobkiewicz, W., Han, S.-R., Beckmann, E., Veerachato, G., Shaid, S., Biehl, S., Dersch, K., Bhakdi, S. & Husmann, M., 2006. Pore-forming Staphylococcus aureus alpha-toxin triggers epidermal growth factor receptor-dependent proliferation. *Cellular microbiology*, 8(10), pp.1591–600.

Hébert, A., Sayasith, K., Sénéchal, S., Dubreuil, P. & Lagacé, J., 2000. Demonstration of intracellular Staphylococcus aureus in bovine mastitis alveolar cells and macrophages isolated from naturally infected cow milk. *FEMS microbiology letters*, 193(1), pp.57–62.

Herrick, S.E., Sloan, P., McGurk, M., Freak, L., McCollum, C.N. & Ferguson, M.W., 1992. Sequential changes in histologic pattern and extracellular matrix deposition during the healing of chronic venous ulcers. *The American journal of pathology*, 141(5), pp.1085–1095.

Hervé, J.-C., Derangeon, M., Sarrouilhe, D., Giepmans, B.N.G. & Bourmeyster, N., 2012. Gap junctional channels are parts of multiprotein complexes. *Biochimica et biophysica acta*, 1818(8), pp.1844–65.

Hinkerohe, D., Smikalla, D., Schoebel, A., Haghikia, A., Zoidl, G., Haase, C.G., Schlegel, U. & Faustmann, P.M., 2010. Dexamethasone prevents LPS-induced microglial activation and astroglial impairment in an experimental bacterial meningitis co-culture model. *Brain research*, 1329, pp.45–54.

Hivnor, C., Williams, N., Singh, F., VanVoorhees, A., Dzubow, L., Baldwin, D. & Seykora, J., 2004. Gene expression profiling of porokeratosis demonstrates similarities with psoriasis. *Journal of cutaneous pathology*, 31(10), pp.657–664.

Hong, S.-W., Choi, E.-B., Min, T.-K., Kim, J.-H., Kim, M.-H., Jeon, S.G., Lee, B.-J., Gho, Y.S., Jee, Y.-K., Pyun, B.-Y. & Kim, Y.-K., 2014. An Important Role

of α-Hemolysin in Extracellular Vesicles on the Development of Atopic Dermatitis Induced by Staphylococcus aureus. *PloS one*, 9(7), p.e100499.

Hu, V.W. & Xie, H.-Q., 1994. Interleukin-1a suppresses gap junction-mediate intercellular communication in human endothelial cells. *Experimental cell research*, 213, pp.218–223.

Huang, G.Y., Cooper, E.S., Waldo, K., Kirby, M.L., Gilula, N.B. & Lo, C.W., 1998. Gap junction-mediated cell-cell communication modulates mouse neural crest migration. *The Journal of cell biology*, 143(6), pp.1725–34.

Huang, R.P., Hossain, M.Z., Huang, R., Gano, J., Fan, Y. & Boynton, A.L., 2001. Connexin 43 (cx43) enhances chemotherapy-induced apoptosis in human glioblastoma cells. *International journal of cancer. Journal international du cancer*, 92(1), pp.130–138.

Hunter, A., Barker, R., Zhu, C. & Gourdie, R.G., 2005. Zonula occludens-1 alters connexin43 gap junction size and organization by influencing channel accretion. *Molecular biology of the cell*, 16(December), pp.5686–5698.

Iacobas, D. a, Scemes, E. & Spray, D.C., 2004. Gene expression alterations in connexin null mice extend beyond the gap junction. *Neurochemistry international*, 45(2-3), pp.243–50.

Isakson, B.E., Evans, W.H. & Boitano, S., 2001. Intercellular Ca2+ signaling in alveolar epithelial cells through gap junctions and by extracellular ATP. *American journal of physiology. Lung cellular and molecular physiology*, 280(2), pp.L221–228.

James, G. a, Swogger, E., Wolcott, R., Pulcini, E. deLancey, Secor, P., Sestrich, J., Costerton, J.W. & Stewart, P.S., 2007. Biofilms in chronic wounds. *Wound repair and regeneration : official publication of the Wound Healing Society [and] the European Tissue Repair Society*, 16(1), pp.37–44.

James, G. & Swogger, E., 2008. Biofilms in chronic wounds. *Wound Repair and …*, 16(1), pp.37–44.

Jara, P.I., Boric, M.P. & Sáez, J.C., 1995. Leukocytes express connexin 43 after activation with lipopolysaccharide and appear to form gap junctions with endothelial cells after ischemia-reperfusion. *Proceedings of the National Academy of Sciences of the United States of America*, 92(15), pp.7011–5.

Jarry, T. & Cheung, A., 2006. Staphylococcus aureus Escapes More Efficiently from the Phagosome of a Cystic Fibrosis Bronchial Epithelial Cell Line than from Its Normal Counterpart. *Infection and immunity*, 74(5), pp.2568–2577.

Jefferson, K., Goldmann, D. & Pier, G., 2005. Use of confocal microscopy to analyze the rate of vancomycin penetration through Staphylococcus aureus biofilms. *Antimicrobial agents and chemotherapy*, 49(6), pp.2467–2473.

Jiang, J.X. & Goodenough, D.A., 1996. Heteromeric connexons in lens gap junction channels. *Proceedings of the National Academy of Sciences of the United States of America*, 93(3), pp.1287–1291.

Johnson, A. & DiPietro, L.A., 2013. Apoptosis and angiogenesis: an evolving mechanism for fibrosis. *FASEB journal : official publication of the Federation of American Societies for Experimental Biology*, 27(10), pp.3893–901.

Johnson, S., Nguyen, V. & Coder, D., 2013. Assessment of cell viability. *Current protocols in cytometrey*, 64, pp.9.2.1–9.2.26.

Johnston, A., Fritz, Y., Dawes, S.M., Diaconu, D., Al-Attar, P.M., Guzman, A.M., Chen, C.S., Fu, W., Gudjonsson, J.E., McCormick, T.S. & Ward, N.L., 2013. Keratinocyte overexpression of IL-17C promotes psoriasiform skin inflammation. *Journal of immunology (*, 190(5), pp.2252–62.

Jung, K.Y., Cha, J.D., Lee, S.H., Woo, W.H., Lim, D.S., Choi, B.K. & Kim, K.J., 2001. Involvement of staphylococcal protein A and cytoskeletal actin in Staphylococcus aureus invasion of cultured human oral epithelial cells. *Journal of medical microbiology*, 50(1), pp.35–41.

Justice, S.S., Hunstad, D. a, Seed, P.C. & Hultgren, S.J., 2006. Filamentation by Escherichia coli subverts innate defenses during urinary tract infection. *Proceedings of the National Academy of Sciences of the United States of America*, 103(52), pp.19884–9.

Kahl, B.C., Goulian, M., van Wamel, W., Herrmann, M., Simon, S.M., Kaplan, G., Peters, G. & Cheung, a L., 2000. Staphylococcus aureus RN6390 replicates and induces apoptosis in a pulmonary epithelial cell line. *Infection and immunity*, 68(9), pp.5385–92.

Kalra, J., Shao, Q., Qin, H., Thomas, T., Alaoui-Jamali, M. a & Laird, D.W., 2006. Cx26 inhibits breast MDA-MB-435 cell tumorigenic properties by a gap junctional intercellular communication-independent mechanism. *Carcinogenesis*, 27(12), pp.2528–37.

Kameritsch, P., Khandoga, N., Pohl, U. & Pogoda, K., 2013. Gap junctional communication promotes apoptosis in a connexin-type-dependent manner. *Cell death & disease*, 4(4), p.e584.

Kanangat, S., Postlethwaite, A., Hasty, K., Kang, A., Smeltzer, M., Appling, W. & Schaberg, D., 2006. Induction of multiple matrix metalloproteinases in human dermal and synovial fibroblasts by Staphylococcus aureus: implications in the pathogenesis of septic arthritis and other soft tissue infections. *Arthritis research & therapy*, 8(6), p.R176.

Kanaporis, G., Mese, G., Valiuniene, L., White, T.W., Brink, P.R. & Valiunas, V., 2008. Gap junction channels exhibit connexin-specific permeability to cyclic nucleotides. *The Journal of general physiology*, 131(4), pp.293–305.

Kandyba, E.E., Hodgins, M.B. & Martin, P.E., 2008. A murine living skin equivalent amenable to live-cell imaging: analysis of the roles of connexins in the epidermis. *The Journal of investigative dermatology*, 128(4), pp.1039–49.

Kang, H.T., Lee, K.B., Kim, S.Y., Choi, H.R. & Park, S.C., 2011. Autophagy impairment induces premature senescence in primary human fibroblasts. *PloS one*, 6(8), p.e23367.

Kang, J., Kang, N., Lovatt, D., Torres, A., Zhao, Z., Lin, J. & Nedergaard, M., 2008. Connexin 43 Hemichannels Are Permeable to ATP. *The Journal of Neuroscience*, 28(18), pp.4702 –4711.

Kanitakis, J., 2002. Anatomy , histology and immunohistochemistry of normal human skin. *European journal of dermatology*, 12(4), pp.390–401.

Karpuk, N., Burkovetskaya, M., Fritz, T., Angle, A. & Kielian, T., 2011. Neuroinflammation leads to region-dependent alterations in astrocyte gap junction communication and hemichannel activity. *The Journal of neuroscience: the official journal of the Society for Neuroscience*, 31(2), pp.414–425.

Kelsell, D.P., Di, W.L. & Houseman, M.J., 2001. Connexin mutations in skin disease and hearing loss. *American journal of human genetics*, 68(3), pp.559–68.

Kelsell, D.P., Wilgoss, a L., Richard, G., Stevens, H.P., Munro, C.S. & Leigh, I.M., 2000. Connexin mutations associated with palmoplantar keratoderma and profound deafness in a single family. *European journal of human genetics : EJHG*, 8(2), pp.141–4.

Kendall, R.T. & Feghali-Bostwick, C. a, 2014. Fibroblasts in fibrosis: novel roles and mediators. *Frontiers in pharmacology*, 5(May), p.123.

Kimura, K., Orita, T., Morishige, N., Nishida, T. & Sonoda, K.-H., 2013. Role of the JNK signaling pathway in downregulation of connexin43 by TNF-α in human corneal fibroblasts. *Current eye research*, 38(9), pp.926–32.

King, L.E., Stratton, C.W. & Mitchell, W.M., 2001. Chlamydia pneumoniae and chronic skin wounds: a focused review. *The journal of investigative dermatology. Symposium proceedings / the Society for Investigative Dermatology, Inc. [and] European Society for Dermatological Research*, 6(3), pp.233–7.

Kintarak, S., Whawell, S.A., Speight, P.M., Packer, S. & Nair, S.P., 2004. Internalization of Staphylococcus aureus by human keratinocytes. *Infection and immunity*, 72(10), pp.5668–5675.

Kirker, K. & James, G., 2012. Differential effects of planktonic and biofilm MRSA on human fibroblasts. *Wound Repair and Regeneration*, 20(2), pp.253–261.

Kirker, K.R., Secor, P.R., James, G.A., Fleckman, P., Olerud, J.E. & Stewart, P.S., 2009. Loss of viability and induction of apoptosis in human keratinocytes exposed to Staphylococcus aureus biofilms in vitro. *Wound Repair and Regeneration: Official Publication of the Wound Healing Society [and] the European Tissue Repair Society*, 17(5), pp.690–699.

Klee, P., Allagnat, F., Pontes, H., Cederroth, M., Charollais, A., Caille, D., Britan, A., Haefliger, J.-A. & Meda, P., 2011. Connexins protect mouse pancreatic β cells against apoptosis. *The Journal of clinical investigation*, 121(12), pp.4870–4879.

Klein, M., Krönke, M. & Krut, O., 2006. Expression of lysostaphin in HeLa cells protects from host cell killing by intracellular Staphylococcus aureus. *Medical microbiology and immunology*, 195(3), pp.159–63.

Kondo, R.P., Wang, S.Y., John, S. a, Weiss, J.N. & Goldhaber, J.I., 2000. Metabolic inhibition activates a non-selective current through connexin hemichannels in isolated ventricular myocytes. *Journal of molecular and cellular cardiology*, 32(10), pp.1859–72.

Koziel, J., Maciag-Gudowska, A., Mikolajczyk, T., Bzowska, M., Sturdevant, D.E., Whitney, A.R., Shaw, L.N., DeLeo, F.R. & Potempa, J., 2009. Phagocytosis of Staphylococcus aureus by macrophages exerts cytoprotective effects manifested by the upregulation of antiapoptotic factors. *PloS one*, 4(4), p.e5210.

Kraus, D. & Peschel, A., 2008. Staphylococcus aureus evasion of innate antimicrobial defense. *Future microbiology*, 3(4), pp.437–51.

Kretz, M., Euwens, C., Hombach, S., Eckardt, D., Teubner, B., Traub, O., Willecke, K. & Ott, T., 2003. Altered connexin expression and wound healing in the epidermis of connexin-deficient mice. *Journal of Cell Science*, 116(16), pp.3443 –3452.

Kristian, S. a, Golda, T., Ferracin, F., Cramton, S.E., Neumeister, B., Peschel, A., Götz, F. & Landmann, R., 2004. The ability of biofilm formation does not influence virulence of Staphylococcus aureus and host response in a mouse tissue cage infection model. *Microbial pathogenesis*, 36(5), pp.237–45.

Krut, O., Utermöhlen, O., Schlossherr, X., Utermo, O. & Kro, M., 2003. Strain-Specific Association of Cytotoxic Activity and Virulence of Clinical Staphylococcus aureus Isolates Strain-Specific Association of Cytotoxic Activity and Virulence of Clinical Staphylococcus aureus Isolates. *Infection adn immunity*, 71(5), pp.2716–2723.

Kubica, M., Guzik, K., Koziel, J., Zarebski, M., Richter, W., Gajkowska, B., Golda, A., Maciag-Gudowska, A., Brix, K., Shaw, L., Foster, T. & Potempa, J., 2008. A potential new pathway for Staphylococcus aureus dissemination: the silent survival of S. aureus phagocytosed by human monocyte-derived macrophages. *PloS one*, 3(1), p.e1409.

Kuilman, T., Michaloglou, C., Mooi, W.J. & Peeper, D.S., 2010. The essence of senescence. *Genes & development*, 24(22), pp.2463–79.

Kurz, D.J., Decary, S., Hong, Y. & Erusalimsky, J.D., 2000. Senescence-associated (beta)-galactosidase reflects an increase in lysosomal mass during replicative ageing of human endothelial cells. *Journal of cell science*, 113 (Pt 2, pp.3613–22.

Labarthe, M.-P., Bosco, D., Saurat, J.-H., Meda, P. & Salomon, D., 1998. Upregulation of Connexin 26 Between Keratinocytes of Psoriatic Lesions. *Journal of Investigative Dermatology*, 111(1), pp.72–76.

Laird, D.W., 2014. Syndromic and non-syndromic disease-linked Cx43 mutations. *FEBS letters*, 588(8), pp.1339–48.

Laird, D.W., Puranam, K.L. & Revel, J.P., 1991. Turnover and phosphorylation dynamics of connexin43 gap junction protein in cultured cardiac myocytes. *The Biochemical Journal*, 273(Pt 1), pp.67–72.

Lamartine, J. et al., 2000. Mutations in GJB6 cause hidrotic ectodermal dysplasia. *Nature genetics*, 26(october), pp.142–144.

Lampe, P.D., Cooper, C.D., King, T.J. & Burt, J.M., 2006. Analysis of Connexin43 phosphorylated at S325, S328 and S330 in normoxic and ischemic heart. *Journal of cell science*, 119(Pt 16), pp.3435–42.

Lampe, P.D., Nguyen, B.P., Gil, S., Usui, M., Olerud, J., Takada, Y. & Carter, W.G., 1998. Cellular interaction of integrin alpha3beta1 with laminin 5 promotes gap junctional communication. *The Journal of cell biology*, 143(6), pp.1735–1747.

Larjava, H., Salo, T., Haapasalmi, K., Kramer, R.H. & Heino, J., 1993. Expression of integrins and basement membrane components by wound keratinocytes. *The Journal of clinical investigation*, 92(3), pp.1425–1435.

Latasa, C., Roux, A., Toledo-Arana, A., Ghigo, J.-M., Gamazo, C., Penadés, J.R. & Lasa, I., 2005. BapA, a large secreted protein required for biofilm formation and host colonization of Salmonella enterica serovar Enteritidis. *Molecular microbiology*, 58(5), pp.1322–39.

Lawrence, T.S., Beers, W.H. & Gilula, N.B., 1978. Transmission of hormonal stimulation by cell-to-cell communication. *Nature*, 272(5653), pp.501–506.

Lee, H.G. & Eun, H.C., 1999. Differences between fibroblasts cultured from oral mucosa and normal skin: implication to wound healing. *Journal of dermatological science*, 21(3), pp.176–82.

Leid, J. & Shirtliff, M., 2002. Human Leukocytes Adhere to , Penetrate , and Respond to Staphylococcus aureus Biofilms Human Leukocytes. *Infection and immunity*, 70(11), pp.6339–6345.

Lemaître, G., Sivan, V., Lamartine, J., Cosset, J.-M., Cavelier-Balloy, B., Salomon, D., Waksman, G. & Martin, M.T., 2006. Connexin 30, a new marker of hyperproliferative epidermis. *The British journal of dermatology*, 155(4), pp.844–846.

Lewis, K., 2010. Persister cells. *Annual review of microbiology*, 64, pp.357–72.

Li, F., Sugishita, K., Su, Z., Ueda, I. & Barry, W.H., 2001. Activation of connexin-43 hemichannels can elevate [Ca(2+)]i and [Na(+)]i in rabbit ventricular myocytes during metabolic inhibition. *Journal of molecular and cellular cardiology*, 33(12), pp.2145–2155.

Liao, C.-K., Wang, S.-M., Chen, Y.-L., Wang, H.-S. & Wu, J.-C., 2010. Lipopolysaccharide-induced inhibition of connexin43 gap junction communication in astrocytes is mediated by downregulation of caveolin-3. *The international journal of biochemistry & cell biology*, 42(5), pp.762–770.

Liebmann, M., Stahr, A., Guenther, M., Witte, O.W. & Frahm, C., 2013. Astrocytic Cx43 and Cx30 differentially modulate adult neurogenesis in mice. *Neuroscience letters*, 545, pp.40–5.

Liechty, B.K.W., Kim, H.B., Adzick, N.S. & Crombleholme, T.M., 2000. Fetal Wound Repair Results in Scar Formation in Interleukin-10–Deficient Mice in a Syngeneic Murine Model of Scarless Fetal Wound Repair. , 35(6), pp.866–873.

Little, T.L., Beyer, E.C., Duling, B.R., Tara, L. & Duling, R., 1995. Connexin 43 and connexin 40 gap junctional proteins present in arteriolar smooth muscle and endothelium are in vivo. *American journal of physiology*, 268, pp.H729–H739.

Liu, C., La Rosa, S. & Hagos, E.G., 2014. Oxidative DNA damage causes premature senescence in mouse embryonic fibroblasts deficient for Krüppel-like factor 4. *Molecular carcinogenesis*, (November 2013), pp.1–11.

Liu, J., Ek Vitorin, J.F., Weintraub, S.T., Gu, S., Shi, Q., Burt, J.M. & Jiang, J.X., 2011. Phosphorylation of connexin 50 by protein kinase A enhances gap junction and hemichannel function. *The Journal of biological chemistry*, 286(19), pp.16914–16928.

Liu, K., Kasper, M., Bierhaus, A., Langer, S. & Müller, M., 1997. Connexin 43 Expression in Normal and Irradiated Mouse Skin. *Radiation research*, 147(4), pp.437–441.

Liu, Y., Petreaca, M., Yao, M. & Martins-Green, M., 2009. Cell and molecular mechanisms of keratinocyte function stimulated by insulin during wound healing. *BMC cell biology*, 10, p.1.

Van der Loo, B., Fenton, M.J. & Erusalimsky, J.D., 1998. Cytochemical detection of a senescence-associated beta-galactosidase in endothelial

and smooth muscle cells from human and rabbit blood vessels. *Experimental cell research*, 241(2), pp.309–15.

Lucke, T., Choudhry, R., Thom, R., Selmer, I.-S., Burden, A.D. & Hodgins, M.B., 1999. Upregulation of Connexin 26 is a Feature of Keratinocyte Differentiation in Hyperproliferative Epidermis, Vaginal Epithelium, and Buccal Epithelium. , 112(3), pp.354–361.

Lygoe, K. a, Wall, I., Stephens, P. & Lewis, M.P., 2007. Role of vitronectin and fibronectin receptors in oral mucosal and dermal myofibroblast differentiation. *Biology of the cell / under the auspices of the European Cell Biology Organization*, 99(11), pp.601–14.

Madeo, J. & Frieri, M., 2014. Bacterial biofilms and chronic rhinosinusitis. *Allergy and asthma proceedings : the official journal of regional and state allergy societies*, 34(4), pp.335–41.

Maestrini, E., Korge, B.P., Ocaña-sierra, J., Calzolari, E., Scudder, P.M., Hovnanian, A. & Munro, C.S., 1999. A missense mutation in connexin26 , D66H , causes mutilating keratoderma with sensorineural deafness (Vohwinkel ' s syndrome) in three unrelated families. *Human molecular genetics*, 8(7), pp.1237–1243.

Mah, W., Jiang, G., Olver, D., Cheung, G., Kim, B., Larjava, H. & Häkkinen, L., 2014. Human gingival fibroblasts display a non-fibrotic phenotype distinct from skin fibroblasts in three-dimensional cultures. *PloS one*, 9(3), p.e90715.

De Maio, A., Gingalewski, C., Theodorakis, N.G. & Clemens, M.G., 2000. Interruption of hepatic gap junctional communication in the rat during inflammation induced by bacterial lipopolysaccharide. *Shock (Augusta, Ga.)*, 14(1), pp.53–59.

Mak, K., Manji, A., Gallant-Behm, C., Wiebe, C., Hart, D.A., Larjava, H. & Häkkinen, L., 2009. Scarless healing of oral mucosa is characterized by faster resolution of inflammation and control of myofibroblast action compared to skin wounds in the red Duroc pig model. *Journal of Dermatological Science*, 56(3), pp.168–180.

Makowski, L., Caspar, D., Phillips, W. & Goodenough, D., 1977. Gap junction structures: Analysis of the x-ray diffraction data. *The Journal of Cell Biology*, 74(2), pp.629–645.

Man, Y.K.S., Trolove, C., Tattersall, D., Thomas, A.C., Papakonstantinopoulou, A., Patel, D., Scott, C., Chong, J., Jagger, D.J., O'Toole, E.A., Navsaria, H., Curtis, M.A. & Kelsell, D.P., 2007. A Deafness-Associated Mutant Human Connexin 26 Improves the Epithelial Barrier In Vitro. *Journal of Membrane Biology*, 218(1-3), pp.29–37.

Mancl, K. a, Kirsner, R.S. & Ajdic, D., 2013. Wound biofilms: lessons learned from oral biofilms. *Wound repair and regeneration : official publication of*

the Wound Healing Society [and] the European Tissue Repair Society, 21(3), pp.352–62.

Markiewicz, M., Margarone, J., Barbagli, G. & Scannapieco, F., 2007. Oral mucosa harvest: an overview of anatomic and biologic considerations. *EAU-EBU Update Series*, 5, pp.179–187.

Martin, P., 1997. Wound healing--aiming for perfect skin regeneration. *Science (New York, N.Y.)*, 276(5309), pp.75–81.

Martin, P., D'Souza, D., Martin, J., Grose, R., Cooper, L., Maki, R. & McKercher, S.R., 2003. Wound healing in the PU.1 null mouse-tissue repair is not dependent on inflammatory cells. *Current Biology: CB*, 13(13), pp.1122–1128.

Martin, P. & Leibovich, S.J., 2005. Inflammatory cells during wound repair: the good, the bad and the ugly. *Trends in Cell Biology*, 15(11), pp.599–607.

Martínez, a D. & Sáez, J.C., 2000. Regulation of astrocyte gap junctions by hypoxia-reoxygenation. *Brain research. Brain research reviews*, 32(1), pp.250–8.

Masgrau-Peya, E., Salomon, D., Saurat, J.H. & Meda, P., 1997. In vivo modulation of connexins 43 and 26 of human epidermis by topical retinoic acid treatment. *The journal of histochemistry and cytochemistry : official journal of the Histochemistry Society*, 45(9), pp.1207–15.

Mashburn, L.M., Jett, A.M., Akins, D.R. & Whiteley, M., 2005. Staphylococcus aureus Serves as an Iron Source for Pseudomonas aeruginosa during In Vivo Coculture. *Journal of Bacteriology*, 187(2), pp.554–566.

Matsuuchi, L. & Naus, C.C., 2013. Gap junction proteins on the move: connexins, the cytoskeleton and migration. *Biochimica et biophysica acta*, 1828(1), pp.94–108.

McCarty, S.M., Cochrane, C. a, Clegg, P.D. & Percival, S.L., 2012. The role of endogenous and exogenous enzymes in chronic wounds: a focus on the implications of aberrant levels of both host and bacterial proteases in wound healing. *Wound repair and regeneration : official publication of the Wound Healing Society [and] the European Tissue Repair Society*, 20(2), pp.125–36.

McKeown, S.T.W., Barnes, J.J., Hyland, P.L., Lundy, F.T., Fray, M.J. & Irwin, C.R., 2007. Matrix metalloproteinase-3 differences in oral and skin fibroblasts. *Journal of dental research*, 86(5), pp.457–462.

McKleroy, W., Lee, T.-H. & Atabai, K., 2013. Always cleave up your mess: targeting collagen degradation to treat tissue fibrosis. *American journal of physiology. Lung cellular and molecular physiology*, 304(11), pp.L709–21.

Meerloo, J. Van, Kaspers, G.J.L. & Cloos, J., 2011. Cell Sensitivity Assays: The MTT Assay I. A. Cree, ed. *Methods in Molecular Biology*, 731, pp.237–245.

Mempel, M., Schnopp, C., Hojka, M., Fesq, H., Weidinger, S., Schaller, M., Korting, H.C., Ring, J. & Abeck, D., 2002. Invasion of human keratinocytes by Staphylococcus aureus and intracellular bacterial persistence represent haemolysin-independent virulence mechanisms that are followed by features of necrotic and apoptotic keratinocyte cell death. *The British journal of dermatology*, 146(6), pp.943–951.

Mendez, M. V, Stanley, a, Park, H.Y., Shon, K., Phillips, T. & Menzoian, J.O., 1998. Fibroblasts cultured from venous ulcers display cellular characteristics of senescence. *Journal of vascular surgery*, 28(5), pp.876–83.

Mendez, M. V., Stanley, A., Park, H.-Y., Shon, K., Phillips, T. & Menzoian, J.O., 1998. Fibroblasts cultured from venous ulcers display cellular characteristics of senescence. *Journal of Vascular Surgery*, 28(5), pp.876–883.

Mendoza-Naranjo, A., Cormie, P., Serrano, A., Hu, R., O'Neill, S., Wang, C.M., Thrasivoulou, C., Power, K.T., White, A., Serena, T., Phillips, A.R.J. & Becker, D.L., 2012. Targeting cx43 and N-cadherin, which are abnormally upregulated in venous leg ulcers, influences migration, adhesion and activation of rho GTPases. *PloS one*, 7(5), p.e37374.

Mendoza-Naranjo, A., Cormie, P., Serrano, A.E., Wang, C.M., Thrasivoulou, C., Sutcliffe, J.E.S., Gilmartin, D.J., Tsui, J., Serena, T.E., Phillips, A.R.J. & Becker, D.L., 2012. Overexpression of the gap junction protein Cx43 as found in diabetic foot ulcers can retard fibroblast migration. *Cell biology international*, 36(7), pp.661–667.

Menke, N.B., Ward, K.R., Witten, T.M., Bonchev, D.G. & Diegelmann, R.F., 2007. Impaired wound healing. *Clinics in dermatology*, 25(1), pp.19–25.

Menzies, B.E., Kourteva, Y., Kaiser, A.B. & Kernodle, D.S., 2002. Inhibition of staphylococcal wound infection and potentiation of antibiotic prophylaxis by a recombinant fragment of the fibronectin-binding protein of Staphylococcus aureus. *The Journal of infectious diseases*, 185(7), pp.937–43.

Mori, R., Power, K. & Wang, C., 2006. Acute downregulation of connexin43 at wound sites leads to a reduced inflammatory response, enhanced keratinocyte proliferation and wound fibroblast migration. *Journal of cell …*, 119(24), pp.5193 –5203.

Mori, R., Shaw, T.J. & Martin, P., 2008. Molecular mechanisms linking wound inflammation and fibrosis: knockdown of osteopontin leads to rapid repair and reduced scarring. *The Journal of experimental medicine*, 205(1), pp.43–51.

Moyer, K.E., Davis, a, Saggers, G.C., Mackay, D.R. & Ehrlich, H.P., 2002. Wound healing: the role of gap junctional communication in rat granulation tissue maturation. *Experimental and molecular pathology*, 72(1), pp.10–6.

Mulcahy, L.R., Burns, J.L., Lory, S. & Lewis, K., 2010. Emergence of Pseudomonas aeruginosa strains producing high levels of persister cells in patients with cystic fibrosis. *Journal of bacteriology*, 192(23), pp.6191–9.

Muller, M., 2006. Premature cellular senescence induced by pyocyanin, a redox-active Pseudomonas aeruginosa toxin. *Free radical biology & medicine*, 41(11), pp.1670–7.

Munro, P., Clément, R., Lavigne, J.-P., Pulcini, C., Lemichez, E. & Landraud, L., 2011. High prevalence of edin-C encoding RhoA-targeting toxin in clinical isolates of Staphylococcus aureus. *European journal of clinical microbiology & infectious diseases : official publication of the European Society of Clinical Microbiology*, 30(8), pp.965–72.

Muramatsu, T., Uekusa, T., Masaoka, T., Saitoh, M., Hashimoto, S., Abiko, Y., Jung, H.-S. & Shimono, M., 2008. Differential expression and localization of connexins 26 and 43 in the rat gingival epithelium. *Archives of histology and cytology*, 71(3), pp.147–154.

Murillo, O., Pachón, M.E., Euba, G., Verdaguer, R., Carreras, M., Cabellos, C., Cabo, J., Gudiol, F. & Ariza, J., 2009. Intracellular antimicrobial activity appearing as a relevant factor in antibiotic efficacy against an experimental foreign-body infection caused by Staphylococcus aureus. *The Journal of antimicrobial chemotherapy*, 64(5), pp.1062–6.

Mustoe, T.A., O'Shaughnessy, K. & Kloeters, O., 2006. Chronic wound pathogenesis and current treatment strategies: a unifying hypothesis. *Plastic and reconstructive surgery*, 117(7 Suppl), p.35S–41S.

Mylvaganam, S., Zhang, L., Wu, C., Zhang, Z.J., Samoilova, M., Eubanks, J., Carlen, P.L. & Poulter, M.O., 2009. Hippocampal seizures alter the expression of the pannexin and connexin transcriptome. *Journal of Neurochemistry*, 112(1), pp.92–102.

Nakatsuji, T., Chiang, H.-I., Jiang, S.B., Nagarajan, H., Zengler, K. & Gallo, R.L., 2013. The microbiome extends to subepidermal compartments of normal skin. *Nature communications*, 4, p.1431.

Niessen, H., Harz, H., Bedner, P., Krämer, K. & Willecke, K., 2000. Selective permeability of different connexin channels to the second messenger inositol 1,4,5-trisphosphate. *Journal of cell science*, 113 (Pt 8, pp.1365–1372.

Nusrat, A., Chen, J.A., Foley, C.S., Liang, T.W., Tom, J., Cromwell, M., Quan, C. & Mrsny, R.J., 2000. The coiled-coil domain of occludin can act to organize structural and functional elements of the epithelial tight junction. *The Journal of biological chemistry*, 275(38), pp.29816–29822.

Oliveira, M., Bexiga, R., Nunes, S.F. & Vilela, C.L., 2011. Invasive potential of biofilm-forming Staphylococci bovine subclinical mastitis isolates. *Journal of Veterinary Science*, 12(1), p.95.

Ongenae, K., Phillips, T. & Park, H., 2000. Level of fibronectin mRNA is markedly increased in human chronic wounds. *Dermatologic surgery*, 26(5), pp.447–451.

Orrenius, B. & Sten, Z., 2001. Assessment of Apoptosis and Necrosis by DNA Fragmentation and Morphological Criteria. *Current Protocols in Cell Biology*, 12(18.3), pp.18.3.1–18.3.23.

Oviedo-Orta, E., Errington, R.J. & Evans, W.H., 2002. Gap junction intercellular communication during lymphocyte transendothelial migration. *Cell biology international*, 26(3), pp.253–63.

Oviedo-orta, E., Hoy, T. & Evans, W., 2000. system: differential expression of connexin40 and 43, and perturbation of gap junction channel functions in peripheral blood and tonsil human lymphocyte. *Immunology*, 99(4), pp.578–590.

Ozawa, H., Matsunaga, T., Kamiya, K., Tokumaru, Y., Fujii, M., Tomita, T. & Ogawa, K., 2007. Decreased expression of connexin-30 and aberrant expression of connexin-26 in human head and neck cancer. *Anticancer Research*, 27(4B), pp.2189–2195.

Ozawa, H., Mutai, H., Matsunaga, T., Tokumaru, Y., Fujii, M., Sakamoto, K., Tomita, T. & Ogawa, K., 2009. Promoted cell proliferation by connexin 30 gene transfection to head-and-neck cancer cell line. *Anticancer research*, 29(6), pp.1981–1985.

P Stephens, K.J.D., 1996. A comparison of the ability of intra-oral and extra-oral fibroblasts to stimulate extracellular matrix reorganization in a model of wound contraction. *Journal of dental research*, 75(6), pp.1358–64.

Pastar, I., Nusbaum, A.G., Gil, J., Patel, S.B., Chen, J., Valdes, J., Stojadinovic, O., Plano, L.R., Tomic-Canic, M. & Davis, S.C., 2013. Interactions of methicillin resistant Staphylococcus aureus USA300 and Pseudomonas aeruginosa in polymicrobial wound infection. *PloS one*, 8(2), p.e56846.

Paznekas, W. a, Boyadjiev, S. a, Shapiro, R.E., Daniels, O., Wollnik, B., Keegan, C.E., Innis, J.W., Dinulos, M.B., Christian, C., Hannibal, M.C. & Jabs, E.W., 2003. Connexin 43 (GJA1) mutations cause the pleiotropic phenotype of oculodentodigital dysplasia. *American journal of human genetics*, 72(2), pp.408–18.

Penes, M.C., Li, X. & Nagy, J.I., 2005. Expression of zonula occludens-1 (ZO-1) and the transcription factor ZO-1-associated nucleic acid-binding protein (ZONAB)-MsY3 in glial cells and colocalization at oligodendrocyte and astrocyte gap junctions in mouse brain. *The European journal of neuroscience*, 22(2), pp.404–418.

Pérez-Novo, C. a, Waeytens, A., Claeys, C., Cauwenberge, P. Van & Bachert, C., 2008. Staphylococcus aureus enterotoxin B regulates prostaglandin E2

synthesis, growth, and migration in nasal tissue fibroblasts. *The Journal of infectious diseases*, 197(7), pp.1036–43.

Plouin-Gaudon, I., Clement, S., Huggler, E., Chaponnier, C., Francois, P., Lew, D., Schrenzel, J., Vaudaux, P. & Lacroix, J., 2006. Intracellular residency is frequently associated withrecurrent Staphylococcus auresus rhinosinusitis. *Rhinology*, 44, pp.249–254.

Pollok, S., Pfeiffer, A.-C., Lobmann, R., Wright, C.S., Moll, I., Martin, P.E.M. & Brandner, J.M., 2011. Connexin 43 mimetic peptide Gap27 reveals potential differences in the role of Cx43 in wound repair between diabetic and non-diabetic cells. *Journal of Cellular and Molecular Medicine*, 15(4), pp.861–873.

Prajsnar, T.K., Hamilton, R., Garcia-Lara, J., McVicker, G., Williams, A., Boots, M., Foster, S.J. & Renshaw, S. a, 2012. A privileged intraphagocyte niche is responsible for disseminated infection of Staphylococcus aureus in a zebrafish model. *Cellular microbiology*, 14(10), pp.1600–19.

Qiu, C., Coutinho, P., Frank, S., Franke, S., Law, L., Martin, P., Green, C.R. & Becker, D.L., 2003. Targeting Connexin43 Expression Accelerates the Rate of Wound Repair. *Current Biology*, 13(19), pp.1697–1703.

Qu, C., Gardner, P. & Schrijver, I., 2009. The role of the cytoskeleton in the formation of gap junctions by Connexin 30. *Experimental cell research*, 315(10), pp.1683–1692.

Radin, J.N., González-Rivera, C., Frick-Cheng, A.E., Sheng, J., Gaddy, J. a, Rubin, D.H., Algood, H.M.S., McClain, M.S. & Cover, T.L., 2014. Role of connexin 43 in Helicobacter pylori VacA-induced cell death. *Infection and immunity*, 82(1), pp.423–32.

Reaume, A.G., Sousa, P.A. De, Kulkarni, S., Langille, B.L., Davies, T.C., Juneja, S.C., Kidder, G.M., Rossant, J. & Zhu, D., 1995. Cardiac Malformation in Neonatal Mice Pr ,. *Science*, 267(5205), pp.1831–1834.

Reilly, S.S., Hudson, M.C., Kellam, J.F. & Ramp, W.K., 2000. In vivo internalization of Staphylococcus aureus by embryonic chick osteoblasts. *Bone*, 26(1), pp.63–70.

Resch, A. & Rosenstein, R., 2005. Differential Gene Expression Profiling of Staphylococcus aureus Cultivated under Biofilm and Planktonic Conditions. *Applied and environmental microbiology*, 71(5), pp.2663–2676.

Retamal, M.A., Schalper, K.A., Shoji, K.F., Bennett, M.V.L. & Sáez, J.C., 2007. Opening of connexin 43 hemichannels is increased by lowering intracellular redox potential. *Proceedings of the National Academy of Sciences of the United States of America*, 104(20), pp.8322–8327.

Reynhout, J.K., Lampe, P.D. & Johnson, R.G., 1992. An activator of protein kinase C inhibits gap junction communication between cultured bovine lens cells. *Experimental cell research*, 198(2), pp.337–342.

Riau, A.K., Barathi, V.A. & Beuerman, R.W., 2008. Mucocutaneous junction of eyelid and lip: a study of the transition zone using epithelial cell markers. *Current Eye Research*, 33(11), pp.912–922.

Richard, G., 2000. Connexins: a connection with the skin. *Experimental dermatology*, 9(2), pp.77–96.

Richard, G., Smith, L.E., Bailey, R. a, Itin, P., Hohl, D., Epstein, E.H., DiGiovanna, J.J., Compton, J.G. & Bale, S.J., 1998. Mutations in the human connexin gene GJB3 cause erythrokeratodermia variabilis. *Nature genetics*, 20(4), pp.366–9.

Richard, G., White, T.W., Smith, L.E., Bailey, R. a, Compton, J.G., Paul, D.L. & Bale, S.J., 1998. Functional defects of Cx26 resulting from a heterozygous missense mutation in a family with dominant deaf-mutism and palmoplantar keratoderma. *Human genetics*, 103(4), pp.393–9.

Van Rijen, H. V, van Kempen, M.J., Postma, S. & Jongsma, H.J., 1998. Tumour necrosis factor alpha alters the expression of connexin43, connexin40, and connexin37 in human umbilical vein endothelial cells. *Cytokine*, 10(4), pp.258–64.

Risek, B., Klier, F.G. & Gilula, N.B., 1992. Multiple gap junction genes are utilized during rat skin and hair development. *Development*, 116(3), pp.639 –651.

Robertson, J., Lang, S., Lambert, P. a & Martin, P.E., 2010. Peptidoglycan derived from Staphylococcus epidermidis induces Connexin43 hemichannel activity with consequences on the innate immune response in endothelial cells. *The Biochemical journal*, 432(1), pp.133–43.

Romanello, M. & D'Andrea, P., 2001. Dual mechanism of intercellular communication in HOBIT osteoblastic cells: a role for gap-junctional hemichannels. *Journal of bone and mineral research: the official journal of the American Society for Bone and Mineral Research*, 16(8), pp.1465–1476.

Rook, M.B., Jongsma, H.J. & van Ginneken, A.C., 1988. Properties of single gap junctional channels between isolated neonatal rat heart cells. *The American Journal of Physiology*, 255(4 Pt 2), pp.H770–782.

Rose, B. & Loewenstein, W.R., 1975. Permeability of cell junction depends on local cytoplasmic calcium activity. *, Published online: 20 March 1975; | doi:10.1038/254250a0*, 254(5497), pp.250–252.

Rosen, D. a, Hooton, T.M., Stamm, W.E., Humphrey, P. a & Hultgren, S.J., 2007. Detection of intracellular bacterial communities in human urinary tract infection. *PLoS medicine*, 4(12), p.e329.

Rosen, D. a, Pinkner, J.S., Jones, J.M., Walker, J.N., Clegg, S. & Hultgren, S.J., 2008. Utilization of an intracellular bacterial community pathway in

Klebsiella pneumoniae urinary tract infection and the effects of FimK on type 1 pilus expression. *Infection and immunity*, 76(7), pp.3337–45.

Rotsch, J., Rohrbeck, A., May, M., Kolbe, T., Hagemann, S., Schelle, I., Just, I., Genth, H. & Huelsenbeck, S.C., 2012. Inhibition of macrophage migration by C. botulinum exoenzyme C3. *Naunyn-Schmiedeberg's archives of pharmacology*, 385(9), pp.883–90.

Rudney, J.D. & Chen, R., 2006. The vital status of human buccal epithelial cells and the bacteria associated with them. *Archives of Oral Biology*, 51(4), pp.291–298.

Rudney, J.D., Chen, R. & Sedgewick, G.J., 2005. Actinobacillus actinomycetemcomitans, Porphyromonas gingivalis, and Tannerella forsythensis are Components of a Polymicrobial Intracellular Flora within Human Buccal Cells. *Journal of Dental Research*, 84(1), pp.59–63.

Rudney, J.D., Chen, R. & Sedgewick, G.J., 2001. Intracellular Actinobacillus actinomycetemcomitans and Porphyromonas gingivalis in buccal epithelial cells collected from human subjects. *Infection and Immunity*, 69(4), pp.2700–2707.

Ryder, V.J., Chopra, I. & O'Neill, A.J., 2012. Increased mutability of Staphylococci in biofilms as a consequence of oxidative stress. *PloS one*, 7(10), p.e47695.

Sadowska, B., Więckowska-Szakiel, M., Paszkiewicz, M. & Różalska, B., 2013. The immunomodulatory activity of Staphylococcus aureus products derived from biofilm and planktonic cultures. *Archivum immunologiae et therapiae experimentalis*, 61(5), pp.413–20.

Sáez, J.C., Connor, J.A., Spray, D.C. & Bennett, M. V, 1989. Hepatocyte gap junctions are permeable to the second messenger, inositol 1,4,5-trisphosphate, and to calcium ions. *Proceedings of the National Academy of Sciences of the United States of America*, 86(8), pp.2708–2712.

Saitoh, M., Oyamada, M., Oyamada, Y., Kaku, T. & Mori, M., 1997. Changes in the expression of gap junction proteins (connexins) in hamster tongue epithelium during wound healing and carcinogenesis. *Carcinogenesis*, 18(7), pp.1319–1328.

Sarieddine, M.Z.R., Scheckenbach, K.E.L., Foglia, B., Maass, K., Garcia, I., Kwak, B.R. & Chanson, M., 2009. Connexin43 modulates neutrophil recruitment to the lung. *Journal of cellular and molecular medicine*, 13(11-12), pp.4560–4570.

Sauer, K., 2003. The genomics and proteomics of biofilm formation. *Genome biology*, 4(6), p.219.

Savage, V.J., Chopra, I. & O'Neill, A.J., 2013. Staphylococcus aureus biofilms promote horizontal transfer of antibiotic resistance. *Antimicrobial agents and chemotherapy*, 57(4), pp.1968–70.

Schierle, C.F., De la Garza, M., Mustoe, T.A. & Galiano, R.D., 2009. Staphylococcal biofilms impair wound healing by delaying reepithelialization in a murine cutaneous wound model. *Wound Repair and Regeneration: Official Publication of the Wound Healing Society [and] the European Tissue Repair Society*, 17(3), pp.354–359.

Schrementi, M.E., Ferreira, A.M., Zender, C. & DiPietro, L.A., 2008. Site-specific production of TGF-β in oral mucosal and cutaneous wounds. *Wound Repair and Regeneration*, 16(1), pp.80–86.

Schröder, A. & Schröder, B., 2006. Staphylococcus aureus Fibronectin Binding Protein-A Induces Motile Attachment Sites and Complex Actin Remodeling in Living Endothelial Cells. *Molecular biology of the cell*, 17(December), pp.5198–5210.

Scibelli, A., Roperto, S., Manna, L., Pavone, L.M., Tafuri, S., Della Morte, R. & Staiano, N., 2007. Engagement of integrins as a cellular route of invasion by bacterial pathogens. *Veterinary journal (London, England : 1997)*, 173(3), pp.482–91.

Sciubba, J.J., Waterhouse, J.P. & Meyer, J., 1978. A fine structural comparison of the healing of incisional wounds of mucosa and skin. *Journal of Oral Pathology*, 7(4), pp.214–227.

Secher, T., Samba-Louaka, A., Oswald, E. & Nougayrède, J.-P., 2013. Escherichia coli producing colibactin triggers premature and transmissible senescence in mammalian cells. *PloS one*, 8(10), p.e77157.

Secor, P.R., James, G.A., Fleckman, P., Olerud, J.E., McInnerney, K. & Stewart, P.S., 2011. Staphylococcus aureus Biofilm and Planktonic cultures differentially impact gene expression, mapk phosphorylation, and cytokine production in human keratinocytes. *BMC Microbiology*, 11, p.143.

Serrano, M., Lin, A., McCurrach, M., Beach, D. & Lowe, S., 1997. Oncogenic ras Provokes Premature Cell Senescence Associated with Accumulation of p53 and p16 INK4a. *Cell*, 88, pp.593–602.

Seth, A., Geringer, M.R., Hong, S.J., Leung, K.P., Galiano, R.D. & Mustoe, T. a, 2012. Comparative analysis of single-species and polybacterial wound biofilms using a quantitative, in vivo, rabbit ear model. *PloS one*, 7(8), p.e42897.

Seth, A.K., Geringer, M.R., Galiano, R.D., Leung, K.P., Mustoe, T.A. & Hong, S.J., 2012. Quantitative Comparison and Analysis of Species-Specific Wound Biofilm Virulence Using an In Vivo, Rabbit-Ear Model. *Journal of the American College of Surgeons*, 215(3), pp.388–399.

Seth, A.K., Geringer, M.R., Galiano, R.D., Leung, K.P., Mustoe, T.A. & Hong, S.J., 2012. Quantitative comparison and analysis of species-specific wound biofilm virulence using an in vivo, rabbit-ear model. *Journal of the American College of Surgeons*, 215(3), pp.388–399.

Shanker, A.J., Yamada, K., Green, K.G., Yamada, K. a & Saffitz, J.E., 2005. Matrix-protein-specific regulation of Cx43 expression in cardiac myocytes subjected to mechanical load. *Circulation research*, 96(5), pp.558–66.

Shannon, D.B., McKeown, S.T.W., Lundy, F.T. & Irwin, C.R., 2006. Phenotypic differences between oral and skin fibroblasts in wound contraction and growth factor expression. *Wound repair and regeneration: official publication of the Wound Healing Society [and] the European Tissue Repair Society*, 14(2), pp.172–178.

Shaw, T.J., Kishi, K. & Mori, R., 2010. Wound-associated skin fibrosis: mechanisms and treatments based on modulating the inflammatory response. *Endocrine, metabolic and immune disorders-drug targets*, 10(4), pp.320–330.

Shaw, T.J. & Martin, P., 2009. Wound repair at a glance. *Journal of cell science*, 122(Pt 18), pp.3209–13.

Simon, A.M., McWhorter, A.R., Chen, H., Jackson, C.L. & Ouellette, Y., 2004. Decreased intercellular communication and connexin expression in mouse aortic endothelium during lipopolysaccharide-induced inflammation. *Journal of vascular research*, 41(4), pp.323–333.

Simpson, K.J., Selfors, L.M., Bui, J., Reynolds, A., Leake, D., Khvorova, A. & Brugge, J.S., 2008. Identification of genes that regulate epithelial cell migration using an siRNA screening approach. *Nature cell biology*, 10(9), pp.1027–38.

Singh, R., Ray, P., Das, A. & Sharma, M., 2010. Penetration of antibiotics through Staphylococcus aureus and Staphylococcus epidermidis biofilms. *The Journal of antimicrobial chemotherapy*, 65(9), pp.1955–8.

Sinha, B., Francois, P., Que, Y.A., Hussain, M., Heilmann, C., Moreillon, P., Lew, D., Krause, K.H., Peters, G. & Herrmann, M., 2000. Heterologously expressed Staphylococcus aureus fibronectin-binding proteins are sufficient for invasion of host cells. *Infection and immunity*, 68(12), pp.6871–6878.

Sinha, B., François, P.P., Nüsse, O., Foti, M., Hartford, O.M., Vaudaux, P., Foster, T.J., Lew, D.P., Herrmann, M. & Krause, K.H., 1999. Fibronectin-binding protein acts as Staphylococcus aureus invasin via fibronectin bridging to integrin alpha5beta1. *Cellular microbiology*, 1(2), pp.101–117.

Sinha, B. & Fraunholz, M., 2010. Staphylococcus aureus host cell invasion and post-invasion events. *International Journal of Medical Microbiology*, 300(2–3), pp.170–175.

Sohl, G. & Willecke, K., 2003. An update on connexin genes and their nomenclature in mouse and man. *Cell communication and adhesion*, 10(4-6), pp.173–180.

Solan, J.L. & Lampe, P.D., 2009. Connexin43 phosphorylation: structural changes and biological effects. *The Biochemical journal*, 419(2), pp.261–72.

Solan, J.L., Marquez-Rosado, L., Sorgen, P.L., Thornton, P.J., Gafken, P.R. & Lampe, P.D., 2007. Phosphorylation at S365 is a gatekeeper event that changes the structure of Cx43 and prevents down-regulation by PKC. *The Journal of cell biology*, 179(6), pp.1301–9.

Somogyi, R., Batzer, A. & Kolb, H.A., 1989. Inhibition of electrical coupling in pairs of murine pancreatic acinar cells by OAG and isolated protein kinase C. *The Journal of membrane biology*, 108(3), pp.273–282.

Soong, G., Martin, F.J., Chun, J., Cohen, T.S., Ahn, D.S. & Prince, A., 2011. Staphylococcus aureus protein A mediates invasion across airway epithelial cells through activation of RhoA GTPase signaling and proteolytic activity. *The Journal of biological chemistry*, 286(41), pp.35891–8.

Sosinsky, G., 1995. Mixing of connexins in gap junction membrane channels. *Proceedings of the National Academy of Sciences of the United States of America*, 92(20), pp.9210–9214.

Souto, R. & Andrade, A., 2006. Prevalence of “non-oral” pathogenic bacteria in subgingival biofilm with chornic periodontitis. *Brazilian Journal of Microbiology*, 37, pp.208–215.

Squier, C. & Brogden, K., 2011. *Human Oral Mucosa: Development, Structure and Function*, John Wiley & Sons.

Squier, C.A. & Kremer, M.J., 2001. Biology of oral mucosa and esophagus. *Journal of the National Cancer Institute. Monographs*, (29), pp.7–15.

Stadelmann, W.K., Digenis, a G. & Tobin, G.R., 1998. Physiology and healing dynamics of chronic cutaneous wounds. *American journal of surgery*, 176(2A Suppl), p.26S–38S.

Stanley, a C., Park, H.Y., Phillips, T.J., Russakovsky, V. & Menzoian, J.O., 1997. Reduced growth of dermal fibroblasts from chronic venous ulcers can be stimulated with growth factors. *Journal of vascular surgery*, 26(6), pp.994–9; discussion 999–1001.

Stanley, A. & Osler, T., 2001. Senescence and the healing rates of venous ulcers. *Journal of Vascular Surgery*, 33(6), pp.1206–1211.

Stanley, A.C., Park, H.-Y., Phillips, T.J., Russakovsky, V. & Menzoian, J.O., 1997. Reduced growth of dermal fibroblasts from chronic venous ulcers can be stimulated with growth factors. *Journal of Vascular Surgery*, 26(6), pp.994–1001.

Statuto, M., Bianchi, C., Perego, R. & Del Monte, U., 2002. Drop of connexin 43 in replicative senescence of human fibroblasts HEL-299 as a possible biomarker of senescence. *Experimental gerontology*, 37(8-9), pp.1113–20.

Stauffer, K.A., 1995. The gap junction proteins beta 1-connexin (connexin-32) and beta 2-connexin (connexin-26) can form heteromeric hemichannels. *The Journal of biological chemistry*, 270(12), pp.6768–6772.

Stein, M., Noorman, M., van Veen, T. a B., Herold, E., Engelen, M. a, Boulaksil, M., Antoons, G., Jansen, J. a, van Oosterhout, M.F.M., Hauer, R.N.W., de Bakker, J.M.T. & van Rijen, H.V.M., 2008. Dominant arrhythmia vulnerability of the right ventricle in senescent mice. *Heart rhythm : the official journal of the Heart Rhythm Society*, 5(3), pp.438–48.

Stephens, P., Davies, K.J., Occleston, N., Pleass, R.D., Kon, C., Daniels, J., Khaw, P.T. & Thomas, D.W., 2001. Skin and oral fibroblasts exhibit phenotypic differences in extracellular matrix reorganization and matrix metalloproteinase activity. *The British journal of dermatology*, 144(2), pp.229–37.

Stojadinovic, O., Brem, H., Vouthounis, C., Lee, B., Fallon, J., Stallcup, M., Merchant, A., Galiano, R.D. & Tomic-Canic, M., 2005. Molecular pathogenesis of chronic wounds: the role of beta-catenin and c-myc in the inhibition of epithelialization and wound healing. *The American journal of pathology*, 167(1), pp.59–69.

Stojadinovic, O., Pastar, I., Vukelic, S., Mahoney, M.G., Brennan, D., Krzyzanowska, A., Golinko, M., Brem, H. & Tomic-Canic, M., 2008. Deregulation of keratinocyte differentiation and activation: a hallmark of venous ulcers. *Journal of cellular and molecular medicine*, 12(6B), pp.2675–2690.

Suci, P.A., Mittelman, M.W., Yu, F.P. & Geesey, G.G., 1994. Investigation of ciprofloxacin penetration into Pseudomonas aeruginosa biofilms. *Antimicrobial agents and chemotherapy*, 38(9), pp.2125–2133.

Sugai, M., Hashimoto, K., Kikuchi, a, Inoue, S., Okumura, H., Matsumoto, K., Goto, Y., Ohgai, H., Moriishi, K. & Syuto, B., 1992. Epidermal cell differentiation inhibitor ADP-ribosylates small GTP-binding proteins and induces hyperplasia of epidermis. *The Journal of biological chemistry*, 267(4), pp.2600–4.

Sumantran, V.N., 2011. Cellular Chemosensitivity Assays: An Overview I. A. Cree, ed. *Methods in Molecular Biology*, 731, pp.219–236.

Susi, F.R., 1968. Studies of cellular renewal and protein synthesis in mouse oral mucosa utilizing H3-thymidine and H3-cystine. *The Journal of Investigative Dermatology*, 51(5), pp.403–408.

Swenson, K.L., Jordan, J.R., Beyer, E.C. & Paul, D.L., 1989. Formation of Gap Junctions in Xenopus Oocyte Pairs by Expression of Connexins in Xenopus Oocyte Pairs. *Cell*, 57, pp.145–155.

Swindell, W.R., Johnston, A., Xing, X., Voorhees, J.J., Elder, J.T. & Gudjonsson, J.E., 2013. Modulation of epidermal transcription circuits in

psoriasis: new links between inflammation and hyperproliferation. *PloS one*, 8(11), p.e79253.

Szpaderska, A.M., Walsh, C.G., Steinberg, M.J. & DiPietro, L.A., 2005. Distinct patterns of angiogenesis in oral and skin wounds. *Journal of Dental Research*, 84(4), pp.309–314.

Szpaderska, A.M., Zuckerman, J.D. & DiPietro, L.A., 2003. Differential Injury Responses in Oral Mucosal and Cutaneous Wounds. *Journal of Dental Research*, 82(8), pp.621 –626.

Tacheau, C., Laboureau, J., Mauviel, A. & Verrecchia, F., 2008. TNF-alpha represses connexin43 expression in HaCat keratinocytes via activation of JNK signaling. *Journal of cellular physiology*, 216(2), pp.438–44.

Tack, K.J. & Sabath, L.D., 1985. increased minimum inhibitory concentration with anaerobiasis for tobramycin, gentamicin and amikacin compared to latamoxef, piperaciliin, chloramphenicol, and clindamycin. *Chemotherapy*, 31, pp.204–210.

Taichman, N., Young, S., Cruchley, A.T., Taylor, P. & Paleolog, E., 1997. Human neutrophils secrete vascular endothelial growth factor. *Journal of leukocyte biology*, 62(September), pp.397–400.

Tan, N.C.-W., Foreman, A., Jardeleza, C., Douglas, R., Tran, H. & Wormald, P.J., 2012. The multiplicity of Staphylococcus aureus in chronic rhinosinusitis: correlating surface biofilm and intracellular residence. *The Laryngoscope*, 122(8), pp.1655–60.

Tan, N.C.-W., Tran, H.B., Foreman, A., Jardeleza, C., Vreugde, S. & Wormald, P.J., 2013. Identifying intracellular Staphylococcus aureus in chronic rhinosinusitis: a direct comparison of techniques. *American journal of rhinology & allergy*, 26(6), pp.444–9.

Taniguchi Ishikawa, E., Ghiaur, G., Dunn, S.K., Ashley, M., Murali, B., Madhu, M., Gutstein, D.E., Fishman, G.I., Barrio, L.C. & Cancelas, J.A., 2012. Connexin-43 prevents hematopoietic stem cell senescence through transfer of reactive oxygen species to bone marrow stromal cells. *Proceedings of the National Academy of Sciences*, 109(31), pp.12834–12835.

Tankersley, A., Frank, M.B., Bebak, M. & Brennan, R., 2014. Early effects of Staphylococcus aureus biofilm secreted products on inflammatory responses of human epithelial keratinocytes. *Journal of inflammation*, 11(1), p.17.

Tarnuzzer, R.W. & Schultz, G.S., 1996. Biochemical analysis of acute and chronic wound environments. *Wound Repair and Regeneration*, 4(3), pp.321–325.

Teubner, B., Michel, V., Pesch, J., Lautermann, J., Cohen-Salmon, M., Sohl, G., Jahnke, H., Winterhager, E., Herberhold, C., Herdelin, J.-P., Petit, C. &

Willecke, K., 2003. Connexin30 (Gjb6)-deficiency causes severe hearing impairment and lack of endocochlear potential. *Human Molecular Genetics*, 12(1), pp.13–21.

Thomas, T., Shao, Q. & Laird, D.W., 2007. Differentiation of organotypic epidermis in the presence of skin disease-linked dominant-negative Cx26 mutants and knockdown Cx26. *The Journal of membrane biology*, 217(1-3), pp.93–104.

Thompson, R.J., Zhou, N. & MacVicar, B.A., 2006. Ischemia opens neuronal gap junction hemichannels. *Science (New York, N.Y.)*, 312(5775), pp.924–927.

Thomson, P.J., Potten, C.S. & Appleton, D.R., 1999. Mapping dynamic epithelial cell proliferative activity within the oral cavity of man: a new insight into carcinogenesis? *The British Journal of Oral & Maxillofacial Surgery*, 37(5), pp.377–383.

Thurlow, L.R., Hanke, M.L., Fritz, T., Angle, A., Aldrich, A., Williams, H., Engebretsen, I.L., Bayles, K.W. & Horswill, A.R., 2012. Staphyloccous auerus biofilms prevent marcophage pahgocytosis and attenuate inflammation in vivo. *Journal of immunology*, 186(11), pp.6585–6596.

Tomasetto, C., Neveu, M.J., Daley, J., Horan, P.K. & Sager, R., 1993. Specificity of gap junction communication among human mammary cells and connexin transfectants in culture. *The Journal of cell biology*, 122(1), pp.157–67.

Tomasz, M., 1995. Mitomycin C: small, fast and deadly (but very selective). *Chemistry & biology*, 2(9), pp.575–9.

Torretta, S., Drago, L., Marchisio, P., Cappadona, M., Rinaldi, V., Nazzari, E. & Pignataro, L., 2013. Recurrences in chronic tonsillitis substained by tonsillar biofilm-producing bacteria in children. Relationship with the grade of tonsillar hyperplasy. *International journal of pediatric otorhinolaryngology*, 77(2), pp.200–4.

Tran Van Nhieu, G., Clair, C., Bruzzone, R., Mesnil, M., Sansonetti, P. & Combettes, L., 2003. Connexin-dependent inter-cellular communication increases invasion and dissemination of Shigella in epithelial cells. *Nature cell biology*, 5(8), pp.720–6.

Traub, O., Look, J., Dermietzel, R., Brummer, F., Husler, D. & Willecke, K., 1989. Comparative Characterization of the 21-kD and 26-kD Gap Junction Proteins in Murine Liver and Cultured Hepatocytes Quantification of Gap Junctional Proteins. *The Journal of cell biology*, 108(March), pp.1039–1051.

Trexler, E.B., Bennett, M. V, Bargiello, T.A. & Verselis, V.K., 1996. Voltage gating and permeation in a gap junction hemichannel. *Proceedings of the National Academy of Sciences of the United States of America*, 93(12), pp.5836–5841.

Turin, L. & Warner, A., 1977. Carbon dioxide reversibly abolishes ionic communication between cells of early amphibian embryo. *Nature*, 270(5632), pp.56–57.

Uchida, Y., Shiba, H., Komatsuzawa, H., Hirono, C., Ashikaga, A., Fujita, T., Kawaguchi, H., Sugai, M., Shiba, Y. & Kurihara, H., 2005. Irsogladine maleate influences the response of gap junctional intercellular communication and IL-8 of human gingival epithelial cells following periodontopathogenic bacterial challenge. *Biochemical and biophysical research communications*, 333(2), pp.502–507.

Usui, M.L., Mansbridge, J.N., Carter, W.G., Fujita, M. & Olerud, J.E., 2008. Keratinocyte migration, proliferation, and differentiation in chronic ulcers from patients with diabetes and normal wounds. *The journal of histochemistry and cytochemistry: official journal of the Histochemistry Society*, 56(7), pp.687–696.

Valle, J., Latasa, C., Gil, C., Toledo-Arana, A., Solano, C., Penadés, J.R. & Lasa, I., 2012. Bap, a biofilm matrix protein of Staphylococcus aureus prevents cellular internalization through binding to GP96 host receptor. *PLoS pathogens*, 8(8), p.e1002843.

Vázquez-Sánchez, E.A., Rodríguez-Romero, M., Sánchez-Torres, L.E., Rodríguez-Martínez, S., Cancino-Diaz, J.C., Rodríguez-Cortes, O., García-López, E.S. & Cancino-Diaz, M.E., 2014. Peptidoglycan from Staphylococcus aureus has an anti-apoptotic effect in HaCaT keratinocytes mediated by the production of the cellular inhibitor of apoptosis protein-2. *Microbiology and immunology*, 58(2), pp.87–95.

Veenstra, R.D., Wang, H.Z., Beblo, D.A., Chilton, M.G., Harris, A.L., Beyer, E.C. & Brink, P.R., 1995. Selectivity of connexin-specific gap junctions does not correlate with channel conductance. *Circulation Research*, 77(6), pp.1156–1165.

Vega, F.M., Fruhwirth, G., Ng, T. & Ridley, A.J., 2011. RhoA and RhoC have distinct roles in migration and invasion by acting through different targets. *The Journal of cell biology*, 193(4), pp.655–65.

Velasquez Almonacid, L., Tafuri, S., Dipineto, L., Matteoli, G., Fiorillo, E., Della Morte, R., Fioretti, A., Menna, L.F. & Staiano, N., 2009. Role of connexin-43 hemichannels in the pathogenesis of Yersinia enterocolitica. *Veterinary journal (London, England : 1997)*, 182(3), pp.452–7.

Velasquez Almonacid, L.A., Tafuri, S., Dipineto, L., Matteoli, G., Fiorillo, E., Della Morte, R., Fioretti, A., Menna, L.F. & Staiano, N., 2009. Role of connexin-43 hemichannels in the pathogenesis of Yersinia enterocolitica. *Veterinary journal (London, England: 1997)*, 182(3), pp.452–457.

Verselis, V.K., Trexler, E.B. & Bukauskas, F.F., 2000. Connexin hemichannels and cell-cell channels: comparison of properties. *Brazilian journal of medical and biological research*, 33(4), pp.379–389.

Vinken, M., Decrock, E., Leybaert, L., Bultynck, G., Himpens, B., Vanhaecke, T. & Rogiers, V., 2012. Non-channel functions of connexins in cell growth and cell death. *Biochimica et biophysica acta*, 1818(8), pp.2002–8.

Vinken, M., Decrock, E., Vanhaecke, T., Leybaert, L. & Rogiers, V., 2012. Connexin43 signaling contributes to spontaneous apoptosis in cultures of primary hepatocytes. *Toxicological sciences: an official journal of the Society of Toxicology*, 125(1), pp.175–186.

Vinken, M., Vanhaecke, T., Papeleu, P., Snykers, S., Henkens, T. & Rogiers, V., 2006. Connexins and their channels in cell growth and cell death. *Cellular Signalling*, 18(5), pp.592–600.

Vollmer, P., Walev, I., Rose-john, S. & Bhakdi, S., 1996. Novel pathogenic mechanism of microbial metalloproteinases : liberation of membrane-anchored molecules in biologically active form exemplified by studies with the human interleukin-6 receptor . Novel Pathogenic Mechanism of Microbial Metalloproteinases : *Infection and immunity*, 64(9), pp.3646–3651.

Waikel, R.L., Kawachi, Y., Waikel, P.A., Wang, X.J. & Roop, D.R., 2001. Deregulated expression of c-Myc depletes epidermal stem cells. *Nature genetics*, 28(2), pp.165–168.

Wall, I.B., Moseley, R., Baird, D.M., Kipling, D., Giles, P., Laffafian, I., Price, P.E., Thomas, D.W. & Stephens, P., 2008. Fibroblast dysfunction is a key factor in the non-healing of chronic venous leg ulcers. *The Journal of investigative dermatology*, 128(10), pp.2526–40.

Wang, C.M., Lincoln, J., Cook, J.E. & Becker, D.L., 2007. Abnormal connexin expression underlies delayed wound healing in diabetic skin. *Diabetes*, 56(11), pp.2809–2817.

Wanke, I., Skabytska, Y., Kraft, B., Peschel, A., Biedermann, T. & Schittek, B., 2013. Staphylococcus aureus skin colonization is promoted by barrier disruption and leads to local inflammation. *Experimental dermatology*, 22(2), pp.153–5.

Watson, A., Morris, V.L. & Chan, B.M.C., 2009. Coordinated integrin and growth factor regulation of primary keratinocyte migration mediated through extracellular signal regulated kinase and phosphoinositide 3-kinase. *Archives of dermatological research*, 301(4), pp.307–317.

Werner, R., Levine, E., Rabadan-Diehl, C. & Dahl, G., 1989. Formation of hybrid cell-cell channels. *Proceedings of the National Academy of Sciences of the United States of America*, 86(14), pp.5380–4.

Wilgoss, A., Leigh, I.M., Barnes, M.R., Dopping-hepenstal, P., Eady, R.A.J., Walter, J.M., Kennedy, C.T.C. & Kelsell, D.P., 1999. Identification of a Novel Mutation R42P in the Gap Junction Protein b -3 Associated with Autosomal Dominant Erythrokeratoderma Variabilis. *The Journal of investigative dermatology*, 113, pp.1119–1122.

Willecke, K., Eiberger, J., Degen, J., Eckardt, D., Romualdi, A., Güldenagel, M., Deutsch, U. & Söhl, G., 2002. Structural and functional diversity of connexin genes in the mouse and human genome. *Biological Chemistry*, 383(5), pp.725–737.

Willoughby, S.G., Hopps, R.M. & Johnson, N.W., 1986. Changes in the rate of epithelial proliferation of rat oral mucosa in response to acute inflammation induced by turpentine. *Archives of Oral Biology*, 31(3), pp.193–199.

Wiszniewski, L., Salomon, D. & Meda, P., 2001. Cx26 affects the in vitro reconstruction of human epidermis. *Cell communication & adhesion*, 8(4-6), pp.409–13.

Wong, J.W., Gallant-Behm, C., Wiebe, C., Mak, K., Hart, D. a, Larjava, H. & Häkkinen, L., 2009. Wound healing in oral mucosa results in reduced scar formation as compared with skin: evidence from the red Duroc pig model and humans. *Wound repair and regeneration : official publication of the Wound Healing Society [and] the European Tissue Repair Society*, 17(5), pp.717–29.

Wright, C.S., Pollok, S., Flint, D.J., Brandner, J.M. & Martin, P.E.M., 2012. The connexin mimetic peptide Gap27 increases human dermal fibroblast migration in hyperglycemic and hyperinsulinemic conditions in vitro. *Journal of cellular physiology*, 227(1), pp.77–87.

Wright, C.S., van Steensel, M.A.M., Hodgins, M.B. & Martin, P.E.M., 2009. Connexin mimetic peptides improve cell migration rates of human epidermal keratinocytes and dermal fibroblasts in vitro. *Wound Repair and Regeneration: Official Publication of the Wound Healing Society [and] the European Tissue Repair Society*, 17(2), pp.240–249.

Xia, J., Liu, X., Tao, X., Hong, Y., Chen, X., Dai, Y., Huang, Y. & Cheng, B., 2009. Expression of gap junctional protein connexin43 during 4-nitroquinoline-1-oxide-induced rat tongue carcinogenesis. *Journal of Molecular Histology*, 40, pp.183–188.

Xu, J. & Clark, R., 1996. Extracellular matrix alters PDGF regulation of fibroblast integrins. *The Journal of cell biology*, 132(1-2), pp.239–249.

Xu, K.D., McFeters, G. a & Stewart, P.S., 2000. Biofilm resistance to antimicrobial agents. *Microbiology (Reading, England)*, 146 (Pt 3(March), pp.547–9.

Xu, X., Francis, R., Wei, C.J., Linask, K.L. & Lo, C.W., 2006. Connexin 43-mediated modulation of polarized cell movement and the directional migration of cardiac neural crest cells. *Development (Cambridge, England)*, 133(18), pp.3629–3639.

Yarwood, J.M., Bartels, D.J., Volper, E.M. & Greenberg, E.P., 2004. Quorum Sensing in Staphylococcus aureus Biofilms Quorum Sensing in Staphylococcus aureus Biofilms. *Journal of bacteriology*, 186(6), pp.1838–1850.

Yeager, M., Unger, V.M. & Falk, M.M., 1998. Synthesis, assembly and structure of gap junction intercellular channels. *Current opinion in structural biology*, 8(4), pp.517–524.

Yeh, T.-H., Hsu, W.-C., Chen, Y.-S., Hsu, C.-J. & Lee, S.-Y., 2005. Lipopolysaccharide decreases connexin 43 expression on nasal epithelial cells in vitro. *Acta oto-laryngologica*, 125(10), pp.1091–1096.

Young, B., Lowe, J., Stevens, A. & Heath, J., 2000. *Wheater's Functional Histology* Fourth Edi., Philadelphia, USA: Churchill Livingstone Elsevier.

Yum, S., Zhang, J., Valiunas, V., Kanaporis, G., Brink, P., White, T. & Scherer, S., 2007. Human connexin26 and connexin30 form functional heteromeric and heterotypic channels. *American Journal of Physiology-Cell Physiology*, 293, pp.C1032–C1048.

Zahler, S. & Hoffmann, A., 2003. Gap-junctional coupling between neutrophils and endothelial cells : a novel modulator of transendothelial migration. *Journal of Leukocyte Biology*, 73, pp.118–126.

Zavizion, B., Bramley, a J., Politis, I., Gilmore, J., Turner, J.D., Patel, a H. & Foster, T.J., 1995. Effects of Staphylococcus aureus toxins on the growth of bovine mammary epithelial cells (MAC-T) in culture. *Journal of dairy science*, 78(2), pp.277–84.

Zglinicki, T. von, Nilsson, E., Docke, W.D. & Brunk, U.T., 1995. lipofuscin accumulation and ageing fibroblasts. *Gerontology*, 41(supplement 2), pp.95–108.

Zhang, X., Chen, X., Wu, D., Liu, W., Wang, J., Feng, Z., Cai, G., Fu, B., Hong, Q. & Du, J., 2006. Downregulation of connexin 43 expression by high glucose induces senescence in glomerular mesangial cells. *Journal of the American Society of Nephrology : JASN*, 17(6), pp.1532–42.

Zhang, Y.-W., Kaneda, M. & Morita, I., 2003. The gap junction-independent tumor-suppressing effect of connexin 43. *The Journal of biological chemistry*, 278(45), pp.44852–44856.

Zhang, Y.W., Morita, I., Ikeda, M., Ma, K.W. & Murota, S., 2001. Connexin43 suppresses proliferation of osteosarcoma U2OS cells through post-transcriptional regulation of p27. *Oncogene*, 20(31), pp.4138–4149.

Zhao, G., Hochwalt, P.C., Usui, M.L., Underwood, R.A., Singh, P.K., James, G.A., Stewart, P.S., Fleckman, P. & Olerud, J.E., 2010. Delayed wound healing in diabetic (db/db) mice with Pseudomonas aeruginosa biofilm challenge: a model for the study of chronic wounds. *Wound repair and regeneration: official publication of the Wound Healing Society [and] the European Tissue Repair Society*, 18(5), pp.467–477.

Zhao, G., Usui, M.L., Lippman, S.I., James, G. a, Stewart, P.S., Fleckman, P. & Olerud, J.E., 2013. Biofilms and Inflammation in Chronic Wounds. *Advances in wound care*, 2(7), pp.389–399.

Zhao, W., Lin, Z. & Zhang, Z., 2004. Cisplatin-induced premature senescence with concomitant reduction of gap junctions in human fibroblasts. *Cell research*, 14(1), pp.60–6.